Universitat de Girona

EVALUACIÓN DE LAS PROPIEDADES MECÁNICAS Y MICROMECÁNICAS DE LOS MATERIALES COMPUESTOS DE POLIPROPILENO REFORZADO CON FIBRAS RESIDUALES PROVENIENTES DEL RECICLADO DE RECORTES EN LA INDUSTRIA TEXTIL

Albert Serra Bruns

Universitat de Girona

Evaluación de las propiedades mecánicas y micromecánicas de los materiales compuestos de polipropileno reforzado con fibras residuales provenientes del reciclado de recortes en la industria textil

Tesis Doctoral

Albert Serra Bruns

2021

Universitat de Girona

Evaluación de las propiedades mecánicas y micromecánicas de los materiales compuestos de polipropileno reforzado con fibras residuales provenientes del reciclado de recortes en la industria textil

Tesis Doctoral

Albert Serra Bruns

2021

PROGRAMA DE DOCTORADO EN TECNOLOGÍA

Dirigida por: Dr. Joaquim Agustí Tarrés Farrés

Tutor: Dr. Pere Mutjé Pujol

Memoria presentada para optar al título de DOCTOR POR LA UNIVERSITAT DE GIRONA

El Dr. Pere Mutjé Pujol, catedrático del Departamento de Ingeniería Química, Agraria y Tecnología Alimentaria de la Universitat de Girona, y el Dr. Joaquim Agustí Tarrés Farrés, investigador ordinario del Departamento de Ingeniería Química, Agraria y Tecnología Alimentaria de la Universitat de Girona,

DECLARAN:

Que el trabajo titulado "Evaluación de las propiedades mecánicas y micromecánicas de los materiales compuestos de polipropileno reforzado con fibras residuales provenientes del reciclado de recortes en la industria textil", que presenta el Sr. Albert Serra Bruns para la obtención del título de doctor ha sido realizado bajo nuestra tutoría y dirección.

Y para que así conste y a los efectos oportunos, firmamos el presente documento

Dr. Pere Mutjé Pujol

Dr. Joaquim Agustí Tarrés Farrés

Girona, 8 d'octubre de 2021.

“I don’t care that they stole my idea… I care that they don’t have any of their own.”

Nikola Tesla

Agraïments

Ara fa quatre anys, els integrants del grup d'investigació LEPAMAP-PRODIS em van animar a realitzar aquesta tesi per tal de poder avançar acadèmicament i professionalment. Per mi, aquell moment va ser difícil ja que s'obria un gran repte en la meva vida. Gràcies al suport de tot el grup de recerca, dels familiars i de les amistats vaig poder acceptar-lo i arribar a la finalització de la present tesis doctoral.

En primer lloc, voldria agrair al meu tutor i director de la tesi durant tres anys i mig, el Dr. Pere Mutjé. Vull agrair-li el seu suport i pels coneixements que m'ha transmès durant aquesta tesi doctoral.

En segon lloc, també voldria expressar el meu agraïment al meu director de tesi el Dr. Joaquim Agustí Tarrés Farrés. Agrair-li la seva implicació, suport i dedicació en el desenvolupament de la tesi.

En tercer lloc, voldria donar les gràcies a tots els companys i companyes del grup LEPAMAP i PRODIS. Cadascun d'ells m'han ajudat a poder desenvolupar la present tesi d'una manera o un altre. Es fa difícil destacar algun membre de l'equip ja que tots ells m'han ofert la seva ajuda i el seu suport des de l'inici del doctorat. A tots ells, moltes gràcies per tot!

També voldria donar les gràcies a la meva família i a les meves amistats. Gràcies Anna, Farners, Francesc, Marta, Jaume, Raquel, Eduard, Sílvia i Xavi per donar-me una empenta en els moments difícils. Tots vosaltres m'heu recolzat i m'heu donat el vostre suport per acabar-la. Gràcies a tots per recolzar-me en tots els moments difícils de la tesi.

ARTÍCULOS QUE COMPONEN LA PRESENTE TESIS

La presente tesis está compuesta por los siguientes artículos:

1. Serra, A., Tarrés, Q., Claramunt, J., Mutjé, P., Ardanuy, M., Espinach, F.X. (2017). "Behaviour of the interphase of dyed cotton residue flocks reinforced" Composites Part B: Engineering, 128, 200-207. **Artículo publicado.**

   Factor de impacto 2017: 4.92, posición 3 de 86 en ENGINEERING, MULTIDISCIPLINARY, 1er Cuartil.

2. Serra, A., Tarrés, Q., Llop, M., Reixach, R., Mutjé, P. Espinach, F.X. (2019). "Recycling dyed cotton textile byproduct fibers as polypropylene reinforcement" Textile Research Journal, 89(11), 2113-2125. **Artículo publicado**.

   Factor de impacto 2019: 1.926, posición 5 de 24 en MATERIAL SCIENCE, TEXTILES, 1er Cuartil.

3. Serra, A., Tarrés, Q., Chamorro, M.A., Soler, J., Mutjé, P., Espinach, F.X., Vilaseca, F. (2019). "Modeling the stiffnesss of coupled and uncoupled recycled cotton fibers reinforced polypropylene composites" Polymers, 11(10), 1725. **Artículo publicado**.

   Factor de impacto 2019: 3.426, posición 16 de 89 en POLYMER SCIENCE, 1er Cuartil.

4. Serra, A., Delgado-Aguilar, M., Ripoll, R., Llorens, M., Espinach, F.X., Tarrés, Q. (2021). "Study of the flexural strength of recycled dyed cotton fiber reinforced polypropylene composites and the effect of the use of maleic anhydride as coupling agent" Journal of Natural Fibers. **Artículo publicado.**

   Factor de impacto 2020: 5.323, posición 1 de 25 en MATERIAL SCIENCE, TEXTILES, 1er Cuartil.

5. Serra, A., Serra-Parareda, F., Vilaseca, F., Delgado-Aguilar, M., M., Espinach, F.X., Tarrés, Q. (2021). "Exploring the potential of cotton industry byproducts in the plastic composite sector: Macro and Micromechanics study of the flexural modulus" Materials, 14(17), 4787. **Artículo publicado.**

   Factor de impacto 2020: 3.623, posición 17 de 80 en METALLURGY & METALLURGICAL ENGINEERING, 1er Cuartil.

El autor de esta tesis contribuyó a los artículos anexos de la siguiente manera:

Artículo 1

Obtuvo los distintos materiales compuestos para el estudio de la interfase entre la borra de algodón y el polipropileno. Evaluó el efecto del tinte y de las distintas cantidades de agente de acoplamiento (MAPP) sobre la interacción fibra-matriz. Calculó las propiedades intrínsecas de las fibras mediante un estudio micromecánico. Efectuó las extracciones de las fibras para realizar los correspondientes ensayos morfológicos. Diseñó los experimentos y evaluó los resultados. Escribió el trabajo junto con los otros autores.

Artículo 2

Realizó la preparación de los materiales y obtención de las probetas normalizadas de los materiales compuestos con distintos porcentajes de polipropileno y borra de algodón para la realización de los ensayos de resistencia a tracción. Aplicó, conjuntamente con los otros autores, modelos micromecánicos para la resolución de la ecuación de Kelly y Tyson mediante el método de Boywer y Bader. Analizó los resultados y contribuyó en la redacción del artículo.

Artículo 3

Realizó los ensayos para la determinación del Módulo de Young de los distintos materiales compuestos obtenidos a partir del residuo de borra de algodón y polipropileno. Participó en la redacción de la primera versión del artículo, así como, en las posteriores revisiones.

Artículo 4

Obtuvo los materiales compuestos necesarios para la realización de los ensayos de resistencia a flexión. Realizó los experimentos y evaluó los resultados obtenidos. Participó en los cálculos micromecánicos y en la redacción del trabajo.

Artículo 5

Obtuvo los materiales compuestos necesarios para la realización de los ensayos de módulo a flexión. Realizó los experimentos y evaluó los resultados obtenidos. Participó en los cálculos micromecánicos.

ABREVIATURAS

α: Ángulo medio de orientación de las fibras (°).

β: Factor del modelo de Hirsch.

CS_2: Disulfuro de carbono.

χ_1: Factor de orientación.

χ_2: Factor de interfase y longitud.

ε^C_f: Deformación del material compuesto a flexión (%).

ε^C_t: Deformación del material compuesto a tracción (%).

η_e: Factor de eficiencia.

η_l: Factor de longitud.

η_o: Factor de orientación.

ρ^C: Densidad del material compuesto ($g.cm^{-3}$)

ρ^F: Densidad de la fibra ($g.cm^{-3}$)

ρ^C: Densidad de la matriz ($g.cm^{-3}$)

σ^c_f: Resistencia máxima a flexión del material compuesto (MPa).

σ^F_f: Resistencia intrínseca a flexión de la fibra (MPa).

σ^{m*}_f: Resistencia a flexión de la matriz en el punto de rotura del material compuesto (MPa).

σ^c_t: Resistencia máxima a tracción del material compuesto (MPa).

σ^F_t: Resistencia intrínseca a tracción de la fibra (MPa).

σ^{m*}_t: Resistencia mecánica de la matriz en el punto de rotura del material compuesto (MPa).

τ: Tensión interfacial de cizalla (MPa).

v: Coeficiente de Poisson.

CF: Fibra de algodón.

D: Coeficiente de difusión.

DC: Demanda catiónica (µeq/g).

d^F: Diámetro aritmético de la fibra (µm).

E^c_f: Módulo a flexión del material compuesto (GPa).

E^F_f: Módulo intrínseco a flexión de la fibra (GPa).

E^m_f: Módulo a flexión de la matriz (GPa).

EPA: United States Enviromental Protection Agency.

E^{11}: Módulo a flexión longitudinal.

E^{22}: Módulo a flexión transversal.

E^{c}_{t}: Módulo de Young del material compuesto (GPa).

E^{F}_{t}: Módulo de Young intrínseco de la fibra (GPa).

E^{m}_{t}: Módulo de Young de la matriz (GPa).

f_c: Factor de acoplamiento.

FFSF: Factor de resistencia a flexión de las fibras (MPa).

FFMF: Factor de módulo a flexión de las fibras (GPa).

FTMF: Factor de módulo a tracción de las fibras (GPa).

FTSF: Factor de resistencia a tracción de las fibras (MPa).

GF: Fibra de vidrio.

HDPE: Polietileno de alta densidad.

HS: Filamentos de Cáñamo.

$I_U{}^C$: Impacto Charpy sin entalla (KJ/m^2).

$I_N{}^C$: Impacto Charpy con entalla (KJ/m^2).

K: Constante cinética de Fick relacionada con las condiciones ambientales.

L: Espesor.

L_a: Longitud aritmética de las fibras (μm).

L_c: Longitud crítica (μm).

LDPE: Polietileno de baja densidad.

LEPAMAP: Laboratori d'enginyeria Paperera i Materials Polímerics.

L_w: Longitud ponderada de las fibras (μm).

KOH: hidróxido de potasio.

MAPP: Polipropileno con injertos de anhídrido maleico.

MT: Millones de toneladas métricas.

M_t: Absorción de agua en un tiempo determinado.

M_∞: Absorción de agua en el punto de saturación (%).

m_0: Peso inicial de una probeta.

m_t: Peso de una probeta en un tiempo t.

n: Constante cinética de Fick relacionada con el tiempo de saturación.

NaOH: Hidróxido de sodio.

ONPF:	Fibras de papel de periódico.
PE:	Polietileno.
PES-NA:	Polietileno sulfonato de sodio.
PP:	Polipropileno.
polyDADMAC:	Cloruro de polidialildimetilamonio.
RoM:	Regla de las mezclas.
SEM:	Microscopio electrónico de barrido.
SGW:	Fibras obtenidas a través de un proceso mecánico de muela de piedra.
t:	Tiempo
UE:	Unión Europea.
V^F:	Fracción volumétrica del refuerzo.
w/w:	Relación entre el peso del componente y el peso total (%).
WPC:	Compuestos de madera plástica.

ÍNDICE

ÍNDICE DE FIGURAS

ÍNDICE DE TABLAS

RESUM

Cada any, la industria tèxtil genera grans quantitats de residu cel·lulòsic durant les etapes de producció i confecció de teixits. Aquest residu es compon de fibres amb longituds inferiors a 10 mm que impedeixen la seva reintroducció en el procés de fabricació de productes tèxtils i acaben abocades o incinerades. En aquesta tesi doctoral s'han obtingut materials compostos de polipropilè reforçats amb residus cel·lulòsics provinents de la indústria tèxtil, per tal de donar-los un valor afegit i reduir el seu impacte mediambiental.

El residu cel·lulòsic que s'ha utilitzat és la borra de cotó doncs, el cotó és la fibra natural que més s'utilitza en la confecció de vestits, procés en el que es genera una major quantitat d'aquests residus.

Per a l'obtenció d'un material compost de polipropilè (PP) reforçat amb fibres naturals és necessària la utilització d'un agent d'acoblament per a garantir una bona interfase entre elles. A més a més, en partir d'una fibra cel·lulòsica tenyida, s'ha aprofitat per estudiar quin efecte té el tint sobre la interfase del material compost. Durant aquest estudi s'ha trobat que els colorants orgànics presents a la borra de cotó afecten la qualitat de la interfase de dues maneres. Per una banda, augmenten la compatibilitat química entre les fibres de cotó i la matriu degut a que disminueixen el caràcter hidrofílic de les fibres. Per una altra banda, els tints limiten l'efecte dels agents d'acoblament degut a que incrementen la dificultat que tenen aquests per reaccionar amb els grups hidroxils presents a la superfície de la fibra.

Aquí mateix s'han analitzat les propietats mecàniques dels diferents materials compostos produïts utilitzant diferents quantitats de reforç i d'agent d'acoblament (MAPP). Els resultats dels assajos a tracció, han mostrat un increment notable de la resistència a tracció de la matriu. No obstant, els compostos formulats amb MAPP han mostrat una resistència a tracció sensiblement més alta que els compostos formulats sense aquest agent d'acoblament. Pel que fa a la rigidesa, s'ha observat una evolució lineal en els valors del Mòdul de Young dels compòsits directament proporcional al contingut de reforç aplicat. Per contra, s'ha constatat que el pendent de l'equació d'ajust lineal obtinguda a través de la representació gràfica esmentada anteriorment, és inferior al d'altres compostos de polipropilè reforçats amb fibres naturals.

Si ens centrem en l'anàlisi a flexió i impacte dels espècimens, els materials obtinguts han mostrat propietats prometedores que demostren la seva capacitat per substituir els compostos reforçats amb fibra de vidre, sent aquest últim el reforç més utilitzat en els materials compostos comercials. També cal tenir en compte l'estudi d'absorció d'aigua a través del que s'ha pogut observar el comportament dels compostos de PP reforçats amb fibres de cotó tenyides en medis amb elevat percentatge d'humitat. S'observa que tot i que les fibres estaven recobertes superficialment pel tint, això no ha estat un impediment per a l'absorció d'aigua en el seu interior.

Paral·lelament a l'estudi de les propietats mecàniques, s'ha avaluat la interfase dels compostos i s'han calculat les propietats intrínseques de les fibres. Per a dur a terme aquesta avaluació, s'ha utilitzat el model de Kelly y Tyson basat en la regla de les mescles modificada. Per tal de resoldre l'equació de quatre incògnites associada al model lineal de Kelly y Tyson , s'agafa com a referencia el model de Bowyer i Bader que ens permet a través d'un seguit de suposicions l'obtenció d'una equació amb una sola incògnita.

En el cas del Mòdul de Young i del mòdul a flexió, s'ha utilitzat el model de Hirsch i el de Tsai i Pagano el qual te en compte la morfologia de les fibres, per calcular els mòduls intrínsecs de les fibres. La obtenció d'aquests dos mòduls intrínsecs ha permès avaluar l'efecte que té la inclusió explícita de la morfologia de les fibres en els resultats. Finalment, s'ha utilitzat una regla modificada de les mescles per obtenir els factors d'eficiència de les fibres i els factors d'orientació i longitud.

RESUMEN

Cada año, la industria textil genera grandes cantidades de residuos celulósicos durante las etapas de producción y fabricación de tejidos. Este residuo se compone de fibras con longitudes inferiores a 10 mm que impiden su reintroducción en el proceso de la fabricación textil y terminan en vertederos o en incineradoras. En esta tesis doctoral, se han obtenido materiales compuestos de polipropileno reforzado con residuos celulósicos provenientes de la industria textil, con el fin de darles un valor añadido y reducir su impacto ambiental.

El residuo celulósico que se ha utilizado es la borra de algodón, dado que el algodón es la fibra natural que más se utiliza en la confección de vestidos y, por lo tanto, es donde se genera la mayor cantidad de estos residuos.

Para la obtención de un material compuesto de polipropileno (PP) reforzado con fibras naturales es necesaria la utilización de un agente de acoplamiento para garantizar una buena interfase entre ellas. En este caso, al partir de una fibra celulósica teñida, se ha aprovechado para estudiar qué efecto tiene el tinte sobre la interfase del material compuesto. Durante este estudio se ha encontrado que los tintes orgánicos presentes en la borra de algodón afectan a la calidad de la interfase de dos maneras distintas. Por un lado, aumentan la afinidad entre las fibras de algodón y la matriz debido a que aumentan el carácter hidrofóbico de las fibras y, en consecuencia, aumentan su compatibilidad química con la matriz. Por otro lado, limitan el efecto de los agentes de acoplamiento debido a la dificultad que tiene el agente de acoplamiento para reaccionar con los grupos hidroxilos superficiales de la fibra a causa de la presencia del tinte.

Se han analizado las propiedades mecánicas de los diferentes materiales compuestos producidos con diferentes cantidades de refuerzo y de agente de acoplamiento (MAPP). Los resultados de los ensayos a tracción, han mostrado un incremento notable de la resistencia a tracción de la matriz. Sin embargo, los compuestos formulados con MAPP han mostrado una resistencia a tracción significativamente más alta que los compuestos formulados sin este agente de acoplamiento. En cuanto a la rigidez, se ha observado una evolución lineal de los valores del Módulo de Young de los compuestos directamente proporcional al contenido de refuerzo aplicado. Por el contrario, se ha constatado que la pendiente de la ecuación de ajuste lineal obtenida a través de la representación gráfica mencionada anteriormente, es inferior al de otros compuestos de polipropileno reforzados con fibras naturales.

Si nos centramos al análisis de flexión y al análisis de impacto de los especímenes, los materiales obtenidos han mostrado propiedades prometedoras que muestran su capacidad para reemplazar compuestos reforzados con fibra de vidrio, siendo este último el refuerzo más utilizado en los materiales compuestos comerciales. También hay que tener en cuenta el estudio de absorción de agua a través del cual se podido observar el comportamiento que tienen los compuestos de PP reforzados con fibras de algodón teñidas en medios con elevado porcentaje de humedad. Aunque las fibras estaban recubiertas superficialmente de tinte, esto no ha sido un impedimento para la absorción de agua en su interior.

Paralelamente al estudio de las propiedades mecánicas, se ha evaluado la interfase de los compuestos y se han calculado las propiedades intrínsecas de las fibras. Para llevar a cabo esta evaluación, se ha utilizado el modelo Kelly y Tyson, basado en la regla de mezclas modificadas. Con el fin de resolver la ecuación de cuatro incógnitas asociada al modelo lineal de Kelly y Tyson,

se toma como referencia el modelo de Bowyer y Bader que nos permite a través de una serie de suposiciones la obtención de una ecuación con una sola incógnita.

En el caso del módulo de Young y del módulo a flexión, se han utilizado el modelo Hirsch y el de Tsai y Pagano que tiene en cuenta la morfología de las fibras, para calcular los módulos intrínsecos de las fibras. La obtención de estos módulos intrínsecos ha permitido evaluar el efecto de la inclusión explícita de la morfología de la fibra en los resultados. Finalmente, se ha utilizado una regla modificada de mezclas para obtener el factor de eficiencia de las fibras y los factores de orientación y longitud.

ABSTRACT

Every year, the textile industry generates large amounts of cellulosic waste during the production and fabrication stages. This waste is made up of fibers, with lengths are less than 10 mm that prevent its reintroduction into the manufacturing process of textile products and they end up dumped or incinerated. In this doctoral thesis, polypropylene composite materials reinforced with cellulosic waste from the textile industry have been obtained, in order to give them added value and reduce their environmental impact.

The cellulosic waste that has been used is cotton wool, due to cotton is the natural fiber that is the most used in making clothes. In this process, a greater amount of this waste is generated.

To obtain a polypropylene (PP) composite material reinforced with natural fibers, it is necessary to use a coupling agent to ensure a good interface between them. In addition, from a dyed cellulosic fiber, it has been used to study the effect of dye on the interface of the composite material. During this study, it was found that the organic dyes present in the cotton wool affect the quality of the interface in two ways. On the one hand, dyes increase the affinity between the cotton fibers and the matrix due to the hydrophilic character of the fibers decreases. So, they increases their chemical compatibility with the matrix. On the other hand, dyes limit the effect of coupling agents because they increase the difficulty they have in reacting with the hydroxyl groups present on the surface of the fiber.

The mechanical properties of the different composite materials produced using different amounts of reinforcement and coupling agent (MAPP) have been analyzed here. The results of the tensile tests have shown a remarkable increase of the tensile strength of the matrix. However, compounds formulated with MAPP have shown significantly higher tensile strength than compounds formulated without this coupling agent. In terms of stiffness, a linear evolution has been observed in the values of the Young's Module of the composites directly proportional to the applied reinforcement content. In contrast, it has been found that the slope of the linear fit equation obtained through the graphical representation mentioned above is lower than that other polypropylene compounds reinforced with natural fibers.

If we focus on the flexural and impact analysis of specimens, the materials obtained have shown promising properties that demonstrate their ability to replace fiberglass-reinforced compounds, which are the most widely used reinforcement in commercial composite materials. It is also necessary to consider the study of water absorption through which it has been possible to observe the behavior of PP compounds reinforced with cotton dyed fibers in media with a high percentage of humidity. It is observed that although the fibers were superficially covered by the dye, this has not been an impediment to the water absorption.

In parallel with the study of the mechanical properties, the interface of the compounds has been evaluated and the intrinsic properties of the fibers have been calculated. To perform this evaluation, the Kelly and Tyson model based on the modified mixing rule was used. In order to solve the equation of four unknowns associated with the linear model of Kelly and Tyson, we take as reference the model of Bowyer and Bader that allows us through a series of assumptions to obtain an equation with a single unknown.

In the case of the Young's Modulus and flexural modulus, the Hirsch model and the Tsai and Pagano model, have been used to calculate the intrinsic modulus of the fibers. Obtaining these intrinsic modules has made it possible to evaluate the effect of the explicit inclusion of fiber morphology on the results. Finally, a modified rule of mixtures was used to obtain the fiber efficiency factor and the orientation and length factors.

Introducción y Estado del Arte

1. Introducción y Estado del Arte

Tal y como se describe en el informe publicado por la organización del Banco Mundial titulado *What a Waste 2.0* anualmente se generan aproximadamente 2010 millones de toneladas de residuos a nivel mundial [1]. En este informe se alerta de la necesidad de adoptar medidas urgentes para evitar una mayor generación de residuos. El informe también subraya que la gestión de los residuos sólidos se encuentra lejos de niveles aceptables. Un porcentaje alrededor de un 4% en los países pobres y de una tercera parte del total en los países ricos.

Laura Tuck, vicepresidenta de Desarrollo Sostenible del Banco Mundial, afirma que "la mala gestión de los desechos está perjudicando la salud humana y los entornos locales, agravando al mismo tiempo los retos que plantea el cambio climático".

A partir del volumen de residuos generados, se estima que durante el año 2016 el tratamiento y la eliminación de estos residuos generó la emisión de 1600 millones de toneladas de dióxido de carbono lo que representa aproximadamente el 5% de las emisiones mundiales [1]. En este sentido, la constitución de sistemas adecuados de gestión de los residuos resulta esencial para construir una economía circular y respetuosa con el medio ambiente [2,3]. Para ello, es necesario que los productos y materiales se diseñen y optimicen para ser reutilizados y reciclados.

Sin embargo, actualmente existen todavía industrias o sectores donde la disminución en la generación de residuos o la gestión de los productos al final de su vida útil todavía resulta complicado. Una de ellas es la industria textil, resultando ser la segunda industria más contaminante del planeta, la cual es responsable del 20% de los tóxicos que se vierten en el agua [4] y que cada año se desechan sus productos por valor de 400.000 millones de dólares [5]. Muchos de ellos terminan desechados en vertederos, como en el vertedero de Hong Kong, en el que cada día se eliminan 253 toneladas de tejidos [6]. En Europa, se generan aproximadamente 10 millones de toneladas de residuos textiles anualmente y suponen aproximadamente el 5% de los vertederos según la Agencia de Protección del Medio Ambiente de la Unión Europea [3]. Aunque la mayor parte de estos residuos se generen en la propia industria, durante el proceso de filamento y la fabricación de piezas de ropa, estos residuos también son generados en el ámbito doméstico cuando las piezas de ropa han cumplido con su utilidad y son desechadas. En la Unión Europea (UE) los consumidores descartan alrededor de 5,8 millones de toneladas de textiles al año que representan aproximadamente el 3% en peso de un contendor municipal [7]. Sin embargo, como mínimo el 50% de los tejidos que desechamos son reciclables, así mismo, la proporción de los residuos textiles reutilizados o reciclados anualmente es de tan solo un 25% [8].

Este fenómeno se puede resumir en dos palabras "fast Fashion". Este es debido al consumismo indiscriminado de la sociedad por estar a la moda y de la gran oferta de productos de baja calidad impuesta por las grandes cadenas textiles [9]. De hecho, este fenómeno empezó desde la década de los 90 y ha provocado un incremento del casi 100% de desechos textiles en los estados unidos según la EPA (United States Enviromental Protection Agency) [10]. En la Tabla 1, se puede observar la cantidad en millones de toneladas y cómo se gestionaron.

Destinación residuo (T)/Año	2000	2005	2010	2015	2017	2018
Desecho en vertederos	6.280	7.570	8.900	10.540	10.540	11.300
Reciclados	1.320	1830	2.050	2.460	2.570	2.510
Incinerados	1880	2110	2.270	3.060	3.170	3.220
Generación de residuos	9.480	11.510	13.220	16.060	16.890	17.300

Tabla 1. *Via de gestión de los residuos textiles estadounidenses en las últimas dos décadas. Fuente EPA.*

La baja tasa de reciclaje de los textiles de los países ricos, provoca que gran parte de estos terminen en vertederos [3], donde a medida que se descomponen contribuyen a la formación de lixiviados. Estos lixiviados pueden terminar contaminado tanto las aguas superficiales como las subterráneas [11]. Otro producto generado en la descomposición de estos materiales es el gas metano, que contribuye al efecto invernadero y al calentamiento global [12].

Otra parte de los residuos textiles es trasladada a incineradores donde son incinerados en grandes cantidades. Se estima que los residuos textiles son el tercer material más incinerado después del plástico y del cartón [6]. Debido a la creciente consciencia ambiental y a las demandas de las autoridades legislativas [13], se está impulsando a la industria textil a desarrollar soluciones para reducir la gran cantidad de residuos que genera. Una de las posibles soluciones pasa por convertir los residuos en productos de valor añadido [14–16]. Sin embargo, se debe tener en cuenta la gran diversidad de residuos fibrosos y de estructuras distintas que genera la industria textil. Esta solución debe, por lo tanto, permitir dotar a la industria textil de una tecnología que funcione de forma integrada y conjunta para que sea efectiva.

1.1. Industria textil

La industria textil es el sector dedicado a la producción de ropa, telas, hilos y productos relacionados. Es una de las actividades económicas más importantes a nivel global, el cual desempeña un papel importante en la industria manufacturera europea al emplear a 1,5 millones de personas y generar una facturación de 162.000 millones de euros [17]. Las exportaciones de la UE representan más del 30% del mercado mundial y los mayores productores europeos son Italia, Francia, Reino Unido, Alemania y España. En conjunto representan aproximadamente tres cuartes partes de la producción de la UE [18].

Tradicionalmente, la producción de textiles se realizó de forma artesanal. Sin embargo, durante la revolución industrial, el crecimiento de la población generó un importante crecimiento en la demanda de productos textiles y surgieron las primeras fábricas textiles [19]. A partir de ese momento, la producción de telas y tejidos se ha desarrollado de forma constante para cubrir las necesidades de la población.

Las materias primeras utilizadas en la industria textil son principalmente las fibras o fibras textiles, tintes, etc [20]. Las fibras textiles son el conjunto de filamentos o hilos que se utilizan

para formar el tejido, las cuales deben cumplir distintas condiciones estructurales y una determinada calidad: finura, longitud, color, brillo, elasticidad, resistencia, entre otros, para ser utilizadas en la industria textil [21]. Habitualmente estas fibras se clasifican según su origen en dos grandes grupos: fibras naturales o fibras manufacturadas [22].

1.1.1. Fibras naturales

Las fibras naturales provienen de componentes animales, vegetales o minerales. En la naturaleza, con la única excepción de la seda, las fibras tienen una longitud limitada que puede oscilar entre 1 y 350 mm para el amianto y algunas clases de lana respectivamente. Este tipo de fibras son habitualmente nombradas fibras discontinuas [23].

Fibras de origen animal

Las fibras naturales de origen animal están formadas a través de la condensación de α-aminoácidos para formar unidades de poliamida repetidas con varios sustituyentes en el átomo de carbono α. Las secuencias y el tipo de aminoácidos que componen las cadenas de proteínas individuales contribuyen a las propiedades generales de la fibra resultante. Existen dos clases principales de fibras proteicas naturales, la queratina (pelo o piel) y las fibras secretadas (insectos) [24].

La fibra natural proteica más utilizada es la lana, cuya fibra se obtiene a partir del pelo de las ovejas. En el año 2019 se produjeron 1,07 millones de toneladas métricas (MT) de lana en todo mundo, cuyo mayor productor fue Sud África con una producción del 63% del total [25]. Su principal propiedad es su enorme capacidad de aislamiento térmico, dado que sus fibras retienen el aire entre ellas. Debido a esta propiedad, se utiliza para la confección de ropa de abrigo (guantes, bufandas, jerseis, etc.), así como mantas, colchas y alfombras [26].

Figura 1. *Posibles fuentes de fibra de origen animal para la producción de textiles.*

Por otra parte, la fibra secretada más utilizada es la seda que se produce a través de las larvas de la mariposa *Bombyx mori* o también conocido como gusano de seda. Aunque la cuota de mercado de la seda es pequeña, se estima que alrededor de 300.00 hogares se benefician de la producción de seda cruda. Alrededor del 75% de toda la seda fue producida en China en el 2019, seguido de la india con un 22% de cuota de mercado. Esto significa que los dos países produjeron el 97% de las 0,16 MT que se produjeron en el mundo [25].

La seda es una fibra monofilamento continua de un alto brillo, resistencia y flexibilidad con buena absorción de agua, suave y que habitualmente se utiliza en la confección de prendas de elevado valor. La seda se utiliza en la industria textil para la confección de ropa interior, camisetas, trajes y vestidos.

Fibras de origen vegetal

Las fibras de origen vegetal se extraen básicamente de las plantas como el algodón, lino, esparto, cáñamo y sisal entre otros (Figura 2), donde la celulosa es el principal contenido químico de la fibra. La celulosa es un polisacárido formado por unidades repetidas de glucosa conectadas entre sí mediante enlaces éter y el número de unidades repetidas en estas fibras (conocido como grado de polimerización) puede variar desde menos de 1000 hasta 18000, dependiendo de la fibra.

Figura 2. *Posibles fuentes de fibra de origen vegetal para la producción de textiles.*

Dentro de las fibras celulósicas, el algodón es la principal fibra natural y la que más importancia tiene dentro del mundo textil. Es la fibra natural más producida anualmente con más de 25 millones de toneladas métricas. Las fibras artificiales han ido disminuyendo su consumo mientras la demanda de algodón está prevista que supere la producción de dicha fibra para la temporada 2021. Como consecuencia se verán reducidas las existencias mundiales en 3,2 millones de fardos de algodón según el departamento de agricultura de los Estados Unidos [27].

Las fibras de algodón proceden del cultivo de la planta en campos de conreo y dependiendo de la variedad sembrada, se obtienen los diferentes tipos de algodón:

- Algodón Egipcio o algodón de fibra larga (*Gossypium barbadense*). Las fibras obtenidas presentan una longitud de 34 a 42 mm y un diámetro de aproximadamente 15 micrómetros.
- Algodón Americano o algodón de fibra media (*Gossypium hirsutum*). Tienen una longitud de fibra de 24 a 34 mm y un diámetro de entre 20 y 25 micrómetros.

- Algodón Indio o algodón de fibra corta (*Gossypium herbaceum*). Sus fibras presentan la menor longitud, inferior a 23 mm y el mayor diámetro, aproximadamente 25 micrómetros.

La fibra de algodón desmontada y limpia contiene aproximadamente un 90% o más de celulosa (Tabla 2). Los otros constituyentes restantes se denominan no celulósicos e incluyen a las proteínas, aminoácidos, etc. Las variaciones que se muestran en la Tabla 2 de estos componentes surgen debido a las diferencias en la madurez de la fibra, la variedad de algodón y las condiciones ambientales (suelo, clima, prácticas agrícolas, etc.) [28].

Componente	Media (%)	Rango (%)
Celulosa	95	88 - 96
Proteína	1,3	1,1 – 1,9
Cera	0,6	0,4 - 1
Ceniza	1,2	0,7 – 1,2
Otros	1,9	–

Tabla 2. *Composición química del algodón.*[28]

Las propiedades de la fibra de algodón son su elevada resistencia que se atribuye a su estructura fibrilar y cristalina [28]. Es un buen conductor del calor, lo que hace que la ropa de algodón sea más fresca. Sin embargo el algodón se seca lentamente cuando absorbe agua, se ensucia fácilmente debido a la superficie rugosa de los hilos de algodón y se encoge al lavar, especialmente cuando se utilizan soluciones de lavado fuertemente alcalinas. Además, se vuelve amarillo y se debilita cuando se expone a la luz solar de forma prolongada, es susceptible a daños por moho (no debe almacenarse húmedo), es muy inflamable y tiene una resistencia bastante pobre al desgaste [24].

Los usos del algodón en la industria textil son muy amplios y se usa principalmente para la confección de ropa como las camisetas, polos, tejanos, vestidos, etc. Esta fibra también se mezcla con toda una variedad de otras fibras para crear telas con diferentes tactos, apariencias y cualidades, todas ellas con un diferente uso. Si se mezcla con poliéster o nylon, las telas pueden adquirir una elasticidad muy útil para la ropa deportiva. Por otro lado, si se mezcla con lana o seda adquiere muy buena calidad, típico de los productos de alta gama como jerséis, camisetas, vestidos y prendas para ocasiones especiales [26].

Fibras de origen mineral

Entre las fibras minerales que provienen de las rocas se encuentra el amianto, cuyo nombre proviene de la palabra griega “asbestos” que significa no arderá, indestructible o inextinguible en referencia a su resistencia al fuego y al calor. Las principales propiedades físicas del amianto son su excelente estabilidad térmica (funde a 1450°C – 1500°C), una elevada resistencia a tracción, químicamente inerte y baja conductividad térmica y eléctrica. Debido a estas propiedades, en la industria textil se utilizaba en la fabricación de prendas ignifugas. Sin embargo, actualmente se ha restringido su uso en la confección de textiles al ser clasificado como material muy cancerígeno y tóxico para el ser humano [29,30].

1.1.2. Fibras manufacturadas

Las fibras manufacturadas o hechas por el hombre son fibras textiles obtenidas mediante la transformación química de las fibras naturales (artificiales) o mediante síntesis química (sintéticas).

Fibras Artificiales

La producción de fibras artificiales consiste en la modificación superficial de las fibras naturales. Mediante la aplicación de los disolventes adecuados y reactivos sobre las fibras de celulosa naturales se obtiene una solución densa y viscosa que al ser filtrada a través de una plancha con varios agujeros da lugar a pequeños filamentos. Estos, una vez secados, constituyen fibras fáciles de adaptar al hilo y a la tela. Este tipo de fibras semisintéticas habitualmente se denominan rayón [11].

La fibra de celulosa es la más producida dentro de las fibras artificiales con una producción anual de 7,1 millones de toneladas métricas y que utiliza principalmente madera o fibras vegetales como materia prima. Dentro de ellas, el rayón más utilizado es el rayón viscoso con un volumen de producción de alrededor de 5,63 MT en 2019 [25].

El rayón viscoso se produce haciendo reaccionar la celulosa con disulfuro de carbono e hidróxido de sodio (Figura 3).

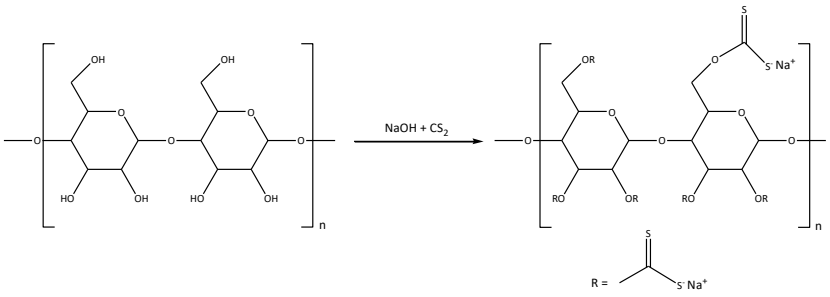

Figura 3. *Reacción de la celulosa con NaOH y CS_2 para la obtención de rayón viscoso*

Este rayón se caracteriza por tener una gran resistencia, no se arruga con facilidad, es compatible con una gran variedad de tintes y es agradable al tacto. Generalmente el rayón se utiliza principalmente para la fabricación de sabanas y camisas, aunque se mezcla con fibras naturales o sintéticas como consecuencia de su pérdida de propiedades cuando se moja [31].

Fibras sintéticas

Las fibras textiles sintéticas son fabricadas por síntesis química, mediante un proceso de polimerización. Uno vez obtenido el polímero, éste se pone dentro de una extrusora juntamente con el colorante deseado para obtener el hilo correspondiente. La incorporación de un tinte en el polímero antes de su hilatura permite obtener un nivel óptimo de estabilidad cromática en la fibra, que elimina la necesidad de realizar operaciones de fijación del color [24].

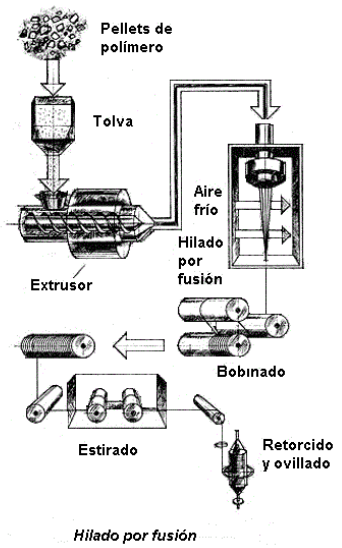

Figura 4. *Hilado por fusión de las fibras sintéticas*[32].

Las fibras de poliéster son las fibras sintéticas más utilizadas en la confección de prendas de ropa. De hecho, el poliéster es la fibra más utilizada en todo el mundo con una producción anual de alrededor de 57,7 millones de toneladas. En el año 2019, la producción de fibras de poliéster supuso aproximadamente el 52% de la producción mundial de fibra en 2019 [25]. Las principales ventajas de este tipo de fibras son su elevada resistencia a cualquier agente externo, la elevada resistencia a tracción y su facilidad ante el lavado. Además, no se arruga presenta una gran resistencia a la proliferación de bacterias y hongos. Habitualmente son fibras utilizadas en la industria textil para la producción de piezas de ropa interior, textiles para el hogar, tapicerías o ropa de deporte. Sin embargo, su principal inconveniente es su carácter higroscópico, que evita la absorción del sudor, no conducen bien el calor y suelen causar irritación en pieles sensibles. Este tipo de fibras suelen mezclarse con fibras naturales para la confección de tejidos [32].

1.1.3. Elaboración de tejidos de algodón

Para poder dotar a la industria textil de soluciones tecnológica y económicamente viables para la gestión de los residuos se debe analizar la generación de estos durante la elaboración de los tejidos.

La obtención de la fibra de algodón se obtiene principalmente mediante el cultivo del algodón en zonas cálidas. Esta condición es muy importante porque su semilla necesita una temperatura mínima de suelo de 15°C para su germinación y una temperatura optima de crecimiento entre 21 y 28°C durante el desarrollo de la campaña. Las necesidades de agua del cultivo del algodón varían entre 7000-13000 m^3/Ha, dependiendo del clima y la duración de la estación de crecimiento. Al inicio del periodo vegetativo son reducidas del orden del 10% del total, pero en el periodo de floración son máximas y representan entre el 50 y 60%. Pasados 150 días de su siembra, el algodón seco se recolecta, se separan las fibras de la semilla y se envían sus fibras a la industria textil [33].

Las fibras procedentes de la recolección del algodón son inicialmente lavadas y desfibradas con el objetivo de que estas sean individualizadas. Una vez individualizadas se producen las bobinas de hilo que posteriormente se utilizaran para la fabricación de los tejidos. La producción de los

tejidos incluye la fabricación de la tela, la tinción y los distintos procesos de finalización como impermeabilización, satinado, etc. Finalmente, las telas obtenidas son utilizadas para la confección de las piezas de ropa [34,35].

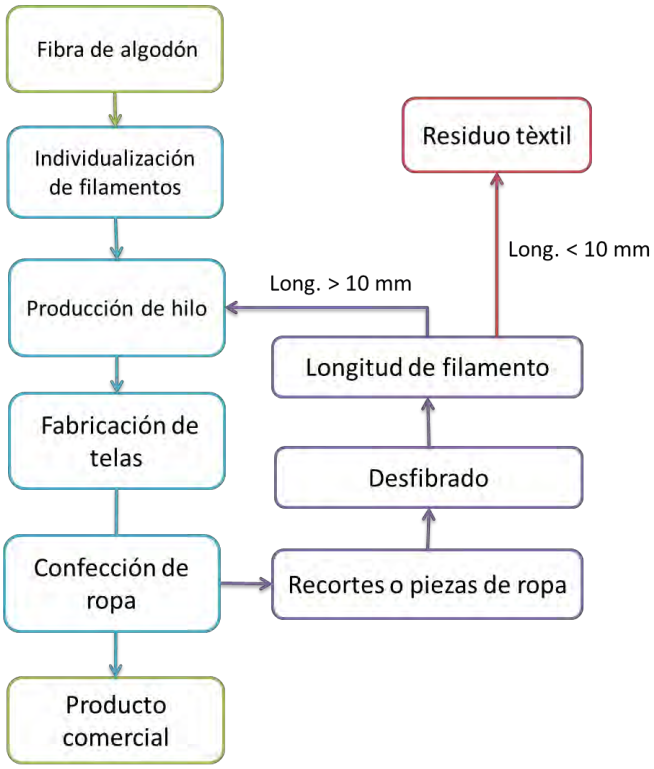

Figura 5. *Esquema del proceso de fabricación de tejidos textiles y su reciclado.*

Durante el proceso de fabricación se generan una gran cantidad de subproductos en forma de hilos, recortes, etc. Estos subproductos son desfibrados y separados en función de la longitud de las fibras. La longitud de las fibras resulta un parámetro determinante para su reutilización, debido a que esta tiene un importante impacto sobre las propiedades mecánicas del hilo que se obtiene. En el esquema de la Figura 5 se muestra como las fibras con una longitud inferior a 10 mm no pueden ser reutilizadas para la producción de hilo y deben ser descartadas como residuo. Actualmente, este residuo constituye entre un 10 y un 20% de la materia primera utilizada que finalmente es vertida o incinerada [36,37].

Sin embargo, tal y como se ha mencionado anteriormente, ambos casos conllevan una considerable contaminación y no ofrecen la posibilidad de incrementar el valor de estos residuos debido a que han sufrido un proceso de tinción [38]. En este sentido, los investigadores están realizando esfuerzos para promocionar e impulsar el aprovechamiento de estos residuos [39,40]. También hay varios estudios donde las fibras de algodón procedentes de pantalones tejanos azules se aprovechan para la confección de materiales compuestos [41,42]. Por lo tanto, una de las posibles vías para dotar a estos residuos de valor añadido y a su vez reducir su impacto ambiental, podría hallarse en su uso en la fabricación de materiales compuestos de matriz termoplástica.

1.2. Materiales compuestos

Un material compuesto es la unión de dos materiales inmiscibles entre sí para la obtención de un nuevo material. Este nuevo material se caracteriza por tener dos fases diferenciadas, matriz y refuerzo por lo que presenta una combinación de las distintas propiedades de los materiales de partida [43,44]. Uno de los principales objetivos de la producción de un material compuesto es el aumento notable de sus propiedades mecánicas. El aumento de estas propiedades está directamente relacionado con la morfología, la orientación y dispersión del refuerzo en el interior de la matriz y la calidad de la interfase producida entre la matriz y el refuerzo [45].

La producción de materiales compuestos de matriz plástica se inició en los años 40 cuando se desarrollaron los primeros compuestos con fibra de vidrio. Estos materiales fueron creados como respuesta a la necesidad de crear vehículos militares más ligeros, pero con la misma resistencia que el acero o incluso superior. El principal inconveniente de dichos materiales fue la elevad fragilidad de las fibras de vidrio, dado que pequeñas imperfecciones superficiales podían reducir sus elevadas prestaciones. Este fenómeno dificultó su implementación en el sector de la aeronáutica en piezas como alas de avión o rotores [46]. Sin embargo, la utilización de fibras cortas permitió la obtención de materiales que experimentaban un importante incremento de las propiedades mecánicas [47]. La baja densidad de los materiales compuestos de matriz plástica permitió la sustitución de piezas tradicionalmente fabricadas con madera y metal.

Aunque el uso de la fibra de vidrio se extendió rápidamente, los programas militares principalmente aeroespaciales, promovieron la sustitución de las fibras de vidrio por fibras de carbono o de boro para la obtención de materiales compuestos durante la guerra fría. Finalmente, en 1964 S. Kwolek produjo las fibras de aramida. Estas fibras sintéticas producidas mediante poliamidas aromáticas presentan una importante resistencia al calor y una resistencia mecánica 5 veces superior al acero [46]. Aun así, durante la década de los 90, se produjo un cambio de paradigma en el sector de los materiales compuestos. El diseño de los materiales compuestos se centró en el estudio de la interacción matriz-refuerzo, con el objetivo de obtener materiales con una mejor estabilidad mediante asociaciones espontaneas entre fases. Este hecho, condujo hacia un mayor conocimiento de los sistemas de compatibilización entre refuerzo y matriz [48].

Actualmente, la fibra más utilizada como refuerzo sigue siendo la fibra de vidrio (GF) y se calcula que de las 4 millones de toneladas de materiales compuestos que se producen al año, más del 90% son reforzadas con fibras de vidrio [49,50]. Este es el refuerzo más utilizado para la gran mayoría de matrices debido a su bajo coste, a su facilidad para obtener las longitudes y diámetros deseados en las GF, por su buena resistencia a la degradación térmica y a la corrosión y por ser capaz de incrementar las propiedades mecánicas de la matriz con un bajo porcentaje de refuerzo [51]. Por ejemplo, cuando una matriz de PP es reforzada con un 20% w/w de GF y con un 6% (w/w) de agente de acoplamiento, su resistencia a tracción (σ^{C}_{T}) aumenta de los 28 a los 68 MPa y su resistencia a flexión (σ^{C}_{F}) de los 40,2 a los 97,3 MPa [52,53].

No obstante, las fibras de vidrio presentan varios inconvenientes, el primero de ellos es la gran cantidad de energía necesaria para producirlas y aunque se incineran, no permiten la

recuperación de dicha energía [54]. El segundo es la manipulación de estas fibras que sin un equipo de protección son muy perjudiciales para la salud humana [55,56] debido a que son muy abrasivas. Además, su uso causa un gran deterioro en la maquinaria [57]. El tercer inconveniente es el impacto medioambiental de los compuestos reforzados con GF debido a su baja biodegradabilidad y a su baja tasa de reciclaje.

Por otra parte, la gran mayoría de matrices utilizadas en la producción de materiales compuestos son las poliolefinas, las cuales derivan del petróleo y son materiales termoplásticos [58–60]. En el año 2019 la demanda de polipropileno (PP), polietileno de baja densidad (LDPE) y polietileno de alta densidad (HDPE) fue del 49,2% en peso de la demanda total de plásticos en la Unión Europea (Figura 6) [61].

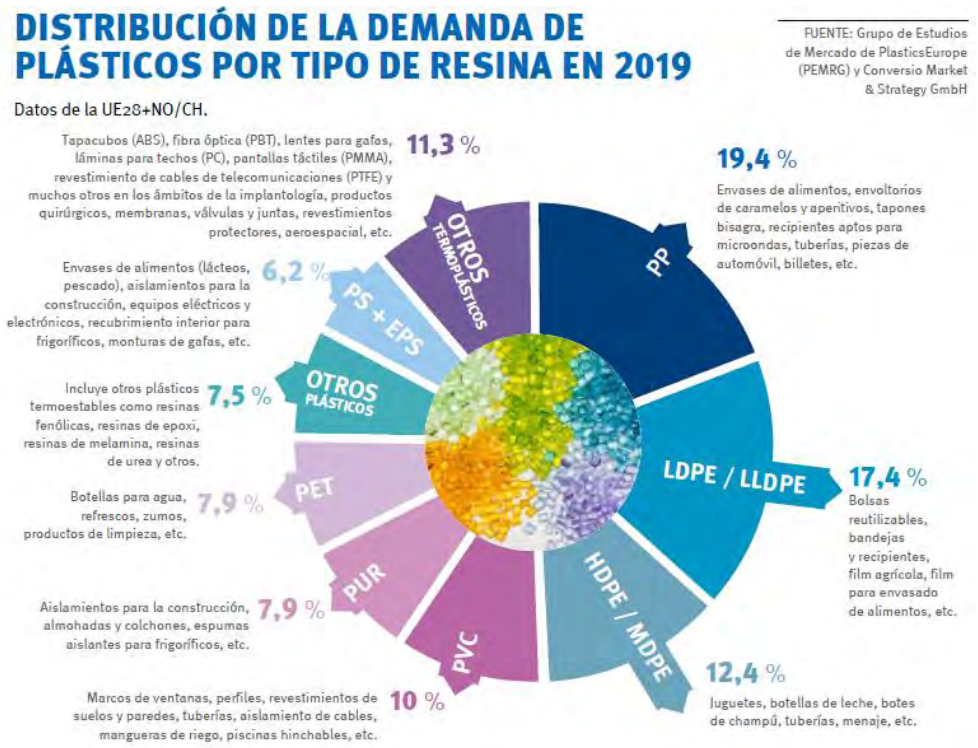

***Figura 6**. Distribución de la demanda de Plásticos por tipo de resina en 2019. Fuente: Grupo de Estudios de Mercado de Plastics Europe (PEMRG) y Convenio Market & Strategy GmbH.*

Esta demanda de poliolefinas es debida a que son los polímeros más utilizados en fabricación de compuestos para los sectores de la automoción, industria de la construcción y otros productos de consumo [62]. La más representativa es el PP debido a su gran versatilidad, a su fácil transformación y reciclaje, a su gran resistencia química frente a los elementos medioambientales y a su temperatura de procesamiento [63,64]. Esta temperatura de procesamiento (190°C) permite su refuerzo con fibras naturales, las cuales presentan una baja temperatura de degradación [65].

Polipropileno

El polipropileno (PP) es un polímero que se obtiene de la polimerización por adición del propileno (C_3H_6). En la polimerización del propileno se utiliza el catalizador estéreo-específico de Ziegler-Natta [66] que permite la obtención de un polímero de un peso molecular promedio de 50.000 y prácticamente isotáctico [67]. Si en el proceso de polimerización no se utilizara dicho catalizador se podrían obtener tres tipos de isómeros (Figura 9) debido al grupo metilo ($-CH_3$) presente cada dos átomos de carbono en su cadena principal.

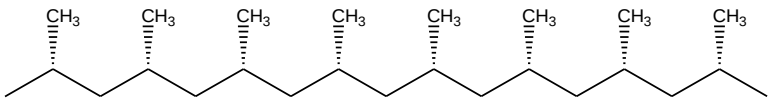

Figura 7. *Isómero isotáctico del propileno.*

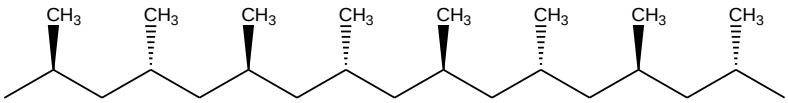

Figura 8. *Isómero sindiotáctico del propileno.*

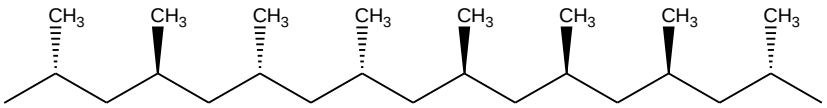

Figura 9. *Isómero atáctico de la polimerización del propileno.*

Las principales diferencias entre los tres isómeros son su punto de fusión y resistencia mecánica. El isómero atáctico presenta un punto de fusión bajo que a temperatura ambiente es un fluido amorfo y tiene una resistencia mecánica nula. Por otra parte, el isómero sindiotáctico presenta cierta cristalinidad, tiene un punto de fusión de 135°C y una resistencia media. El isómero isotáctico tiene mayor cristalinidad que los isómeros anteriores y es el que presenta una mayor resistencia a tracción. El polímero obtenido a partir del isómero isotáctico tiene una densidad de 0,9 g/cm^3, un punto de fusión de 170°C y es insoluble en los disolventes orgánicos habituales [68]. Sus propiedades mecánicas a baja temperatura son similares a las del polietileno de alta densidad (HDPE) y se puede utilizar hasta una temperatura alrededor de 140°C.

El polipropileno es el plástico más ligero y ofrece una buena relación de propiedades térmicas (superiores al polietileno) y químicas, teniendo en cuenta sus propiedades mecánicas moderadas. Se caracteriza por ser un material tenaz, con buena resistencia a flexión y a impacto para temperaturas superiores a 0°C y por mostrar una excelente resistencia química [68]. Su elevada capacidad aditiva le confiere una gran versatilidad que ha permitido el aumento de sus

aplicaciones. Su bajo coste y baja densidad han hecho del polipropileno un polímero muy demandado que ofrece flexibilidad y sencillez de reciclaje [69].

Materiales compuestos a partir de fibras naturales

Debido a la creciente conciencia medioambiental, los investigadores están investigando cómo sustituir los refuerzos minerales no renovables por los naturales [70]. Estos materiales compuestos formados como mínimo por una de las fases de origen renovable, ofrecen la posibilidad de producir productos con propiedades adecuadas para su aplicación con una importante mejora medioambiental [71–73].

Las fibras naturales representan una fuente renovable de materiales de refuerzo, cuyos compuestos podrían incinerarse y parte de la energía podría recuperarse. Además, las fibras naturales son menos abrasivas que las GF y en consecuencia, más respetuosas con la maquinaria. Destacar que además su manipulación no se considera perjudicial [63]. Sin embargo las propiedades químicas, mecánicas y morfológicas de las fibras naturales no son tan fáciles de establecer y es habitual encontrar datos muy dispersos para una misma familia de refuerzos. Las propiedades de las fibras naturales están muy ligadas a su origen y también al clima (pluviometría, temperatura…) por lo que las desviaciones estándar de sus propiedades mecánicas suelen ser enormes. Además su morfología, especialmente su longitud y diámetro, también varía de un lote a otro [74].

Durante los últimos años, los materiales compuestos reforzados con fibras naturales han sido habitualmente nombrados compuestos de madera plástica (WPC) y han recibido una atención notable por parte de la comunidad científica [75–78]. Los estudios científicos sobre los WPC aumentan año tras año y muestran propiedades mecánicas de los compuestos basados en fibras naturales competitivas lo que permite su uso en la industria [79]. Este tipo de materiales compuestos también pueden ser nombrados como biocompuestos y su uso se presenta como una oportunidad para aplicaciones en la industria del automóvil o en la construcción ligera [80]. Hoy en día las compañías automovilísticas están intentando reducir el uso de fibras artificiales mediante la adición de fibras naturales en los componentes plásticos que no forman parte de la estructura de los vehículos [81]. Este proceso ha sido iniciado como consecuencia de la mayor consciencia ecológica de la sociedad actual y a las acciones legislativas de los gobiernos que promueven el estudio y uso de materiales de base biológica. En este sentido, los compuestos reforzados con fibras naturales están emergiendo como nuevos materiales [82].

Sin embargo, las fibras naturales presentan algunas limitaciones para ser combinadas con una matriz polimérica. La temperatura de fusión de la matriz polimérica que se combina con la fibra debe ser inferior a 220°C debido a que esta es la temperatura de degradación de la celulosa [83]. Por otra parte, la interfase entre las fibras hidrofílicas y las matrices poliméricas de naturaleza hidrofóbica resulta incompatible. Para solucionar esta incompatibilidad y obtener una unión interfacial fuerte entre las fibras y la matriz se pueden seguir dos metodologías diferentes [84].

Un primer método consiste en la modificación superficial de las fibras lignocelulósicas mediante reacciones químicas [85–88]. Éste es uno de los más adoptados y estudiados debido a la alta densidad de grupos hidroxilos en la superficie de las fibras, sobre la cual se podría emprender una amplia variedad de reacciones. Mediante estas reacciones se puede llevar a cabo la

sustitución de los grupos hidroxilos por otro grupo funcional que mejore compatibilidad entre ambos componentes del material compuesto.

Otra metodología consiste en mejorar la interfase fibra-matriz mediante la utilización de agentes de acoplamiento. Mediante el uso de dichos agentes se mejora la adhesión interfacial entre las fibras y la matriz, mejorando de esta forma las propiedades físicas y mecánicas del material compuesto resultante [89–92].

Un ejemplo consistiría en el uso de MAPP como agente de acoplamiento, que evitaría el uso de reactivos costosos y tóxicos (Figura 10) [91].

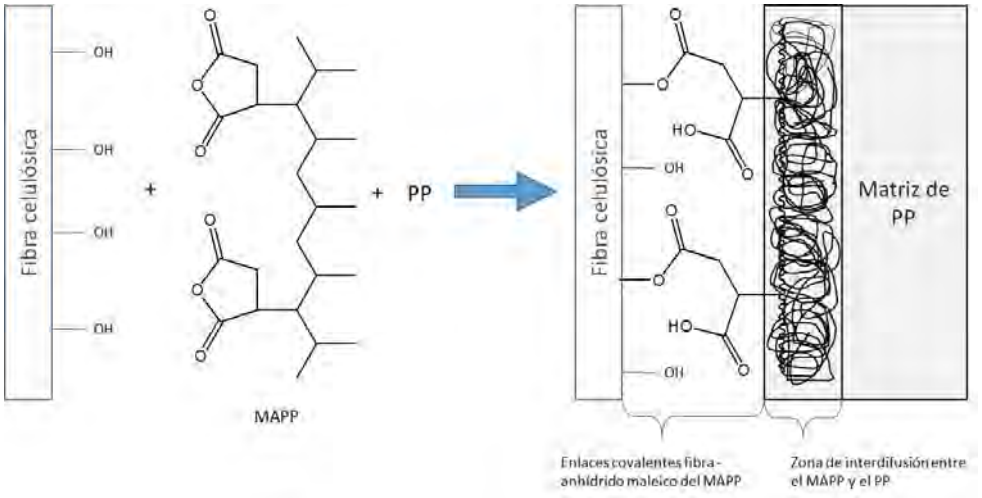

Figura 10. *Mejora de la interfase de los compuestos con fibras naturales con el uso de agentes de acoplamiento.*

Este agente está constituido por una matriz polimérica de PP modificada químicamente con grupos funcionales (anhídrido maleico) que pueden reaccionar con los grupos hidroxilos presentes en la superficie de la fibra a las temperaturas de procesado [93,94] y presentan una doble función: la interacción con la matriz polimérica y la capacidad de reacción con los grupos hidroxilos de las fibras a elevadas temperaturas (160-220°C) dando lugar a enlaces covalentes [95–97].

Utilización de la borra de algodón como refuerzo de PP.

Durante las dos últimas décadas, los investigadores han realizado esfuerzos para sustituir a los compuestos de PP reforzados con GF, cuyos compuestos se consideran productos básicos y se utilizan ampliamente en la industria de la automotriz, el diseño de productos básicos y como materiales de construcción [98]. Esta investigación se ha centrado principalmente a la substitución de las fibras de vidrio por las fibras naturales manteniendo la matriz termoplástica dónde las fibras naturales han mostrado su capacidad de refuerzo [63,99,100].

No obstante, la substitución de los compuestos de PP reforzados con GF solo se llevará a cabo si las especificaciones técnicas y propiedades de los compuestos son similares a los que están disponibles y en uso. Actualmente, parte de esta sustitución se está llevando a cabo en la industria automotriz mediante compuestos de PP reforzados con filamentos o hebras como el yute, el cáñamo, el ramio o el lino [101–103] Dado que el algodón es una hebra similar, esta hebra también podría ser utilizada para el refuerzo de PP.

Por lo tanto, una forma atractiva de valorizar el residuo de fibras de algodón podría ser su incorporación en matrices poliméricas para la obtención de materiales compuestos. Aunque se parta de un residuo lignocelulósico producido por la industria textil, no debe suponer un impedimento para su utilización como refuerzo. En la literatura hay varios estudios sobre el uso de residuos agrícolas [89,104–106] pero solo unos cuantos de ellos informan del uso de estos subproductos como refuerzo de la matriz de PP [107–109].

Este residuo de fibras de algodón presenta algunas ventajas como el bajo costo y disponibilidad. Pero también presenta algunos inconvenientes evidentes como la presencia de tintes textiles [109]. Sin embargo, estos tintes podrían tener un efecto similar al que muestra un tinte índigo en la tela de mezclilla, que provoca un aumento de la impermeabilidad de dicha tela y mayor compatibilidad con una matriz hidrofóbica [110].

En este contexto, la presente investigación tiene como objetivo la obtención de materiales compuestos de PP reforzados con este subproducto textil de algodón, con el propósito de valorizar el residuo, contribuir a una economía circular, reducir la presión sobre los recursos naturales y desarrollar compuestos competitivos.

Objetivo y justificación de la tesis

2. Objetivo y justificación de la tesis

2.1. Justificación

La presente tesis doctoral surge de la necesidad de la industria textil de encontrar una utilidad al residuo de filamentos de algodón, el cual es un subproducto del proceso de desfibrilación que hoy en día no presenta ningún valor ni uso en la industria textil. Este residuo está compuesto de fibras teñidas debido a los procesos de tinción a los que han sido sometidas. Estas fibras también se caracterizan por tener longitudes inferiores a los 10 mm, cuya característica hace que no sean aptas para la producción de hilo y deben ser descartadas como residuo. Mayoritariamente, este residuo en forma de borra de algodón es incinerado o desechado en vertederos.

Con la finalidad de evitar su vertido, la tesis presentada propone como solución la utilización de la borra de algodón para la fabricación de materiales compuestos de polipropileno, reduciendo el impacto ambiental de este residuo y añadiéndole una utilidad. La solución aportada se fundamenta en la multitud de estudios sobre la obtención de materiales compuestos de polipropileno reforzado con fibras naturales de origen vegetal, dónde estos materiales han mostrado buenas propiedades mecánicas. Debido a las elevadas propiedades intrínsecas de las fibras del algodón, superiores a las de otras fibras naturales, se consideró la posibilidad de obtener materiales compuestos con propiedades mecánicas próximas a las de los materiales compuestos reforzados con fibra de vidrio.

Actualmente, en la literatura existen pocas publicaciones sobre el aprovechamiento de residuos industriales, sobre todo en la utilización de las fibras de algodón como refuerzo de matrices poliméricas. Este hecho se debe principalmente a dos motivos: el primero es debido a un mayor interés de los investigadores hacia el aprovechamiento de residuos agrícolas que hacia los desechos de fibras textiles; y el segundo es debido a las dificultades para la obtención de un material compuesto con un alto contenido de refuerzo, y en la formación de agregados de las fibras de algodón sin tratamiento previo. Este último se ha resuelto mediante la amplia experiencia del grupo de investigación LEPAMAP-PRODIS, que permitió resolver los problemas de formación de agregados y del bajo contenido en refuerzo en la obtención de los materiales compuestos.

La presente tesis está basada en cinco artículos que en su conjunto analizan las propiedades mecánicas y micromecánicas de los compuestos reforzados con borra de algodón. En el primer artículo “Behaviour of the interphase of dyed cotton residue flocks reinforced” se determinó la cantidad de agente de acoplamiento necesaria para conseguir la máxima resistencia a tracción. Esto se determinó midiendo la resistencia máxima de los compuestos sin agente de acoplamiento y con porcentajes crecientes de MAPP. Aunque los compuestos con un 6% (w/w, respecto del contenido de fibra) mostraban un mayor incremento de la resistencia a tracción de la matriz (σ^m_t), los compuestos sin agente de acoplamiento también mostraron un incremento notable de la σ^m_t. Seguidamente, se estudió el impacto de la presencia de colorantes orgánicos en la superficie de las fibras de algodón, cuyos tintes parecen afectar la calidad de la interfase de dos maneras distintas: por un lado aumentan la afinidad entre las fibras de algodón y la matriz, mejorando la interfase entre ellos. Por otro lado, cuando se incorporó un agente de acoplamiento a la formulación de los compuestos, los colorantes obstaculizaron las interacciones químicas entre el ácido maleico y los grupos OH de las fibras celulósicas. Para

investigar más a fondo el comportamiento de la interfase, se utilizaron los modelos micromecánicos que permitieron evaluar las propiedades intrínsecas de los compuestos.

En el segundo artículo "Recycling dyed cotton textile byproduct fibers as polypropylene reinforcement" se estudió la evolución de la resistencia en función del contenido de refuerzo de los materiales formulados con un 0 y 6% (w/w) de MAPP. Los ensayos mostraron que los materiales reforzados con un 50% (w/w) de fibra de algodón (CF) y formulados con MAPP presentan una resistencia a tracción similar a los compuestos comerciales fabricados con un 10% de fibra de vidrio (GF) y MAPP. Tras el resultado positivo obtenido, debido a un aumento lineal de la resistencia a tracción de los materiales formulados con un 0 y 6% (w/w) de MAPP, se realizó el estudio micromecánico mediante el modelo de Kelly-Tyson, basado en la regla de las mezclas modificada (RoM) y se resolvió mediante el método propuesto por Bowyer y Bader. Este método permitió el cálculo de la tensión interfacial de cizalla, indicativo de la calidad de la calidad de las interacciones matriz y el refuerzo, y de la resistencia intrínseca a tracción de las fibras. Este trabajo también demostró que se puede utilizar borra de algodón como refuerzo sin más tratamiento, aumentando la cadena de valor de la industria textil y disminuyendo los tratamientos químicos necesarios para reciclar o eliminar las fibras textiles teñidas.

Una vez establecida la resistencia a tracción de los compuestos, el tercer paso fue estudiar su Módulo de Young o rigidez (E_t^C). En el tercer artículo titulado "Modeling the stiffnesss of coupled and uncoupled recycled cotton fibers reinforced polypropylene composites", se reportó que los compuestos de fibra de algodón presentan un efecto casi nulo sobre el E_t^C con la adicción de un agente de acoplamiento y muestran una evolución lineal de los módulos de Young de los compuestos frente al contenido de refuerzo. Sin embargo, la pendiente de la línea de regresión fue menor que la de otros compuestos de polipropileno reforzado con hebras naturales. Seguidamente, se estudió el efecto de las fibras en el módulo del compuesto a través del FTMF (Fiber Tensile Modulus Factor) y se compararon los resultados con los compuestos de polipropileno reforzados con GF y fibras naturales. Además, se calculó el módulo intrínseco de las fibras de algodón, el cual duplicó los valores publicados anteriormente, mediante los modelos de Hirsh y Tsai Pagano. El uso de estos dos modelos de micromecánicos diferentes permitió evaluar el impacto de la morfología de las fibras en el módulo de Young.

El análisis de la resistencia a flexión y su comparativa con otros compuestos de PP se presentó en el artículo titulado "Study of the flexural strength of recycled dyed cotton fiber reinforced polypropylene composites and the effect of the use of maleic anhydride as coupling agent". Primeramente, se estudió el efecto del contenido de MAPP sobre los compuestos reforzados con CF, donde se determinó que el porcentaje óptimo de MAPP era de un 6% (w/w). Posteriormente se analizó el efecto del contenido de refuerzo de los compuestos formulados con un 0 y 6% (w/w) de agente de acoplamiento. Se observó que los compuestos mostraban una evolución no lineal de la resistencia a flexión respecto al contenido de refuerzo y una desviación respecto al valor teórico. Con la finalidad de analizar las posibles causas de esta desviación, se empleó la regla de las mezclas modificada (RoM) para analizar la resistencia intrínseca a flexión de las fibras y los factores de acoplamiento. Mediante los resultados obtenidos, se determinó que la desviación era producida por los tintes, los cuales inhibían la creación de una interfase completamente fuerte y dicho efecto aumentaba con la cantidad de refuerzo.

En el quinto artículo "Exploring the potential of cotton industry byproducts in the plastic composite sector: Macro and Micromechanics study of the flexural modulus" se reportaron los resultados del módulo a flexión de los compuestos de CF (E_F^C). Estos presentaron un aumento linealmente con el contenido de fibra y un efecto mínimo sobre los módulos de flexión con la adicción de MAPP, un comportamiento similar al E_t^C. Seguidamente, se estudió el efecto de las fibras en el módulo del compuesto a través del FFMF (Fiber Flexural Modulus Factor) y se realizó la medición del módulo de flexión de las fibras (E_f^F) mediante el modelo de Hirsch, el modelo de Tsai-Pagano y un modelo que utiliza como base la relación FFMF / FTMF. Este último se ha propuesto en estudios recientes como un método simple para calcular el módulo de flexión intrínseco de las fibras naturales debido a las similitudes de comportamiento entre E_t^C y E_F^C.

A parte de las propiedades mecánicas y micromecánicas descritas en estas cinco publicaciones, la presente tesis doctoral también aporta los resultados obtenidos de la resistencia a impacto y absorción de agua de los materiales reforzados con CF.

2.2. Objetivos generales

El objetivo principal de la presente tesis doctoral es la obtención de materiales compuestos, con propiedades competitivas, a partir de polipropileno y borra de algodón teñida como refuerzo. Adicionalmente, se valorará la posibilidad de utilizar estos materiales como sustitutos de los principales *commodities* actuales basados en polipropileno y fibra de vidrio.

2.3. Objetivos específicos

En base a los objetivos generales y la problemática planteada, los objetivos específicos de esta tesis doctoral son los que se numeran a continuación:

1. Obtener compuestos de PP con contenidos de residuo celulósico entre el 20 y el 50 % en peso.
2. Estudiar el efecto del agente de acoplamiento sobre las propiedades mecánicas de los materiales compuestos, teniendo en cuenta distintos porcentajes de este agente.
3. Determinar las propiedades mecánicas a nivel macroscópico a través de los ensayos a tracción, flexión e impacto.
4. Estudiar el posible cambio morfológico de las fibras de algodón durante la fabricación del material compuesto mediante la extracción de las fibras de los diferentes materiales compuestos y su posterior ensayo a tracción.
5. Evaluar la calidad de la interfase y las resistencias intrínsecas de las fibras mediante la modelización de los materiales compuestos.
6. Modelizar el comportamiento del E_t^C y el módulo elástico a flexión (E_f^C), para determinar los factores de eficacia (η_e), orientación (η_o) y longitud (η_l).
7. Evaluar mediante las propiedades mecánicas de los compuestos obtenidos en esta tesis, si son un posible substituto de los compuestos reforzados con fibra de vidrío.
8. Estudiar el comportamiento de los diferentes materiales en ambientes húmedos para evaluar su utilización en condiciones similares.

Metodología y modelizaciones

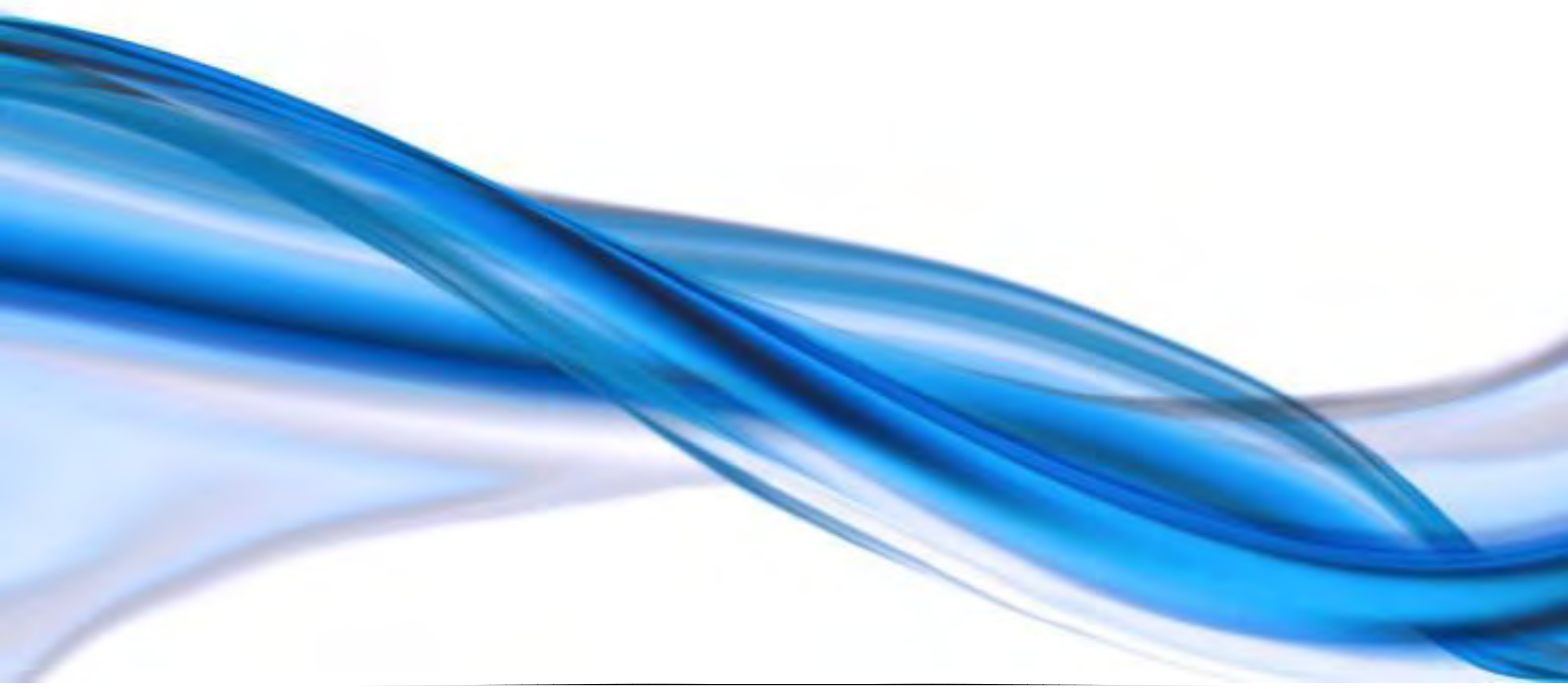

3. Materiales, metodología y modelizaciones.

3.1. Materiales

Los residuos de filamento de algodón provenientes de la industria textil (borra de algodón), utilizados como refuerzo para la obtención de materiales compuestos, fueron suministrados por Fontfilva S.L. (Olot, Girona, España). Estas fibras (Figura 11) son un residuo producido en la confección de tejidos, las cuales se caracterizan por ser tratadas con un tinte reactivo y por no ser aptas para su uso en la producción de hilos, debido a sus longitudes inferiores a 10 mm. Una vez recibidas, las fibras se cortaron mediante un molino de cuchillas equipado con un tamiz de 1 mm para su posterior incorporación en el material polimérico.

Figura 11. *Residuo de fibras de algodón con tinte, provenientes de la industria textil.*

La matriz polimérica utilizada en la presente tesis fue el polipropileno (PP) Isplen PP090 62 M, el cual fue suministrado por Repsol-YPF (Tarragona, España). Con el fin de mejorar la compatibilidad entre los residuos de algodón y la matriz de PP, se utilizó como agente de acoplamiento el polipropileno funcionalizado con anhídrido maleico (MAPP) Epolene G3015. Este agente se caracteriza por tener un número ácido de 15 mg de KOH/g, un peso molecular de 24800 y fue proveído por Eastman Chemical Products (San Roque, España).

El hidro sulfito de sodio ($Na_2S_2O_4$) se utilizó para eliminar los tintes de los residuos de algodón y fue proporcionado por Sigma Aldrick (Barcelona, España). La decalina (decahidronaftaleno) de Fischer Scientific (Madrid, España), con un punto de ebullición de 190°C y un 97% de pureza se usó como disolvente de la matriz polimérica. Este reactivo se utilizó para disolver la matriz PP en la extracción de las fibras de los compuestos. Todos los reactivos utilizados para la caracterización de las fibras de algodón fueron adquiridos a Scharlau España (Barcelona, España) y utilizados sin más purificación.

3.2. Metodología.

3.2.1. Caracterización de las fibras

Composición química de las fibras

La determinación de la composición química de la fibra de algodón se realizó a partir de la fibra virgen debido a las interferencias causadas por el tinte en los análisis de composición química, afectando significativamente a los resultados. Para dichos análisis, se trituró una pequeña cantidad de fibra virgen de algodón y se determinó su sequedad con el analizador de humedad (Sartorius, Goettingen).

A continuación, se determinó el contenido en compuestos extraíbles mediante una extracción Soxhlet, de acuerdo con la norma estándar TAPPI 207 cm-97 [111]. Para llevar a cabo la determinación de los compuestos extraíbles, primeramente, se trituró la fibra de algodón virgen y luego se tamizó mediante un tamiz de 0,40 mm hasta obtener 5 gramos de fibra tamizada. Esta cantidad se puso dentro del cartucho de celulosa para extracción Soxhlet, se tapó la fibra tamizada con algodón y se realizó la extracción Soxhlet durante 6 horas mediante una mezcla etanol-benceno en proporciones volumétricas 1:2. Transcurrido el tiempo de 6 horas, se sacó la fibra tamizada de dentro del filtro, que posteriormente se secó a 100°C durante 24 horas y se guardó para la determinación de lignina.

El contenido mineral de las fibras de algodón fue realizado a través de un análisis gravimétrico siguiendo la norma estándar T 413 om-93 [112]. Este análisis se llevó a cabo por duplicado y antes de realizar el análisis se prepararon dos crisoles los cuales habían sido calentados a 900°C durante 12 horas y luego enfriados gradualmente hasta temperatura ambiente. Después se pesó aproximadamente un gramo de fibras de algodón virgen en cada crisol y las muestras fueron sometidas a un proceso de incineración donde se calentó gradualmente hasta alcanzar una temperatura de 900°C.

La determinación del contenido en lignina Klason fue realizada a partir de las fibras libres de extraíbles, mediante el procedimiento T 222 om-98 [113]. Mediante este proceso se procede a la disolución de la fracción celulósica de la muestra con ácido sulfúrico mientras que la lignina permanece insoluble. Una vez determinado el contenido de lignina, se obtiene el contenido de holocelulosas, mediante el cálculo de la diferencia entre el contenido de materia sin extractivos y el contenido de lignina.

La determinación de la cantidad de α-celulosas se ha realizado según la norma T 203 om-93 [114], mediante la extracción de la lignina, hemicelulosas y β-celulosas con hidróxido sódico.

Grado de polimerización

El grado de polimerización de las fibras de algodón se determinó según la norma ISO 5351:2010 [115], utilizando etilendiamina de cobre (II) como disolvente. A partir de la viscosidad intrínseca se calculó el peso molecular promedio del polímero de celulosa usando la ecuación (1):

$$\mu = K.M^{a} \quad (1)$$

donde μ es la viscosidad intrínseca, K es una constante con valor igual a 2,28, a es igual a 0,72 y M es el peso molecular promedio en número [116]. Finalmente, se calculó el grado de polimerización siendo este el resultado de la división entre el peso molecular promedio del polímero y el peso molecular del monómero.

Determinación de la longitud y diámetro de las fibras

Las longitudes y diámetros de las fibras de algodón provenientes de la industria textil se caracterizaron por medio de un analizador Kajaanni (FS-300). A lo largo del periodo de tiempo comprendido entre dos y cinco minutos se analizó una suspensión acuosa de fibras diluida al 1% de consistencia y se evaluó su longitud teniendo en cuenta una cantidad de fibras individuales en el rango de 2500 y 3000 unidades. El analizador Kajaanni permite procesar las imágenes y las medidas de longitud de fibras, según la norma ISO 16065:2014 [117]. Los principales parámetros y medidas proporcionados por el analizador son: la longitud promedio de las fibras; la distribución de longitudes; el diámetro promedio de fibra; la masa lineal (*coarseness*) y el contenido en finos.

Por otra parte, las fibras también se analizaron mediante microscopía óptica con un microscopio Leica DMR-XA con una resolución óptica de 2 μm.

Extracción de las fibras de los compuestos

El análisis de las fibras de algodón una vez procesado el material compuesto se realizó sobre las fibras extraídas. Dicha extracción se realizó mediante un aparato Soxhlet empleando decalina como disolvente, durante un tiempo de extracción de 24 horas. Inicialmente, tres gramos de material compuesto fueron triturados y se colocaron en el interior de un filtro de cartucho de celulosa. Una vez realizada la extracción, las fibras de algodón recuperadas se lavaron en primera instancia con acetona y posteriormente con agua destilada con el objetivo de eliminar los residuos de disolventes presentes en las muestras. Finalmente, las fibras se secaron en una estufa a 105°C durante 24 horas.

Blanqueo de la borra de algodón

La eliminación del tinte presente en los residuos de algodón se realizó mediante un blanqueo con hidro sulfito sódico al 25 % en peso, durante 2h a temperatura ambiente. Transcurrido el tiempo de blanqueo las fibras obtenidas fueron lavadas repetidamente con agua y finalmente se secaron a 50°C.

Demanda catiónica

La demanda catiónica de las fibras de algodón vírgenes y de la borra de algodón se determinó mediante un detector de carga de partículas Mütek PCD 04. Inicialmente, se pesaron 0,2 gramos de fibra seca y se diluyeron en 15 ml de agua destilada, a los que se añadieron 50 ml de cloruro de polidialildimetilamonio (polyDADMAC). Seguidamente se mantuvo la suspensión en agitación magnética durante 5 minutos, y transcurrido este tiempo, la muestra se centrifugó en una centrifugadora Sigma Laborzentrifugen modelo 6 K 15 durante 20 min a 10000 rpm. A continuación, la carga de 10 ml del sobrenadante se neutralizó en el equipo Mütek, mediante la adición de polietilen sulfonato de sodio (PES-Na). A partir del volumen adicionado del polímero aniónico PES-Na, de concentración conocida, se calculó el valor de la demanda catiónica de las fibras de algodón según la ecuación (2).

$$D.C. = \frac{\left(C_{Poly-DADMAC} \cdot 0{,}05\right) - \left(C_{PES-NA} \cdot V_{PES-NA\ gastado} * 7\right)}{P_{seco\ total}} \quad (2)$$

donde D.C. es la demanda catiónica en (eq/l), $C_{Poly\text{-}DADMAC}$ es la concentración del polímero catiónico (eq/l), $V_{PES\text{-}NA\ gastado}$ es el volumen necesario para neutralizar los 10 ml de sobrenadante (l), $C_{PES\text{-}NA}$ es la concentración de polímero aniónico en (eq/l) y $P_{seco\ total}$ es el peso de la muestra seca (g).

Análisis de las propiedades a tracción de las fibras

La fuerza de rotura y el alargamiento de rotura de las diferentes fibras de algodón provenientes de la industria textil se obtuvieron a través de su respectiva curva tensión-deformación, siguiendo el estándar ASTM D3822-01. La medición se realizó mediante una máquina universal de ensayos mecánicos INSTRON 5500R (suministrado por INSTRON, Cerdanyola del Vallès, España) equipada con una célula de carga de 5 kg. La experiencia se repitió a cuatro longitudes de calibre distintas; 25,4, 19,05, 12,7 y 6,35 mm, utilizando velocidades cruzadas de 2,54, 1,905, 1,27 y 0,635 mm/min, respectivamente. Se muestrearon una cantidad de hasta 100 fibras individuales para cada longitud del medidor y se evaluaron sus fuerzas máximas. Se obtuvieron imágenes de microscopía donde se determinó el diámetro y la anchura de las fibras obteniéndose un valor promedio de 3 medidas.

3.2.2. Obtención de los materiales compuestos

El residuo de filamentos de algodón suministrado por Fontfilva S.L. se molió usando un molino equipado con un tamiz de 1 mm, para lograr una mejor dispersión de las fibras dentro de la matriz polimérica. Estas fibras tamizadas, junto con la matriz polimérica y el agente de acoplamiento se mezclaron en diferentes proporciones (peso/peso) mediante al mezclador interno Brabender Plastograph de Brabender® (Duisburg, Alemania). Los materiales se mezclaron a 185 °C y 80 rpm durante 10 minutos para garantizar una buena dispersión de los componentes. Las mezclas realizadas se dejaron enfriar antes de ser molidas mediante un molino de cuchillas (Reisch, Hann) para la adquisición de granzas de granulometría adecuadas a

la alimentación de la inyectora. Finalmente, las distintas granzas obtenidas se secaron y almacenaron a 80°C durante 24 horas como mínimo antes de su inyección.

El proceso de inyección de las distintas granzas fue realizado en una máquina de inyección Meteor-40 (Mateu & Solé, España). Las probetas requeridas para los ensayos de tracción, flexión e impacto fueron obtenidas mediante la inyección de las granzas en los correspondientes moldes con las dimensiones requeridas en los estándares ASTM D638 y ASTM D790. A continuación, se resumen las condiciones de procesado durante la inyección de los materiales compuestos:

- Temperatura 1ª zona husillo: 175°C
- Temperatura 2ª zona husillo: 175°C
- Temperatura 3ª zona husillo: 190°C
- Calefacción en la boquilla: 30%
- Velocidad de inyección: 30%
- Velocidad del husillo: 220 rpm
- Carga: 55 mm
- Descompresión del material: 76 mm
- Primera presión: 120 kg/cm^2
- Segunda presión: 37,5 kg/cm^2
- Graduación segunda presión: 80 mm
- Tiempo de inyección: 10 s
- Tiempo de carga: 9,9 s
- Tiempo de refrigeración: 10 s

El régimen de inyección utilizado fue semiautomático, lo que implica que cada vez que se completaba un ciclo, era necesario volver a iniciar manualmente el proceso para iniciar un nuevo ciclo.

Antes de iniciar el primer ciclo, se esperó a que la inyectora alcanzara las diferentes temperaturas en el husillo. Cuando alcanzó dichas temperaturas, el material de la tolva empezó a alimentar el husillo. Mientras el material es transportado hacia la punta del husillo, el material se plastifica y homogeniza debido a los esfuerzos de cizalla y a la calefacción de las resistencias del cilindro calefactor. Se dejó salir material compuesto fundido durante 20 segundos para evitar contaminaciones de inyecciones anteriores en las primeras probetas.

Durante el ciclo, primero se cerró el molde lentamente y a baja presión hasta su cierre completo. Seguidamente se elevó la presión de cierre del molde para mantenerlo cerrado durante la inyección. Si la fuerza de cierre es menor a la fuerza generada por la presión de inyección dentro del molde, éste se abrirá, provocando que la pieza salga con exceso de plástico, a la cual habrá que darle un acabado o ser molida para reprocesarla. Seguidamente la punta del husillo hizo contacto con el molde para efectuar la inyección del material en las cavidades del molde, con una predeterminada presión y velocidad de inyección. Después de la inyección, la presión de sostenimiento se mantuvo hasta que el material se enfrió y se solidificó.

El tiempo de cierre necesario para enfriar la pieza se ajusta en un regulador de tiempo. Cuando éste termina se abre el molde. Un mecanismo de expulsión separa el artículo del molde y la máquina se encuentra lista para iniciar el próximo ciclo.

3.2.3. Caracterización de los materiales compuestos

La caracterización de las propiedades mecánicas se realizó sobre las probetas estándar obtenidas por inyección y se analizaron un mínimo de 10 probetas para todos los ensayos. Las probetas se acondicionaron previamente en una cámara climática (Dycometal, España) a 50% de humedad relativa y 23°C durante al menos 48 horas tal y como indica la norma ASTM D618 [118]. Antes de proceder a los ensayos mecánicos, se midió la anchura y el espesor de cada probeta con un micrómetro.

Evaluación de las propiedades de resistencia a tracción

El ensayo a tracción consiste en medir la fuerza necesaria para deformar las probetas normalizadas cuando éstas se someten a estiramiento mediante una máquina de ensayos universal TM 1122 (Instron, Estados Unidos). Los ensayos a tracción se pueden realizar a diferentes temperaturas y velocidades de deformación, sin embargo, se ha empleado la metodología descrita en la norma ISO 527-1:2000. Para la realización de estos ensayos se utilizó una celda de carga de 5 kN, donde la probeta se sujeta a dos mordazas con una distancia inicial entre ellas de 11,5 cm. Una mordaza permanece fija y la otra se desplaza a velocidad controlada, estirando la probeta a una velocidad constante de ensayo de 2 mm/min (Figura 12).

Figura 12. *Esquema del ensayo a tracción*

Tal y como es ampliamente conocido la tensión necesaria para deformar un material depende, entre otras características, de sus dimensiones. En consecuencia, la resistencia a tracción se expresa como el esfuerzo nominal (MPa). De esta forma se obtiene la resistencia a tracción del material sin la influencia de la sección de la probeta medida (espesor y anchura).

Para la determinación de la rigidez de los materiales se realizó según la norma ASTM D3039 [119] y se utilizó el extensómetro MFA2 (Metrotec, España) debido a la necesidad de realizar mediciones más precisas de deformación. Su utilización hace que las condiciones de ensayo sean distintas dependiendo de si se está midiendo el Módulo de Young o llevando la probeta a rotura. Para la medida del Módulo de Young, se colocó la probeta en las mordazas y después se colocó el extensómetro en la probeta. El Módulo de Young fue determinado entre los valores 0,05 y 0,25% de deformación. Al determinar el Módulo de Young, el cual mide la dificultad de un material para deformarse en unidades de fuerza/superficie (GPa), en la zona elástica, puede aplicarse la ley de Hook (ecuación (3)):

$$\sigma = E.\varepsilon \tag{3}$$

donde σ es el esfuerzo expresado en MPa, E el módulo de Young y ε es la deformación expresada como incremento de longitud dividido entre la longitud inicial.

Para el ensayo a tracción se llevó la probeta al punto de rotura y se trabajó sin extensómetro. El procedimiento es similar al caso anterior, pero se permite una elongación máxima superior a la que se supone que ofrecerá la probeta.

Estos dos ensayos han permitido obtener la deformación en el punto de máxima fuerza, el esfuerzo máximo alcanzado durante el ensayo expresado en MPa y la rigidez de cada material.

Evaluación de las propiedades de resistencia a flexión

Por otra parte, el ensayo a flexión permite determinar la resistencia a flexión, el módulo elástico en la región elástica y la deformación máxima a flexión. Al igual que el ensayo a tracción se realizó mediante una máquina de ensayos universal TM 1122 (Instron, Estados Unidos) a una velocidad constante de 2mm/min según la norma ASTM D790 [120].

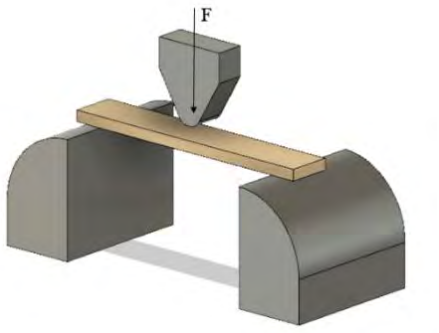

Figura 13. *Esquema del ensayo a flexión*

El cálculo de la resistencia máxima a flexión se realizó según la siguiente ecuación:

$$\sigma_F = \frac{3 \cdot F \cdot L}{2 \cdot w \cdot h^2} \tag{4}$$

Donde σ_F es la resistencia máxima a flexión, F la fuerza máxima del ensayo, L la distancia entre los dos puntos de apoyo, w la anchura de la probeta y h el espesor.

El módulo elástico se obtiene en la región elástica de la curva del ensayo según la ecuación:

$$E_F = \frac{L^3 \cdot F}{4 \cdot w \cdot h^3 \cdot \delta} \quad (5)$$

Donde E_F es el módulo elástico y δ la deflexión de la probeta.

Evaluación de las propiedades de resistencia al impacto

El ensayo a impacto permite conocer el comportamiento de los distintos materiales ante una fuerza ejercida a velocidad elevada. En este trabajo se han estudiado las dos principales metodologías para el ensayo de impacto: Charpy e Izod utilizando en el caso de la metodología Charpy probetas entalladas y sin entallar según las normativas ISO 179 e ISO 180 [121,122]. El procedimiento es similar para ambas metodologías. Para realizar el análisis, se sube el martillo (Ceast, Pianezza) a una altura determinada y se deja caer el martillo. Este golpea la probeta y alcanza una altura inferior debido a la absorción de energía potencial del martillo por parte la probeta en el momento del impacto. Por lo tanto, la diferencia de energías potenciales corresponderá a la energía absorbida por la probeta durante el impacto (Figura 5). El mismo equipo realiza el cálculo y muestra el valor de la energía absorbida (kJ/m^2) en su pantalla.

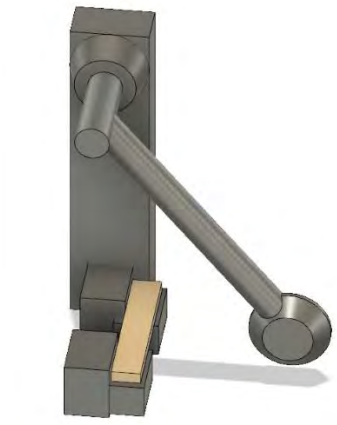

Figura 14. *Esquema del ensayo a impacto.*

Determinación de la absorción de agua

La absorción de agua de las fibras se produce por la formación de enlaces de hidrógeno entre los grupos hidroxilo de la superficie de la celulosa y el agua. La absorción del agua provoca hinchamiento en los materiales compuestos reforzados con fibras naturales debido a la absorción de humedad por parte del refuerzo. Esto puede ser un factor negativo que se debe tener en cuenta y que puede limitar sus aplicaciones.

Para determinar la cantidad de agua absorbida por una probeta de dimensiones definidas se utilizaron los procedimientos descritos en la norma UNE-EN ISO 62:1999. El análisis de absorción de agua se realizó por triplicado para cada material preparado. El procedimiento ha consistido en un primer proceso de secado previo de las probetas en un horno a 100°C durante un mínimo

de 24 horas. A continuación, se dejan enfriar dentro de un desecador y se pesan para conocer el peso inicial del material. Las probetas secas son expuestas a 23 °C y 50% de humedad en una cámara climática y se pesan regularmente, según indica la norma, hasta que el peso de las probetas se estabiliza. De cada probeta se ha calculado el porcentaje de cambio de masa (% humedad absorbida), relativa a la masa inicial, según la ecuación (6):

$$M_t = \frac{m_t - m_0}{m_0}.100 \quad (6)$$

donde M_t es el porcentaje de absorción de agua, m_t es la masa de la probeta en un tiempo t del ensayo y m_0 es la masa de la probeta seca (tiempo inicial del ensayo).

El parámetro que mesura la rapidez de permeación del agua a través de un material compuesto es el coeficiente de difusión (D) y viene expresado en m^2/s. Para calcularlo se aplica la ley de Fick, y se parte de la ecuación (7):

$$\left(\frac{M_t}{M_\infty}\right) = k.t^n \quad (7)$$

donde k y n son constantes, y M_∞ la masa de agua porcentual cuando ha alcanzado el estado de equilibrio de absorción. Para encontrar los valores de K y n se linealiza la anterior ecuación (8) y se obtiene:

$$Log\left(\frac{M_t}{M_\infty}\right) = \log(K) + n.\log(t) \quad (8)$$

A partir de los datos experimentales, se calculan el $log\left({M_t}/{M_\infty}\right)$ y el log(t) de varios puntos y se calcula la regresión lineal de estos puntos. Los coeficientes n y k se obtienen a partir de la recta, donde n será la pendiente de la recta ajustada y el log (k) su ordenada en el origen. Finalmente se utiliza la ecuación (9) para calcular el coeficiente de difusión si los valores de $\left({M_t}/{M_\infty}\right)$ son inferiores a 0,5.

$$\left(\frac{M_t}{M_\infty}\right) = \frac{4}{L}\sqrt{\frac{4.D}{\pi}} \quad (9)$$

Donde L es el espesor de probeta y t el tiempo de exposición. Obteniendo como resultado el coeficiente de difusión.

3.2.4. Cálculos y modelizaciones

A continuación, se presentan los modelos y cálculos usados.

Cálculo de las longitudes ponderadas

En la modelización de la resistencia máxima y del Módulo de Young se han usado longitudes ponderadas. Aunque el mismo equipo ofrece este dato, la ecuación (10) y la ecuación (11) muestran los métodos de cálculo de la longitud aritmética y ponderada, respectivamente:

$$l_a^F = \frac{\sum_i n_i . l_i}{\sum_i n_i} \tag{10}$$

$$l_a^F = \frac{\sum_i n_i . l_i^2}{\sum_i n_i \, l_i} \tag{11}$$

donde l_i es la longitud de cada fibra y n_i el porcentaje de fibras que presentan la longitud l_i.

Cálculo de la fracción volumétrica de los materiales

A partir de la siguiente ecuación (12) se realiza el cálculo de la fracción volumétrica:

$$V^F = \frac{w^F . \rho^m}{w^m . \rho^f + w^F . \rho^m} \tag{12}$$

donde ρ^F y ρ^m las densidades de la fibra y de la matriz, y w^F y w^m son las fracciones másicas de la fibra y de la matriz respectivamente.

Modificando la ecuación anterior, se obtiene la densidad de la fibra a partir del siguiente cálculo:

$$\rho^F = \frac{w^F . \rho^m . \rho^c}{(w^F + w^m) . \rho^m - w^m . \rho^F} \tag{13}$$

donde ρ^c es la densidad del material compuesto de fracción másica w^F, y las densidades ρ^c y ρ^m se determinan experimentalmente siguiendo la norma ISO 118-3.

Regla de las mezclas modificada para la resistencia a tracción

La resistencia mecánica del compuesto progresa de forma lineal en función de la cantidad del refuerzo utilizado en su elaboración. Este comportamiento permite la aplicación de modelos lineales. Uno de estos modelos es el conocido como regla de las mezclas modificada, que se expresa:

$$\sigma_t^C = f_c . \sigma_t^F . V^F + (1 - V^F) . \sigma_t^{m*} \tag{14}$$

donde σ_t^c es la resistencia máxima del material compuesto, σ_t^F es la resistencia máxima de la fibra, σ_t^m* es la resistencia de la matriz en el punto de deformación máxima del material compuesto y f_c es el factor de eficacia. Éste último (Ecuación (15)), es producto de dos factores, el primer factor (χ_1) tiene en cuenta la pérdida de propiedades debido a la orientación de las fibras en el compuesto. Por otro lado, el segundo factor (χ_2) tiene en cuenta la interfase entre fibra y matriz y la longitud de las fibras y se expresa según la ecuación (15):

$$f_c = \chi_1 . \chi_2 \tag{15}$$

A su vez, χ_2 se calcula a través de la longitud crítica, también conocida como longitud de fibra mínima para cargar completamente una fibra según el modelo de shear lag [123]). Ésta se calcula a partir de la ecuación (16):

$$L_c^F = \frac{d^F . \sigma_t^F}{2.\tau} \tag{16}$$

donde d^F es el diámetro de la fibra y τ la tensión interfacial. Una vez calculado el valor de L_C^F, se compara con L^F y se procede al cálculo de χ_2. Si la longitud de la fibra (L^F) es menor que la longitud crítica de la fibra (L_C^F), se aplica la Ecuación (17), en cambio, si L^F es mayor o igual que L^F se aplica la ecuación (18).

$$\chi_2 = \frac{L^F}{2.L_c^F} \tag{17}$$

$$\chi_2 = 1 - \frac{L_c^F}{2.L^F} \tag{18}$$

La reordenación de la Ecuación (14) da lugar al concepto "factor de resistencia tracción de la fibra" (FTSF) que representa la resistencia efectiva que es capaz de proporcionar un refuerzo y se expresa como:

$$FTSF = \frac{\sigma_t^c - (1 - V^F).\sigma_t^{m*}}{V^F} = f_c.\sigma_t^F \tag{19}$$

Mediante este factor es posible comparar las aportaciones de diferentes refuerzos sobre materiales compuestos que tengan la misma matriz polimérica.

Modelo de Kelly y Tyson

Kelly y Tyson modelaron el comportamiento de la resistencia a tracción de materiales compuestos reforzados con fibras orientadas basándose en la regla de las mezclas [124] y obtuvieron la ecuación (20):

$$\sigma_t^C = \sum_{i=0}^{i=l_C} \left[\frac{\tau.l_i^F.V_i^F}{d^F}\right] + \sum_{j=l_C}^{j=\infty} \left[\sigma_t^F.V_j^F\left(1 - \frac{\sigma_t^F.d^F}{4.\tau.l_j^F}\right)\right] + (1 - V^F).\sigma_t^{m*} \tag{20}$$

Esta expresión reformulada a partir de la regla de las mezclas separa la contribución de las fibras en dos tipos de fibras según sus longitudes; supercríticas y subcrítricas. La longitud crítica (L_c) se define a partir de la ecuación (16) y es la longitud que separa las fibras subcríticas de las supercríticas. Por otra parte, se considera que todas las fibras están orientadas en la misma dirección, por lo tanto, cuando las fibras no estén alienadas se debe incorporar el factor de la orientación dentro de la expresión. Resultando en la siguiente ecuación:

$$\sigma_t^C = \chi_1.\left(\sum_{i=0}^{i=l_C} \left[\frac{\tau.l_i^F.V_i^F}{d^F}\right] + \sum_{j=l_C}^{j=\infty} \left[\sigma_t^F.V_j^F\left(1 - \frac{\sigma_t^F.d^F}{4.\tau.l_j^F}\right)\right]\right) + (1 - V^F).\sigma_t^{m*} \tag{21}$$

Para resolver el modelo de Kelly y Tyson que presenta cuatro incógnitas: χ_1, τ, $\sigma^F{}_t$ y $L_C{}^F$, Bowyer y Bader propusieron un método que permitía la resolución de esta ecuación.

Solución de Bowyer y Bader

Bowyer y Bader consideraron que la resistencia intrínseca de las fibras a tracción puede ser aproximada a [125]:

$$\sigma_t^F = E_t^F . \varepsilon_t^C \tag{22}$$

El Módulo de Young intrínseco de la fibra se determina usando el modelo de Hirsch, por lo tanto, se obtiene un valor aproximado de la fuerza intrínseca a tracción. Las contribuciones de las fibras subcríticas, fibras de longitud supercríticas y la matriz se pueden expresar como X, Y, y Z, respectivamente. Por lo tanto, la ecuación (21) se puede reescribir como:

$$\sigma_t^C = \chi_1 (X + Y) + Z \tag{23}$$

Para la resolución del modelo, el compuesto de máxima fuerza es comparado entre dos niveles de fuerza distintos, y se expresa como la relación (24):

$$R = \frac{\sigma_{t1}^c - Z_1}{\sigma_{t2}^c - Z_2} \tag{24}$$

$$R^* = \frac{(X_1 + Y_1)}{(X_2 + Y_2)} \tag{25}$$

Siendo posible de este modo descartar χ_1 de la ecuación. Sin embargo, la ecuación todavía presenta dos incógnitas: τ y L_c. Los métodos numéricos se utilizarán para encontrar valores que se ajusten entre R y 1/4 R*. Una vez determinado τ y L_c, será posible obtener χ_1 y $\sigma^F{}_t$.

Regla de las mezclas modificada para el módulo.

El módulo de Young tiene el mismo comportamiento que la fuerza a tracción, al seguir el Módulo de Young una evaluación lineal al aumentar la cantidad de fibra. Por ello también puede aplicarse la regla modificada de las mezclas, y se obtiene la siguiente expresión para materiales semiorientados y reforzados con fibras.

$$E_t^C = \eta_e . E_t^F . V^F + (1 - V^F) . E_t^m \tag{26}$$

Donde $E_t{}^C$ y $E_t{}^m$ son el módulo del material compuesto y de la matriz, los cuales se obtienen de forma experimentalmente; $E_t{}^F$ es el módulo intrínseco de la fibra y η_e el factor de eficiencia. Este último factor, ηe es el producto entre el factor de eficiencia de orientación η_0 y el factor de eficiencia de longitud η_l.

A diferencia de la ecuación de Kelly Tyson para determinar la resistencia máxima del compuesto (ecuación (20)) que presentaba 4 incógnitas, la expresión de la regla de las mezclas modificada

para el módulo presenta dos incógnitas. Estas dos son el factor de eficiencia y el módulo de Young de la fibra, el cual podrá ser obtenido fácilmente a partir del modelo de Hirsch.

Contribución neta de las fibras al Módulo de Young.

La contribución neta de los refuerzos al módulo de Young del material compuesto está representada por $\eta_e.E_T^F$ en la RoM. Por lo tanto, a partir de la ecuación (26), aislando el factor de eficiencia con el módulo de Young se obtiene la ecuación (27). Luego, si la contribución neta se representa frente a la fracción de volumen del refuerzo, se obtiene una línea de regresión donde el pendiente de dicha línea se conoce en la literatura como el factor de módulo de tracción de la Fibra (FTMT).

$$FTMF = \eta_e.E_t^F = \frac{E_t^C - (1 - V^F).E_t^m}{V^F} \tag{27}$$

Este factor se puede utilizar para mesurar la capacidad de refuerzo de una fibra y para la comparación de diferentes materiales compuestos que tienen la misma matriz.

Modelo de Hirsch

El modelo de Hirsch [126] describe el Módulo de Young de los materiales compuestos a partir de la siguiente expresión (28):

$$E_t^C = \beta.\left(E_t^F.V^F + E_t^m.(1 - V^F)\right) + (1 - \beta).\frac{E_t^F.E_t^m}{E_t^m.V^F + E_t^F.(1 - V^F)} \tag{28}$$

Donde E_t^C es el módulo del material compuesto, E_t^m es el módulo de la matriz, E_t^F es el módulo del refuerzo y β es un parámetro que determina la eficiencia de transmisión de esfuerzos entre la fibra y la matriz. Las variables E_t^m y E_t^C se pueden determinar experimentalmente y a la variable β se le asigna el valor bibliográfico de 0,4 [127], cuyo valor se ajusta con el comportamiento de materiales compuestos con fibras cortas semialineadas.

Modelo de Cox y Krenchel

Una vez obtenido el módulo de Young de la fibra a través del modelo de Hirsch, utilizando la expresión (26), se podrá calcular η_e. No obstante, se necesitará el modelo de Cox Krenchel [128] para la obtención de η_l y η_0 a partir de las siguientes ecuaciones:

$$\eta_l = 1 - \frac{\tanh\left(\frac{\beta.L^F}{2}\right)}{\frac{\beta.L^F}{2}} \tag{29}$$

$$\beta = \frac{1}{r}\sqrt{\frac{E_t^m}{E_t^F.(1 - \nu).\ln\sqrt{\pi/4V^F}}} \tag{30}$$

Siendo r el radio de las fibras y υ el coeficiente de poison de la matriz. Finalmente a través de η_e y η_l se puede determinar el factor de orientación mediante la siguiente ecuación (31):

$$\eta_e = \eta_l . \eta_o \tag{31}$$

Modelado del módulo de Flexión

Los compuestos reforzados con fibras naturales exhiben un comportamiento complejo bajo tensión, lo que respalda aún más el uso de modelos de micromecánica. Una de las formas más sencillas de calcular la contribución de las fibras y de la matriz al módulo de flexión del material compuesto es mediante una regla de mezclas modificada. Ésta se adaptó al módulo de flexión a partir de la regla de las mezclas para modelar el Módulo de Young [129], obteniendo la siguiente ecuación:

$$E_f^C = \eta_e . E_f^F . V^F + (1 - V^F) . E_f^m \tag{32}$$

Donde E^C_f, E^F_f, y E^m_f son el módulo de flexión del material compuesto, la fibra y la matriz, respectivamente. La fracción de volumen de la fibra está representada por V^F, mientras que la contribución de las fibras al módulo de flexión del material compuesto se corrige incorporando un factor de eficiencia del módulo (η_e).

Contribución neta de las fibras al módulo de flexión

La contribución de las fibras al módulo de flexión al material compuesto se puede determinar a partir de un factor de módulo de flexión de fibra (FFMF) que se obtiene reordenado la ecuación (32).

$$FFMF = \eta_e . E_f^F = \frac{E_f^C - (1 - V^F) . E_f^m}{V^F} \tag{33}$$

La contribución de las fibras al módulo de flexión del compuesto, se representa gráficamente como una función de la fracción de volumen de fibra (V^F) en cada contenido de fibra (Ecuación (33)). El FFMF se obtiene de la pendiente de la línea de regresión que une las aportaciones en diferentes fracciones de volumen de refuerzo.

Modelo de Hirsch para el módulo de flexión

El modelo de Hirsch [126] también se puede aplicar para modelar el módulo de flexión de los materiales compuestos a partir de la siguiente expresión (34) :

$$E_f^C = \beta . \left(E_f^F . V^F + E_f^m . (1 - V^F) \right) + (1 - \beta) . \frac{E_f^F . E_f^m}{E_f^m . V^F + E_f^F . (1 - V^F)} \tag{34}$$

Donde E_f^C es el módulo de flexión del material compuesto, E_f^M es el módulo de flexión de la matriz, E_f^F es el módulo de flexión de las fibras y β es un parámetro que determina la eficiencia de transmisión de esfuerzos entre la fibra y la matriz. En general, en aquellos compuestos poliméricos de fibra corta procesados mediante moldeo por inyección, el valor de β cercano a 0,4 ha mostrado una buena concordancia entre los valores teóricos y experimentales [130].

Modelo de Tsai-Pagano

A diferencia del modelo de Hirsch, donde solo se utilizan datos experimentales de la prueba de flexión, el modelo de Tsai-Pagano tiene en cuenta las características morfológicas de las fibras, como la longitud media de la fibra (l^F) y el diámetro (d^F). Este modelo se describe en la Ecuación (35), mientras que el módulo longitudinal (E^{11}) y el módulo transversal (E^{22}) pueden determinarse siguiendo las ecuaciones de Halpin-Tsai según las ecuaciones (36) y (37).

$$E_f^C = \frac{3}{8} \cdot E^{11} + \frac{5}{8} \cdot E^{22} \tag{35}$$

$$E^{11} = \frac{1 + 2 \cdot (l^F/d^F) \cdot \eta_l \cdot V^F}{1 - \eta_l \cdot V^F} \cdot E_f^m \; ; \; \eta_l = \frac{\left(E_f^F/E_f^M\right) - 1}{\left(E_f^F/E_f^M\right) + 2 \cdot (l^F/d^F)} \tag{36}$$

$$E^{22} = \frac{1 + 2 \cdot \eta_t \cdot V^F}{1 - \eta_t \cdot V^F} \cdot E_f^m \; ; \; \eta_t = \frac{\left(E_f^F/E_f^M\right) - 1}{\left(E_f^F/E_f^M\right) + 2} \tag{37}$$

Càlculo de η_e, η_l y η_o a partir del módulo de flexión Intrínseca

Una vez calculado el módulo de flexión intrínseca, ya sea por los modelos Hirsch o TP&HT, el factor de eficiencia del módulo puede obtenerse a partir de la Ecuación (33). Dicho factor de eficiencia de módulo está influenciado principalmente por la orientación y la longitud de las fibras dentro del compuesto, lo que permite descomponer el factor en un factor de orientación de módulo (η_l) y un factor de longitud de módulo (η_o) de acuerdo con la Ecuación (31).

Tanto η_l como η_o se pueden obtener calculando inicialmente el η_l a través del modelo de Cox y Krenchel (Ecuación (38)) [33,34], y luego aislando el η_o de la Ecuación (31). Cabe señalar que el factor (38) en la Ecuación 8 se refiere a la tasa de concentración de tensión en los extremos de las fibras, mientras que ν es la relación de Poisson de la matriz, en este caso, 0,36 para PP.

$$\eta_l = 1 - \frac{\tan h\,(\xi \cdot l^F/2)}{\xi \cdot l^F/2} \; ; \; \xi = \frac{1}{(d^F/2)} \cdot \sqrt{\frac{E_f^M}{E_f^F \cdot (1-\nu) \cdot \sqrt{\ln\,(\pi/4V^F)}}} \tag{38}$$

$$\eta_o = \frac{\sin(\alpha_o)}{\alpha_o} \cdot \left(\frac{3-\nu}{4} \cdot \frac{\sin(\alpha_o)}{\alpha_o} + \frac{1-\nu}{4} \cdot \frac{\sin(3\alpha_o)}{3\alpha_o}\right) \tag{39}$$

Resultados

4. Resultados

4.1. Artículo I

Manuscript Details

Manuscript number	JCOMB_2017_1203
Title	Behavior of the interphase of dyed cotton residue flocks reinforced polypropylene composites
Article type	Full Length Article

Abstract

Textile industry produces a high amount of residues that, nowadays, are poorly treated. The majority of such wastes are dumped and landfilled. The cotton yarning industries produce wastes in the shape of fiber flocks, with lengths smaller than 10 mm that prevent their reintroduction in the textiles manufacturing process. Nonetheless, such waste cotton strands could be used as reinforcement for short fiber mould injected composites. This paper reports on the behavior of the interphase between the cotton strands and a polypropylene matrix. The recycled strands were treated with an organic dye that seem to affect the quality of the interphase, in one hand by increasing the affinity between the natural fibers and the matrix, and on the other hand by limiting the effect of the coupling agents. Micromechanic models are used to further research the quality of the interphase and the intrinsic properties of the composites.

Keywords	Fabrics/textiles; fibres; Interphase; Strength; Injection molding
Manuscript region of origin	Europe
Corresponding Author	F.X. Espinach
Corresponding Author's Institution	Universitat de Girona, Escola Politècnica Superior
Order of Authors	Albert Serra, Quim Tarrés, Josep Claramunt, Pere Mutje, Monica Ardanuy, F.X. Espinach
Suggested reviewers	Carlos Negro, Fernando Julian, Josep Tresserras, Nour-Eddine El-Mansouri, sami boufi

Submission Files Included in this PDF

File Name [File Type]

cover letter.doc [Cover Letter]

manuscript.docx [Manuscript File]

figures.docx [Figure]

To view all the submission files, including those not included in the PDF, click on the manuscript title on your EVISE Homepage, then click 'Download zip file'.

Girona, April 4, 2017

Dear Editor,

Please find attached our manuscript for publication in Composites Part B entitled:

Behavior of the interphase of dyed cotton residue flocks reinforced polypropylene composites.

By: Serra, A., Tarrés, Q., Claramunt, J., Mutjé, P., Aradanuy, M. and Espinach, FX.

This work uses a by-product of the textile industry, in the shape of cotton flocks to produce composite materials. Usually, the textile industry has no use for the fibers with lengths inferior to 10mm, and thus landfilled or dumped them. Indeed, such fibers could be used to prepare composite materials, adding value to the by-product, extending the value chain of the textile industry and stimulating a circular economy.

The material was received dyed fibers. It was found that the organic dye decreased the hydrophilicity of the cotton fibers, stimulating the creation of a good interphase with the polypropylene. Nonetheless, when coupling agents were added to the composite it was found that the tensile strength of the composites was lower than expected. Thus, the same dyes were suspected to hinder the action of the coupling agents, affecting the quality of the interphase.

We confirm that this manuscript has not been published elsewhere, is not under consideration by another journal, and all authors have approved the manuscript and agree with its submission to Composites Part B.

Should you have any questions, please do not hesitate to contact us anytime.

The corresponding author is

Francesc Xavier Espinach

Dpt. of Organization, Business Management and Product Design

Escola Politecnica Superior. Avda. Lluis Santalo, s/n, 17071 Girona, Spain

Phone: 34 972 418 920,

E-mail: franciso.espinach@udg.edu

Behavior of the interphase of dyed cotton residue flocks reinforced polypropylene composites.

By:
Serra, A[a]., Tarrés, Q[a]., Claramunt, J[b]., Mutjé, P[a]., Ardanuy, M[c]., Espinach, FX[d*].

[a] LEPAMAP Group, Department of Chemical Engineering, University of Girona, Girona 17071, Spain
[b] Agri-Food Engineering and Biotechnology Dept., Polytechnic University of Catalunya, Castelldefels 08860, Spain
[c] Materials Science and Metallurgic Engineering Dept., Polytechnic University of Catalunya, Barcelona 08019, Spain
[d] Design, Development and Product Innovation, Dept. of Organization, Business, University of Girona, Girona 17071, Spain
[*] Escola Politecnica Superior. Avda. Lluis Santalo, s/n, 17071 Girona, Spain.
Francisco.espinach@udg.edu, tlf. +34 972 418 920, FAX +34 972 418 399

Abstract

Textile industry produces a high amount of residues that, nowadays, are poorly managed. The majority of such wastes are dumped and landfilled. Among all the textile value chain, cotton yarning factories produce wastes in the shape of fiber flocks, with lengths smaller than 10 mm that prevent their reintroduction in the textiles manufacturing process. Nonetheless, such waste cotton flocks could be used as reinforcement for short fiber mould injected composites. This paper reports on the behavior of the interphase between the cotton flocks and a polypropylene matrix. It was found that the organic dyes present on the cotton flocks seem to affect the quality of the interphase in two ways: on the one hand by increasing the affinity between the cotton fibers and the matrix, and on the other hand by limiting the effect of the coupling agents. Micromechanic models are used to further research the quality of the interphase and the intrinsic properties of the composites.

Keywords: A, Fabrics/textiles, fibres; B, Interphase, Strength; E, Injection molding

1 Introduction

Since the textile industry is generating huge amounts of residues, the increasing environmental consciousness and demands of legislative authorities is driving this sector to look for solutions to deliver the remainders into recycling processes and convert these waste products into valuable byproducts [1, 2]. However, the rate of textile recycling is still relatively low. On average, approximately 10 million tons of textile waste is currently dumped in Europe and America each year. Considering the

diversity of fibrous waste and structures, many technologies must work in concert in an integrated industry in order to increase the rate of recycling [3, 4].

Textiles represent about 3 wt.% of a household bin. At least 50% of the textiles we throw away are recyclable; however, the proportion of textile wastes reused or recycled annually is only around 25%. Although the majority of textile waste provides from household sources, waste textiles also arise during yarn and fabric manufacture, garment-making processes and from the retail industry. In this sense, textile waste can be classified as either pre-consumer or post-consumer. Pre-consumer textile waste consists of by-product materials from the textile, fiber and cotton industries. Each year 750,000 tons of this waste is recycled into new raw materials for the automotive, furniture, mattress, coarse yarn, home furnishings, paper and other industries. Through the efforts of this industry approximately 75% of the pre-consumer textile waste that is generated is diverted from our landfills and recycled. Some post-industrial waste is recycled 'in-house', usually in the yarn and fabric manufacturing sector. The rest, aside from going to landfill or incineration, is sent to merchants [5]. As an example, in Hong Kong, there are 253 tons of textiles through up to landfill daily, and the U.S. Environmental Protection Agency estimates that textile waste supposes nearly 5% of all landfill space. The post-consumer waste goes to jumble sales and charities but more typically are disposed of into the trash and end up in municipal landfills. Together, they provide a vast potential for recovery and recycling, which can provide both environmental and economic benefits.

Textile waste in landfill contributes to the formation of ‘leachate’ (the noxious fluid produced in landfill sites) as it decomposes, which has the potential to contaminate both surface and groundwater sources [6]. Another product of decomposition in landfill is methane gas, which is a major greenhouse gas and a significant contributor to global warming, although it can be used if collected. Textile waste is also incinerated in large quantities, and comes third after plastics and cardboard.

In the particular case of cotton-based textiles, the process used to prepare the fabrics, generates byproducts in the form of cotton flocks. As can be seen in Figure 1, to produce cotton fabrics, on the first step, cotton fibers are yarned to manufacture high quality yarns. These yarns are the used to manufacture fabrics. The manufacturing process produces a large number of byproducts in the shape of fabric trims. These fabric trims are submitted to a defibration process, obtaining cotton fibers. These fibers are yarned and used for the manufacturing of fabrics that will be used to manufacture

denim. Anyhow, the defibration process produces fibers with length under 10mm. Such fibers are unable to be yarned and thus are a byproduct of the process without any value or use for the textile industry. This byproduct has the shape of cotton flocks. Moreover, as the yarns used are previously subjected to dying processes, these cotton flocks are composed by dyed fibers.

Although a lot of studies about the reinforcement of polypropylene with wood- and non-wood cellulose fibers can be found in the literature, only few of them report the use these cotton flocks byproduct as reinforcement for polypropylene-based composites [7-10]. The use of cotton waste is also limited as reinforcement of other polymers, with few publications in the literature [11].

One of the main limitations of these composites is the maximum wt.% of cotton flocks content due to the flock aggregation without any prior treatment. In this sense, Petrucci et al. [9] use a pretreatment of the flocks with a vinyl-acetate water solution to obtain compressed sheets that are subsequently milled, then mixed with PP in a twin screen extruder and finally injection molded. The maximum amount of fiber introduced in this study was 16 wt.%. Araujo et al. [7] prepared composites with until 20 wt.% of reinforcement after dye removal and silanization or acetylation treatment. The composites in this case were mixed in a twin screen extruder and compression molded to form the composites.

In this work, waste dyed cotton flocks were used as reinforcement for polypropylene-based composites. The cotton flocks were used without any chemical treatment and only were cut down to ensure their correct individualization and dispersion in the matrix. Composites with 30 and 40 wt.% of waste cotton strands (WCS) were prepared. Percentages of polypropylene functionalized with maleic anhydre (MAPP) ranging from 0 to 8 wt.% were added to the composites to find the highest tensile strengths. The results showed tensile strengths higher than expected for the uncoupled composites. Then, the effect of the dye on the interphase was investigated by preparing composites reinforced with virgin cotton fibers. Additionally, the virgin cotton flocks were chemically analysed. A modified rule of mixtures was used to compute the intrinsic tensile strength of the WCS. Initially a good interphase was hypothesised for all the coupled composites. The intrinsic tensile strength of the dyed strands was found to be noticeably inferior to that of the virgin fibers, indicating a negative effect of the dye on the quality of the interphase. Single fiber tensile tests were carried out to obtain the tensile strength of the WCS. The obtained results were

submitted to a Weibull analysis to find the characteristic strength of the WCS. The results were tabulated against the fibers length and it was possible to find the characteristic strength of the WCS used in the composites, after its morphologic analysis. Then, the modified Kelly and Tyson equation was used to define the interfacial shear strength of the interphase and the orientation factor.

2 Materials and methods

2.1 Materials

The cotton flocks residues, treated with a reactive dye, from textile industry and with not enough length for spinning, were kindly supplied by Fontfilva S. L. (Olot, Girona, Spain). Figure 1 shows the aspect of the provided cotton residue flocks.

The polymer matrix used was polypropylene (PP) (Isplen PP090 62M) and was kindly supplied by Repsol-YPF (Tarragona, Spain). In order to improve the compatibility between cotton residues and PP, polypropylene functionalized with maleic anhydre (MAPP) (Epolene G3015), with an acid number of 15 mg KOH/g and Mn of 24800, was used as a coupling agent. This was acquired from Eastman Chemical Products (San Roque, Spain).

Sodium hydrosulphite ($Na_2S_2O_4$) was used to remove the dyes from the cotton residues and was provided by Sigma Aldrick (Barcelona, Spain). Decalin (Decahydronaphthalene) was acquired from Fischer Scientific (Madrid, Spain) and had 190ºC boiling point and 97% purity. This reagent was used to dissolve PP matrix in the fiber extraction from composites. All reactants used for cotton flocks characterization were bought from Scharlau Spain (Barcelona, Spain) and used without further purification.

2.2 Methods

2.2.1 Composite processing

The cotton residues were cut down to a nominal length of 1 mm using a blade mill in order to obtain a better dispersion in the composite. Then, PP, MAPP and cotton flocks residues were mixed at different wt./wt. ratios in an intensive melt mixer Brabender Plastograph (Brabender, Duisburg, Germany) at 185 ºC for 10 min, and at 80 rpm, in order to ensure to obtain a well-dispersed material. The blends were cut down to pellets with a particle size in the range of 10 mm using a pelletizer equipped with a set of knifes and different grids. The pellets were dried and stored at 80ºC for 24h. After

that, the composite blends were injection-moulded in a Meteor-40 injection machine (Mateu & Solé, Spain). The machine is equipped with three heating areas working at 175, 175 and 190 ºC, the highest temperature corresponding to the nozzle. First and second pressures were 120 and 37.5 $Kg.cm^{-2}$, respectively. This process allowed acquisition of specimens for mechanical characterization (ASTM D638).

2.2.2 Mechanical characterization

Processed materials were placed in a conditioning chamber (Dycometal) at 23ºC and 50% relative humidity during 48 hours, in accordance with ASTM D618, prior to testing. Afterwards, samples were mechanically studied by using a Universal testing machine (instrom TM 1122), fitted with a 5 kN load cell. Tensile specimens were shaped like a dog-bone (of approx. 160x13.3x3.2 mm), according to the ASTM D790 standard. Results were obtained from the average of at least 5 samples.

2.2.3 Fiber extraction from composites

Cotton residues were extracted from composites by matrix solubilisation using a Soxhlet apparatus and Decalin as a solvent. Small pieces of composites were cut and placed inside a specific cellulose filter and set into a Soxhlet equipment. A small cotton tab was used to prevent the fibers from getting out of the filtering tube. The fiber extraction was carried out during 24 hours. Afterwards, fibers were rinsed with acetone and then with distilled water in order to remove the solvent residue. Finally the fibers were dried in an oven at 105 ºC for 24 hours.

2.2.4 Determination of the fiber length and fiber diameter

Fiber length distribution and fiber diameter of the extracted cotton fibers were characterized by means of a Kajanni analyzer (FS-300). A diluted aqueous suspension (1 wt.% consistency) of fibers was analyzed during 2 to 5 minutes, and the length of the fibers was evaluated considering an amount of individual fibers in the range of 2500 to 3000 units. Minimums of two samples were analyzed. The Kajanni analyzer offers complete fiber, fines and shiv morphology characterization, but only the fiber length and fiber diameter distribution were used the present work.

The fibers were also measured with a Leica DMR-XA optic microscope with a 2µm optical resolution.

2.2.5 Cotton strands characterization

2.2.5.1 Degree of polymerisation

The degree of polymerisation (DP) of cotton fibers was determined according to UNE 57-039-92. The viscosimetric average molecular weight was calculated from the equation $\eta = K \cdot M^a$, where η is the intrinsic viscosity, $K = 2.28$ and $a = 0.76$ [12].

2.2.5.2 The solvent used was a copper (II) ethylenediamine by Scharlau Spain (Barcelona, Spain). Cationic demand

The cationic demand of cotton fiber was determined using a Mütek PCD 04 particle charge detector. First, 0.2 g (dried weight) of cotton fiber was diluted in 15 ml distilled water. Then 25 ml of cationic polymer polydiallyldimethylamonium chloride (polyDADMAC) was added to before fiber solution and it was mixed for 5 minutes with magnetic stirring. After this time the mixture was centrifuged in a Sigma Laborzentrifugen model 6 K 15 for 90 min at 4,000 rpm. Then, 10 ml of the supernatant was taken to the Mütek equipment. Anionic polymer (Pes-Na) was then added to the sample drop by drop with a pipette until the equipment reached 0 mV. The volume of anionic polymer consumed was used to calculate the cationic demand though:

$$CD = \frac{(C_{PD} \cdot V_{PD}) - (C_{AP} \cdot V_{AP})}{W_s} \quad (1)$$

where CD is the cationic demand (μeq/l), C_{PD} = cationic polymer concentration (g/l), V_{PD} = used volume of cationic polymer (ml), C_{AP} = anionic polymer concentration (g/l), V_{AP} = used volume of anionic polymer (ml) and W_S = sample's dry weight (g).

2.2.5.3 Chemical composition

Extractives and lignin of cotton fiber residues were determined following TAPPI standard methods, T222 om-88 and T223 cm-84, respectively. Cellulose content was measured according to Wise et al. (1946).

.

2.2.5.4 Single fiber tensile test

The tensile strength of the cotton flocks was obtained from the force-displacement curves, following ASTM D3822-01 standard. The measurement was conducted using the INSTRON 5500R testing device (supplied by INSTRON, Cerdanyola del Vallès, Spain) equipped with 5kg force cell. The experiment was repeated at four different gauge lengths; 25.4, 19.05, 12.7 and 6.35 mm, using cross speed rates of 2.54, 1.905, 1.27 and 0.635 mm/min, respectively. An amount up to 100 single fibers was tested for each gauge length and the maximum force was evaluated.

The diameter of the fibers was determined by optical microscopy. Microscopy images were obtained and the width of the fibers was evaluated as a mean value of 3 measures

2.2.5.5 Fiber fading

To remove the dye from the cotton flocks, one dry gram of cotton residues was submerged into a hot Sodium hydrosulphite solution (25 wt.%) for two hours. Then, cotton flocks were water rinsed and dried at 50ºC.

3 Results and discussion

When hydrophilic natural fibers, as cotton, are used as reinforcement for a hydrophobic matrix, as PP, the use of coupling agents as MAPP is a common practice to obtain good tensile and flexural strength [13-15]. Consequently, searching the percentage of MAPP against fiber content that renders the best tensile strengths (σ_t^C) was the first step proposed by the authors to obtain competitive composite materials. Figure 2 shows the behavior of the tensile strength of the PP-based composite materials containing 30 and 40 wt.% waste cotton strands (WCS) contents, when increasing contents of MAPP were added to the composite formulation.

It was found that adding MAPP increased progressively the tensile strength of the composites besides the reinforcement content. The composites with a 30 wt.% of WCS increased their tensile strength a 57.2, 63.7 and a 70.6% against the matrix when 2, 4 and 6% of MAPP was added, respectively. If the same values are compared with the composite without MAPP the respective increases were 13.6, 18.3 and 23.3%. Further MAPP contents caused a drop of the tensile strength of the composite. The most probable cause could be the self-entanglement of the MAPP chains [16]. The composites with a 40 wt.% content of WCS showed a similar behavior, with a maximum observed tensile strength when a 6% of MAPP was added to its formulation. Such MAPP content rendered 94.2 and 28.5% increases of the tensile strength, compared to the matrix and the uncoupled composite, respectively. While the increases against the matrix were found to be significant, the tensile strength of the uncoupled composites was found to be remarkably high [13, 17].

The uncoupled composite materials with 30 and 40 wt.% WCS increased the tensile strength of the matrix a 38.4 and a 51.1%, respectively. Such increases are really significant when compared with other uncoupled cellulosic fiber reinforced composites. A probable cause for such behavior could be due to the dye agents affecting surface

chemical character of the cotton flocks. In that sense, the cationic demand of the dyed cotton residue flocks, expressed in micro-equivalents of polyDACMAC per gram of reinforcement, was estimated at 16.39 μeq. g/g, while the virgin cotton fibers showed a 58.7 μeq. g/g demand [18]. The change on the superficial hydrophilicity of the dyed cotton is significant, increasing its hydrophobicity, and consequently increasing its affinity with the PP. The effect is similar to that obtained by diminishing the hydrophilic nature of natural fibers by surface treatment with alkyl ketene dimmer (AKD) [19, 20]. Then, some cotton residue flocks were faded, and their cationic demand was measured to be 48.9 μeq. g/g. Besides, some dyed and faded flocks were suspended in a water/hexane mixture (50/50%). Figure 3 shows the result.

It was found that the dyed and the faded cotton flocks had affinity with the organic phase (hexane), and aqueous phase, respectively. Consequently, it was apparent that the dying agents changed the surface character of the cotton fibers, increasing their hydrophobicity, and consequently their affinity with the PP, and thus resulting in comparatively high tensile strengths for the uncoupled composites [21].

Nonetheless, it is probable that such dying agents also affect the interactions of the cotton fiber surfaces with the MAPP, limiting its strengthening power. To that effect, a modified Rule of Mixtures (mRoM) was used to analyze the experimental results (Eq. 1).

$$\sigma_t^C = f_c \cdot \sigma_t^F \cdot V^F + (1 - V^F) \cdot \sigma_t^{m*} \quad (1)$$

Were σ_t^C, σ_t^F *and* σ_t^{m*} are the tensile strength of the composite, the intrinsic tensile strength of the strands, and the tensile strength of the matrix at the composites' failure strain. The value of σ_t^{m*} was computed with a polynomial 4th regression of the stress strain curve of the matrix (Eq.2).

$$\sigma_t^{m*} = -0.0001 \cdot (\varepsilon_t^C)^5 + 0.0014 \cdot (\varepsilon_t^C)^4 + 0.0468 \cdot (\varepsilon_t^C)^3 - 1.1307 \cdot (\varepsilon_t^C)^2 + 9.0559 \cdot \varepsilon_t^C \quad (2)$$

V^F is the volume fraction of the reinforcement, and f_c is the coupling factor that is used to account for the effect of the fiber length and orientation, and the quality of the interface between the fibers and the matrix. It has been reported that bell bonded semi-aligned short fiber composites show coupling factor with 0.2 values [17, 22, 23].

The mRoM was used to obtain the value of the intrinsic tensile strengths of the cotton fibers, using the experimental results (Figure 3, Table 1), and a 0.2 coupling factor, assuming a high quality interphase in the case of the composites containing a 6% of MAPP.

The obtained σ_t^F were 658.2 and 624.5 MPa for the 30 and 40% coupled composites, respectively. Such intrinsic tensile strengths are sensibly higher to previously reported values [24, 25]. Nonetheless, if the dying agents affect the interactions between the fiber surface and the MAPP it means that the composites could not be defined as well bonded, and consequently, lower values of the coupling factor were expected. Anyhow, lower values of the coupling factor will produce higher intrinsic tensile strengths (a 0.15 coupling factor renders 1005 MPa intrinsic tensile strength). In the literature there are references to the intrinsic tensile strength of cotton fibers in the range from 287 to 800 MPa [26, 27]. The large variability of such value is common to natural fibers.

For comparison purposes, virgin cotton flocks were used to prepare a composite with a 20% of such fibers as reinforcement (the composite was coupled with a 6% of MAPP). Once tensile tested its tensile strength was 46.86 MPa and its strain at break was 4.9%. These new experimental data were used anew to back calculate the correspondent intrinsic tensile strength of virgin cotton flocks, by using the mRoM, and assuming a 0.2 coupling factor, obtaining a 1017.4 MPa value. The dyed and the virgin cotton strands are very similar, being its main difference the presence or not of dying agents and consequently its effect on the reactivity between the strands surface and the MAPP. Then, if the intrinsic strength of the cotton flocks is established at a value around 1000 MPa, it is clear that the coupling factor in the case of the dyed cotton strands-based composites is lower than 0.2, and such composites could not considered fully well bonded. It is known that the contribution of a reinforcing fiber to the tensile strength of a composite depends on its intrinsic tensile strength, but also in the nature of the bonds between the matrix and the fibers, and the number of such bonds per volume fraction. These virgin cotton flocks were chemically analyzed (table 2), and their chemical composition and its degree of polymerization (DP) further support high intrinsic tensile strengths for such fibers.

It was found that the cellulose and the alpha-cellulose contents, and its degree of polymerization were comparatively very high. A bleached pine Kraft pulp (BPKP) shows lesser cellulose contents (84.1 wt.%, with a 15.9 wt.% of hemicelluloses), and a polymerization degree of 1197. A PP-based composite material reinforced with a 40 wt.% of BPKP, coupled with a 6% of MAPP reported that the intrinsic tensile strength of the BPKP is 474.6 MPa. The qualitative and quantitative differences with the cotton

fibers are clear. With the objective of clarifying the value of the intrinsic tensile strength of the cotton flocks single fiber tensile tests were performed.

3.1 Cotton flocks intrinsic mechanical properties.

Figure 4 shows two representative samples of the evaluation of the mean diameter (width) of the fibers submitted to single fiber tensile test.

The width of the single fibers was very regular, fiber to fiber, with slight variation between them. The mean diameter of all the evaluated fibers was 17.35 μm. Then, the fibers were submitted to tensile test. Figure 5 shows the results of the single fiber tests against the gauge length.

The intrinsic properties of the Cotton fibers were computed after a Weibull analysis of the single fiber tests experimental results. The Weibull analysis describes the probability of failure of a fiber under stress. The probability of failure under a given stress (σ) is directly linked to the presence of a defect in the fiber surface with the size that allows crack propagation [28]. The failure stress is distributed accordingly to a Weibull distribution, described by equation 3:

$$P_f(\sigma) = 1 - e^{\left[-\left(\frac{\sigma}{\eta}\right)^{\beta}\right]} \quad (3)$$

Where, β is known as the Weibull modulus, and is a measure of the dispersion of the strength values. The higher the Weibull modulus is, the shorter is the scatter of the strength values. In the same equation, σ and η are the measured fiber tensile strengths, and the scale factor or the characteristic strength of the fiber. With the objective of measuring the intrinsic tensile strength of the fibers the gauge length of the Instron universal dynamometer were established at four different positions; 1, ¾, ½, and ¼ inches (25.40, 19.05, 12.70 and 6.35mm). At least 100 fibers were tested for each gauge lengths. The strength of a fiber is highly dependent on its length, as the higher the length, higher id the probability of finding a defect. Besides, natural fibers usually show high standard deviations on their mechanical properties, thus a scatter on their properties was expected. Upper and lower strength values were omitted in agreement with the research by Thomason [29].

Figure 6 shows the linearized representation of the probability of failure against the natural logarithm of the measured intrinsic fiber tensile strength.

Table 2 shows the experimental mean intrinsic tensile strengths (σ_t^F) and its standard deviations. As expected the experimental values were higher for the shorter fibers. For comparison purposes the table also adds the specific mean tensile strengths of the fibers ($\sigma_t^{F,\ specific}$). In that sense, the specific intrinsic tensile strength of a glass fiber is around 580 MPa/g cm^3, and a flax fiber around 600 MPa/g cm^3 [30]. The Weibull modulus and the characteristic strengths were computed after the statistical analysis and are also shown in table 3.

The low value of the Weibull modulus reflects the exhibited wide scatter. The measured mean intrinsic tensile strengths are similar to their respective characteristic strengths. The characteristic strengths also visualize the highest probability of failure for the longest fibers. Figure 5 shows a linear evolution of the tensile strength of the single fibers against the gauge length. This gauge length is equivalent to the fiber length and a linear regression of the intrinsic tensile strength of the fibers (σ_t^F) against its length (L^F) delivers Eq. 3:

$$\sigma_t^F = 952 - 16.504 \cdot L^F \quad (3)$$

Usually the mean lengths of the fibers inside the composites show values much shorter than that of the gauge lengths. The regression equation can be used to compute the intrinsic tensile strength of the reinforcing fibers, once such fibers are morphologically characterized. This morphological analysis indicated that the mean diameter of the fibers was 16.5 µm. Figure 7 shows the length distribution of the cotton fibers extracted from the matrix, for the case of the coupled composite with a 40% of WCS.

It was found that the mean arithmetic lengths of the coupled composites with 30 and 40 wt.% WCS contents were 239 and 210 µm, respectively. In the same way, the respective single weighted length was 374 and 339 µm. The equation presented with the figure 5 was used to compute the respective intrinsic tensile strength; obtaining 948.0 and 948.5 MPa values for the 239 and 210 µm mean lengths, respectively. The values are very similar to those obtained by using the mRoM while assuming a good interphase. Nonetheless, there are studies that observe notable differences between the intrinsic tensile strengths of the fibers if a re experimentally measured or back-computed by using micromechanical models [31].

With the morphologic data of the reinforcing fibers and the results of the tensile tests of the matrix and the composites it was possible to use the modified Kelly and Tyson model [32-34] (Eq. 4) to assess the quality of the interphase.

$$\sigma_t^C = \chi_1 \left(\sum_i \left[\frac{\tau \cdot l_i^F \cdot V_i^F}{d^F} \right] + \sum_j \left[\sigma_t^F \cdot V_j^F \left(1 - \frac{\sigma_t^F \cdot d^F}{4 \cdot \tau \cdot l_j^F} \right) \right] \right) + (1 - V^F) \cdot \sigma_t^{m*} \quad (4)$$

In Equation 4 the d^F and $l^F_{i,j}$ terms represent the fiber diameter and length, respectively. χ_1 is the orientation factor, modifying the original Kelly and Tyson model, developed for aligned reinforcements. Finally, τ is the interfacial shear strength, accounting for the ability of the interphase to transmit loads from the matrix to the fiber [35].

Previous works found that the orientation angle was highly influenced by the machinery used during the mould injection of the specimens. It was found that such parameter also rendered values between 0.25 and 0.35. It is accepted that the relation between the orientation factor and the mean orientation angle (α) is represented by: $\alpha=cos^4(\chi_1)$. Accordingly, the mean orientation angles were between 40 and 45º. It is also known that Von Mises criteria: $\tau=\sigma_t^c/3^{1/2}$ could be used to predict the value of the interfacial shear strength in the case of very good interphases, and also an upper bound for such value (cites). As the used PP had an tensile strength of 27.6 MPa, Von Mises criteria establishes a 15.9 MPa value for τ.

A numerical solution for the Kelly and Tyson equation was proposed in order to know the value of the interfacial shear strength and the orientation factor for the composites that added a 6% of MAPP. If the equation is handled individually for both composites shows two incognita, being impossible to solve. On the other hand it is wise thinking that both values will be similar for the composites with a 40 and 30% of cotton fiber reinforcement, being the case in previous researches [17, 23]. Thus, a numerical iterative method was applied to find a value for the interfacial shear strength and the orientation factor for both composites that showed the lowest distance between the computed values. The initialization values were a 0.3 orientation factor and 16 MPa interfacial shear strength. The method converged very fast to interfacial shear strengths around 14.8 MPa and an orientation factors in the range from 0.33 to 0.34. The interfacial shear strength was inferior to Von Mises, showing that the interphase has possibilities to be improved, supporting that the dye somehow limited the interaction between the fibers and the polymer. At the same time, the orientation factor was inside the 0.25 to 0.35 range found in previous works [14, 17]. Besides the value coincides with the mean value of the orientation factor predicted by other researchers [36]. The

orientation factor was used to compute the theoretical interfacial shear strength of the uncoupled composites, obtaining 6.5 and 8.3 MPa values for the 30 and 40% composites, respectively. Such values are in line with those shown by other natural fiber reinforced polypropylene composites [17, 23].

Finally, the mRoM (Eq.1) was used to compute the value of the coupling factor of the coupled and uncoupled WCS-based composites. The coupled composites with 30 and 40 wt.% WCS contents rendered 0.159 and 0.146 coupling factor values, respectively. The value is far from 0.2, pointing out improvable interphases, and further adding to the negative effect of the dyes on such interphases. On the other hand, the same uncoupled composites showed coupling 0.117 and 0.105 coupling factors, respectively. Such values are high in comparison with other natural fiber uncoupled composites, which show slightly positive values [13, 23, 37, 38].

4 Conclusions

A by-product of the textile industry in the shape of waste cotton flocks was used to reinforce polypropylene. This use could inertize such by-product and extend the value chain of the textile industries.

It was found that the organic dyes favored the interphase between the cotton flocks and the matrix, as long as their composite materials showed comparatively relevant tensile strength, without any coupling agent. At the same time, it was apparent that the aforementioned dyes affected negatively the action of the coupling agents.

The tested cotton flocks presented intrinsic tensile strengths superior to that found in the bibliography. With such strengths, its composites could replace glass fiber-based reinforced composites.

The intrinsic tensile strengths of the cotton flocks were obtained by single fiber tensile test, and as it is known that the fibers suffer morphologic changes when composed. Thus, it is probable that its intrinsic tensile strength inside the composite is different to that outside. A more accurate micro-mechanics analysis could unveil possible deviations from the experimental values.

The interfacial tensile strength and the orientation factor obtained in the analysis are consistent with the literature.

References

[1] Mishra R, Behera B, Militky J. Recycling of Textile Waste Into Green Composites: Performance Characterization. Polymer Composites. 2014;35(10):1960-7.
[2] DeVallance DB, Gray J, Lentz H. PROPERTIES OF WOOD/RECYCLED TEXTILE COMPOSITE PANELS. Wood Fiber Sci. 2012;44(3):310-8.
[3] Mulinari DR, Voorwald HJC, Cioffi MOH, Lima CAA, Baptista C, Rocha GJM. Composite materials obtained from textile fiber residue. Journal of Composite Materials. 2011;45(5):543-7.
[4] Barbero-Barrera MdM, Pombo O, Navacerrada MdlÁ. Textile fibre waste bindered with natural hydraulic lime. Composites Part B: Engineering. 2016;94:26-33.
[5] Ryu C, Phan AN, Sharifi VN, Swithenbank J. Combustion of textile residues in a packed bed. Exp Therm Fluid Sci. 2007;31(8):887-95.
[6] Jha MK, Kumar V, Maharaj L, Singh RJ. Studies on leaching and recycling of zinc from rayon waste sludge. Industrial & Engineering Chemistry Research. 2004;43(5):1284-95.
[7] Araújo RS, Rezende CC, Marques MF, Ferreira LC, Russo P, Emanuela Errico M, et al. Polypropylene- based composites reinforced with textile wastes. J Appl Polym Sci. 2017.
[8] Haque MS. Processing and characterization of waste denim fiber reinforced polymer composites. 2014.
[9] Petrucci R, Nisini E, Puglia D, Sarasini F, Rallini M, Santulli C, et al. Tensile and fatigue characterisation of textile cotton waste/polypropylene laminates. Composites Part B: Engineering. 2015;81:84-90.
[10] Taşdemır M, Koçak D, Usta I, Akalin M, Merdan N. Properties of polypropylene composite produced with silk and cotton fiber waste as reinforcement. International Journal of Polymeric Materials. 2007;56(12):1155-65.
[11] Tserki V, Matzinos P, Panayiotou C. Effect of compatibilization on the performance of biodegradable composites using cotton fiber waste as filler. J Appl Polym Sci. 2003;88(7):1825-35.
[12] Henriksson M, Berglund LA, Isaksson P, Lindstrom T, Nishino T. Cellulose nanopaper structures of high toughness. Biomacromolecules. 2008;9(6):1579-85.
[13] Reixach R, Espinach FX, Arbat G, Julián F, Delgado-Aguilar M, Puig J, et al. Tensile Properties of Polypropylene Composites Reinforced with Mechanical, Thermomechanical, and Chemi-Thermomechanical Pulps from Orange Pruning. BioResources. 2015;10(3):4544-56.
[14] Granda LA, Espinach FX, Lopez F, Garcia JC, Delgado-Aguilar M, Mutje P. Semichemical fibres of Leucaena collinsii reinforced polypropylene: Macromechanical and micromechanical analysis. Compos Pt B-Eng. 2016;91:384-91.
[15] Li Y, Pickering KL, Farrell RL. Determination of interfacial shear strength of white rot fungi treated hemp fibre reinforced polypropylene. Composites Science and Technology. 2009;69(7-8):1165-71.
[16] Beckermann GW, Pickering KL. Engineering and evaluation of hemp fibre reinforced polypropylene composites: Micro-mechanics and strength prediction modelling. Composites Part A-Applied Science and Manufacturing. 2009;40(2):210-7.

[17] Vallejos ME, Espinach FX, Julian F, Torres L, Vilaseca F, Mutje P. Micromechanics of hemp strands in polypropylene composites. Composites Science and Technology. 2012;72(10):1209-13.
[18] Carrasco F, Mutjé P, Pelach MA. Control of retention in paper-making by colloid titration and zeta potential techniques. Wood Science and Technology. 1998;32(2):145-55.
[19] Mutje P, Girones J, Lopez A, Llop MF, Vilaseca F. Hemp strands: PP composites by injection molding: Effect of low cost physico-chemical treatments. Journal of Reinforced Plastics and Composites. 2006;25(3):313-27.
[20] Vilaseca F, Lopez A, Llauro X, Pelach MA, Mutje P. Hemp strands as reinforcement of polystyrene composites. Chemical Engineering Research & Design. 2004;82(A11):1425-31.
[21] Zhou Y, Fan M, Chen L. Interface and bonding mechanisms of plant fibre composites: An overview. Composites Part B: Engineering. 2016;101:31-45.
[22] Sanadi AR, Young RA, Clemons C, Rowell RM. Recycled newspaper fibers as reinforcing fillers in thermoplastic: 1 analysis of tensile and impact properties in polypropylene Journal of Reinforced Plastics and Composites. 1994;13(1):54-67.
[23] Reixach R, Franco-Marquès E, El Mansouri N-E, de Cartagena FR, Arbat G, Espinach FX, et al. Micromechanics of Mechanical, Thermomechanical, and Chemi-Thermomechanical Pulp from Orange Tree Pruning as Polypropylene Reinforcement: A Comparative Study. BioResources. 2013;8(3).
[24] Kompella MK, Lambros J. Micromechanical characterization of cellulose fibers. Polymer Testing. 2002;21(5):523-30.
[25] Bledzki AK, Gassan J. Composites reinforced with cellulose based fibres. Progress in Polymer Science. 1999;24(2):221-74.
[26] Yan L, Kasal B, Huang L. A review of recent research on the use of cellulosic fibres, their fibre fabric reinforced cementitious, geo-polymer and polymer composites in civil engineering. Composites Part B: Engineering. 2016;92:94-132.
[27] Kong C, Lee H, Park H. Design and manufacturing of automobile hood using natural composite structure. Composites Part B: Engineering. 2016;91:18-26.
[28] Rösler J, Harders H, Baeker M. Mechanical behaviour of engineering materials: metals, ceramics, polymers, and composites: Springer Science & Business Media; 2007.
[29] Thomason J. On the application of Weibull analysis to experimentally determined single fibre strength distributions. Composites Science and Technology. 2013;77:74-80.
[30] Cañigueral N, Vilaseca F, Méndez JA, López JP, Barberà L, Puig J, et al. Behavior of biocomposite materials from flax strands and starch-based biopolymer. Chemical Engineering Science. 2009;64(11):2651-8.
[31] Shah DU, Nag RK, Clifford MJ. Why do we observe significant differences between measured and 'back-calculated' properties of natural fibres? Cellulose. 2016;23(3):1481-90.
[32] Kelly A, Tyson W. Tensile porperties of fibre-reinforced metals - copper/tungsten and copper/molybdenum. Journal of the Mechanics and Physics of Solids. 1965;13(6):329-38.
[33] Espinach FX, Granda LA, Tarrés Q, Duran J, Fullana-i-Palmer P, Mutjé P. Mechanical and micromechanical tensile strength of eucalyptus bleached fibers reinforced polyoxymethylene composites. Composites Part B: Engineering. 2017;116:333-9.

533 [34] Granda LA, Espinach FX, López F, García JC, Delgado-Aguilar M, Mutjé P.
534 Semichemical fibres of Leucaena collinsii reinforced polypropylene:
535 Macromechanical and micromechanical analysis. Composites Part B: Engineering.
536 2016;91:384-91.
537 [35] Serrano A, Espinach FX, Julian F, del Rey R, Mendez JA, Mutje P. Estimation of
538 the interfacial shears strength, orientation factor and mean equivalent intrinsic
539 tensile strength in old newspaper fiber / polypropylene composites. Composites
540 Part B: Engineering. 2013(50):232-8.
541 [36] Fu SY, Lauke B. Effects of fiber length and fiber orientation distributions on
542 the tensile strength of short-fiber-reinforced polymers. Composites Science and
543 Technology. 1996;56(10):1179-90.
544 [37] Serrano A, Espinach FX, Tresserras J, del Rey R, Pellicer N, Mutje P. Macro and
545 micromechanics analysis of short fiber composites stiffness: The case of old
546 newspaper fibers-polypropylene composites. Materials & Design. 2014;55:319-24.
547 [38] Lopez JP, Mendez JA, Espinach FX, Julian F, Mutje P, Vilaseca F. Tensile
548 Strength characteristics of Polypropylene composites reinforced with Stone
549 Groundwood fibers from Softwood. BioResources. 2012;7(3):3188-200.
550
551 Figure Captions
552 **Figure 1: Cotton textiles manufacturing roadmap.**

553 **Figure 2: Tensile strength of the composites against its MAPP content. (a) Composites with a 30% of**
554 **cotton strands, (b) composites with a 40% of cotton strands**

555 **Figure 3: Dyed and faded cotton residue suspended in a water/hexane mixture.**

556 **Figure 4: Evaluation of the mean diameter of the single cotton fibers.**

557 **Figure 5: Intrinsic tensile strength of the dyed cotton strands submitted to single fiber tensile test,**
558 **against the gauge length**

559 **Figure 62: Linearized cumulative probability of failure against the natural logarithm of the**
560 **measured fiber tensile strengths for each gauge length.**

561 **Figure 7: Fiber length distribution of the WCS extracted from the 40% reinforced coupled composite.**

562

563 **Tables**
564 **Table 1: Experimental results used to solve the mRoM**

Fiber type	Fiber Content (%)	MAPP (%)	V^F	ε_l^C (%)	σ_l^{m*} (Mpa)
WCS	30	0	0.205	3.5	20.0
WCS	40	0	0.287	3.3	19.4
WCS	30	6	0.205	3.9	21.1
WCS	40	6	0.287	3.7	20.6
Virgin cotton	20	6	0.131	4.9	23.2

565

566 **Table 2: Chemical composition of the Surface and degree of polymerization of the virgin cotton strands**

Cellulose	α cellulose	Lignin	Extractives	Ash	Others	D. P.
93.8%	89.95%	0.55%	2.85%	1.15%	1.15%	4727

567

568 **Table 3: Experimental mean intrinsic tensile strengths of the fibers, and the Weibull analysis**

569 **outputs.**

Gauge length (mm)	σ_t^F ± SD (MPa)	$\sigma^F_{t,\,specific}$ (MPa/g cm^3)	Weibull shape factor β	Characteristic strength η (MPa)
6.35	739 ± 356	493	2.2	854
12.70	638 ± 310	425	2.3	735
19.05	540 ± 273	360	2.4	632
25.40	478 ± 256	319	2.4	539

570

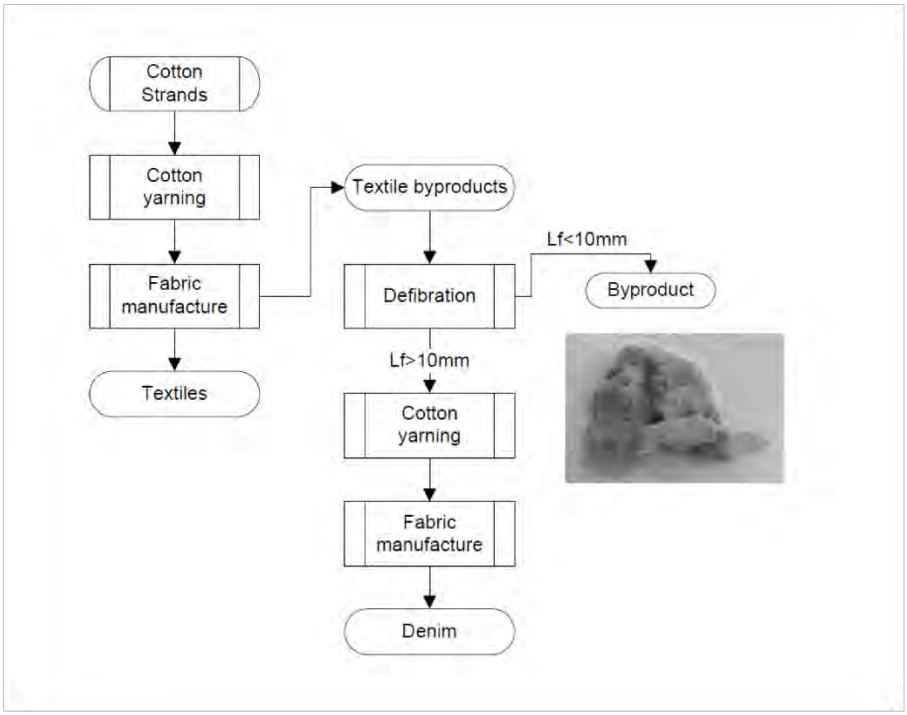

Figure 1: Cotton textiles manufacturing roadmap.

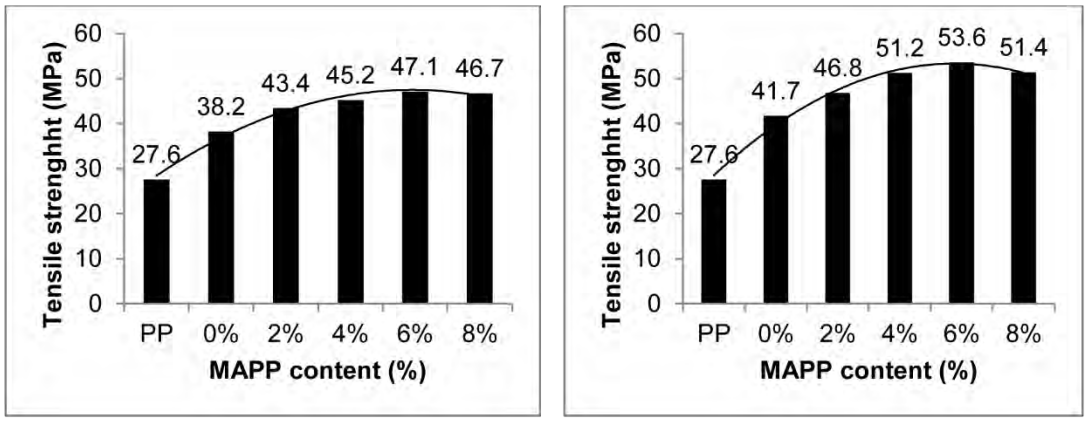

a b

Figure 2: Tensile strength of the composites against its MAPP content. (a) composites with a 30% of cotton strands, (b) composites with a 40% of cotton strands

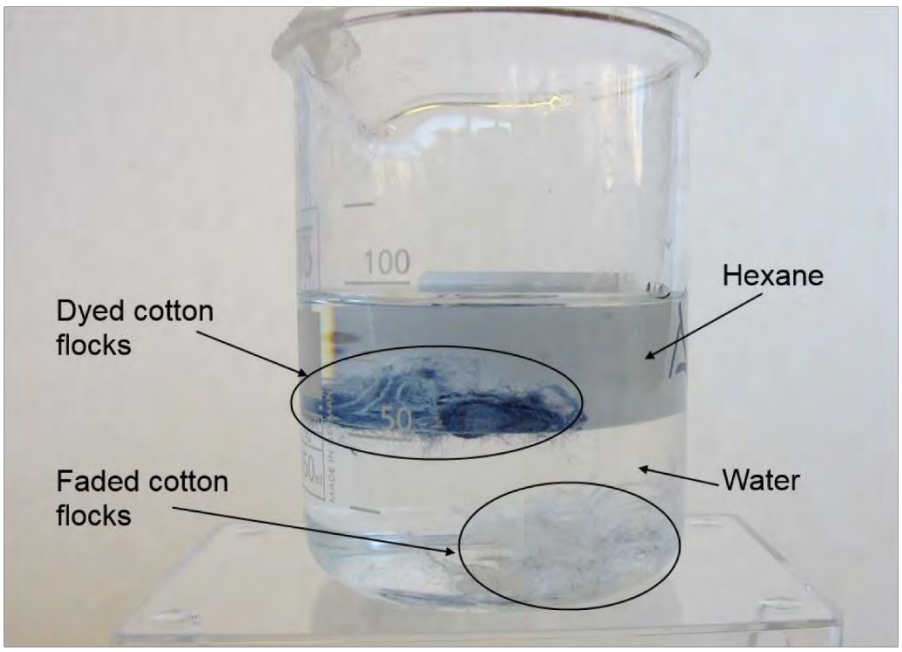

Figure 3: Dyed and faded cotton residue suspended in a water/hexane mixture.

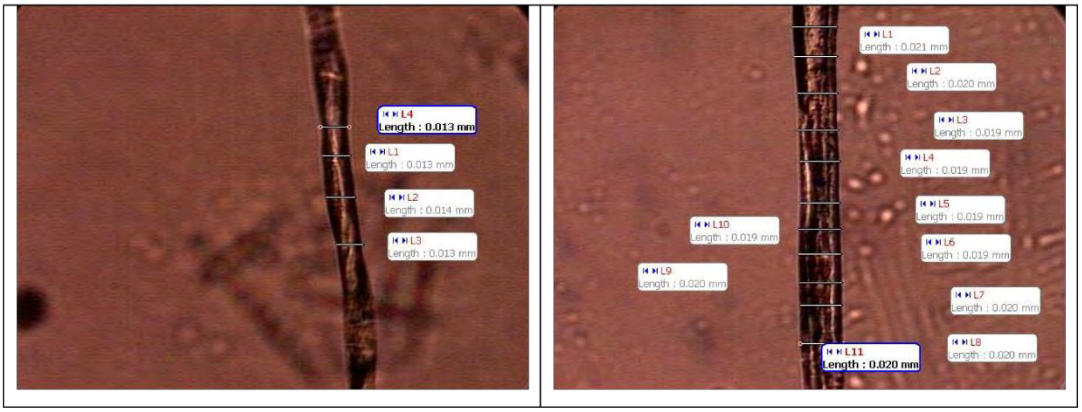

Figure 4: Evaluation of the mean diameter of the single cotton fibers.

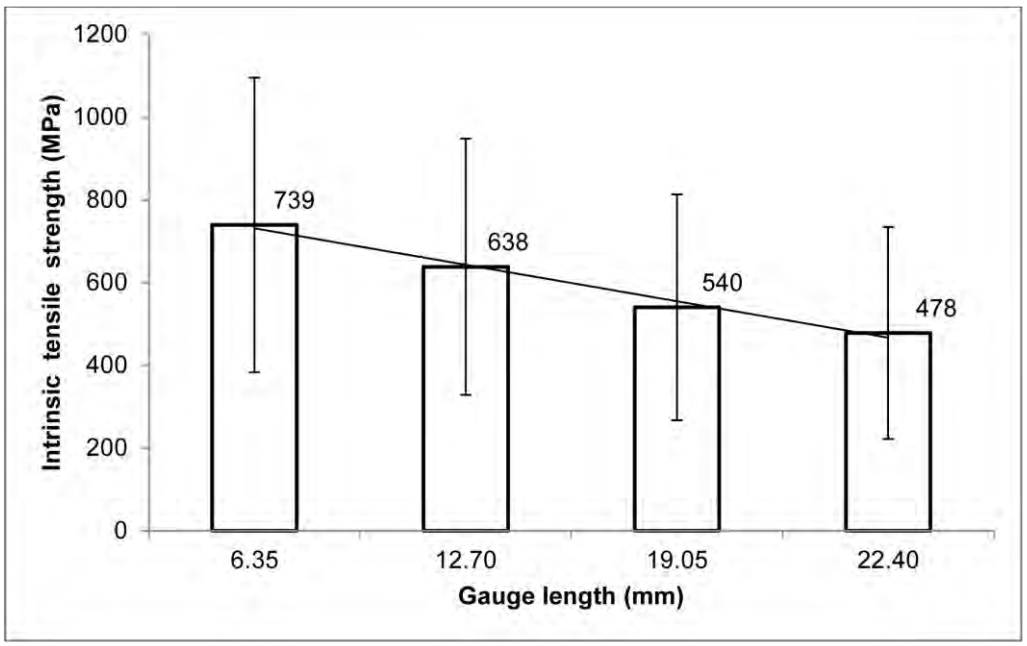

Figure 5: Intrinsic tensile strength of the dyed cotton strands submitted to single fiber tensile test, against the gauge length

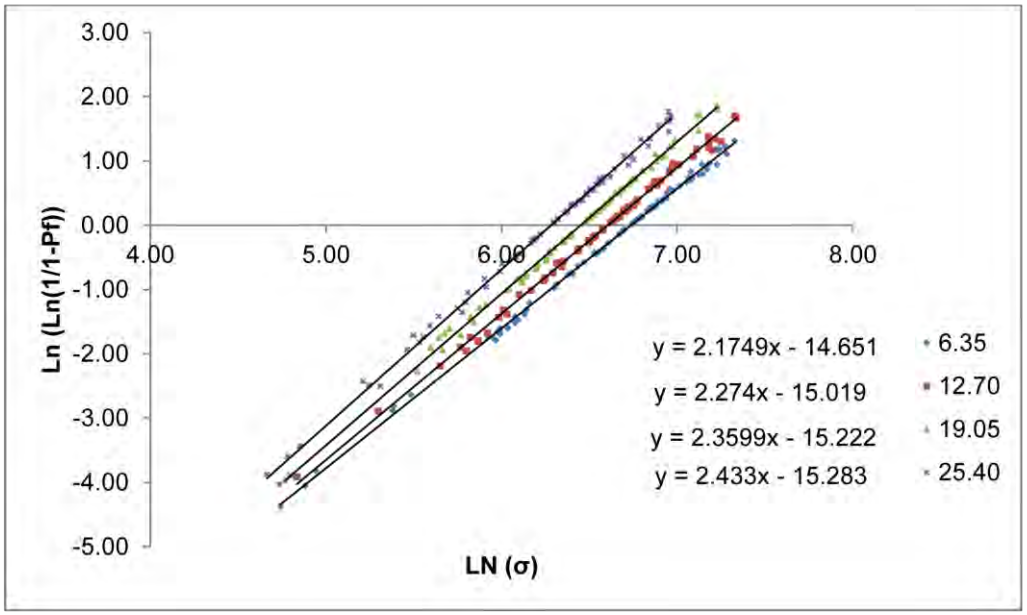

Figure 6: Linearized cumulative probability of failure against the natural logarithm of the measured fiber tensile strengths for each gauge length.

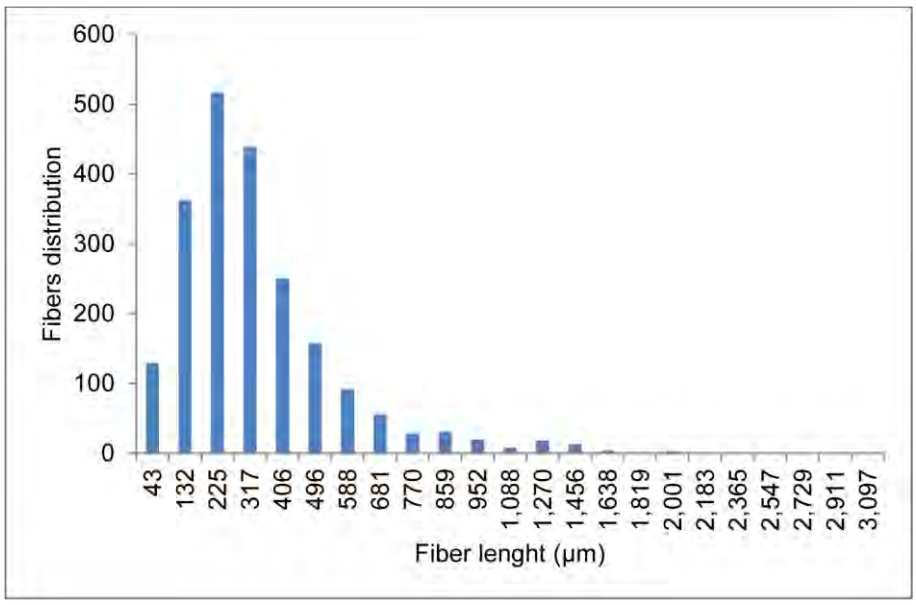

Figure 7: Fiber length distribution of the WCS extracted from the 40% reinforced coupled composite.

4.2. Artículo II

Textile Research Journal

Recycling dyed cotton textile byproduct fibers as polypropylene reinforcement

Journal:	*Textile Research Journal*
Manuscript ID	Draft
Manuscript Type:	Original Manuscript
Keywords:	Byproduct Cotton fibers, composites < Materials, Interfacial shear strength, Intrinsic fiber tensile strength, Mean fiber orientation angle
Abstract:	Textile industry generates a big amount of by-products that must be treated before being recycled or disposed. The treatments to extract the colorant agents are mandatory and involve costs and interacting with toxic reagents. A relevant amount of such by-products are short cotton dyed fibers. Cotton fibers are high quality cellulosic fibers and can be used as composite reinforcement. In this paper, dyed cotton fibers were used to formulate, obtain and tensile test composite materials. The impact of the presence of colorants was studied and such colorants enhanced the interphase between the matrix and the reinforcement. On the other hand, when a coupling agent was incorporated to the formulation of the composites, the dyes hindered the chemical interactions between the maleic acid and the OH groups of the cellulosic fibers. Nonetheless, the composite materials showed competitive mechanical properties, better than other natural fiber reinforced composites and comparable to some glass fiber-based ones. Dyed cotton fibers can be used as reinforcement without further treatments, increasing the value chain of the textile industry and decreasing the chemical treatments necessary to recycle or dispose of dyed textile fibers.

Girona, February 22, 2018

Dear Editor,

Please find attached our manuscript for publication in Textile Research journal:

Recycling dyed cotton textile byproduct fibers as polypropylene reinforcement.

By: Albert Serra, Quim Tarrés, Miquel F. LLop, Rafel Reixach, Pere Mutjé and Francesc X. Espinach

This work analyses the tensile properties of cotton fibres reinforced polypropylene composites. The cotton fibres are a by-product of the textile yarning industry, and due to its low length have no further use for such industry. Furthermore, the cotton fibres provide from inked textiles.

Inked textiles are difficult to recycle or dispose of, mainly because the colorants must be extracted before disposing. Such colouring agents are known to be carcinogenic or toxic, thus, any alternative use that encapsulates these reagents will be environmentally beneficial.

Additionally, the colorants change the polarity of the cotton fibre surfaces, allowing a better compatibility between such surfaces and the matrices.

The work provides information about the tensile properties and the quality of the interphase of inked cotton fibres reinforced composites, and shows that it is possible to obtain competitive materials using a by-product of the textile industry.

We therefore believe that our work, as described in this manuscript, would be very much of interest to Scientifics. Our aim is to show the scientific community how they can benefit from the use of a by-product from the textile industry, obtaining composite materials with tensile properties comparable to commercial products, with a relatively low cost and weight.

We confirm that this manuscript has not been published elsewhere and is not under consideration by another journal, and all authors have approved the manuscript and agree with its submission to Textile Research Journal.

In case of any questions please do not hesitate to contact us anytime.

The corresponding author is

Dr. Quim Tarrés

For all the authors.

Group LEPAMAP, Department of Chemical Engineering

Escola Politècnica Superior. C/M. Aurèlia Campmany, 61, 17003 Girona, Spain

Phone : 34 669 996 998,

FAX +34 972 418 39

Original article

Abstract

Textile industry generates a big amount of by-products that must be treated before being recycled or disposed. The treatments to extract the dyeing agents are mandatory and involve costs and interacting with toxic reagents. A relevant amount of such by-products are short cotton dyed fibers. Cotton fibers are high quality cellulosic fibers and can be used as composite reinforcement. In this paper, dyed cotton fibers were used to formulate, obtain and tensile test composite materials. The impact of the presence of dyes was studied and such dyes enhanced the interphase between the matrix and the reinforcement. On the other hand, when a coupling agent was incorporated to the formulation of the composites, the dyes hindered the chemical interactions between the maleic acid and the OH groups of the cellulosic fibers. Nonetheless, the composite materials showed competitive mechanical properties, better than other natural fiber reinforced composites and comparable to some glass fiber-based ones. Dyed cotton fibers can be used as reinforcement without further treatments, increasing the value chain of the textile industry and decreasing the chemical treatments necessary to recycle or dispose of dyed textile fibers.

Keywords

Byproduct Cotton fibers, Composites, Interfacial shear strength, Intrinsic fiber tensile strength, Mean fiber orientation angle

Introduction

Environmental concern has increased the sensitiveness of the whole society towards greener products and processes. In this sense, the scientific community has devoted a great effort in substituting mineral fiber reinforcements like glass fiber with more sustainable alternatives, like natural fibers.[1] The literature reveals a positive evolution of the mechanical properties of natural fiber-based composites as consequence, among others, of the achievement of: strong interphases between the fibers and the matrices and mixing methods that ensure better aspect ratios and good dispersions of the reinforcements inside the composites.[2] The literature also shows an increasing interest in the use of recycled fibers or fibers from byproducts, like agroforestry waste, pruning or used newspaper. Such fibers were used to prepare polyolefin-based composites and obtained quite competitive mechanical properties.[3-5]

The abovementioned environmental concern has impacted the textile industry. This industry is in the search of an strategic balance between “fashion and nature”.[6] This industry generates a high amount of wastes estimated to 12.4 and 26.0 million tons in the United States and China alone.[7] There are a wide variety of proposals to reuse or recycle such wastes; from biogas production or ethanol production, to its regeneration or its use as composite reinforcement.[8-13] Nonetheless, a big amount of textile wastes incorporate dyes causing difficulty for its recycling or disposal. These dyes must be removed before any of such actions. Besides, these dyes are known to be carcinogenic or toxic.[14] Nonetheless, such dyes also reduce the hydrophilic nature of the cotton fibers. This

impact is favorable if these fibers must be blended with hydrophobic matrices to prepare composite materials.[8, 15] In that sense, a lower hydrophilicity can enhance the fiber/matrix interphase without using coupling agents. Thus, the exploitation of dyes as a sort of coupling agent answers two needs. On the one hand, fibers are not deinked and the dyes are not discharged to the environment. On the other hand, the interphase can be enhanced and the use of further reactants is limited agreeing with the principles of green chemistry. In a previous article, some of the authors used a simplified method to research the tensile strength of short recycled fibers from cotton flocks reinforced polypropylene composites.[15] In this work, the authors used a Kelly and Tyson modified equation, and the experimental results of the tensile tests of the composites adding 30 and 40% w/w of reinforcement. Two sets of such materials were prepared, a first without coupling agents and a second adding 6% of MAPP (with respect to the reinforcement content). Additionally, a morphologic analysis allowed knowing the distribution of fiber length's and its mean lengths and diameters. With the objective of knowing the intrinsic tensile strength of the cotton fibers, single specimens of such fibers were submitted to tensile test at different gauge lengths (1", ¾", ½" and ¼"). A Weibull analysis of the results was used to obtain the theoretical tensile strength of a cotton fiber with the mean length of the reinforcements used to prepare the composites. A numerical method provided a solution for the Kelly and Tyson modified equation were the orientation factor and the interfacial shear strength of the coupled 30 and 40% reinforced composites converged to the same values. Previous researches endorsed such hypotheses.[16-18] The solution converged quickly towards 14.8 MPa interfacial shear strengths and 0.33 orientation factor values. Then, the obtained orientation factor was used to compute the interfacial shear strength of the uncoupled composites, obtaining values around 7 MPa. While the obtained values were in line with the literature, the proposed method was based in a number of assumptions that can impact the results. Moreover, some author consider controversial the use of intrinsic tensile strengths of individual fibers experimentally measured in front of back calculated values.[19]

In this work, the Kelly and Tyson modified equation was solved using the Bowyer and Bader method, a widely accepted strategy for modelling the micromechanics of a short fiber reinforced composite. Composites adding 20, 30, 40 and 50% of reinforcement were considered the most interesting form an engineering and industrial point of view, due to their mechanical properties. Lower reinforcement contents provided uncompetitive mechanical properties, and higher contents resulted in materials with high mold flow indexes, and difficult to use in injection molding machines. The intention of the researchers is presenting a possible mean to recycle textile wastes in the shape of reinforcements for composite materials. Of course, the developed and tested materials must show mechanical properties similar to that of commercial materials or other materials profusely investigated as wood fiber reinforced polyolefin. Consequently, recycled cotton reinforced polypropylene composites were formulated, obtained and tested. The tensile strength of such composites were compared with commodities as glass fiber reinforced polypropylene. Finally, the quality of the interphases of the materials was investigated by using micromechanics models to obtain the intrinsic tensile strength of the fibers, the interfacial shear strengths and the orientation factors. The values were compared with those previously obtained and the differences were discussed.[15]

Materials and methods

Materials

The cotton residues (CF) were kindly supplied by Fontfilva S. L. (Olot, Girona, Spain). These residues were already been treated with a reactive dye. A polypropylene (PP) (Isplen PP090 62M) was used as matrix and was provided by Repsol-YPF (Tarragona, Spain). A maleic-grafted polypropylene (MAPP) (Epolene G3015) from Eastman Chemical Products (San Roque, Spain), was used as coupling agent to improve the compatibility between the cotton residues and the PP. This MAPP had an acid number of 15 mg KOH/g and Mn of 24800.
Decalin (Decahydronaphthalene) with a 190ºC boiling point and 97% purity, was used, without further purification, to dissolve PP matrix in the fiber extraction from composites. Decalin was acquired from Fischer Scientific (Madrid, Spain).

Methods

Composite processing

While the cotton residue had inadequate length for spinning, its length was too long to ensure a proper dispersion of the reinforcement in the composite. Thus, the CF were cut to 1mm mean length in a blade mill. The resulting fibers were mixed with the PP matrix at different rates. Batches with and without coupling agent were prepared. The mixing was carried out in a mixer Brabender Plastograph intensive melt mixer (Brabender, Duisburg, Germany). The operation lasted 10 min, at 185ºC and 80rpm. The obtained blends were pelletized in a blades mill. The pellets were stored in a climatic chamber at 80ºC during at least 24h.
The composites will be tagged using the code *x*CF*y*PP*z*MAPP, were *x*, *y* and *z* are the reinforcement, matrix and coupling agent contents, respectively.

Sample obtaining

The standard dog bone specimens, in accordance with ASTM D638 [20], were obtained by mound injection in a Meteor-40 injection machine (Mateu & Solé, Spain). The processing parameters were; first and second pressures 120 and 37.5 kg/cm^3, respectively, and 175,175 and 190ºC in the three heating areas. At least 10 specimens for each composite formulation were obtained. Prior to their mechanical characterization, and in accordance with ASTM D618 [21], the samples were stored in a conditioning chamber at 50% relative humidity and 23ºC for at least 48 hours.

Mechanical characterization

The specimens were tensile tested in a Universal testing machine instrom TM 1122), fitted with a 5 kN load cell and operating at a rate of 2 mm/min, in agreement with ASTM D638 [20]. Results were obtained from the average of at least 5 samples.

Morphological analysis of the fibers

The cotton fibers were extracted from the composites by matrix solubilization in a Soxhlet apparatus. The extraction of the fibers from the composite was considered necessary its morphology usually changes during composite preparation and specimen obtaining processes. The extraction lasted 24h. The obtained fibers were rinsed with

acetone and distilled water to remove any solvent residue. These fibers were morphologically characterized in a Kajanni analyser (FS-300). The equipment returned mean length and diameter, as well as diameter and length distributions after measuring 2500 to 3000 sample fibers. A minimum of two samples were analyzed.

Micromechanics

Modified rule of mixtures

An original modified rule of mixtures was developed for the Young's modulus of short fiber reinforced composites.[22] Nonetheless, such equation was quickly adapted to the tensile strength of these composite materials. This modified rule of mixtures (mRoM) models the tensile strength of the composite as the contribution of two phases, the matrix and the reinforcement:

$$\sigma_t^C = f_c \cdot \sigma_t^F \cdot V^F + (1 - V^F) \cdot \sigma_t^{m*} \quad (1)$$

Where σ_t^C and σ_t^F are the ultimate tensile strength of the composite and the intrinsic tensile strength of the reinforcement, respectively. V^F is the volume fraction of the reinforcement, and σ_t^{m*} is the contribution of the matrix at the ultimate strain of the composite. In order to add the effects of the quality of the interphase and the orientation and morphology of the reinforcement, a coupling factor (f_c) was added to the original rule of mixtures. This coupling factor can be also found as the multiplication of an orientation and a length factors, α_1 and α_2, respectively. It is accepted that well bonded composites show coupling factors ranging from 0.18 to 0.2.[18]

The main problem using this mRoM (equation 1) is obtaining the value of the intrinsic tensile strength of the reinforcement. In its absence the mRoM shows two incognita, f_c and σ_t^C. While the intrinsic tensile strength of the fibers can be obtained by experimentation, these methods are usually difficult or expensive due to the morphology of the fibers. Moreover, natural fibers show a high dispersion of their mechanical properties, and therefore it is necessary to perform a huge amount of single fiber tests. Besides, as mentioned in the introduction, some authors state that the properties of a reinforcement inside a composite can oscillate noticeably from its properties as a single fiber.[19] In any case, a considerable number of authors advocate in favor of the use of micromechanics models like the Kelly and Tyson modified equation with the solution provided by Bowyer and Bader to compute such intrinsic tensile strengths.[17, 23-25]

However, it is possible to recombine the mRoM and evaluate the neat contribution of the reinforcements as a function of its volume fraction. This reformulation is known as the Fiber Tensile Strength Factor (*FTSF*) and was previously used to evaluate the meat contribution of different fibers to the tensile strength of composites:

$$\frac{\sigma_t^C - (1 - V^F) \cdot \sigma_t^{m*}}{V^F} = f_c \cdot \sigma_t^F \quad (2)$$

Equation 2 is a line that goes through the origin and has a slope that reflects the neat contribution of the fibers against its volume fraction. Such line is obtained by linear regression of the points obtained by introducing the experimental data in equation 2.

Kelly and Tyson modified equation

Kelly and Tyson developed their original equation to deal with the micromechanics of aligned short fiber reinforced composites[23]. Later, a modified equation was proposed to

include the effect of the orientation of the fibers to their contribution to the final tensile strength of the composites. Kelly and Tyson based their equation in the mRoM and considered two kinds of fibers depending on their lengths; subcritical and supercritical fibers. The classification is based on the shear lag theory and the critical length is defined by:

$$l_C = \frac{\sigma_t^F \cdot d^F}{2 * \tau} \quad (3)$$

Were τ is the interfacial shear strength that defines the maximum shear loads transfers allowed by the interphase between the reinforcement and the matrix and d^F is the mean fiber diameter. In that sense only the supercritical fibers will have enough area to break during composite loading, as the tensile strength of the specimen is transferred to the fibers by shear load along the fiber matrix interphase. Thus, the contribution of the fibers, under these theory, is highly influenced by its length, and by its consideration as supercritical or subcritical.

The Kelly and Tyson modified equation can be expressed as:

$$\sigma_t^C = \chi_1(X + Y) + Z \quad (4)$$

Were X and Y are the contributions of the subcritical and supercritical fibers, respectively, and Z the contribution of the matrix to the tensile strength of the composite. Both kinds of fibers show different load states. As aforementioned, the contributions of the fibers are equalized by an orientation factor, already introduced with the mRoM.

The load states of the fibers and the matrix are defined by:

$$X = \sum_{l=0}^{l=lc} \left[\frac{\tau \cdot l \cdot V_l^F}{d^F}\right] \quad (5)$$

$$Y = \sum_{l=lc}^{\infty} \left[\sigma_t^F \cdot V_l^F \cdot \left(1 - \frac{\sigma_t^F \cdot d^F}{4 \cdot \tau \cdot l}\right)\right] \quad (6)$$

$$Z = (1 - V^F) \cdot \sigma_t^{m*} \quad (7)$$

Almost all the variables are already defined. Here, d^F and l are the diameter and the length of the fibers along a distribution obtained during the morphological analysis were the volume fraction for a certain men length (V_l^F) will be also defined.

In its presented shape, the Kelly and Tyson modified equation can't be solved because shows three incognita; the interfacial shear strength, the orientation angle and the intrinsic tensile strength of the reinforcement. Even so, Bowyer and Bader proposed a method to solve the equation.

Bowyer and Bader solution

The solution was based in a hypothesis: when a composite is loaded under tensile stress it shows a deformation. Bowyer and Bader supposed that the composite and the fibers showed the same deformations or strains[24]. Thus, the strain of the composite (ε_t^C) was the same than the fibers' (ε_t^F). On the other hand, it is know that for elastic materials a load state is expressed by the multiplication of the strain by its young's modulus. Thus, under elastic conditions, the stress state of a fiber under a certain strain will be defined by:

$$\sigma_1^F = \varepsilon_1^F \cdot E_t^F = \varepsilon_1^C \cdot E_t^F \quad (8)$$

Where F and C refer to the fiber and the composite, respectively. E_t^F is the intrinsic Young modulus of the reinforcement.

Bowyer and Bader demonstrated that picking the experimental data of two strain states were able to compute the values of the orientation factor and the interfacial shear

strength, allowing the use of the modified Kelly and Tyson equation to compute the intrinsic tensile strength.
The intrinsic Young's modulus of the fiber was computed by using the Hirsch equation.[26]

Results and discussion

The chemical compatibility between the different phases of a composite it's a main factor to obtain a strong interphase. Natural fibers from annual plants or wood show a lignocellulosic chemistry in its surfaces and a hydrophilic nature. On the other hand, polyolefin like polypropylene have a hydrophobic nature. Thus, both phases are incompatible and it is impossible to obtain strong interphases as an effective wetting of the fibers will not be obtained[25-27]. Usually, uncoupled composite materials based on polyolefin reinforced with natural fibers show slight increases of the tensile strength of their matrix for low reinforcement contents, and in some cases, high reinforcement contents render strengths lower than the matrix's[3, 30, 31]. Thus, the use of chemical treatments as alkali or the use of coupling agents are needed to obtain a strong interphase. The literature shows that fiber alkali treatments can increase the compatibility between the natural fibers and the matrix. Such alkali treatments decrease the hydrophilic nature of the fibers, slightly increasing the quality of the interphase between the reinforcement and the matrix[3, 32]. Anyhow, these treatments involve the use of reactants and the generation of byproducts, decreasing the yield of the reinforcement. In this sense, it is possible to obtain high yield mechanical pulps with a 99% yield, while obtaining chemi-thermomechanical pulps reduced the yield to 90%[32]. Nonetheless, all the mentioned processes involve using raw materials and generating different percentages of byproducts. The literature also shows that, in the case of lignocellulosic fibers reinforced polypropylene, the best results are obtained by using MAPP as coupling agent. MAPP interacts with both phases. On the one hand the PP chains of the MAPP entangle with the matrix, obtaining a strong mechanical anchoring. On the other hand, the maleic acid created hydrogen bonds and covalent ester links between its anhydride groups and the hydroxyl groups present at the fiber surfaces.
Figure 1 shows the stress strain curves for the composites adding a 50% of reinforcement content.

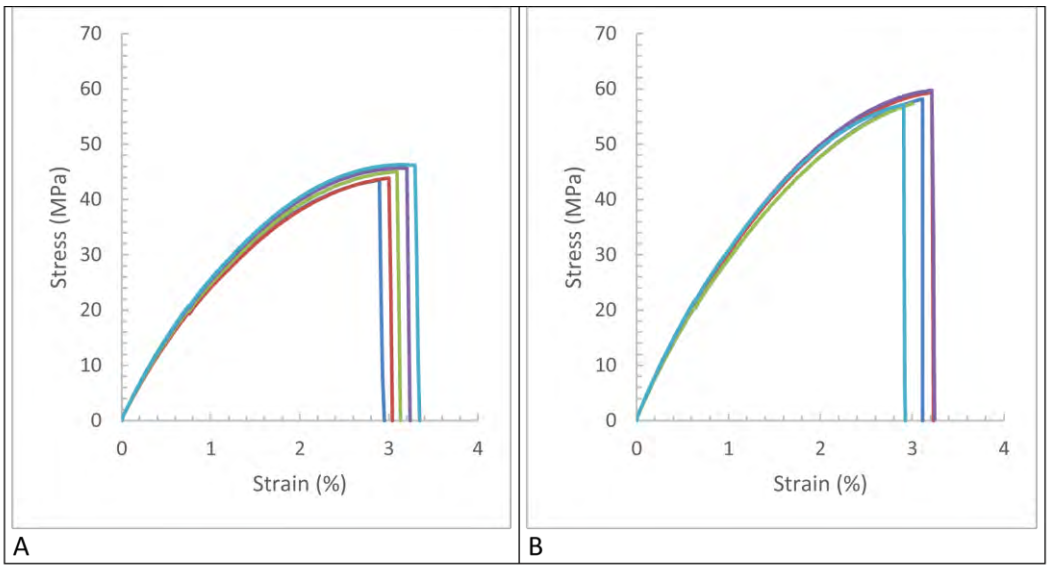

Figure 1: Stress-strain curves of the coupled and uncoupled composites adding 50% w/w of reinforcement. A: Uncoupled composites, B: composites adding a 6% of MAPP.

Five samples of every composite were tested obtaining the experimental values shown at table 1. It was found that both, coupled and uncoupled composites increased noticeably the tensile strength of the matrix. It was found also that both kinds of composites showed similar strains at break. Nonetheless, the coupled ones obtained noticeably higher tensile strengths. The shape of the curves, with similar initial slopes, but increases of the curvature in the case of the uncoupled composites indicates the premature failure of one of the phases, presumably the interphase.

The materials with lower reinforcement contents showed similar behaviors (table 1).

Table 1: Experimental results of the tensile tests of the coupled and uncoupled composites, contribution of the matrix and neat contribution of the reinforcement to the tensile strength of the composites.

Composite	V^F (%)	σ_t^C (MPa)	ε_t^C (%)	σ_t^{m*} (MPa)	$f_c \cdot \sigma_t^F \cdot (V^F)$
PP	-	27.6 ± 0.51	9.3 ± 0.23	-	-
20CF80PP0MAPP	0.127	35.0 ± 0.45	3.8 ± 0.12	20.86	16.8
30CF70PP0MAPP	0.200	38.2 ± 0.78	3.5 ± 0.09	20.01	22.2
40CF60PP0MAPP	0.280	41.7 ± 0.84	3.3 ± 0.14	19.38	27.7
50CF50PP0MAPP	0.368	45.4 ± 1.14	3.1 ± 0.16	18.70	33.6
20CF80PP6MAPP	0.127	41.7 ±0.66	4.3 ± 0.18	22.08	22.4

30CF70PP6MAPP	0.200	47.1 ±0.74	3.9 ± 0.15	21.13	30.2
40CF60PP6MAPP	0.280	53.6 ±0.97	3.7 ± 0.13	20.59	38.8
50CF50PP6MAPP	0.368	58.3 ±1.23	3.2 ± 0.08	19.05	46.26

Despite the reinforcement content, uncoupled and coupled composites showed noticeable increases of their tensile strength when the percentage of reinforcement was increased. The uncoupled composites increased the tensile strength of the matrix a 27%, 38%, 51% and 64% when the reinforcement contents increased from 20 to 50%. This was not the expected behavior for the uncoupled composites. The literature shows that uncoupled composite materials based on polyolefin reinforced with natural fibers show slight increases of the tensile strength of their matrix for low reinforcement contents, and in some cases, high reinforcement contents render strengths lower than the matrix's (figure 2)[3, 30, 31]. The reason of the increase of the tensile strength of the uncoupled composites was attributed to the presence of dyes in the cotton fibers. This dyes modify the polarity of the cotton fiber surface in a manner similar to an alkali treatment.[15] The literature shows that uncoupled cotton reinforced PP composites showed tensile strengths lower that the matrix when percentages or reinforcement ranging from 10 to 30% were incorporated to the composite[34]. Thus, the increasing of the tensile strength of the uncoupled composites reinforced with recycled and dyed cotton fibers was attributed to the presence of the dyeing agents.

One of the goals of a new material is increasing at least one or more properties of existing ones, while maintaining other properties. In the case of short fiber reinforced composites, glass fiber reinforced polypropylene are considered commodities and are widely used in the automotive industry, product design and as building materials[35-37]. The literature also shows the intense effort made by the researchers to employ more sustainable reinforcements as wood fibers, obtaining noticeable results. The literature also shows efforts to use recycled fibers as those from old newspaper, obtaining also materials able to substitute GF reinforced PP materials[38]. Figure 2 shows the evolution of the tensile strength of some of the abovementioned composites against its reinforcement volume fractions.

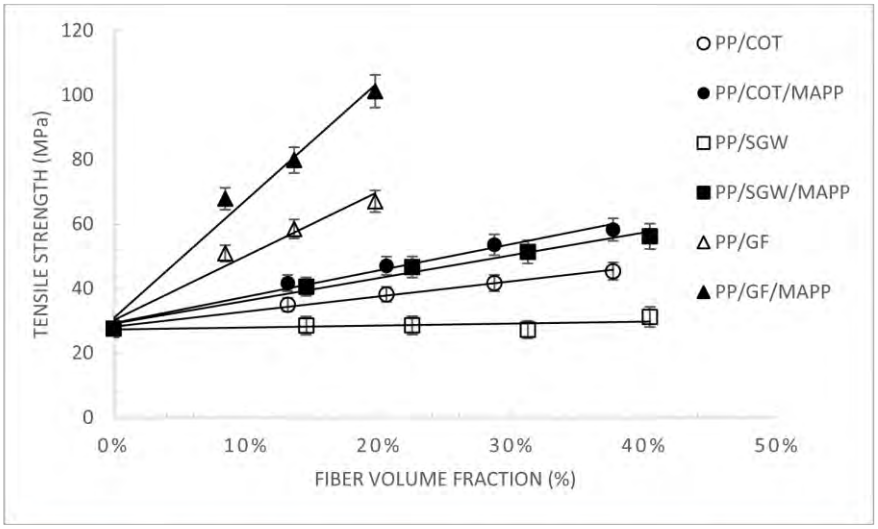

Figure 2: Tensile strength of short semi-aligned reinforced polypropylene composites against reinforcement contents.

Figure 2 shows the tensile strength of stone groundwood (SGW) reinforced PP composites.[2, 18] SGW is a widely available mechanical pulp usually used in the papermaking industry. The chemistry of the surface of both fibers is quite different, on the one hand, the cotton fibers surface is almost cellulose, with 93.8%, and only 0.05% of lignin.[15] On the other hand, SGW presents a lower 68.4% content of cellulose and higher 27.6% lignin content.[18] Nonetheless, the presence of higher cellulose contents in the cotton fiber surfaces can be seen as an advantage, as the presence of OH groups will be higher. The uncoupled cotton fiber-based composites, compared to uncoupled SGW-based composites showed a clearly different behavior. The SGW composites did not showed noticeable changes of their tensile strength whatever its reinforcement contents. On the other hand, the uncoupled cotton composites showed noticeable and linear increases of their tensile strength when the percentage of reinforcement increased. This behavior was similar to old newspaper fibers (ONF) reinforced PP uncoupled composites[38, 39]. Newspaper fibers are also a byproduct but, unlike SGW, were submitted to a mild bleaching process that impacted the polarity of the ONF surface. ONF uncoupled composites showed increases of their tensile strength up to 30% w/w fiber contents. Higher ONP contents rendered decreasing tensile strengths. Thus, the impact of the chemical treatments of the fiber surfaces showed a lower impact on the tensile strength of the composites than the presence of dyes. Thus, provably dyes impacted the quality of the interphase between the matrix and the reinforcements, obtaining higher values than those obtained by chemical fiber surface treatments.

Figure 1 also shows the tensile strength of uncoupled glass fibers reinforced PP composites.[2] It is clear that the tensile strengths of uncoupled cotton-based composites are far from GF-based ones. Nonetheless, this is also true for the rest of natural fiber reinforced polyolefin composites. The tensile strength of an uncoupled 50% cotton reinforced composites is equivalent to a 5% GF uncoupled composite.

As it was mentioned, the use of coupling agents like maleic-grafted polyolefin is a common strategy used to obtain strong interphases between natural fibers and

polyolefin.[40-42] The coupled composites rendered higher tensile strengths than the uncoupled ones at the same reinforcement contents (Table 1). These composites increased the tensile strength of the matrix a 51%, 70%, 94% and 111% when the reinforcement contents were increased from 20 to 50%, respectively. Compared to the uncoupled composites, at the same reinforcement contents, the strengths were 19%, 22%, 28% and 28% higher, respectively. Thus, the addition of a coupling agent in the formulation of the composites impacted positively the tensile strength of the composites. Compared with the SGW- based composites at the same reinforcement contents, the behavior of the tensile strength was similar, increasing linearly with the reinforcement content (Figure 1). Moreover, the strengths of the cotton-based composites were always higher than the SGW-based ones. The main reason can be due to the higher intrinsic tensile strength of cotton fibers than SGW's. The intrinsic tensile strength of SGW and cotton fibers used as reinforcement were reported to be 612 MPa and 950MPa, respectively.[2] Nonetheless, the intrinsic tensile strength of the cotton fibers was obtained by single fibers tensile test and the value for SGW by micromechanics models. Anyhow, and despite the measuring method, the intrinsic tensile strength of cotton fibers was noticeably higher than SGW's. Thus, the tensile strength of the cotton-based composites was expected to be noticeably higher than SGW-based ones. Thus, the quality of the interphase between the cotton fibers and the PP increased but not as much as expected due to MAPP presence. In order to establish the impact of the dyes in the tensile strength of the composites a batch of coupled materials, based on 20% w/w un-dyed cotton contents, were prepared and tensile tested.[15] These coupled composites rendered a tensile strength of 46.9 ±1.56 MPa and a strain at break of 4.9±0.24%. The results are noticeably higher than the obtained with coupled composites based on dyed cotton reinforcements (table 1). This fact shows that while the presence of dyes helps obtaining an interphase also hinders obtaining stronger interphases in the presence of MAPP.[15]

Compared with the GF-based composites, cotton-based composites showed tensile strengths similar to uncoupled GF composites up to 20% w/w GF contents. The coupled GF composites showed tensile strengths higher than the other composites. Nonetheless a 50% cotton composite had a tensile strength not far from a 10% GF coupled composite. While both values are different, a clever engineering design can allow the substitution of GF composites by CF-reinforced composites.

From an environmental point of view, 10% GF-based composited add 90% w/w of a PP oil-based polyolefin, and 10% w/w of a high energy production demanding reinforcement. On the other hand, 50% cotton-based composites reduces to 50% w/w the content of oil-based materials, adds a little content of MAPP, and around 50% w/w of a byproduct as reinforcement. The use of such reinforcement avoids undying processes and landfill or incineration of the byproduct.

Nonetheless, while uncoupled cotton-based composites showed comparatively strong interphases, the coupled composites showed presumably improved interphases. A fiber tensile strength factor (*FTSF*) was obtained to obtain the net contribution of the fibers to the tensile strength of the composite (Figure 3)

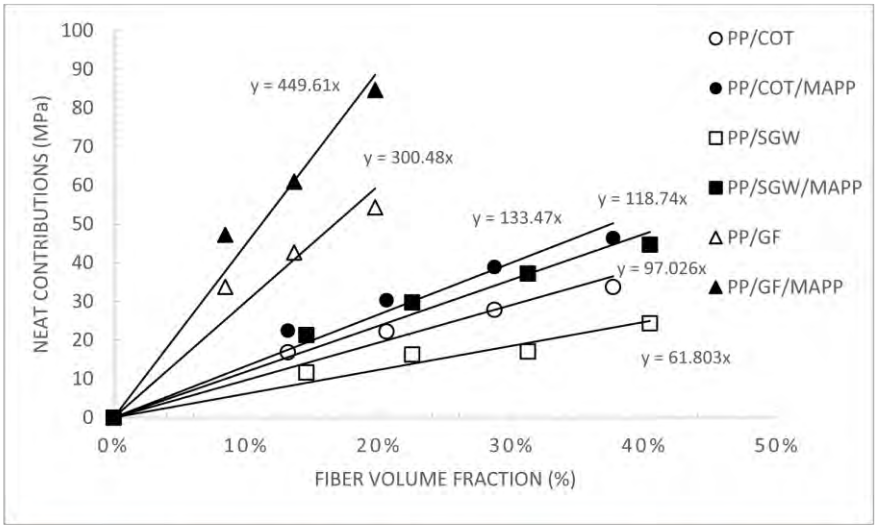

Figure 3: Neat contribution of the reinforcements to the tensile strengths of the composites.

The quality of the interphase hinders the neat contribution of the fibers, because if an interphase is weak the load transfer by shear loads in the interphase will be limited. The *FTSF* shows that the contribution of cotton fibers increased from uncoupled to coupled composites a 37.5%, with a neat increase of 36.4 MPa. This increase is noticeably lower than the obtained for SGW fibers with a 92%, 56.9 MPa increase. Thus, presumably, the quality of the interphase of the SGW-based composites increased more than the cotton based one. The GF-based composites increased their *FTSF* a 49.6%, but the neat increase was 149.1 MPa. Compared to cotton composites, the rest of materials showed noticeable increases of the neat contribution of the fibers, and presumably higher increases of the quality of their interphases. Thus, a micromechanics modelling was proposed in order to evaluate the quality of the interphase of cotton-based composites.

Micromechanics

The method proposed to evaluate the quality of the interphase and the intrinsic tensile strength of the reinforcements was the Kelly and Tyson modified equation, with the solution provided by Bowyer and Bader. This equation incorporates the morphology of the reinforcements to group the fibers among subcritical and supercritical ones. Figure 4 shows the length distribution of the fibers extracted from the coupled composite with 20% reinforcement contents.

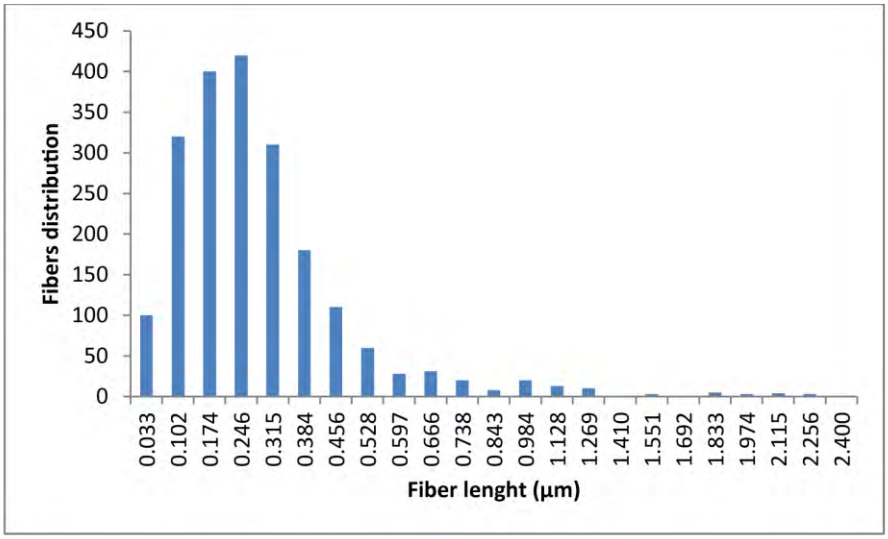

Figure 4: Length distribution of the fibers extracted from the coupled composite with a 20% of reinforcement.

As it was mentioned in the methods section cotton fibers were cut to 1mm mean lengths. The distribution of the fibers extracted from the composite shows the notable decrease in the number of fibers longer than 1mm with a noticeable decrease of the mean length of the fibers. The length of the fibers decreases during the mixing and mold injection processes due to attrition. This phenomena increases with the reinforcement content. Table 2 show the main morphologic properties of the reinforcements extracted from all the composites.

Table 2: Morphology of the reinforcements.

Composite	L_a (µm)	L_l (µm)	d^F (µm)	L_a/d^F
20CF80PP0MAPP	284	512	16.5	17.2
30CF70PP0MAPP	274	459	16.5	16.6
40CF60PP0MAPP	250	396	16.5	15.2
50CF50PP0MAPP	222	351	16.5	13.5
20CF80PP6MAPP	293	509	16.5	17.8
30CF70PP6MAPP	253	406	16.5	15.3
40CF60PP6MAPP	210	339	16.5	12.7
50CF50PP6MAPP	185	299	16.5	11.2

As it was expected, the mean length of the fibers decreased at the same time as its content in the composites increased. It was also found that coupled composites showed lower

mean lengths than the uncoupled ones. Although the mixing time was reduced due to the use of a multi-kinetic mixer, it was enough for the better interphase to transfer higher shear loads to the fibers and reduce its length. The shape of the fiber length distributions also changed with the amounts of reinforcement. The composites with higher amounts of reinforcement showed a higher presence of short fibers and a gradual diminution of long fiber presence (>1.5mm). The mean diameter of the fibers remained very stable at 16.5 µm. A weighted length was computed and used during micromechanics modelling. The use of weighted lengths instead of the arithmetic lengths is proposed to equalize the contribution of long fibers.[4, 17, 28]

The Bowyer and Bader solution is based on the evaluation of the contributions of the matrix and the reinforcement at two strain points in the elastic section of the stress strain curve of the composite. Figure 5 shows the stress strain curves of the composites and the matrix, and the stress values used to solve the equation. The intermediate strain points were ¼ and ½ of the strain at break of the composites.

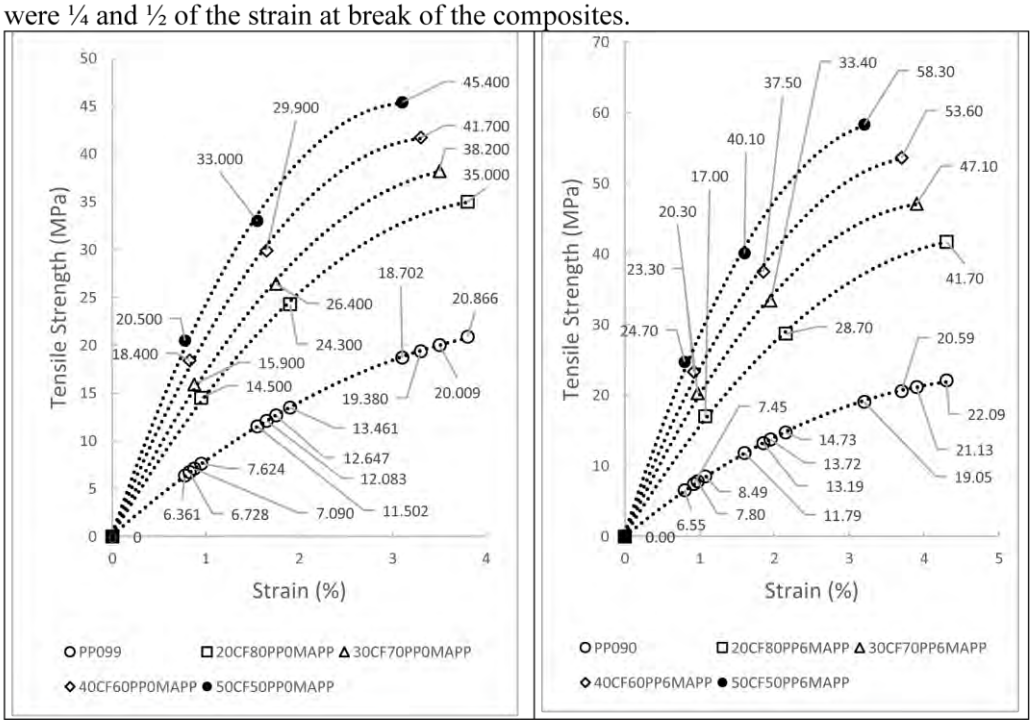

Figure 5: Stress-strain curves of the coupled and uncoupled composites and values at two intemediat strain states used to solve the Kelly and Tyson modified equation.

The stress strain diagrams show the increases of the tensile strength of the composites and the decreases of the strain at break against the reinforcement content. The diagrams also show the contribution of the matrix to the tensile strength of the composite, at failure and at the two intermediate points used to solve the Kelly and Tyson equation. The intrinsic Young's modulus of the reinforcements was obtained using the Hirsch model. The mean value was 27.5 GPa for the coupled and uncoupled composites.

Table 3 shows the obtained micromechanics properties.

Table 3: Micromechanics properties of the interphase and the fibers after solving the Kelly and Tyson modified equation.

Composite	χ_1	τ (MPa)	lc (µm)	σ_t^F (Mpa)
20CF80PP0MAPP	0.312	9.14	878	973
30CF70PP0MAPP	0.307	8.70	861	908
40CF60PP0MAPP	0.293	9.31	833	940
50CF50PP0MAPP	0.301	9.17	746	829
20CF80PP6MAPP	0.297	14.41	710	1240
30CF70PP6MAPP	0.316	13.96	686	1162
40CF60PP6MAPP	0.310	14.55	776	1368
50CF50PP6MAPP	0.310	14.53	735	1295

The obtained orientation angles showed values in the range from 0.29 to 0.32. These values agreed with prior researches were it was found that the orientation factor was mainly influenced by the equipment used to obtain the specimens.[2, 32, 43] In these prior researches it was found that the orientation factor presented values in the range from 0.25 to 0.35.[17, 32, 44] The orientation factor can be translated to theoretical mean orientation angles as: $\chi_1 = cos^4(\alpha)$.[17] Then, around 61° mean orientation angles were found for the coupled and uncoupled composites.

The interfacial shear strength varied noticeably from the uncoupled to the coupled composites. Its mean values were 9.1±0.26 and 14.36±0.27 MPa, respectively. In the case of short fibers semi-aligned composites, it is accepted that von Mises criteria ($\sigma_t^m \cdot 3^{-1/2}$) returns the equivalent to a very strong interphase, being 15.9 MPa for Isplen PP090 62M-based composites.[17] The interfacial shear strength of the uncoupled composites was 74% lower than von Mises. Nonetheless, the values were noticeably better than those obtained for uncoupled SGW reinforced PP composites, with values below 4Mpa. Thus, as expected, uncoupled composites showed a weak interphase, but better than other natural fiber-reinforced uncoupled composites. Thus, probably, dyes reduced the hydrophilicity of the fibers and increased the compatibility between the reinforcement and the matrix. On the other hand, the coupled composites returned higher interfacial shear strengths, only 11% lower than Von Mises criteria. Hence, the interphase can be rated as strong. However, coupled SGW-based composites showed higher interfacial shear strengths, with values around 16MPa.[2] At the same time, old newspaper-based composites showed also similar interfacial shear strengths. Thus, probably the dyes hindered the interaction between the maleic acid and the OH groups in the fibers surfaces, preventing better interphases. However, this value was similar to 14.8 MPa obtained previously.[15]

Figure 6 shows micrographs of the rupture section of the uncoupled and coupled composites adding 20% of reinforcement.

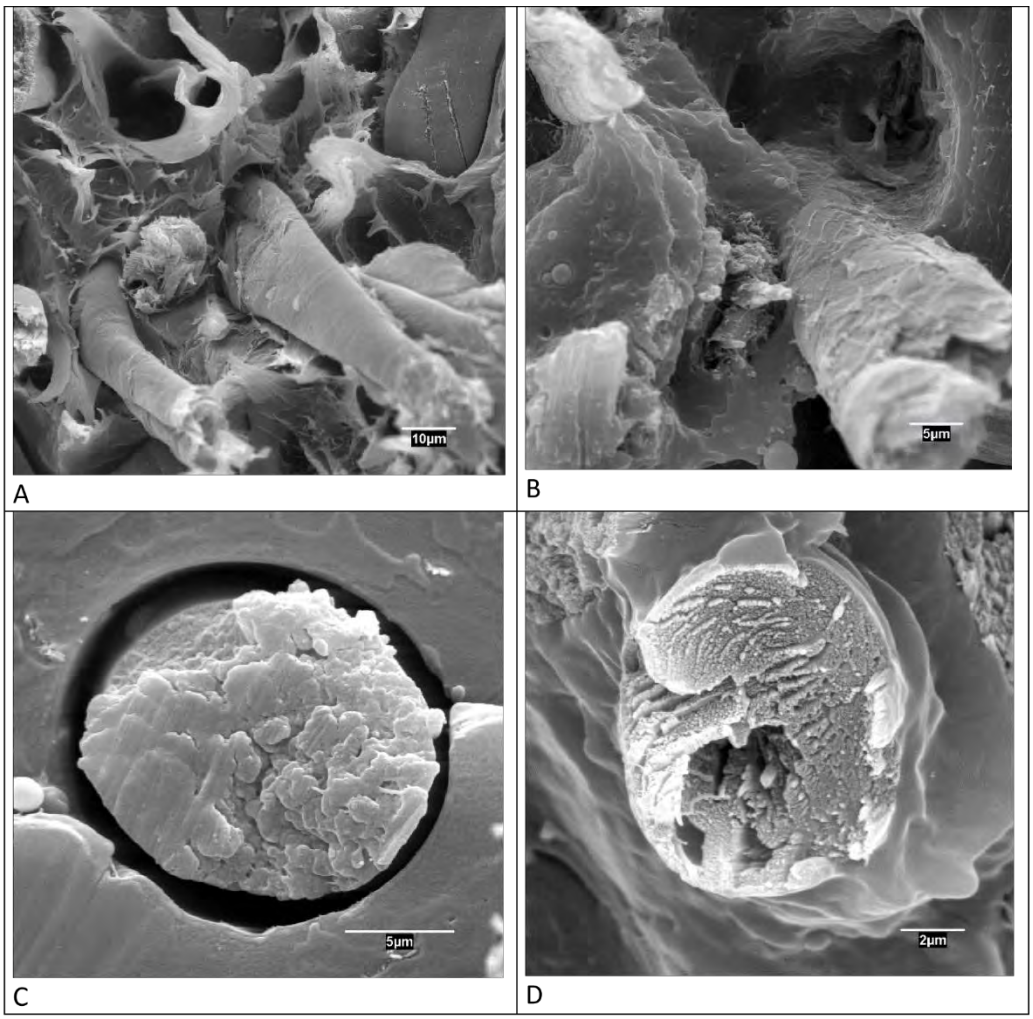

Figure 6: SEM micrographs of the coupled and uncoupled composites. A and C correspond to uncoupled composites with 20% reinforcement content. B and D correspond to coupled composites with the same reinforcement contents.

Micrograph 6A shows a correct dispersion of the fibers. The reinforcements are distributed without forming bundles. Micrographs A and C, corresponding to the uncoupled composites showed voids in the space occupied by the interphase. This was most noticeable in figure 6C. Figure 6A shows fibers totally slipped out from the matrix, another indication of a feeble interphase. On the other hand, the coupled composites (figures 6B and 6D) showed a correct wetting of the fibers. The observed fibers were shorter than in the case of the uncoupled composites and the presence of voids due to fiber slippage was minor. In the case of the uncoupled composites it seems that the facture mainly propagated around the interphase as it was the weakest phase of the composite, resulting in the mentioned fiber slippages. In the case of the coupled composite the mechanism was similar, but with a stronger interphases that resulted in a

lower number of fiber slippages and a propagation of the fracture along the interphase and the matrix with an ultimate fiber breaking.

The intrinsic tensile strengths of the fibers changed from the uncoupled to the coupled composites. This agreed with researchers pointing out that the properties of a reinforcement experimentally measured can vary from those back calculated.[19] In a previous research, the intrinsic tensile strength of the cotton fibers was obtained by single fiber tensile testing, obtaining values around 950MPa.[15] While such methods are useful to measure the strength and mechanical properties of textiles, can sub estimate the strengthening capabilities of the fibers.[45] The 950 MPa value is similar to the value for the cotton fibers inside the uncoupled composites. The cotton fibers inside the coupled composites showed mean intrinsic tensile strengths of 1266±87MPa, 33% higher that the uncoupled.

The critical length was used to divide the fibers between the subcritical and subcritical sets, and compute their contribution to the tensile strength of the composite (equations 5 and 6). In all the cases the critical length was higher than the mean length of the fibers, indicating a major presence of short fibers. Figure 7 shows the percentage contribution of the different phases to the tensile strength of the matrix, for the uncoupled and coupled composites.

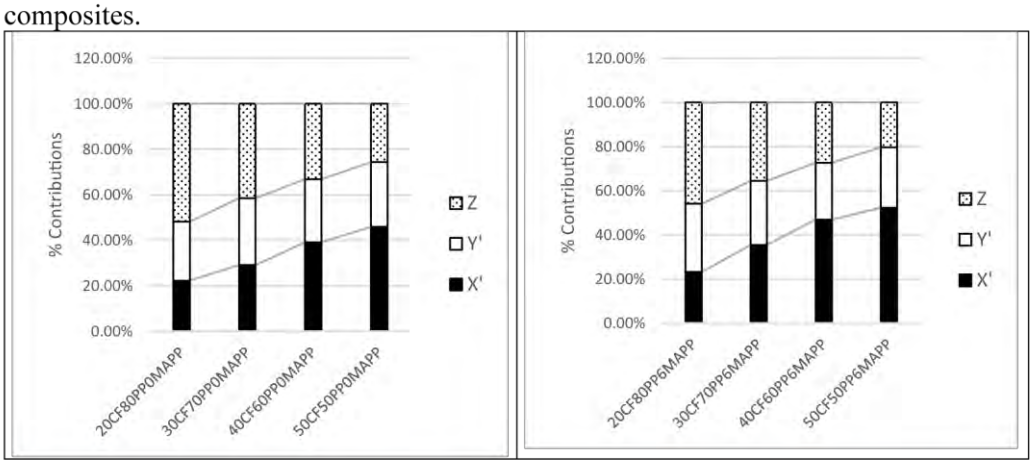

Figure 7: Contribution of the subcritical and supercritical fibers and the matrix to the tensile strength of the uncoupled and coupled composites.

The coupled composites showed higher contributions of the fibers to the tensile strength than the uncoupled. This was caused by a feebler interphase in the case of the uncoupled composites that hindered a total exploitation of the strengthening capabilities of the fibers. The contribution of the supercritical fibers remained almost constant and around 30%, despite the presence of coupling agents or the amount or reinforcement. The contribution of the matrix decreased with the presence of reinforcement. On the one hand it was due to the decrease of the strain at break, reducing the contribution of the matrix, and on the other hand to the decrease of the presence of the matrix, limiting also its contribution. The contribution of the short fibers increased noticeably with the percentage of reinforcement. On the one hand due to the decrease of the contribution of the matrix, and on the other hand due to the increase of the percentage of short fibers. The contribution of the subcritical fibers was noticeably higher than the observed for other natural fibers-based composites, around 10%.[32] The quality of the interphase hinders a

full exploitation of the strengthening capabilities of the supercritical fibers, but totally exploits the subcritical fibers.

Conclussions

Coupled and uncoupled composite materials were formulated using polypropylene as matrix and dyed cotton fibers as reinforcement. The tensile properties of such materials showed promising and competitive in front of another natural fiber reinforced materials. The coupled composites showed a tensile strength similar to low content glass fiber reinforced polypropylene composites.
The gap between the tensile strength of the uncoupled and the coupled composites was found smaller that the gap found for natural fiber or glass fiber coupled and uncoupled composites. This indicates the presence of a better than expected interphase in the uncoupled composites. This interphase can be due to the presence of dyes. The dyes decrease the hydrophilicity of the cotton fibers increasing the compatibility between these fibers and the hydrophobic matrix.
The neat contribution of the fibers to the tensile strength of the composites also showed that the strengthening capabilities of the cotton fibers were possibly not fully exploited. This indicated that the quality of the coupled composites was lower than expected due to the presence of a coupling agent. This can be explained by the effect of the dyes hindering the creation of bonds between the maleic acid and the OH groups on the surface of the cotton fibers.
The micromechanics revealed that the interphase of the uncoupled composites was better than other natural fiber reinforced polypropylene composites. This agreed with an impact of the dyes on the quality of the interphase. On the other hand, the quality of the interphase of the coupled composites showed good values but also possibilities to obtain better ones. This corroborates the impact of the dyes on the chemical interactions between the coupling agents and the cotton fiber surfaces.
The back calculated intrinsic tensile strength of the fibers showed that this property vary noticeably from the experimentally measured.
The composites based on dyed cotton fibers showed that it is possible recovering and valuing a textile by-product. Moreover, the use of tinted fibers allowed obtaining composite materials with relevant tensile properties. The use of such fibers as reinforcement is an alternative to the difficult textile recycling or disposal of tinted textile by-products, obligated to remove the dyes.

The Authors declares that there is no conflict of interest.

References

1. Schwarzkopf MJ and Burnard MD. Wood-Plastic Composites—Performance and Environmental Impacts. Environmental Impacts of Traditional and Innovative Forest-based. *Bioproducts*. Springer, 2016, p. 19-43.

2. Lopez JP, Mendez JA, El Mansouri NE, Mutje P and Vilaseca F. Mean intrinsic tensile properties of stone groundwood fibers from softwood. *BioResources*. 2011; 6: 5037-49.

3. Reixach R, Espinach FX, Arbat G, et al. Tensile Properties of Polypropylene Composites Reinforced with Mechanical, Thermomechanical, and Chemi-Thermomechanical Pulps from Orange Pruning. *BioResources*. 2015; 10: 4544-56.

4. Granda LA, Espinach FX, Lopez F, Garcia JC, Delgado-Aguilar M and Mutje P. Semichemical fibres of Leucaena collinsii reinforced polypropylene: Macromechanical and micromechanical analysis. *Compos Part B-Eng*. 2016; 91: 384-91.

5. Robertson NLM, Nychka JA, Alemaskin K and Wolodko JD. Mechanical performance and moisture absorption of various natural fiber reinforced thermoplastic composites. *J Appl Polym Sci.* 2013; 130: 969-80.

6. Illge L and Preuss L. Strategies for sustainable cotton: comparing niche with mainstream markets. *Corp Soc Resp Env Ma*. 2012; 19: 102-13.

7. Pensupa N, Leu S-Y, Hu Y, et al. Recent Trends in Sustainable Textile Waste Recycling Methods: Current Situation and Future Prospects. *Top Curr Chem*. 2017; 375: 76.

8. Araújo RS, Rezende CC, Marques MFV, et al. Polypropylene-based composites reinforced with textile wastes. *J Appl Polym Sci*. 2017; 134: 45060-n/a.

9. Jeihanipour A and Taherzadeh MJ. Ethanol production from cotton-based waste textiles. *Bioresource Technol*. 2009; 100: 1007-10.

10. Isci A and Demirer G. Biogas production potential from cotton wastes. *Renew Energ*. 2007; 32: 750-7.

552 11. De Silva R and Byrne N. Utilization of cotton waste for regenerated cellulose fibres:
553 Influence of degree of polymerization on mechanical properties. *Carbohyd Polym*.
554 2017; 174: 89-94.

555 12. Nirmal U, Lau ST, Hashim J and Devadas A. Effect of kenaf particulate fillers in
556 polymeric composite for tribological applications. *Text Res J*. 2015; 85: 1602-19.

557 13. Yalcin I, Sadikoglu TG, Berkalp OB and Bakkal M. Utilization of various non-
558 woven waste forms as reinforcement in polymeric composites. *Text Res J*. 2013; 83:
559 1551-62.

560 14. Ertaş M, Acemioğlu B, Alma MH and Usta M. Removal of methylene blue from
561 aqueous solution using cotton stalk, cotton waste and cotton dust. *J Hazard Mater*.
562 2010; 183: 421-7.

563 15. Serra A, Tarrés Q, Claramunt J, Mutjé P, Ardanuy M and Espinach F. Behavior of
564 the interphase of dyed cotton residue flocks reinforced polypropylene composites.
565 *Compos Part B-Eng*. 2017; 128: 200-7.

566 16. Serrano A, Espinach FX, Tresserras J, del Rey R, Pellicer N and Mutje P. Macro and
567 micromechanics analysis of short fiber composites stiffness: The case of old
568 newspaper fibers-polypropylene composites. *Mater Design*. 2014; 55: 319-24.

569 17. Vallejos ME, Espinach FX, Julian F, Torres L, Vilaseca F and Mutje P.
570 Micromechanics of hemp strands in polypropylene composites. *Compos Sci Technol*.
571 2012; 72: 1209-13.

572 18. Lopez JP, Mendez JA, Espinach FX, Julian F, Mutje P and Vilaseca F. Tensile
573 Strength characteristics of Polypropylene composites reinforced with Stone
574 Groundwood fibers from Softwood. *BioResources*. 2012; 7: 3188-200.

575 19. Shah DU, Nag RK and Clifford MJ. Why do we observe significant differences
576 between measured and 'back-calculated' properties of natural fibres?. *Cellulose*.
577 2016; 23: 1481-90.

20. International A. Standard Test Method for Tensile Properties of Plastics. West Conshohocken, PA: ASTM International, 2010.

21. International A. Standard Practice for Conditioning Plastics for Testing. West Conshohocken, PA: ASTM International, 2013.

22. Thomason JL. Interfacial strength in thermoplastic composites - at last an industry friendly measurement method?. *Compos Part A-Appl S*. 2002; 33: 1283-8.

23. Kelly A and Tyson W. Tensile porperties of fibre-reinforced metals - copper/tungsten and copper/molybdenum. *J Mech Phys Solid*. 1965; 13: 329-38.

24. Bowyer WH and Bader HG. On the reinforcement of thermoplastics by imperfectly aligned discontinuous fibres. *J Mater Sci*. 1972; 7: 1315-2.

25. Colom X, Carrasco F, Pages P and Canavate J. Effects of different treatments on the interface of HDPE/lignocellulosic fiber composites. Composites Science and Technology. 2003; 63: 161-9.

26. de Carvalho FP, Felisberti MI, Oviedo MAS, Vargas MD, Farah M and Ferreira MPF. Rice Husk/Poly(propylene-co-ethylene) Composites: Effect of Different Coupling Agents on Mechanical, Thermal, and Morphological Properties. J Appl Polym Sci. 2012; 123: 3337-44.

27. Osman H, Ismail H and Mustapha M. Effects of Maleic Anhydride Polypropylene on Tensile, Water Absorption, and Morphological Properties of Recycled Newspaper Filled Polypropylene/Natural Rubber Composites. Journal of Composite Materials. 2010; 44: 1477-91.

28. Li Y, Pickering KL and Farrell RL. Determination of interfacial shear strength of white rot fungi treated hemp fibre reinforced polypropylene. *Compos Sci Technol*. 2009; 69: 1165-71.

602 29. Jiménez AM, Espinach FX, Granda L, et al. Tensile strength assessment of injection-
603 molded high yield sugarcane bagasse-reinforced polypropyene. BioResources. 2016;
604 11: 6346-61.

605 30. Naghmouchi I, Espinach FX, Mutjé P and Boufi S. Polypropylene composites based
606 on lignocellulosic fillers: How the filler morphology affects the composite
607 properties. Materials & Design. 2015; 65: 454-61.

608 31. Hirsch T. Modulus of elasticity of concrete affected by elastic moduli of cement
609 paste matrix and aggregate. *ACI J.* 1962; 59: 427-51.

610 32. Reixach R, Franco-Marquès E, El Mansouri N-E, et al. Micromechanics of
611 Mechanical, Thermomechanical, and Chemi-Thermomechanical Pulp from Orange
612 Tree Pruning as Polypropylene Reinforcement: A Comparative Study. *BioResources*.
613 2013; 8: 3231-46.

614 33. Mendez JA, Vilaseca F, Pelach MA, et al. Evaluation of the reinforcing effect of
615 ground wood pulp in the preparation of polypropylene-based composites coupled
616 with maleic anhydride grafted polypropylene. J Appl Polym Sci. 2007; 105: 3588-
617 96.

618 34. Kim S-J, Moon J-B, Kim G-H and Ha C-S. Mechanical properties of
619 polypropylene/natural fiber composites: comparison of wood fiber and cotton fiber.
620 Polymer testing. 2008; 27: 801-6.

621 35. Galan-Marin C, Rivera-Gomez C and Garcia-Martinez A. Use of Natural-Fiber Bio-
622 Composites in Construction versus Traditional Solutions: Operational and Embodied
623 Energy Assessment. Materials. 2016; 9.

624 36. Siengchin S. Potential use of'green'composites in automotive applications.
625 BUDAPEST UNIV TECHNOL & ECON DEPT POLYMER ENG, MUEGYETEM
626 RKP 3, BUDAPEST, H-1111, HUNGARY, 2017.

627 37. Julian F, Espinach FX, Verdaguer N, Pelach MA and Vilaseca F. Design and
628 Development of Fully Biodegradable Products from Starch Biopolymer and Corn
629 Stalk Fibres. Journal of Biobased Materials and Bioenergy. 2012; 6: 410-7.

630 38. Serrano A, Espinach FX, Tresserras J, Pellicer N, Alcala M and Mutje P. Study on
631 the technical feasibility of replacing glass fibers by old newspaper recycled fibers as
632 polypropylene reinforcement. Journal of Cleaner Production. 2014; 65: 489-96.

633 39. Serrano A, Espinach FX, Julian F, del Rey R, Mendez JA and Mutje P. Estimation of
634 the interfacial shears strength, orientation factor and mean equivalent intrinsic tensile
635 strength in old newspaper fiber / polypropylene composites. *Compos Part B-Eng*.
636 2013: 232-8.

637 40. Birnin-Yauri A, Ibrahim N, Zainuddin N, Abdan K, Then Y and Chieng B. Effect of
638 Maleic Anhydride-Modified Poly(lactic acid) on the Properties of Its Hybrid Fiber
639 Biocomposites. *Polymers*. 2017; 9: 165.

640 41. Fuqua MA, Chevali VS and Ulven CA. Lignocellulosic byproducts as filler in
641 polypropylene: Comprehensive study on the effects of compatibilization and loading.
642 *J Appl Polym Sci*. 2013; 127: 862-8.

643 42. de Carvalho FP, Felisberti MI, Oviedo MAS, Vargas MD, Farah M and Ferreira
644 MPF. Rice Husk/Poly(propylene-co-ethylene) Composites: Effect of Different
645 Coupling Agents on Mechanical, Thermal, and Morphological Properties. *J Appl*
646 *Polym Sci*. 2012; 123: 3337-44.

647 43. Jiménez AM, Espinach FX, Granda L, et al. Tensile strength assessment of injection-
648 molded high yield sugarcane bagasse-reinforced polypropyene. *BioResources*. 2016;
649 11: 6346-61.

650 44. Oliver-Ortega H, Granda LA, Espinach FX, Mendez JA, Julian F and Mutjé P.
651 Tensile properties and micromechanical analysis of stone groundwood from

softwood reinforced bio-based polyamide11 composites. *Compos Sci Technol*. 2016; 132: 123-30.

45. Üreyen ME and Kadoglu H. Regressional estimation of ring cotton yarn properties from HVI fiber properties. *Text Res J*. 2006; 76: 360-6.

4.3. Artículo III

polymers

MDPI

Article

Modeling the Stiffness of Coupled and Uncoupled Recycled Cotton Fibers Reinforced Polypropylene Composites

Albert Serra [1], Quim Tarrés [1,2], Miquel-Àngel Chamorro [3], Jordi Soler [3], Pere Mutjé [1,2], Francesc X. Espinach [4,*] and Fabiola Vilaseca [5]

1 LEPAMAP Group, Department of Chemical Engineering, University of Girona, 17003 Girona, Spain; albert.serra@udg.edu (A.S.); joaquimagusti.tarres@udg.edu (Q.T.); pere.mutje@udg.edu (P.M.)
2 Càtedra de Processos Industrials Sostenibles, University of Girona, 17003 Girona, Spain
3 Department of Architecture and Construction, 17003 Girona, Spain; mangel.chamorro@udg.edu (M.-À.C.); jordi.soler@udg.es (J.S.)
4 Design, Development and Product Innovation, Dept. of Organization, Business, University of Girona, 17003 Girona, Spain
5 Advanced Biomaterials and Nanotechnology, Dpt. of Chemical Engineering, University of Girona, 17003 Girona, Spain; fabiola.vilaseca@udg.edu
* Correspondence: francisco.espinach@udg.edu

Received: 3 October 2019; Accepted: 17 October 2019; Published: 21 October 2019

check for updates

Abstract: The stiffness of a composite material is mainly affected by the nature of its phases and its contents, the dispersion of the reinforcement, as well as the morphology and mean orientation of such reinforcement. In this paper, recovered dyed cotton fibers from textile industry were used as reinforcement for a polypropylene matrix. The specific dye seems to decrease the hydrophilicity of the fibers and to increase its chemical compatibility with the matrix. The results showed a linear evolution of the Young's moduli of the composites against the reinforcement contents, although the slope of the regression line was found to be lower than that for other natural strand reinforced polypropylene composites. This was blamed on a growing difficulty to disperse the reinforcements when its content increased. The micromechanics analysis returned a value for the intrinsic Young's modulus of the cotton fibers that doubled previously published values. The use of two different micromechanics models allowed evaluating the impact of the morphology of the fibers on the Young's modulus of a composite.

Keywords: recycled cotton fibers; stiffness; micromechanics; Young's modulus

1. Introduction

The use of fibrous industrial byproducts as reinforcement for polymer-based composites has increasingly been attracting the attention of researchers. The use of byproducts is in line with the principles of green chemistry and the actual demands of the society for greener materials and more environmentally friendly products [1–3]. The literature shows the opportunity to use agroforestry wastes such as prunings, used paper fibers, or textile byproducts [4–8]. These studies reveal how the nature of the reinforcements has a high impact on the mechanical properties of its composites. In this sense, artificial fibers like glass fibers, aramids, or carbon fibers show the highest strengthening and stiffening abilities [9,10]. Natural fiber strands and wood fibers also show notable capabilities as polyolefin reinforcements. Nonetheless, strands like jute or hemp showed higher stiffening potential than wood fibers [11–15]. In this sense, cotton strands have been used as polyolefin reinforcement successfully [16–18]. While some of the studies have used raw cotton as reinforcing fibers, a vast

majority prefer to use recycled fibers from the textile industry [7,13,19,20], however, the number of published studies are still limited.

Cotton fibers recovered from the textile industry have some advantages, such as low cost and availability, but also some apparent drawbacks, since usually these fibers contain textile dyes [7,20]. Additionally, there is a large quantity of discarded textiles that are directly landfilled [21]. Moreover, landfilled textiles contribute to the formation of 'leachate' that can contaminate ground and underground waters [22]. Thus, the use of such textiles as composite reinforcement can contribute to widen the value chain of the textile sector on the one hand, and to decrease landfilling and contamination on the other hand.

Cotton fibers are almost 100% cellulosic fibers, and thus have a high presence of hydroxyl groups in their surface, and a high potential to create hydrogen bonds under favorable conditions. Therefore, they tend to aggregate, making their individualization and dispersion on a polymeric phase difficult [8]. In addition, cotton fibers are hydrophilic, while the vast majority of polymeric matrices are hydrophobic.

A previous study revealed that the presence of dyes diminished the hydrophilicity of cotton fibers, allowing the obtaining of better interphases without using any coupling agent [7,20]. The same dyes eased the dispersion of the fibers without any treatment. Nonetheless, the tensile strength of the composites reinforced with dyed cotton fibers were lower than those obtained with other natural fiber strands. Some authors claim that the same dyes hindered the action of coupling agents [7], although these researchers did not publish any results concerning the stiffness of the composites. According to the literature, the intrinsic Young's modulus of cotton fibers is found between 5 and 13 GPa, however, this value seems too low compared with the values obtained for other strands [11,12,23–28].

This paper examines the Young's modulus of cotton fiber (CF) reinforced polypropylene (PP) composites. CFs were recovered from a yarning process where all the fibers with lengths below 10mm were discarded. The byproduct has the shape of cotton dyed flocks that must be individualized prior to its use as reinforcement [20]. Composite materials adding CF percentages ranging from 20 to 50 wt% were formulated. Two batches of every formulation were prepared, one with 6 wt% of coupling agent added, and the other without. The composites were mold injected to obtain the standard specimens, and later on tested under tensile conditions. The Young's moduli of the materials were evaluated and discussed. The Young's moduli of the composites were not coherent with the intrinsic Young's modulus for CFs found in the literature. Therefore, a micromechanical analysis was proposed to analyze the properties of CF. First, the Hirsch model provided a value for the intrinsic Young's modulus of CF that doubled those on the literature [29]. Then, the efficiency factors allowed discussing a possible poor dispersion of the fibers at high reinforcement contents. Finally, the Tsai and Pagano model in combination with Halpin and Tsai equations [30,31] allowed incorporating the morphology of the reinforcements to back-calculate a theoretical Young's modulus for the composites. The paper actualizes the value of the intrinsic Young's modulus of cotton fibers, and proposes a series of composites that reuse textile byproducts, and thus avoids their landfilling or incineration.

2. Materials and methods

2.1. Materials

The cotton fibers (CF) used as reinforcement were recovered from cotton flock residues. These cotton flocks are textile industry byproducts and are composed of entangled cotton fibers with lengths too short for spinning. The flocks were previously treated with a reactive dye and were kindly supplied by Fontfilva S. L. (Olot, Girona, Spain).

A polypropylene (PP) Isplen PP090 62M by Repsol-YPF (Tarragona, Spain) was kindly supplied by its producer and used as the polymeric matrix. The use of a coupling agent was proposed in order to prevent chemical incompatibilities between the hydrophilic reinforcements and the hydrophobic matrix. Epolene G3015 polypropylene functionalized with maleic anhydride (MAPP) by Eastman

Chemical Products (San Roque, Spain) was purchased for this purpose. This reactive has an acid number of 15 mg KOH/g and a Mn of 24800.

Decalin (decahydronaphthalene) was acquired from Fischer Scientific (Madrid, Spain) and had a 190 °C boiling point and 97% purity. This reagent was used to dissolve the PP matrix in the fiber extraction from composites.

Figure 1 shows the workflow for the research, from the production of cotton flocks by the textile industry to the measurement and evaluation of the mechanical properties.

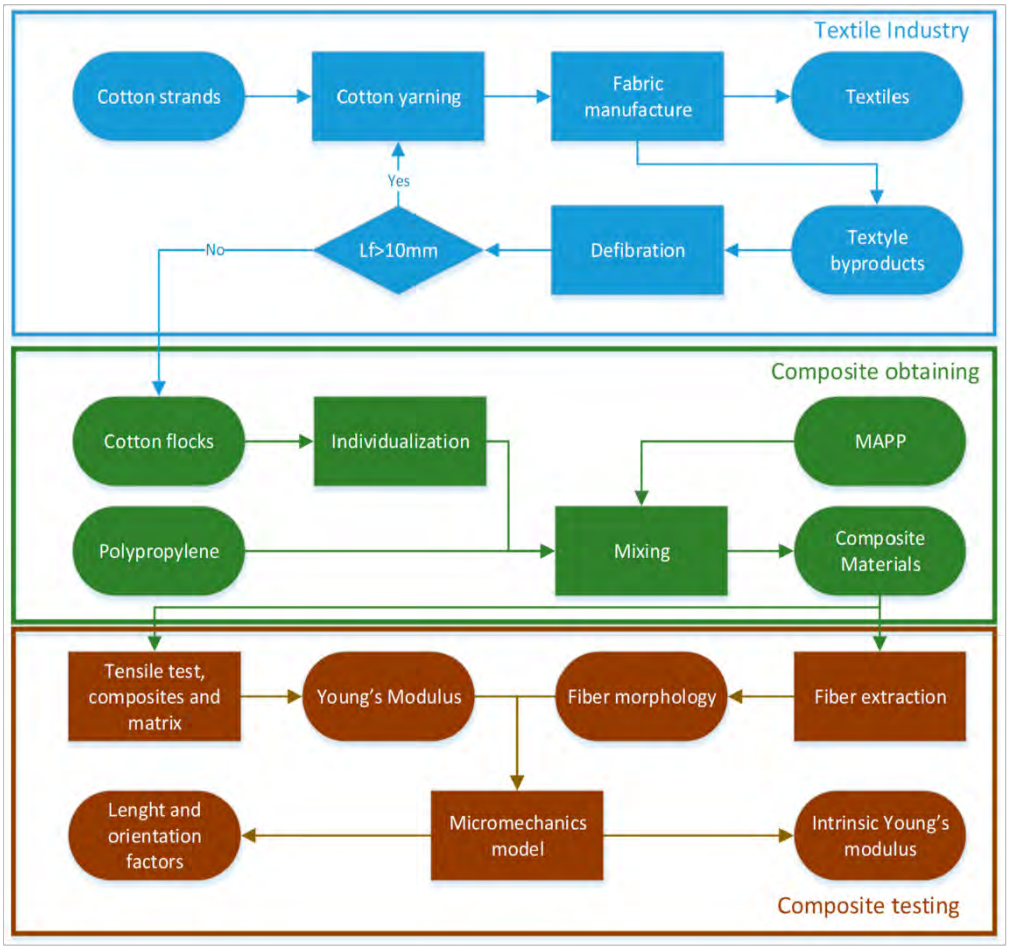

Figure 1. Workflow of the research, including the production of cotton flock byproducts, composite mixing and material testing.

2.2. Cotton Flocks Treatment and Composites Preparation

The cotton residues were passed through a blade mill in order to individualize the entangled fibers. The mill was provided with a 1mm sieve to obtain cotton fibers able to attain a good dispersion. These CFs were mixed with the PP in a Brabender Plastograph kinetic mixer by Brabender® (Duisburg, Germany). The coupled composites added a 6 wt% of MAPP at the same time than the other phases. The process took 10 min, at 185 °C and at a speed of 80 rpm. Coupled and uncoupled composites with CF contents ranging from 20 to 50 wt% were prepared. The obtained blends were cut down to 8 mm pellets able to be mold injected. These pellets were stored for 24 h in an oven at 80 °C to eliminate the humidity.

2.3. Composite and Standard Specimen Preparation

The composite pellets were injection molded in the shape of standard dog bone specimens, in agreement with ASTM D638. The injection molding machine was a Meteor-40 by Mateu & Solé (Barcelona, Spain). The machine has three heating areas that were operated at 175 °C, 175 °C, and 190 °C, corresponding to the highest to the nozzle. The injection pressure was 120 kg/cm^{-2} and the maintaining pressure was 37.5 kg/cm^{-2}. A steel mold with a cavity in the shape of the standard specimen was used, and at least ten specimens for every one of the composite formulations were obtained.

2.4. Mechanical Test

Prior to any mechanical test, the specimens were stored in a conditioning chamber by Dycometal. The stabilization of the specimens took 48 h, and the conditions were at 23 °C with 50% relative humidity.

The specimens were placed in the gauges of an Instron TM 1122 universal testing machine. The machine was fitted with a 5 Kn load cell. The test was performed in agreement with ASTM D790 standard. An extensometer MFA2 was used to measure the strains with addequate precision. The measurements were the result of testing at least 5 samples for every composite formulation.

2.5. Morphologic Analysis of the Reinforcements

Some micromechanics models use the morphology of the reinforcements as input. As soon as the literature accepts that the morphology of such reinforcements changes noticeably during composite preparation, the study was performed to reinforcements extracted from the polymeric matrix. The extraction was obtained by matrix solubilization using a Soxhlet apparatus and using Decalin as a solvent. Composite material pieces approximately 10 × 10mm were placed inside a cellulose filter into the Soxhlet equipment. The process lasted 24 h until the matrix was totally dissolved. Then, the fibers were rinsed with acetone and distilled water.

The morphology of the fibers was measured in a FS-300 Kajanni analyzer. The equipment measured from 2500 to 3000 fibers and returned a fiber length distribution, mean length, and diameter and the percentage of fines (fibers shorter than 70 μm).

3. Results and Discussion

3.1. Young's Modulus of the Composites

Table 1 shows the Young's moduli of the coupled and uncoupled composites ($E_t{}^C$) reinforced with CF contents ranging from 20 to 50 wt%. The table also shows the tensile strength of the composites ($\sigma_t{}^C$), the percentage of reinforcement in weight (W^F), and its volume fraction (V^F).

Table 1. Young's modulus and tensile strength of the cotton fiber (CF)/polypropylene (PP) composites.

		0%MAPP		6%MAPP	
W^F	V^F	$E_t{}^C$ (GPa)	$\sigma_t{}^C$ (MPa)	$E_t{}^C$ (GPa)	$\sigma_t{}^C$ (MPa)
0	0	1.5 ± 0.1	27.6 ± 0.5	1.5 ± 0.1	27.6 ± 0.5
20%	0.131	3.2 ± 0.1	35.0 ± 0.5	3.3 ± 0.1	41.7 ± 0.7
30%	0.205	3.9 ± 0.2	38.2 ± 0.8	3.9 ± 0.1	47.1 ±0.7
40%	0.287	4.7 ± 0.2	41.7 ± 0.8	4.8 ± 0.2	53.6 ± 1.0
50%	0.376	5.6 ± 0.2	45.4 ± 1.1	5.4 ± 0.2	58.3 ± 1.2

It was found that the use of a coupling agent had a low effect on the Young's modulus of the composites. In fact, an ANOVA analysis (at 95% confidence rate) reveals that the differences between the Young's moduli of the composites with the same percentage of reinforcement, despite adding or not adding a coupling agent, were not statistically relevant. This result was expected as it has been reported previously in the literature [5,32]. The same materials revealed totally different behaviors in

the case of the tensile strength, where the presence of MAPP considerably increased the strength of the materials [7,20]. Thus, while the coupling agent has a noticeable effect on the tensile strength of the composites, its impact is not statistically relevant in the case of the Young's modulus. Some authors prefer to state that the strength of the interphase between the matrix and the reinforcements has a limited impact on the stiffness of the composites [6,11]. Other authors prefer to justify the differences on the methods used to evaluate the strength and the modulus. While the strength is measured at the maximum strain, where the interphase has been fully put to test, the Young's modulus is measured at low strains [32].

The Young's modulus of a semi-aligned short fiber reinforced composite is mainly affected by the properties of the phases and its contents, the morphology of the reinforcement, its mean orientation, and its grade of dispersion. In the case of a correctly dispersed reinforcement, the increase of the Young's modulus against reinforcement content was expected to be linear (Figure 2) [32].

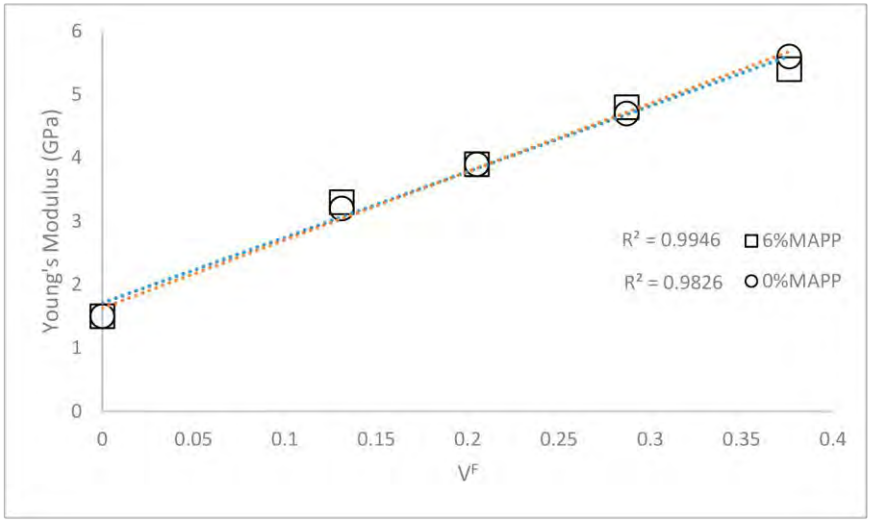

Figure 2. Young's modulus of the coupled and uncoupled CF-PP composites against reinforcement content.

Both, coupled and uncoupled composites showed a linear evolution of its Young's moduli against CF content. Thus, a proper dispersion of the reinforcement was assumed. Nonetheless, the higher the percentage of reinforcement the harder it becomes to obtain a good or proper dispersion. In the case of the coupled composite at 50 wt% of CF, the Young's modulus seems to start to decrease under the regression line. Besides, CF incorporates a textile dye that seems to increase the strength of the interphase and ease the dispersion at low reinforcement rates. Nonetheless, it was impossible to corroborate this evolution due to the impossibility of preparing materials with higher reinforcement contents that are still able to be mold injected. From now on, and due to the equivalence between coupled and uncoupled CF-based composites, the analysis will be referring to the coupled materials.

The literature shows multiple studies on the evolution of the Young's modulus against the fiber contents. We have chosen stone groundwood fibers (SGW), commonly used for papermaking, hemp strands (HS), as a byproduct of agroforestry, old newspaper fibers (ONPF), as recycled fibers, and glass fibers (GF) as an industrial commodity and the most commonly used reinforcement [11,14,33]. Table 2 shows the Young's moduli of SGW, HS, ONPF and GF reinforced PP composites.

Table 2. Young's moduli of stone groundwood, hemp strands, and glass fiber reinforced polypropylene coupled composites.

	SGW	HS	ONPF	GF
20%	2.7 ± 0.1	2.8 ± 0.1	2.8 ± 0.1	4.1 ± 0.1
30%	3.5 ± 0.1	3.8 ± 0.1	3.8 ± 0.1	5.7 ± 0.1
40%	4.3 ± 0.1	5.2 ± 0.1	4.2 ± 0.1	7.7 ± 0.1
50%	5.2 ± 0.1	6.3 ± 0.1	5.3 ± 0.1	-

The Young's moduli of natural fiber reinforced polypropylene composites are similar, with slight advantages for those reinforced with strands, especially at high reinforcement contents. Cotton fibers showed Young's moduli as superior to SGW and ONPF, and in line with the other strands. Nonetheless, cotton fibers are recycled and a byproduct of the textile industry, while hemp strands can be considered virgin materials. ONPF are recycled fibers that come from the disintegration of used newspaper. The Young's moduli of ONPF and SGW based composites are very similar, showing that recovering the fibers from the paper had little effect on the stiffening potential of the reinforcements. Moreover, CF showed higher Young's moduli than ONPF based composites. All the natural-based composites showed a linear evolution of their Young's moduli against fiber contents, but different slopes on their regression lines.

On the other hand, GF-based materials showed noticeably higher Young's moduli than natural fiber-based composites. At the same reinforcement contents, Young's modulus of CF-based composites is noticeably lower than GF-based ones. It was necessary to increase 20 wt% the amount of CF to obtain a Young's moduli similar to GF.

3.2. Neat Contribution of the Reinforcements

Attending to the above-mentioned parameters that affect the Young's modulus of a composite, the differences must be related with the morphology of the reinforcements, its mean orientation, or the intrinsic properties of the phases. The modified rule of mixtures (RoM) for the Young's modulus summarizes all these parameters (Equation (1)):

$$E_t^C = \eta_e \cdot E_t^F \cdot V^F + \left(1 - V^F\right) \cdot E_t^M \quad (1)$$

where $E_t{}^C$, $E_t{}^F$, and $E_t{}^M$ are the Young's moduli of the composite, reinforcement, and matrix, respectively. V^F represents the reinforcement volume fraction, and η_e is a modulus efficiency factor that equalizes the contribution of the reinforcements to the Young's modulus of the composite. This efficiency factor is seldom presented as a length efficiency factor times an orientation efficiency factor ($\eta_e = \eta_l \cdot \eta_o$). At the exception of the intrinsic Young's modulus of the reinforcements and the modulus efficiency factor, the rest of the values can be easily obtained during the tensile test of the composites. Clearly, the RoM can only be used if the Young's modulus of the composite evolves linearly against reinforcement content.

In any case, the neat contribution of the reinforcements to the Young's modulus of the composite is represented by $\eta_e \cdot E_t^F$ in the RoM. Thus, the RoM can be rearranged to account for such neat contribution as:

$$\eta_e \cdot E_t^F = \frac{E_t^C - \left(1 - V^F\right) \cdot E_t^M}{V^F} \quad (2)$$

Then, if the neat contribution is represented against the reinforcement volume fraction, a regression line is obtained, and the slope of such a line has been referred to in the literature as a fiber tensile modulus factor (FTMF) [6,32]. This factor can be used as a measure of the stiffening capabilities of a reinforcement. Figure 3 shows the FTMF for different fibers as polypropylene reinforcement.

The FTMF of CF was between HS and SGW. This value ensures good stiffening abilities for CF as PP reinforcement because the literature shows possible applications for materials with similar FTMF for building or product design purposes [34,35]. Moreover, some researchers used an ONPF-based

composite to substitute a GF-based one [36]. On the other hand, GF showed higher stiffening capabilities than the rest of the reinforcements. This is not a surprise, having in account that GF is a man-made material with more stable intrinsic properties and a regular morphology. The FTMF of the reinforcements shows a similar behavior than the Young's moduli of its composites. Thus, the differences between such moduli seem to be focused on the neat contribution of the fibers, specifically, the intrinsic Young's modulus of the reinforcement and the modulus efficiency factor. In order to analyze such differences, the researchers propose a micromechanics analysis.

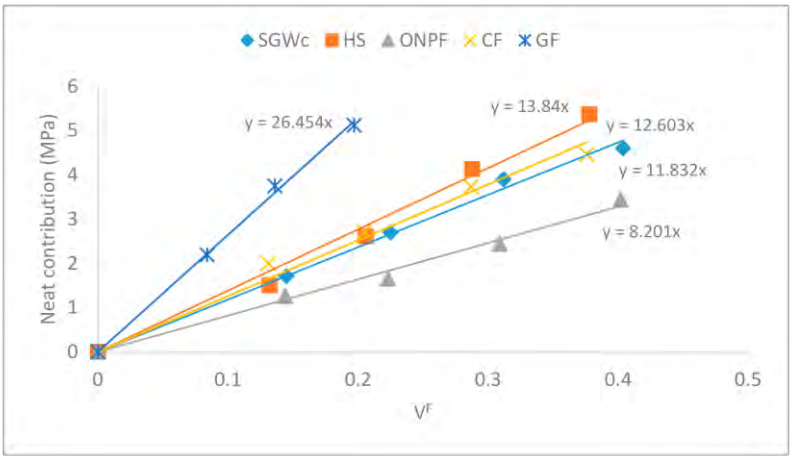

Figure 3. Neat contribution of the reinforcements to the Young's modulus of the polymers.

3.3. Micromechanics Analysis of the Young's Modulus

The RoM (Equation (1)) shows two unknowns that coincide with the neat contribution of the fibers: $\eta_e \cdot E_t{}^F$. While it is possible to measure the intrinsic Young's modulus of the fibers, and more so in the case of the strands, some authors defend the use of micromechanics methods as an alternative [11,37,38]. In addition, a high number of experiments are necessary due to the foreseeable standard deviations of the mechanical properties of natural fiber reinforcements. Thus, the Hirsh model was proposed as a means to evaluate the intrinsic Young's modulus of CF.

$$E_t^C = \beta \cdot (E_t^F \cdot V^F + E_t^M (1 - V^F) + (1 - \beta) \frac{E_t^F \cdot E_t^M}{E_t^F \cdot V^F + E_t^m (1 - V^F)} \quad (3)$$

where β is a parameter that modules the stress transference between both phases of the composite material. In the case of semi-aligned short fibers reinforced composites β has a value of 0.4 [14]. Table 3 shows the micromechanical parameters obtained after the analysis.

Table 3. Micromechanics of the Young's moduli of CF reinforced polypropylene coupled composites.

V^F	$E_t{}^F$ (GPa)	η_e	η_l	η_o	α_o
0.131	31.48	0.52	0.89	0.58	48.8
0.205	28.06	0.47	0.89	0.53	53.3
0.287	26.48	0.45	0.89	0.51	55.1
0.376	25.46	0.45	0.90	0.49	56.2
Mean	27.87 ± 2.63	0.47 ± 0.03	0.89 ± 0.01	0.53 ± 0.04	53.3 ± 3.3

The mean intrinsic Young's modulus of CF was found to be 27.87 ± 2.63 GPa, similar to HS, with a value of 26.8 GPa [11]. This coincidence agrees with the already similarities found in the neat contributions of such fibers (Figure 3). Nonetheless, the computed intrinsic Young's modulus of CF

contrasts heavily with the neatly inferior values found in the literature. Some authors place this intrinsic Young's modulus in the range from 5 to 13 GPa [26–28]. Using such values with the RoM is not possible to reach the obtained experimental values without using modulus efficiency factors outside the usual range.

On the other hand, the value for CF is noticeably higher than the value obtained for SGW and ONPF, 21.2 ± 1.9 and 22.8 ± 1.8 GPa, respectively [14,39]. This also agrees with the neat contributions of such fibers. Similarly, GF showed an intrinsic Young's modulus of 76 GPa, justifying the differences obtained in the Young's modulus of its composites [11,40].

Consequently, the intrinsic Young's moduli of the different reinforcements affected heavily the Young's moduli of its composites. Nonetheless, CF showed a higher intrinsic Young's modulus than HS, but HS-based composites showed higher Young's moduli, at the same reinforcement contents than CF-based composites. Thus, the differences are expected to be found in the modulus efficiency factor (Table 3).

The values for the modulus efficiency factor were obtained by using all the experimental data (Table 1) and the mean intrinsic Young's modulus of CF (Table 3). The mean value was found to be 0.47 ± 0.03. The value is inside the usual range of values, between 0.45 and 0.56 for such factor [11,12,14,40]. Nonetheless, it is worth noting that the obtained value is in the lower half bound of the expected values. Thus, presumably, CF based composites have not taken advantage of the stiffening capabilities of CF. Particular values decrease when the CF contents increase (Table 3). The composite with a 20 wt% of CF exhibits a modulus efficiency factor higher than the other CF-based composites, and also a higher intrinsic Young's modulus, indicating a higher yield on the stiffening capabilities of CF. The reasons must be found on the mean orientation of the fibers, the morphology of the reinforcements or its dispersion.

In the case of HS the modulus efficiency factor was evaluated at 0.50 ± 0.02. This value is higher than CF and can compensate the difference between the intrinsic Young's moduli of the reinforcements and justify the higher moduli of the HS-based composites. In the case of ONPF, the value of η_e was evaluated at 0.49 ± 0.04, a value similar to HS. Finally, SGW showed the highest values for η_e, with a mean of 0.56 ± 0.02.

In order to find the impact of the morphology and the mean orientation of CF, the morphology and orientation efficiency factors were computed. The length efficiency factor was calculated according to Cox-Krenchel's model (Equations (4) and (5)) [41]:

$$\eta_l = 1 - \frac{tanh\left(\frac{\mu \cdot L^F}{2}\right)}{\left(\frac{\mu \cdot L^F}{2}\right)} \tag{4}$$

with

$$\mu = \frac{1}{r^F}\sqrt{\frac{E_t^M}{E_t^F \cdot (1-v) \cdot Ln\left(\sqrt{\pi/4 \cdot V^F}\right)}} \tag{5}$$

where L^F and r^F are the reinforcement mean weighed length and radius, respectively. The Poisson's ratio of the matrix is represented by v and μ is a coefficient of the stress concentration rate at the end of the fibers. The Poisson ratio was 0.36, as found in the literature [22]. The orientation factor η_o was obtained from $\eta_o = \eta_l/\eta_e$. Table 3 shows the obtained values.

The length efficiency factor remained almost the same for all the composite formulations, with a mean value of 0.89 ± 0.01. Usually this factor decreases when the percentage of reinforcement increases [5]. This is due to the changes in the mean length of the reinforcements during compounding, when reinforcements are exposed to attrition phenomena and tend to break. There is a decrease in the mean length of such reinforcements as the reinforcement content increases [32]. Thus, these changes are expected to affect the Young's moduli of the composites. In the case of CF based composites,

the impact of the morphology of the fibers seems to little impact the Young's modulus, although the reinforcements decreased their mean length from 293 to 185 μm [7]. This hypothesis will be put to test later on by applying a different micromechanics model.

On the other hand, the orientation efficiency factor clearly changed with the amount of reinforcement (Table 3). This factor showed a mean value of 0.53 ± 0.04 and ranged from 0.58 to 0.49. Usually, the orientation efficiency factor is more stable than the length efficiency factor, because the mean orientation of the fibers is heavily impacted by the geometry of the injection mold and the parameters used during the mold injection [42,43].

Fukuda and Kawata [44] studied the tensile modulus of short fiber reinforced thermoplastics, and the orientation of the fibers inside the composites. The authors proposed different fiber distributions, but based on the literature, a rectangular distribution (square packing) renders adequate results for short fiber semi-aligned reinforced composites [32,45]. The authors present an equation that computes the orientation efficiency factor from a mean orientation angle (α):

$$\eta_o = \frac{sin(\alpha)}{\alpha}\left(\frac{3-\upsilon}{4}\frac{sin(\alpha)}{\alpha} + \frac{1-\upsilon}{4}\frac{sin(3\alpha)}{3\alpha}\right) \quad (6)$$

Equation (6) was used to compute the mean orientation angles of the reinforcements (Table 3). The mean orientation angle was found to be 53.3 ± 3.3°. This value is in line with other natural fiber reinforced composites, thought in the upper bounds, meaning that the reinforcements are les oriented than the expected. It must be stressed that the orientation decreased with the amount of reinforcement, from 48.8° for the composite containing 20 wt% of CF to 56.2° for the composite containing 50 wt%. In other cases, it was found that the composites with higher fiber contents showed higher orientations [11]. In these studies, it was assumed that the shorter fibers were easily aligned than the longer ones. Nonetheless, the RoM does not incorporate a factor taking in account the dispersion of the fibers, and as has been previously commented, the authors suspect that the dispersion of the composites at high-reinforcement contents was improvable.

3.4. Effect of the Morphology of the Reinforcements

While the rule of mixtures (Equation (1)) and Hirsch's equation (Equation (3)) are elegant models that allow predicting the Young's modulus of a composite from a variety of parameters, they do not incorporate any morphological property of the reinforcements. The morphology of the reinforcements is known to greatly impact the mechanical properties of a composite, especially the ratio between its mean length and diameter, known as aspect ratio [12,46,47]. Thus, the authors propose using the Tsai and Pagano model (Equation (7)) in combination with Halpin and Tsai equations (Equations (8)–(10)) to evaluate a theoretical Young's modulus of the composites.

In agreement with Tsai and Pagano model, the stiffness in the fiber direction is given by:

$$E_t^C = \frac{3}{8}E^{11} + \frac{5}{8}E^{22} \quad (7)$$

where, E^{11} and E^{22} are the longitudinal and transversal elastic modulus, calculated by the Halpin–Tsai equations [11]:

$$E^{11} = \frac{1 + 2\left(L^F/2r^F\right)\cdot\lambda_l V^F}{1-\lambda_l V^F}E_t^M \quad (8)$$

with

$$\lambda_l = \frac{\left(E_t^F/E_t^M\right) - 1}{\left(E_t^F/E_t^M\right) + 2\left(L^F/2r^F\right)} \quad (9)$$

and:

$$E^{22} = \frac{1 + 2\lambda_t V^F}{1-\lambda_t V^F}E_t^M \quad (10)$$

with

$$\lambda_t = \frac{\left(E_t^F / E_t^M\right) - 1}{\left(E_t^F / E_t^M\right) + 2} \tag{11}$$

Table 4 presents the obtained values. The values obtained by using the micromechanics model show a good alignment with the experimental values, especially at reinforcement contents higher than 20 wt%. In these cases, the error goes to a maximum of 5.6%, which is assumable when modeling a mechanical property of a natural fiber reinforcement composite. In fact, the standard deviation of the experimental values is higher than this maximum of 5.6% (Table 1). The higher errors found for the composite with a 20 wt% of CF can be explained by the intrinsic Young's modulus derived from these composites (Table 2). The value of such a parameter is 11.5% higher than the mean value. If the 31.48 GPa value is used as input for the Tsai and Pagano model, the theoretical Young's modulus increases to 3.02 GPa. This value is more similar to the value obtained experimentally. Moreover, the authors blame the differences between the experimental and theoretical values to deviations from a totally linear evolution of the Young's moduli against reinforcement contents—due to possible auto entanglements between the CF—and thus showing a slightly worse dispersion of the CF.

Table 4. Theoretical Young's moduli of the composites computed by using the Tsai and Pagano model in combination with Halpin andTsai equations.

	Experimental		**Tsai-Pagano**		**Error (GPa)**		**Error (%)**	
V^F	0% MAPP	6% MAPP	0% MAPP	6% MAPP	0% MAPP	6% MAPP	0% MAPP	6% MAPP
0.131	3.2	3.3	2.9	2.9	0.3	0.4	9.4	12.1
0.205	3.9	3.9	3.7	3.7	0.2	0.2	5.1	5.1
0.287	4.7	4.8	4.7	4.6	0	0.2	0	4.2
0.376	5.6	5.4	5.8	5.7	–0.2	–0.3	–3.6	–5.6

The obtained values were plotted against the experimental ones to find the grade of correlation between both values (Figure 4).

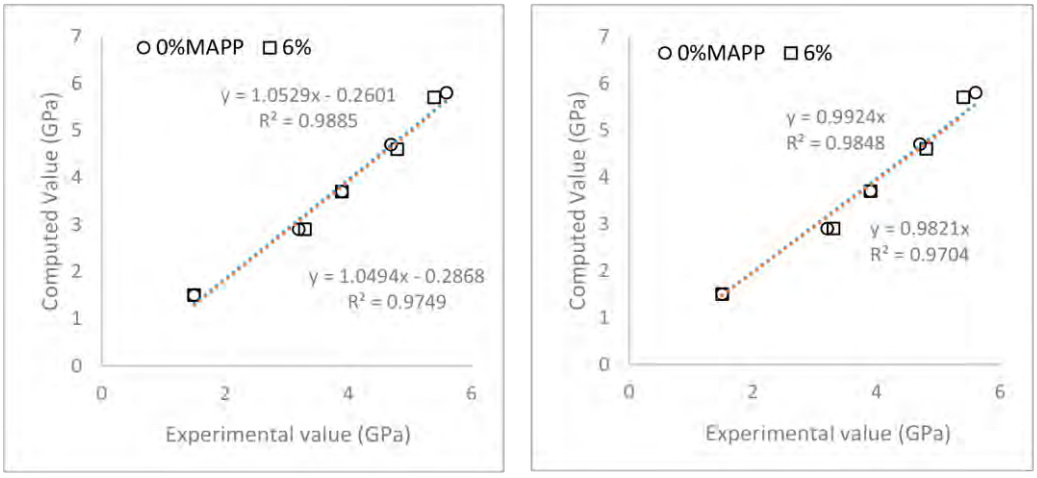

A **B**

Figure 4. Correlation between the experimental Young's moduli of the composites and the computed ones by using the Tsai and Pagano model in combination with Halpin and Tsai equations: (**A**) Unweighted correlation; (**B**) correlation line adding the condition of such line going through the origin.

The regression lines for the uncoupled and coupled composites using the experimental and theoretic values (Figure 4A) show 1.05 slopes, with a high correlation. This slope shows a high coincidence between the computes and experimental values. A second regression line was proposed, passing thorough the origin (Figure 4B). In this case the slopes were found to be 0.99 and 0.98 for the uncoupled and coupled composite, respectively. As mentioned above, these results prove the accuracy of the values predicted from the model. The values also prove the impact of the morphology of the reinforcements in the Young's moduli of the polymers, as Tsai and Pagano model uses these values as the input.

4. Conclusions

Composite materials with CF as reinforcement and PP as the matrix were formulated with 20 to 50 wt% CF contents. Two batches were prepared, one including a 6 wt% of coupling agent and another without.

The Young's moduli of the composites were little impacted by the presence of coupling agents and thus by the strength of the interphase. Thus, for applications where stiffness is paramount, uncoupled composites can be used with the same response under load as the coupled composites. On the other hand, in the case of semi-structural uses, the coupled composites ensure a higher tensile strength and similar deformations under load than the uncoupled ones.

The Young's moduli of the composites were similar to those obtained for natural strands reinforced composites and higher than wood fibers reinforced composites. The presence of a textile dye in the CF decreased its hydrophilicity but also seemed to increase the difficulty in obtaining a good dispersion of the fibers inside the composite, and the decrease in the quality of the dispersion decreased the stiffening yield of CF.

A value of the intrinsic Young's modulus of CF was obtained by using Hirsh's model. The mean value of the modulus was found to be 27.87 GPa, lower than other strands. Nonetheless, this value doubles the values previously published. The value obtained for the CF in a composite with 20 wt% of reinforcement reached 31.48 GPa, a value more proper to other natural strands like hemp.

The micromechanics properties of the Young's modulus of the composites showed the effect of the orientation and the morphology of the fibers. Nonetheless, the authors found some deviations from a linear behavior of the Young's modulus against CF contents. The authors assume that the dispersion of the fibers can be improved to increase the Young's moduli of the composites with high rates of reinforcement. Nonetheless, further research is needed to prove this point.

This paper shows the opportunity of recovering textile cotton fibers, which are useless for the textile industry, to obtain composite materials able to replace glass fiber reinforced materials. In doing so, the dumping and incinerating of such fibers is avoided and the value chain of the textile industry is widened.

Author Contributions: A.S. performed the experiments and wrote the first version of the manuscript; M.-À.C. and J.S. conceived and designed the experiments; F.X.E. and Q.T. performed the calculus and represented the data; F.V. and P.M. guided the project. All the authors contributed to writing and correcting the document.

Funding: The authors wish to acknowledge the financial support of the Càtedra de Processos Industrials Sostenibles of the University of Girona.

Conflicts of Interest: The authors declare no conflict of interest.

References

1. Anastas, P.T.; Warner, J. *Green Chemistry: Theory and Practice*; Oxford University Press: Oxford, UK, 1998.
2. Schumann, A. Plastics-the Environmentally Friendly Design Material. *ATZ Heavy Duty Worldw.* **2019**, *12*, 74. [CrossRef]
3. Ferreira, F.V.; Pinheiro, I.F.; Mariano, M.; Cividanes, L.S.; Costa, J.C.; Nascimento, N.R.; Kimura, S.P.; Neto, J.C.; Lona, L.M. Environmentally friendly polymer composites based on PBAT reinforced with natural fibers from the amazon forest. *Polym. Compos.* **2019**. [CrossRef]

4. Reixach, R.; Espinach, F.X.; Franco-Marquès, E.; Ramirez de Cartagena, F.; Pellicer, N.; Tresserras, J.; Mutjé, P. Modeling of the tensile moduli of mechanical, thermomechanical, and chemi-thermomechanical pulps from orange tree pruning. *Polym. Compos.* **2013**, *34*, 1840–1846. [CrossRef]
5. Serrano, A.; Espinach, F.X.; Tresserras, J.; del Rey, R.; Pellicer, N.; Mutje, P. Macro and micromechanics analysis of short fiber composites stiffness: The case of old newspaper fibers-polypropylene composites. *Mater.Des.* **2014**, *55*, 319–324. [CrossRef]
6. Espinach, F.X.; Chamorro-Trenado, M.A.; Llorens, J.; Tresserras, J.; Pellicer, N.; Vilaseca, F.; Pèlach, A. Study of the Flexural Modulus and the Micromechanics of Old Newspaper Reinforced Polypropylene Composites. *BioResources* **2019**, *14*, 3578–3593.
7. Serra, A.; Tarrés, Q.; Llop, M.; Reixach, R.; Mutjé, P.; Espinach, F.X. Recycling dyed cotton textile byproduct fibers as polypropylene reinforcement. *Text. Res. J.* **2019**, *89*, 2113–2125. [CrossRef]
8. Petrucci, R.; Nisini, E.; Puglia, D.; Sarasini, F.; Rallini, M.; Santulli, C.; Minak, G.; Kenny, J. Tensile and fatigue characterisation of textile cotton waste/polypropylene laminates. *Compos. Pt B-Eng.* **2015**, *81*, 84–90. [CrossRef]
9. Kallel, T.K.; Taktak, R.; Guermazi, N.; Mnif, N. Mechanical and structural properties of glass fiber-reinforced polypropylene (PPGF) composites. *Polym. Compos.* **2018**, *39*, 3497–3508. [CrossRef]
10. Thomason, J.; Jenkins, P.; Yang, L. Glass Fibre Strength—A Review with Relation to Composite Recycling. *Fibers* **2016**, *4*, 18. [CrossRef]
11. Espinach, F.X.; Julian, F.; Verdaguer, N.; Torres, L.; Pelach, M.A.; Vilaseca, F.; Mutje, P. Analysis of tensile and flexural modulus in hemp strands/polypropylene composites. *Compos. Pt. B-Eng.* **2013**, *47*, 339–343. [CrossRef]
12. Vilaseca, F.; Valadez-Gonzalez, A.; Herrera-Franco, P.J.; Pelach, M.A.; Lopez, J.P.; Mutje, P. Biocomposites from abaca strands and polypropylene. Part I: Evaluation of the tensile properties. *Bioresource Technol.* **2010**, *101*, 387–395. [CrossRef] [PubMed]
13. Mishra, R.; Behera, B.; Militky, J. Recycling of Textile Waste Into Green Composites: Performance Characterization. *Polym. Compos.* **2014**, *35*, 1960–1967. [CrossRef]
14. Lopez, J.P.; Mutje, P.; Pelach, M.A.; El Mansouri, N.E.; Boufi, S.; Vilaseca, F. Analysis of the tensile modulus of PP composites reinforced with Stone grounwood fibers from softwood. *BioResources* **2012**, *7*, 1310–1323. [CrossRef]
15. Espinach, F.X.; Mendez, J.A.; Granda, L.A.; Pelach, M.A.; Delgado-Aguilar, M.; Mutje, P. Bleached kraft softwood fibers reinforced polylactic acid composites, tensile and flexural strengths. In *Natural Fibre-Reinforced Biodegradable and Bioresorbable Polymer Composites*; Lau, A., Ed.; Woodhead Publishing Limited: Cambridge, UK, 2017.
16. Araújo, R.S.; Rezende, C.C.; Marques, M.F.V.; Ferreira, L.C.; Russo, P.; Emanuela Errico, M.; Avolio, R.; Avella, M.; Gentile, G. Polypropylene-based composites reinforced with textile wastes. *J. Appl. Polym. Sci.* **2017**, *134*, 45060. [CrossRef]
17. Monteiro, S.N.; Lopes, F.P.D.; Barbosa, A.P.; Bevitori, A.B.; Da Silva, I.L.A.; Da Costa, L.L. Natural Lignocellulosic Fibers as Engineering Materials-An Overview. *Metall. Mater. Trans. A-Phys. Metall. Mater. Sci.* **2011**, *42*, 2963–2974. [CrossRef]
18. Reddy, N.; Yang, Y.Q. Properties and potential applications of natural cellulose fibers from the bark of cotton stalks. *Bioresource Technol.* **2009**, *100*, 3563–3569. [CrossRef]
19. De Silva, R.; Byrne, N. Utilization of cotton waste for regenerated cellulose fibres: Influence of degree of polymerization on mechanical properties. *Carbohyd. Polym.* **2017**, *174*, 89–94. [CrossRef]
20. Serra, A.; Tarrés, Q.; Claramunt, J.; Mutjé, P.; Ardanuy, M.; Espinach, F. Behavior of the interphase of dyed cotton residue flocks reinforced polypropylene composites. *Compos. Pt. B-Eng.* **2017**, *128*, 200–207. [CrossRef]
21. Ryu, C.; Phan, A.N.; Sharifi, V.N.; Swithenbank, J. Combustion of textile residues in a packed bed. *Exp. Therm. Fluid Sci.* **2007**, *31*, 887–895. [CrossRef]
22. Jha, M.K.; Kumar, V.; Maharaj, L.; Singh, R.J. Studies on leaching and recycling of zinc from rayon waste sludge. *Ind. Eng. Chem. Res.* **2004**, *43*, 1284–1295. [CrossRef]
23. Bledzki, A.K.; Franciszczak, P.; Osman, Z.; Elbadawi, M. Polypropylene biocomposites reinforced with softwood, abaca, jute, and kenaf fibers. *Ind. Crop. Prod.* **2015**, *70*, 91–99. [CrossRef]

24. Lopez, J.P.; Boufi, S.; El Mansouri, N.E.; Mutje, P.; Vilaseca, F. PP composites based on mechanical pulp, deinked newspaper and jute strands: A comparative study. *Compos. Pt. B-Eng.* **2012**, *43*, 3453–3461. [CrossRef]
25. Bledzki, A.K.; Mamun, A.A.; Faruk, O. Abaca fibre reinforced PP composites and comparison with jute and flax fibre PP composites. *Express Polym. Lett.* **2007**, *1*, 755–762. [CrossRef]
26. Bledzki, A.K.; Gassan, J. Composites reinforced with cellulose based fibres. *Prog. Polym. Sci.* **1999**, *24*, 221–274. [CrossRef]
27. Rogovina, S.; Prut, E.; Berlin, A. Composite Materials Based on Synthetic Polymers Reinforced with Natural Fibers. *Polym. Sci. Ser. A* **2019**, *61*, 417–438. [CrossRef]
28. Faruk, O.; Bledzki, A.K.; Fink, H.P.; Sain, M. Progress report on natural fiber reinforced composites. *Macromol. Mater. Eng.* **2014**, *299*, 9–26. [CrossRef]
29. Hirsch, T. Modulus of elasticity of concrete affected by elastic moduli of cement paste matrix and aggregate. *J. Am. Concr. Inst.* **1962**, *59*, 427–451. [CrossRef]
30. Halpin, J.C.; Tsai, S.W. *Effects of Environmental Factors on Composite Materials*; Technical Report AFML-TR-67-423; National Institute of Occupational Safety and Health: Cincinnati, OH, USA, 1969.
31. Halpin, J.C.; Pagano, N.J. The Laminate Approximation for Randomly Oriented Fibrous Composites. *J. Compos. Mater.* **1969**, *3*, 720–724. [CrossRef]
32. Granda, L.A.; Espinach, F.X.; Mendez, J.A.; Tresserras, J.; Delgado-Aguilar, M.; Mutje, P. Semichemical fibres of Leucaena collinsii reinforced polypropylene composites: Young's modulus analysis and fibre diameter effect on the stiffness. *Compos. Pt. B-Eng.* **2016**, *92*, 332–337. [CrossRef]
33. Tarrés, Q.; Vilaseca, F.; Herrera-Franco, P.J.; Espinach, F.X.; Delgado-Aguilar, M.; Mutjé, P. Interface and micromechanical characterization of tensile strength of bio-based composites from polypropylene and henequen strands. *Ind. Crop. Prod.* **2019**, *132*, 319–326. [CrossRef]
34. Julian, F.; Mendez, J.A.; Espinach, F.X.; Verdaguer, N.; Mutje, P.; Vilaseca, F. Bio-based composites from stone groundwood applied to new product development. *BioResources* **2012**, *7*, 5829–5842. [CrossRef]
35. Oliver-Ortega, H.; Chamorro-Trenado, M.À.; Soler, J.; Mutjé, P.; Vilaseca, F.; Espinach, F.X. Macro and micromechanical preliminary assessment of the tensile strength of particulate rapeseed sawdust reinforced polypropylene copolymer biocomposites for its use as building material. *Constr. Build. Mater.* **2018**, *168*, 422–430. [CrossRef]
36. Serrano, A.; Espinach, F.X.; Tresserras, J.; Pellicer, N.; Alcala, M.; Mutje, P. Study on the technical feasibility of replacing glass fibers by old newspaper recycled fibers as polypropylene reinforcement. *J. Clean. Prod.* **2014**, *65*, 489–496. [CrossRef]
37. Shah, D.U.; Nag, R.K.; Clifford, M.J. Why do we observe significant differences between measured and 'back-calculated' properties of natural fibres? *Cellulose* **2016**, *23*, 1481–1490. [CrossRef]
38. Facca, A.G.; Kortschot, M.T.; Yan, N. Predicting the elastic modulus of natural fibre reinforced thermoplastics. *Compos. Pt. A-Appl. Sci.* **2006**, *37*, 1660–1671. [CrossRef]
39. Serrano, A.; Espinach, F.X.; Julian, F.; del Rey, R.; Mendez, J.A.; Mutje, P. Estimation of the interfacial shears strength, orientation factor and mean equivalent intrinsic tensile strength in old newspaper fiber/polypropylene composites. *Compos. Pt. B-Eng.* **2013**, *50*, 232–238. [CrossRef]
40. Vallejos, M.E.; Espinach, F.X.; Julian, F.; Torres, L.; Vilaseca, F.; Mutje, P. Micromechanics of hemp strands in polypropylene composites. *Compos. Sci. Technol.* **2012**, *72*, 1209–1213. [CrossRef]
41. Krenchel, H. *Fibre Reinforcement*; Akademisk Forlag: Copenhagen, Denmark, 1964.
42. Del Rey, R.; Serrat, R.; Alba, J.; Perez, I.; Mutje, P.; Espinach, F.X. Effect of Sodium Hydroxide Treatments on the Tensile Strength and the Interphase Quality of Hemp Core Fiber-Reinforced Polypropylene Composites. *Polymers* **2017**, *9*, 377. [CrossRef]
43. Reixach, R.; Franco-Marquès, E.; El Mansouri, N.-E.; de Cartagena, F.R.; Arbat, G.; Espinach, F.X.; Mutjé, P. Micromechanics of Mechanical, Thermomechanical, and Chemi-Thermomechanical Pulp from Orange Tree Pruning as Polypropylene Reinforcement: A Comparative Study. *BioResources* **2013**, *8*, 3231–3246. [CrossRef]
44. Fukuda, H.; Kawata, K. On Young's modulus of short fibre composites. *Fibre Sci. Technol.* **1974**, *7*, 207–222. [CrossRef]
45. Espinach, F.X.; Julián, F.; Alcalà, M.; Tresserras, J.; Mutjé, P. High stiffness performance alpha-grass pulp fiber reinforced thermoplastic starch-based fully biodegradable composites. *BioResources* **2013**, *9*, 738–755. [CrossRef]

46. Thomason, J.L. The influence of fibre length and concentration on the properties of glass fibre reinforced polypropylene: 5. Injection moulded long and short fibre PP. Compos. Pt. A-Appl. Sci. 2002, 33, 1641–1652. [CrossRef]
47. Lopez, J.P.; Mendez, J.A.; Espinach, F.X.; Julian, F.; Mutje, P.; Vilaseca, F. Tensile Strength characteristics of Polypropylene composites reinforced with Stone Groundwood fibers from Softwood. BioResources 2012, 7, 3188–3200. [CrossRef]

4.4. Artículo IV

Journal of Natural Fibers

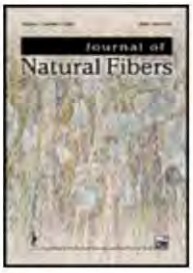

Study of the flexural strength of recycled dyed cotton fiber reinforced polypropylene composites and the effect of the use of maleic anhydride as coupling agent.

Journal:	*Journal of Natural Fibers*
Manuscript ID	Draft
Manuscript Type:	Original Article
Keywords:	cellulose, recycled fibers, cotton, dyes, flexural strength, micromechanics

Girona, March 26, 2021

Dear Editor,

Please find attached our manuscript for publication in Journal of Natural Fibers entitled:

Study of the flexural strength of recycled dyed cotton fiber reinforced polypropylene composites and the effect of the use of maleic anhydride as coupling.

By: Albert Serra, Marc Delgado-Aguilar, Ramon Ripoll, Miquel Llorens, Francesc X. Espinach, Quim Tarrés.

This work uses a by-product of the textile industry, in the shape of cotton flocks to produce composite materials. Usually, the textile industry has no use for the fibers with lengths inferior to 10mm, and thus landfilled or dumped them. Indeed, such fibers could be used to prepare composite materials, adding value to the by-product, extending the value chain of the textile industry and stimulating a circular economy.

The material was received dyed fibers. It was found that the organic dye decreased the hydrophilicity of the cotton fibers, stimulating the creation of a good interphase with the polypropylene. Nonetheless, when coupling agents were added to the composite it was found that the flexural strength of the composites was lower than expected. Thus, the same dyes were suspected to hinder the action of the coupling agents, affecting the quality of the interphase.

We confirm that this manuscript has not been published elsewhere, is not under consideration by another journal, and all authors have approved the manuscript and agree with its submission to Journal of Natural Fibers.

Should you have any questions, please do not hesitate to contact us anytime.

The corresponding author is

Francesc Xavier Espinach

Dpt. of Organization, Business Management and Product Design

Escola Politecnica Superior. Avda. Lluis Santalo, s/n, 17071 Girona, Spain

Phone: 34 972 418 920,

E-mail: franciso.espinach@udg.edu

Study of the flexural strength of recycled dyed cotton fiber reinforced polypropylene composites and the effect of the use of maleic anhydride as coupling agent.

Albert Serra[a], Marc Delgado-Aguilar[a], Ramon Ripoll[b], Miquel Llorens[c], Francesc X. Espinach[d*], Quim Tarrés[a].

[a]LEPAMAP-PRODIS Group, Department of Chemical Engineering, University of Girona, Girona 17003, Spain; [b]Department of Architecture and Construction Engineering, University of Girona, Girona 17003, Spain; [c]Department of Mechanical Engineering and Industrial Construction, University of Girona, Girona 17003, Spain; [d]LEPAMAP-PRODIS Group, Dept. of Organization, Business, University of Girona, Girona 17003, Spain partment of Architecture and Construction Engineering, University of Girona, Girona 17003, Spain

Francesc X. Espinach, Dept. of Organization, Business, Polytechnic school, Building 1, Maria Aurèlia Capmany Str. 61, Montilivi campus, University of Girona, Girona 17003. Francisco.espinach@udg.edu

Albert Serra: PhD student at the university of Girona, Lic in Chemistry, specialized in organic Chemistry. His line of research is devoted no natural fiber reinforced composites.

Marc Delgado-Aguilar: Chemical engineer, currently holds a tenure-track lecturer position at the Department of Chemical and Agricultural Engineering and Agrifood Technology, University of Girona. He also serves as the head of the Departmental Section of Chemical Engineering at Polytechnic School. His main areas of expertise are nanocellulose-based materials, lignocellulose-reinforced composites, and advanced applications of bio-based and biodegradable materials. He is a Serra Húnter Fellow.

Ramón Ripoll: Architect, Senior Lecturer at the University of Girona. His main interests are the preservation of Catalan architectural heritage and the use of innovative and environmentally conscientious solution to the architecture.

Miquel Llorens: Engineer, Lecturer at the University of Girona. His main interests are the numerical simulation of materials and the development of innovative solutions for the industrial building sector.

Francesc X. Espinach: Mechanical engineer and Industrial Engineer. Professor at the University of Girona. Main research interests in the field of product desing and development, innovation, social responsibility, green desing and the development of sustainable materials and processes.

Quim Tarres: Chemical engineer, Researcher at the University of Girona, head of the laboratories of paper engineering and composite materials, and secretary of the Chair of Sustainable Industrial Processes at the University of Girona. Main research interests are Composite Materials reinforced with vegetable fibres, textile materials, nanocomposites and polymeric materials.

Study of the flexural strength of recycled dyed cotton fiber reinforced polypropylene composites and the effect of the use of maleic anhydride as coupling agent.

Albert Serra[a], Marc Delgado-Aguilar[a], Ramon Ripoll[b], Miquel Llorens[c], Francesc X. Espinach[d*], Quim Tarrés[a].

[a]*LEPAMAP-PRODIS Group, Department of Chemical Engineering, University of Girona, Girona 17003, Spain;* [b]*Department of Architecture and Construction Engineering, University of Girona, Girona 17003, Spain;* [c]*Department of Mechanical Engineering and Industrial Construction, University of Girona, Girona 17003, Spain;* [d]*LEPAMAP-PRODIS Group, Dept. of Organization, Business, University of Girona, Girona 17003, Spain partment of Architecture and Construction Engineering, University of Girona, Girona 17003, Spain*

Francesc X. Espinach, Dept. of Organization, Business, Polytechnic school, Building 1, Maria Aurèlia Capmany Str. 61, Montilivi campus, University of Girona, Girona 17003. Francisco.espinach@udg.edu

Albert Serra: PhD student at the university of Girona, Lic in Chemistry, specialized in organic Chemistry. His line of research is devoted no natural fiber reinforced composites.

Marc Delgado-Aguilar: Chemical engineer, currently holds a tenure-track lecturer position at the Department of Chemical and Agricultural Engineering and Agrifood Technology, University of Girona. He also serves as the head of the Departmental Section of Chemical Engineering at Polytechnic School. His main areas of expertise are nanocellulose-based materials, lignocellulose-reinforced composites, and advanced applications of bio-based and biodegradable materials. He is a Serra Húnter Fellow.

Ramón Ripoll: Architect, Senior Lecturer at the University of Girona. His main interests are the preservation of Catalan architectural heritage and the use of innovative and environmentally conscientious solution to the architecture.

Miquel Llorens: Engineer, Lecturer at the University of Girona. His main interests are the numerical simulation of materials and the development of innovative solutions for the industrial building sector.

Francesc X. Espinach: Mechanical engineer and Industrial Engineer. Professor at the University of Girona. Main research interests in the field of product desing and development, innovation, social responsibility, green desing and the development of sustainable materials and processes.

Quim Tarres: Chemical engineer, Researcher at the University of Girona, head of the laboratories of paper engineering and composite materials, and secretary of the Chair of Sustainable Industrial Processes at the University of Girona. Main research interests are Composite Materials reinforced with vegetable fibres, textile materials, nanocomposites and polymeric materials.

Study of the flexural strength of recycled dyed cotton fiber reinforced polypropylene composites and the effect of the use of maleic anhydride as coupling agent.

The flexural strengths of composite materials composed of polypropylene reinforced with cotton fibers recycled from textile waste are presented. Materials with and without coupling agents were prepared. The analysis of the flexural strength of the specimens showed promising properties, both, in the case of the coupled and uncoupled materials, showing their ability to substitute glass fiber reinforced composites. The presence of dyes in the recycled fibers had a noticeable impact on the properties of the composite. A micromechanics analysis showed that the interphase between the matrix and the reinforcements was stronger than expected for uncoupled materials and weaker than expected for coupled ones. The presence of dyes in the fiber surface had a positive effect by decreasing the hydrophilicity of the fibers, and at the same time inhibited the full exploitation of the coupling agents.

Keywords: cellulose; recycled fibers; cotton, dyes; flexural strength

Introduction

The textile industry produces a large number of byproducts with a low or null value. The vast majority of textile waste goes to landfills, with all the environmental problems that it entails (Shuhua et al. 2020). Although the textile industry, in the last decades, has made a great effort to reduce the amount of waste, only a small amount of the textile waste is nowadays recycled, and in 2050, the textile sector is expected to be responsible for 26% of the world carbon budget (Foundation 2017; Shirvanimoghaddam et al. 2020). Furthermore, in the last decades, textile production and consumption have doubled their numbers, with the potential increase of waste creation and groundwater contamination due to the formation of 'leachate' (Shirvanimoghaddam et al. 2020; Jha et al. 2004). These problems have aroused the need for new regulations looking after a reduction of residues and the environmental impact of the textile sector (Serra et al.

2018; Mishra, Behera, and Militky 2014; Hole and Hole 2020). Thus, any effort in increasing the percentage of textile waste decrease is worth considering.

The waste considered in this paper is produced during the preparation of cotton fabrics. This process produces waste in the shape of cotton flocks that are mainly cotton fibers with less than 10mm length (figure 1).

Figure 1: Cotton flocks as received from the textile industry

The cotton flocks provide form the defibration process of cotton trims, used to produce fabrics to manufacture denim (Serra et al. 2017). This is the reason why the cotton fibers are dyed. The presence of dyes adds a layer of complexity to the recycling of the fibers because huge amounts of water, energy, and reactants are needed to eliminate such dyes (Ertaş et al. 2010). Therefore, these cotton flocks remain a waste with little use inside the textile value chain.

The use of lignocellulosic fibers as polyolefin reinforcement has been vastly dealt with in the literature and there are plenty examples of successful examples (Gholampour and Ozbakkaloglu 2020; Kerni et al. 2020; Thomason and Rudeiros-Fernández 2018). The main sources for lignocellulosic reinforcements are wood fibers, annual plants, and agroforestry or industrial waste. Hardwood and softwood fibers have been tested as

reinforcements with notable results, showing the opportunities of such source (Alcala et al. 2013; Chan et al. 2018; Granda et al. 2016 in press.). Anyhow, virgin wood is more prone to be used for other purposes like the furniture of paper pulp. Moreover using trees as a resource involves deforestation and other environmental concerns (Alves et al. 2010). On the other hand, annual plants, in addition to their seeds also produce stems, stalks, and stalks that can be used as reinforcement. Examples are hemp, flax, sisal, and other annual plants (Kumar et al. 2019; Davis et al. 2019; Zuccarello and Scaffaro 2017; Sullins et al. 2017). The main difference between wood fibers and fibers from annual plants is the chemical composition of its surface, which has a main role in the strength of the interphase between the reinforcements and the matrix. Fibers from annual plants show lesser concentrations of lignin and higher percentages of celluloses. The use of waste from agroforestry or industry has also been investigated, but the examples are less common. Old newspaper or textile fibers have been used to produce composites (Serra et al. 2018; Yallew, Kumar, and Singh 2016; Espinach et al. 2019). Anyhow, there are only a few examples of the use of cotton textile waste as composite reinforcement. In the case of dyed cotton fibers, to the best knowledge of the authors, only a few papers researching the tensile properties of such fibers and their composites are available in the literature (Serra et al. 2017; Serra et al. 2018; Sood and Dwivedi 2018; Pensupa et al. 2017), and few of them refer to mold injected materials.

When a short fiber-reinforced composite is mold injected, the fibers orient themselves depending on the geometry of the injection mold, the process parameters, the rheological properties of the composite, and the morphology of the fibers. Consequently, reinforcements semi-align, and thus, the composite shows anisotropy concerning its mechanical properties. Therefore, the tensile and flexural strengths of this kind of composites are noticeably different. The literature shows usually flexural

strengths 1.2 to 1.7 times higher than the tensile strengths for the same composites (Granda et al. 2016; Espinach et al. 2015; Sood and Dwivedi 2018). The main reason for such difference is the fact that a short fiber-reinforced composite is not homogeneous, thus the anisotropy. The differences are also due to the characteristics of the tests. In the case of a three bending test, the maximum tensile stresses are concentrated in the area below the neutral axis, while a tensile test subjects the whole area of the specimen to the same tensile loads.

The differences between the tensile and flexural strength of any material must be taken into account because the larger the difference between both values, the higher the anisotropy of the material, and thus the doubts on its behavior under use conditions. On the other hand, when the composite is used to obtain a part, the load conditions and displacement constraints that will be applied to such part will define its load state. Then, using tensile properties to calculate the geometry of a part under flexural loads will result in an overestimation of such geometry. This overestimation can have economic and environmental consequences as more materials and energy than necessary will be required. Thus the importance of knowing the flexural behavior of the composites and the impacts of coupling agent presence and percentage of reinforcement over such properties.

In this paper, short cotton fibers were used to produce polypropylene-based composites. Amounts of maleic anhydride, ranging from 0 to 10 wt% were used to test the impact of such coupling agent over the flexural strength of the composites. The percentage of coupling agent that returned the highest flexural impact was used to produce composites at 20, 30, 40, and 50 % content of cotton fibers. The impact of the reinforcement percentage on the flexural strength of coupled and uncoupled composites was presented and discussed. A micromechanics model was used to establish the net contribution of

the fibers to the flexural strength of the composites and the intrinsic flexural strength of the fibers.

Materials and methods.

Materials

Fontfilva S. L. (Olot, Girona, Spain) provided Cotton flocks (Figure 1) as a waste of its spinning processes. The flocks are an aggregate of not individualized cotton fibers with lengths lower than 10mm. Moreover, the residues are treated with a reactive dye.

A polypropylene (PP) (Isplen PP090 62M), kindly supplied by Repsol-YPF (Tarragona, Spain), was used as the matrix for the composites. Based on prior experiments, a polypropylene functionalized with maleic anhydride (MAPP) coupling agent, with the commercial name (Epolene G3015) by Eastman Chemical Products (San Roque, Spain), was used to increase the compatibility between the cotton fibers and polypropylene. This reagent has a Mn of 24800 and an acid number of 15 mg KOH/g.

Composite processing

Cotton waste was treated in a blade mill to shorten its length to around 1 mm. This length allows a proper dispersion of the reinforcements inside the composite during mixing operations. An intensive mixer Brabender Plastograph (Brabender, Duisburg, Germany) was used to obtain the composites. Both phases were added to the mixer at different fiber matrix ratios. The mixer was operated at 80 rpm, and the temperature of the blends raised to 185ºC after 10 minutes, when the composites were discharged.

To mold inject the composites, the mixer product has to be pelletized in a knife mill, obtaining pellets with a mean diameter of 8mm. These pellets were stored in an oven at

80ºC for 24 h to prevent moisture absorption.

Mold injection of the specimens

Flexural test specimens following ASTM D618-13, with a mean 127x23x3mm^3 dimensions, were mold injected. The operation followed ASTM D3641. A Meteor-40 injection machine (Mateu & Solé, Spain) was used to obtain the specimens. The equipment was operated at temperatures ranging from 160 to 190ºC at the different heating areas, being the higher temperature that of the injection nozzle. The injection pressure increased from 30 to 70 bars as the percentage of cotton was increased. Likewise, the second pressure increased from 10 to 30 bars due to the same reason.

Mechanical characterization

The specimens were submitted to a three-point bending test following ASTM D618-13 standard in a DTC-10 dynamometer by IDMtest (San Sebastián, Spain). This equipment is equipped with a 5000N load cell. At least five specimens for every composite formulation were tested.

Results and discussion

Effect of coupling agents on the flexural strength of the composites.

Figure 2 shows the evolution of the flexural strength of composites with a 30 wt% of reinforcement against coupling agent percentages.

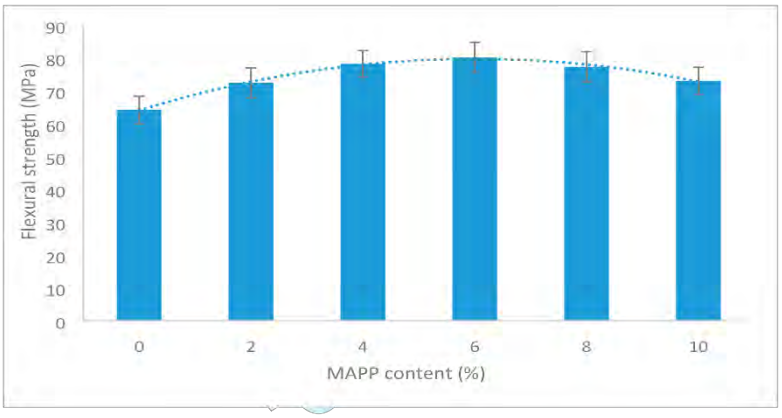

Figure 2: Evolution of the flexural strength of composites adding a 30wt% of reinforcement against coupling agent contents.

The presence of MAPP facilitates the creation of chemical bonds between the OH groups on the surface of the fibers. The accepted mechanism is on the one hand, the creation of hydrogen bonds and covalent ester linkages between hydroxyl groups of the surface of the fibers and the anhydride groups of the MAPP. On the other hand, the PP chains of the MAPP interlock with the matrix (Lopez et al. 2011; Sullins et al. 2017) (Figure 3)

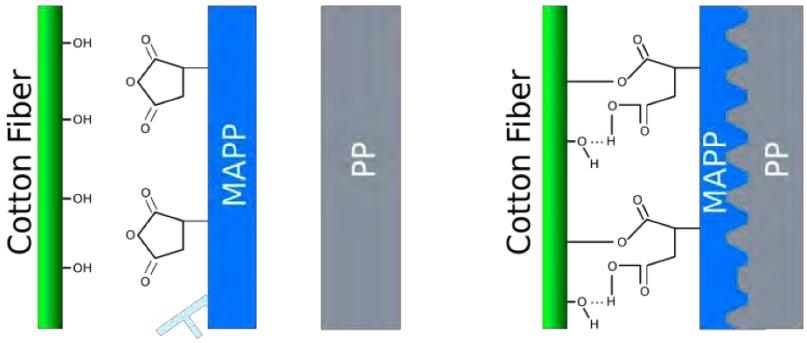

Figure 3: Proposed mechanisms of interaction between the fiber surface, the polypropylene matrix, and the polypropylene functionalized with maleic anhydride.

The literature shows how uncoupled composites tend to show a flexural strength similar or slightly superior to that of the matrix (Tarrés et al. 2019; Sood and Dwivedi 2018). This is due to the incompatibility between the hydrophilic natural fibers and the hydrophobic matrix. Thus, it is common that the interphase region is mostly composed of voids and thus the mechanical anchorage or the creation of chemical bond is highly restricted. In the case of the dyed cotton fiber-reinforced composites, uncoupled materials showed a flexural strength 59% higher than the matrix. This is unusual because points out the presence of interactions in the interphase without using any coupling agent. Thus, the authors think that the dyes can act somehow as coupling agents. The most probable mechanism is that the dyes partially waterproof the surface of the cotton fibers, increasing the compatibility between both phases. Similar effects have been observed in the literature, where the presence of an indigo dye in denim fabric increased the waterproof of such fabric (Zhong et al. 2020). The skeletal formula of indigo dye shows some similarities with the maleic acid (figure 3), thus some interactions cannot be discarded.

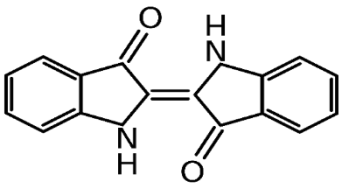

Figure 4: Skeletal formula of indigo dye

Figure 2 shows how when the percentage of MAPP was increased up to 6%, the flexural strength of the composites increased likewise. A local maximum flexural strength was obtained for a 6wt% of MAPP. Higher percentages of coupling agents returned composite materials with decreasing flexural strengths. The literature shows how the presence of excessive percentages of MAPP harms the strength of the composites. This can be explained by the self entanglement of MAPP chains (Oliver-Ortega et al. 2018).

An ANOVA of the data shows that at a 95% confidence ratio, the effects of a 4, 6 and, 8% of MAPP are statistically similar. Nonetheless, the authors used the percentage of MAPP that returned the highest flexural strength, to prepare composites at different reinforcement contents. Thus, coupled and uncoupled material were prepared and tested, to evaluate the impact of the reinforcement percentages of the tensile strength of the composites.

Impact of the cotton fiber contents on the flexural strength

Table 1 shows the mean flexural strengths and strains at break of the composite materials. It was observed that in both cases the flexural strength of the composites increased with increasing percentages of reinforcement. This is usually the case for coupled composites, and the literature shows multiple examples (Tarrés et al. 2019; Sood and Dwivedi 2018; Espinach, Mendez, et al. 2017). Moreover, uncoupled

composites tend to show slight increases in the flexural strength of the matrix, but in some cases, for high fiber contents, uncoupled composites tend to decrease the flexural strength of the matrix (Granda et al. 2016). This is mainly due to the strength of the interphase between the fibers and the matrix. Weak or null interphases do not oppose resistance to fiber pull-outs, and the contribution of the fibers is highly compromised.

Table 1: Evolution of the flexural strength of uncoupled and coupled composites against cotton fiber contents.

Fiber content (%)	V^F	MAPP content (%)	σ_f^C (MPa)	ε_f^C (%)
0	0	0	40.2 ± 0.84	9.6 ± 0.32
20	0.131	0	56.7 ± 0.95	5.8 ± 0.21
30	0.205	0	64.2 ± 1.05	4.7 ± 0.14
40	0.287	0	70.9 ± 1.16	4.0 ± 0.16
50	0.301	0	78.9 ± 1.24	3.8 ± 0.22
20	0.131	6	70.1 ± 1.14	6.7 ± 0.19
30	0.205	6	80.2 ± 1.19	5.5 ± 0.23
40	0.287	6	88.3 ± 2.07	4.9 ± 0.22
50	0.301	6	96.2 ± 2.15	4.1 ± 0.16

For the uncoupled composites, the use of 20 to 50 wt% of cotton fibers increased the flexural strength of the matrix 41, 59.7, 76.4, and 96.3%, respectively. In the case of the coupled composites, the increases were 74.4, 99.5, 119.7, and 139.3% for the same percentages of reinforcement contents. These values were higher than the expected for uncoupled composites, and the expected for coupled materials. The literature shows how with 50% of stone groundwood, abaca, or old newspapers, coupled PP-based composites showed flexural strengths of 98.6, 103.9, and 86.9 MPa, respectively (Lopez et al. 2013; Granda et al. 2016). Nonetheless, if the values of the flexural strength are plotted against fiber volume fractions, it can be observed that this value did not evolve linearly (Figure 5). Uncoupled composites showed a more linear evolution of their flexural strength against reinforcement contents. A linear evolution of the property is a sign of regular interphase between the fibers and the matrix. The figure seems to show a

deterioration of the contribution of the reinforcements to the flexural strength of the composite. Figure 5 presents the theoretical evolution of the flexural strength of the composites. Then it is clear that higher flexural strengths can be expected.

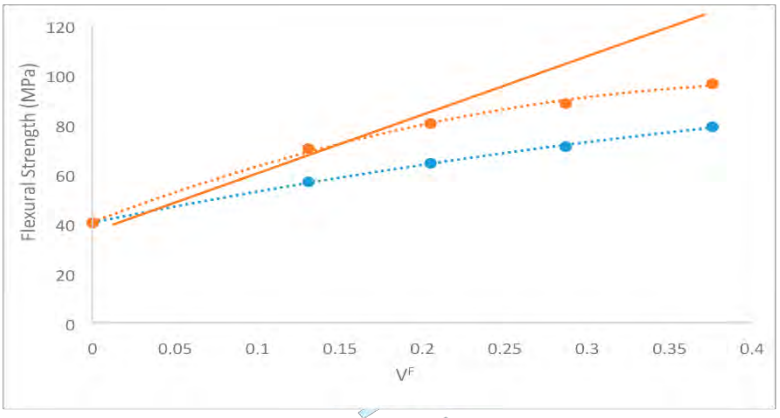

Figure 5: Evolution of the flexural strength of uncoupled and coupled composites against fiber content. The figure also adds a regression line that shows the theoretical linear evolution of the flexural strength of coupled composites.

Notwithstanding, the values obtained for the cotton fiber-reinforced composites can be competitive in front of glass fiber reinforced PP composites under some considerations. On the one hand, the percentage of cotton fibers will be higher than the percentage of glass fibers to obtain similar strengths. In this sense, composites containing a 20 and a 30 wt% of Glass fiber sized, return flexural strengths of 78.0 and 88.1 MPa (Tarrés et al. 2019). In the case of cotton reinforced composites, these values can be obtained partially by uncoupled composites and fully with coupled ones (Table 1). If a coupling agent is added to the Glass fiber-based composites, 97.3 and 125.1 MPa were obtained (Tarrés et al. 2019). The first value can be obtained with coupled composites but the value obtained for the composite with a 30 wt% of glass fiber was not reached with the tested material. It is worth noting that if a linear behavior of the flexural strength was

potential values near 125MPa were possible.

As mentioned above, the presence of dyes in the cotton fibers can have two opposite effects. On the one hand, waterproof the surface of the fibers and increase their compatibility with the matrix. This is indicated by the evolution of the flexural strength of uncoupled composites against fiber content. On the other hand, the presence of the dye can inhibit or limit the effect of the coupling agent. This can be explained by interactions between the maleic anhydride and the colorants or by the concealment of hydroxyl groups due to the presence of the dye (Serra et al. 2017; Serra et al. 2018). Thus, the analysis of the net contribution of the reinforcements to the flexural strength of the composites is of interest.

Micromechanics of the flexural strength

A micromechanics analysis was used to evaluate the contribution of the phases of a composite to its mechanical properties. In this case, knowing the net fiber contributions, evaluating the strength of the interphase and the intrinsic flexural strength of the fibers is the objective. The results will be used to discuss the effect of the presence of dyes on the mechanical properties of the composites. The first step is to evaluate a fiber flexural strength factor (FFSF) as a measure of the net contribution of the fibers to the flexural strength of the composites.

Fiber flexural strength factor

This factor, based on rearranging a rule of mixtures for the flexural strength of a semi-aligned short fiber-reinforced composite (Equation 1), has been used in previous researches to evaluate the contribution of other natural fibers to the strength of such materials (Serra-Parareda et al. 2019; Espinach et al. 2019; Espinach, Granda, et al.

2017).

$$\sigma_f^C - (1 - V^F)\sigma_f^{M*} = f_c \sigma_f^F V^F \quad (1)$$

In the equation, σ_f^C, σ_f^F, σ_f^{M*}, are the flexural strength of the composite, the intrinsic flexural strength of the reinforcement, and the contribution of the matrix understood as its load state at the strain at break of the composite. The value for the contribution of the matrix can be obtained from its stress-strain curve. The data used for the analysis was obtained from a curve fitting of such a curve to a quartic equation (figure 6).

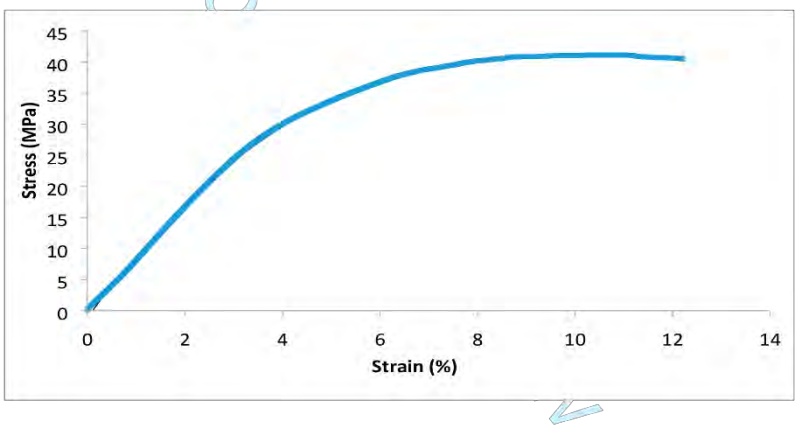

Figure 6: Stress-strain curve for the three-point bending test of the composite specimens.

The volume fraction of the fibers is indicated as V^F, and f_c is a coupling factor that equalizes the contribution of the fibers by having into account the effects of the strength of the interphase, the morphology of the fibers, and its mean orientation (Serra-Parareda et al. 2019; Espinach et al. 2019; Espinach, Granda, et al. 2017). The first term of equation 1 is the flexural strength of the composite minus the contribution of the matrix, thus the contribution of the fibers. The second term of equation 1, $f_c \cdot \sigma_f^F \cdot V^F$, has two constants ($f_c \cdot \sigma_f^F$), and the variable V^F, and thus has the shape of a line with $f_c \cdot \sigma_f^F$ slope.

The slope of the regression lines for the uncoupled and coupled composites and thus its FFSF was 170.9 and 222.7, respectively. These values show better exploitation of the strengthening capabilities of the cotton fibers in the presence of the coupling agent. This factor has the sense to compare the strengthening capabilities of other reinforcements. Alfa fibers, as reinforcement of polypropylene, returned 173 and 335 values (Espinach et al. 2015). While the value for the uncoupled composites is similar, the strengthening capabilities of alfa fibers seem higher than cotton. One explanation can be due to the intrinsic properties of both fibers, another due to flexural strength of alfa fiber reinforced polypropylene composites evolving linearly against the fiber contents, unlike cotton reinforced composites (figure 5) (Espinach et al. 2015). Abaca fibers, when used in coupled PP-based composites returned a FFSF of 209, in line with the results obtained for cotton. Glass fibers return a FFSF of 383.5, showing its strengthening capabilities, and how lesser amounts of glass fiber are needed to obtain composites with high flexural strengths.

Equation 1 has two unknowns, the coupling factor, and the intrinsic flexural strength of the fibers. While these values can be obtained by testing single fibers, the literature shows that there could be differences between the values obtained when a fiber is measured outside or inside a composite (Shah, Nag, and Clifford 2016). The measurements of a single fiber correspond to its properties, and the values obtained from the composite to the exploitation of the properties of such reinforcement. Thus, the authors opted for the use of validated models to compute the value of the intrinsic flexural strength of the fibers.

Intrinsic flexural strength

As commented in the introduction, semi-aligned short-fiber reinforced composites are

anisotropic in terms of mechanical properties. The higher the alignment of the fibers the higher will be such anisotropy. Thus, it is expected that the tensile and flexural properties of these composites will be different, but keep related. Some authors use this relation to calculate the intrinsic flexural strength of fiber from its tensile properties. One interesting proposal relates the tensile strength of the fibers and a fiber tensile strength factor (FTSF) with the flexural strength of the fibers and a fiber flexural strength factor (FFSF) (Tarrés et al. 2019). The FTSF comes from a reformulation of the rule of mixtures for the tensile strength and is similar to equation 1, only changing the subscript from "f" to "t", to indicate tensile. If both equations are divided, we obtain:

$$\frac{\sigma_t^c - (1-V^F)\sigma_t^{M*} = f_c\sigma_t^F V^F}{\sigma_f^c - (1-V^f)\sigma_f^{M*} = f_c\sigma_f^f V^F} \quad (2)$$

This model assumes that the coupling factor under tensile and flexural loads is the same. Considering that, the coupling factor accounts for the fiber morphology, the mean orientation of the fibers, and the strength of the interphase and that, the specimens for tensile and flexural tests were obtained with the same materials and equipment, this assumption can be considered. Then, the coupling factors and the volume fractions can be deleted from the second term of equation 2, and the divider and dividend of the first term substituted by FTSF and FFSF, being FTSF/FFSF= σ_t^F/σ_f^F. In the literature, there are values for all the data concerning the tensile strength (Serra et al. 2017; Serra et al. 2018). Table 2 shows the values for the intrinsic flexural strength of the fibers obtained from equation 2.

Table 2: Evaluation of the intrinsic flexural strength of cotton fibers from recycled textile

Fiber content (%)	MAPP content (%)	τ (MPa)	L_f (μm)	σ_t^F (MPa)	FTSF	FFSF	σ_f^F (MPa)
20	0	9.1	512	973	97.02	170.88	1713

30	0	8.7	459	908	97.02	170.88	1599
40	0	9.3	396	940	97.02	170.88	1655
50	0	9.2	351	829	97.02	170.88	1460
20	6	14.4	509	1240	133.47	222.73	2069
30	6	13.9	406	1162	133.47	222.73	1939
40	6	14.6	339	1368	133.47	222.73	2282
50	6	14.5	299	1295	133.47	222.73	2161

The theoretical intrinsic flexural strengths of uncoupled composites are noticeably higher than those of coupled materials. This is evidence of the exploitation of the strengthening potential of the reinforcements and agrees with the authors that preview differences between intrinsic properties measures experimentally and by using micromechanics methods (Shah, Nag, and Clifford 2016). The minimum value is 1460 MPa and the highest 2282MPa. This does not mean that the intrinsic property changes from one composite to another because the raw materials used to prepare the composites were the same. The results can be read as boundaries, and in all the cases, the intrinsic property of the reinforcement is equal or higher to the highest computed values. Thus, the intrinsic flexural strength of cotton dyed fibers as polypropylene is equal to or higher than 2282 MPa. The differences between the obtained values will be explained by the exploitation of the strengthening potential of the fibers and the limitation to such exploitation due to the strength of the interphase, the morphology of the fibers, and the mean orientation of such fibers.

Table 2 shows the interfacial shear strengths obtained by using the Kelly and Tyson equation for the tensile specimens (Serra et al. 2017; Serra et al. 2018; Kelly and Tyson 1965). Here, a notable difference between coupled and uncoupled composites is observed. Coupled composites showed higher interfacial shear strength and thus a higher ability to transfer loads from the matrix to the fiber. Additionally, the mean length of the fibers decreased with the amount of fiber in the composites but remained similar for coupled and uncoupled composites reinforced with the same amount of

reinforcement. The decrease of the fiber length is attributed to attrition phenomena during composite preparation. This attrition increases with the amount of reinforcement at the same time that the viscosity of the composites increases (Granda et al. 2016). Thus, the main reason for a change in the exploitation of the strengthening abilities of the fibers is most probably due to the changes in the strength of the interphase. Additionally, strong interphases suppose lower critical lengths (L_c), with an increase in the potential contribution of the fibers.

Finally, a rule of mixtures for the flexural strength (Equation 3) was used to verify the strength of the interphase for the flexural specimen by computing the value of the theoretical coupling factor for all the composites.

$$\sigma_f^C = f_c \sigma_f^F V^F + (1 - V^F)\sigma_f^{M*} \quad (3)$$

The value of the intrinsic tensile strength was established to be 2282 MPa for all the cases. Table 3 shows the obtained results.

Table 3: Evaluation of the coupling factor for the composites, assuming that the intrinsic flexural strength of cotton fibers amounts to 2282 MPa.

Fiber content (%)	MAPP content (%)	σ_f^{M*} (MPa)	σ_t^F (MPa)	f_c
20	0	36.4	2282	0.083
30	0	37.2	2282	0.082
40	0	29.6	2282	0.076
50	0	28.6	2282	0.071
20	6	38.5	2282	0.122
30	6	35.5	2282	0.111
40	6	33.5	2282	0.098
50	6	30.1	2282	0.090

The literature shows that strong interphases for semi-aligned short-fiber reinforced composites return coupling factors in the range from 0.18 to 0.20 (Espinach et al. 2019; Serra-Parareda et al. 2019). The values obtained for the coupled composites are far from

the values expected for strong interphases although coupling agents were used to ensure such interphase. Moreover, the value of the coupling factor decreased with the number of fibers, announcing low exploitation of such fibers. On the other hand, the values obtained for uncoupled composites are higher than the expected (Granda et al. 2016). This supports the role of dyes in the strength of the interphase. On the one hand, reduce the hydrophilicity of the fibers and allow creating weak interphase between the fibers and the matrix, but enough to allow load transfer. On the other hand, dyes inhibit a full deployment of the coupling agents and prevent the creation of fully strong interphase. This effect increases with the amount of reinforcement and does not allow a linear evolution of the flexural strength of the composites (Figure 5).

Conclusions

Composites reinforced with fibers from dyed cotton flocs were used as reinforcement for a polypropylene matrix. Percentages of cotton fibers ranging from 20 to 50 wt% were used. At the same time, different percentages of a coupling agent were assayed to ensure the maximization of the flexural strengths and thus the obtention of strong interphases.

A 6 wt% of coupling agent was the dosage that returned the highest flexural strengths for composites reinforced with 30 wt% of cotton fibers. This dosage was used to obtain coupled composites at other cotton fiber contents. The impact of the presence of a coupling agent was lower than the expected, as uncoupled composites increased the flexural strength of the matrix noticeably. A possible effect of the presence of dyes in this behavior was established.

The flexural strength of the composites increased with the presence of reinforcement, both for uncoupled and coupled composites. Nonetheless, the evolution of the flexural

strength for uncoupled composites was almost linear while the evolution of the coupled composites was not. Composites with increased cotton percentages returned lower flexural strengths than those expected by a linear evolution. This was attributed to the presence of interphases less strong than expected. The obtained flexural strengths were similar to those of glass fiber reinforced composites, but with lesser contents of such reinforcement.

The net contribution of the fibers was in line with other natural fibers and lower than glass fiber. The micromechanics analysis allowed establishing that the intrinsic flexural strength of the fibers was at least 2282 MPa. Whit this value, the strength of the interphase was computed to be stronger than expected for uncoupled composites and weaker than expected for coupled ones. This was attributed to the presence of dyes that decreased the hydrophilicity of the fibers, but at the same time inhibit the action of the coupling agents.

The use of a waste from the textile industry as reinforcement allows extending the value chain of the textile industry by adding value to such waste and decrease the amount of textile waste.

References

Alcala, M., I. Gonzalez, S. Boufi, F. Vilaseca, and P. Mutje. 2013. "All-cellulose composites from unbleached hardwood kraft pulp reinforced with nanofibrillated cellulose." *Cellulose* 20 (6):2909-21. doi: 10.1007/s10570-013-0085-2.

Alves, C, AJ Silva, LG Reis, M Freitas, LB Rodrigues, and DE Alves. 2010. "Ecodesign of automotive components making use of natural jute fiber composites." *Journal of Cleaner Production* 18 (4):313-27.

Chan, Clement Matthew, Luigi-Jules Vandi, Steven Pratt, Peter Halley, Desmond Richardson, Alan Werker, and Bronwyn Laycock. 2018. "Composites of Wood

and Biodegradable Thermoplastics: A Review." *Polymer Reviews* 58 (3):444-94. doi: 10.1080/15583724.2017.1380039.

Davis, Aubrey M., Laura E. Hanzly, Barbara L. DeButts, and Justin R. Barone. 2019. "Characterization of dimensional stability in flax fiber reinforced polypropylene composites." *Polymer Composites* 40 (1):132-40. doi: 10.1002/pc.24614.

Ertaş, Murat, Bilal Acemioğlu, M Hakkı Alma, and Mustafa Usta. 2010. "Removal of methylene blue from aqueous solution using cotton stalk, cotton waste and cotton dust." *Journal of Hazardous Materials* 183 (1-3):421-7.

Espinach, F. X., J. A. Mendez, L. A. Granda, M. A. Pelach, M. Delgado-Aguilar, and P. Mutje. 2017. "Bleached kraft softwood fibers reinforced polylactic acid composites, tensile and flexural strengths." In *Natural Fibre-reinforced Biodegradable and Bioresorbable Polymer Composites*, edited by A. Lau. UK: Elsevier.

Espinach, Francesc X, Miquel A Chamorro-Trenado, Joan Llorens, Josep Tresserras, Neus Pellicer, Fabiola Vilaseca, and Angels Pèlach. 2019. "Study of the Flexural Modulus and the Micromechanics of Old Newspaper Reinforced Polypropylene Composites." *Bioresources* 14 (2):3578-93.

Espinach, Francesc X., Luis A. Granda, Quim Tarrés, Josep Duran, Pere Fullana-i-Palmer, and Pere Mutjé. 2017. "Mechanical and micromechanical tensile strength of eucalyptus bleached fibers reinforced polyoxymethylene composites." *Composites Part B: Engineering* 116:333-9. doi: 10.1016/j.compositesb.2016.10.073.

Espinach, FX, M Delgado-Aguilar, J Puig, F Julian, S Boufi, and P Mutjé. 2015. "Flexural properties of fully biodegradable alpha-grass fibers reinforced starch-based thermoplastics." *Composites Part B: Engineering* 81:98-106. doi: 10.1016/j.compositesb.2015.07.004.

Foundation, Ellen MacArthur. 2017. "A new textiles economy: Redesigning fashion's future." In.: Ellen MacArthur Foundation Cowes, Isle of Wight, UK.

Gholampour, Aliakbar, and Togay Ozbakkaloglu. 2020. "A review of natural fiber composites: Properties, modification and processing techniques, characterization, applications." *Journal of Materials Science* 55 (3):829-92.

Granda, L., Q. Tarres, F. X. Espinach, F Julian, A. Mendes, M. Delgado-Aguilar, and P Mutje. 2016 in press. "Fully biodegradable polylactic composites reinforced with bleached softwood fibers." *Cellulose, Chemistry and Technology*.

Granda, LA, FX Espinach, JA Méndez, F Vilaseca, M Delgado-Aguilar, and P Mutjé. 2016. "Semichemical fibres of Leucaena collinsii reinforced polypropylene composites: Flexural characterisation, impact behaviour and water uptake properties." *Composites Part B: Engineering* 97:176-82.

Hole, Glenn, and Anastasia S Hole. 2020. "Improving recycling of textiles based on lessons from policies for other recyclable materials: A minireview." *Sustainable Production and Consumption*.

Jha, M. K., V. Kumar, L. Maharaj, and R. J. Singh. 2004. "Studies on leaching and recycling of zinc from rayon waste sludge." *Industrial & Engineering Chemistry Research* 43 (5):1284-95. doi: 10.1021/ie020949p.

Kelly, A., and W. Tyson. 1965. "Tensile porperties of fibre-reinforced metals - copper/tungsten and copper/molybdenum." *Journal of the Mechanics and Physics of Solids* 13 (6):329-38. doi: 10.1016/0022-5096(65)90035-9

Kerni, Love, Sarbjeet Singh, Amar Patnaik, and Narinder Kumar. 2020. "A review on natural fiber reinforced composites." *Materials Today: Proceedings* 28:1616-21.

Kumar, R., M. I. Ul Haq, A. Raina, and A. Anand. 2019. "Industrial applications of natural fibre-reinforced polymer composites - challenges and opportunities." *International Journal of Sustainable Engineering* 12 (3):212-20. doi: 10.1080/19397038.2018.1538267.

Lopez, J. P., J. Girones, J. A. Mendez, M. A. Pelach, F. Vilaseca, and P. Mutje. 2013. "Impact and flexural properties of stone-ground wood pulp-reinforced polypropylene composites." *Polymer Composites* 34 (6):842-8. doi: 10.1002/pc.22486.

Lopez, J. P., J. A. Mendez, N. E. El Mansouri, P. Mutje, and F. Vilaseca. 2011. "Mean intrinsic tensile properties of stone groundwood fibers from softwood." *Bioresources* 6 (4):5037-49. doi: 10.15376/biores.6.4.5037-5049.

Mishra, R., B. Behera, and J. Militky. 2014. "Recycling of Textile Waste Into Green Composites: Performance Characterization." *Polymer Composites* 35 (10):1960-7. doi: 10.1002/pc.22855.

Oliver-Ortega, Helena, Miquel Àngel Chamorro-Trenado, Jordi Soler, Pere Mutjé, Fabiola Vilaseca, and Francesc X Espinach. 2018. "Macro and micromechanical preliminary assessment of the tensile strength of particulate rapeseed sawdust reinforced polypropylene copolymer biocomposites for its use as building

material." *Construction and Building Materials* 168:422-30. doi: 10.1016/j.conbuildmat.2018.02.158.

Pensupa, Nattha, Shao-Yuan Leu, Yunzi Hu, Chenyu Du, Hao Liu, Houde Jing, Huaimin Wang, and Carol Sze Ki Lin. 2017. "Recent Trends in Sustainable Textile Waste Recycling Methods: Current Situation and Future Prospects." *Topics in Current Chemistry* 375 (5):76.

Serra-Parareda, F., Q. Tarres, M. Delgado-Aguilar, F. X. Espinach, P. Mutje, and F. Vilaseca. 2019. "Biobased Composites from Biobased-Polyethylene and Barley Thermomechanical Fibers: Micromechanics of Composites." *Materials* 12 (24):13. doi: 10.3390/ma12244182.

Serra, A, Q Tarrés, J Claramunt, P Mutjé, M Ardanuy, and FX Espinach. 2017. "Behavior of the interphase of dyed cotton residue flocks reinforced polypropylene composites." *Composites Part B: Engineering* 128:200-7. doi: https://doi.org/10.1016/j.compositesb.2017.07.015.

Serra, Albert, Quim Tarrés, Miquel Llop, Rafel Reixach, Pere Mutjé, and Francesc X Espinach. 2018. "Recycling dyed cotton textile byproduct fibers as polypropylene reinforcement." *Textile Research Journal*:2113-25. doi: https://doi.org/10.1177/0040517518786278.

Shah, D. U., R. K. Nag, and M. J. Clifford. 2016. "Why do we observe significant differences between measured and 'back-calculated' properties of natural fibres?" *Cellulose* 23 (3):1481-90. doi: 10.1007/s10570-016-0926-x.

Shirvanimoghaddam, Kamyar, Bahareh Motamed, Seeram Ramakrishna, and Minoo Naebe. 2020. "Death by waste: Fashion and textile circular economy case." *Science of The Total Environment* 718:137317.

Shuhua, Wang, Yu Xiaoying, Chen Xiaogang, Hou Wensheng, and Niu Mei. 2020. "Recycling of Cotton Fibers Separated from the Waste Blend Fabric." *Journal of Natural Fibers* 17 (4):520-31.

Sood, Mohit, and Gaurav Dwivedi. 2018. "Effect of fiber treatment on flexural properties of natural fiber reinforced composites: A review." *Egyptian journal of petroleum* 27 (4):775-83.

Sullins, Theresa, Selvum Pillay, Alastair Komus, and Haibin Ning. 2017. "Hemp fiber reinforced polypropylene composites: The effects of material treatments." *Composites Part B: Engineering* 114:15-22. doi: https://doi.org/10.1016/j.compositesb.2017.02.001.

Tarrés, Quim, Helena Oliver-Ortega, F Xavier Espinach, Pere Mutjé, Marc Delgado-Aguilar, and José A Méndez. 2019. "Determination of Mean Intrinsic Flexural Strength and Coupling Factor of Natural Fiber Reinforcement in Polylactic Acid Biocomposites." *Polymers* 11 (11):1736.

Thomason, James L, and José Luis Rudeiros-Fernández. 2018. "A review of the impact performance of natural fiber thermoplastic composites." *Frontiers in Materials* 5:60.

Yallew, Temesgen Berhanu, Pradeep Kumar, and Inderdeep Singh. 2016. "Mechanical behavior of nettle/wool fabric reinforced polyethylene composites." *Journal of Natural Fibers* 13 (5):610-8.

Zhong, Tuhua, Renuka Dhandapani, Dan Liang, Jinwu Wang, Michael P Wolcott, Dana Van Fossen, and Hang Liu. 2020. "Nanocellulose from recycled indigo-dyed denim fabric and its application in composite films." *Carbohydrate Polymers* 240:116283.

Zuccarello, B., and R. Scaffaro. 2017. "Experimental analysis and micromechanical models of high performance renewable agave reinforced biocomposites." *Composites Part B: Engineering* 119:141-52. doi: https://doi.org/10.1016/j.compositesb.2017.03.056.

4.5. Artículo V

materials

MDPI

Article

Exploring the Potential of Cotton Industry Byproducts in the Plastic Composite Sector: Macro and Micromechanics Study of the Flexural Modulus

Albert Serra [1], Ferran Serra-Parareda [1], Fabiola Vilaseca [2], Marc Delgado-Aguilar [1], Francesc X. Espinach [1] and Quim Tarrés [1,3,*]

[1] LEPAMAP-PRODIS Research Group, University of Girona, Maria Aurèlia Capmany 61, 17003 Girona, Spain; albert.serra@udg.edu (A.S.); ferran.serrap@udg.edu (F.S.-P.); m.delgado@udg.edu (M.D.-A.); francisco.espinach@udg.edu (F.X.E.)
[2] Advanced Biomaterials and Nanotechnology, Department of Chemical Engineering, University of Girona, Maria Aurèlia Capmany 61, 17003 Girona, Spain; fabiola.vilaseca@udg.edu
[3] Chair on Sustainable Industrial Processes, University of Girona, Maria Aurèlia Capmany 61, 17003 Girona, Spain
* Correspondence: joaquimagusti.tarres@udg.edu

Abstract: The textile sector produces yearly great quantities of cotton byproducts, and the major part is either incinerated or landfilled, resulting in serious environmental risks. The use of such byproducts in the composite sector presents an attractive opportunity to valorize the residue, reduce its environmental impact, and decrease the pressure on natural and synthetic resources. In this work, composite materials based on polypropylene and dyed cotton byproducts from the textile industry were manufactured. The competitiveness of the resulting composites was evaluated from the analyses, at macro and micro scales, of the flexural modulus. It was observed that the presence of dyes in cotton fibers, also a byproduct from the production of denim items, notably favored the dispersion of the phases in comparison with other cellulose-rich fibers. Further, the presence of a coupling agent, in this case, maleic anhydride grafted polypropylene, enhanced the interfacial adhesion of the composite. As a result, the flexural modulus of the composite at 50 wt.% of cotton fibers enhanced by 272% the modulus of the matrix. From the micromechanics analysis, using the Hirsch model, the intrinsic flexural modulus of cotton fibers was set at 20.9 GPa. Other relevant micromechanics factors were studied to evaluate the contribution and efficiency of the fibers to the flexural modulus of the composite. Overall, the work sheds light on the potential of cotton industry byproducts to contribute to a circular economy.

Keywords: cotton fibers; textile byproduct; flexural modulus; composites; circular economy

Citation: Serra, A.; Serra-Parareda, F.; Vilaseca, F.; Delgado-Aguilar, M.; Espinach, F.X.; Tarrés, Q. Exploring the Potential of Cotton Industry Byproducts in the Plastic Composite Sector: Macro and Micromechanics Study of the Flexural Modulus. Materials 2021, 14, 4787. https://doi.org/10.3390/ma14174787

Academic Editor: It-Meng (Jim) Low

Received: 28 July 2021
Accepted: 20 August 2021
Published: 24 August 2021

1. Introduction

The circular economy has recently evolved and gained acceptance mainly due to the increasing environmental awareness in our society, scarcity of resources, and environmental legislation [1,2]. One major goal of the circular economy is the minimization of waste generation in industrial processes, or otherwise, the implementation of systems that promote conscientious management of such wastes via, for example, its valorization in other sectors [3]. In this context, the textile sector has experienced considerable growth in recent years, reaching up to approximately 105 million tons per year of textile fibers by 2018 [4], which by consequence has driven the generation of high amounts of textile byproducts [5]. A large fraction of such textile byproducts with low-added value are landfilled or incinerated, resulting in serious environmental risks, whilst only a minor part is recycled. As reported, only 15% of the textile byproducts worldwide are currently recycled or reused, and it is estimated that nowadays such wastes occupy 5% of the mass of landfills [6]. To enhance the sustainability of the textile sector and reduce the environmental

impact resulting from the improper waste management strategies, the application of a circular economy and valorization of the byproducts is of utmost importance.

It is estimated that a great part, about 35–40%, of the textile waste produced globally consists of cotton [7,8]. The production of cotton fabrics consists of a first step where the cotton fibers are yarned to produce high-quality yarns, which are then destined to the manufacturing of fabrics and the obtention of textiles. This step generates high content of fibrous residues in the shape of cotton trims, which are posteriorly submitted to a defibration process to obtain cotton fibers. Again, these fibers are yarned for the final production of textiles that will be used for the manufacturing of denim products. These fibers used to produce denim items are generally more than 10 mm in length, whereas those fibers less than 10 mm in length are unable to be yarned and thus have no value to the textile industry. Such fibrous-like material stemming from the yarning of cotton trims has usually been referred to, owing to its shape and appearance, as cotton flocks, which are regarded as a lignocellulosic byproduct of the textile industry. Additionally, the dyes applied for the production of denim products remain in such cotton flocks, which indeed add a layer of complexity to its recycling, as huge amounts of water, energy, and reactants may be needed to eliminate the dyes, making these operations economically and environmentally unfeasible [9].

An attractive way to valorize dyed cotton flocks could be by its incorporation in polymer matrixes to provide improved strength and/or stiffness to composite materials. Such composite materials have been typically produced using synthetic fibers (i.e., glass, carbon, or aramid); though, in recent years, there has been an increasing interest in substituting such materials with natural fibers [10–12]. This is mainly due to the much more eco-friendly character of natural fibers over synthetic ones due to their biobased, renewable, recyclable, and biodegradable nature [13]. Additionally, mixing natural fibers and plastic materials may contribute to low-weight, non-abrasive, non-toxic, low-cost, and biodegradable properties [14]. Natural fiber composites (NFC) have been traditionally developed using flax, abaca, bamboo, hemp, sisal, and wood, amongst others [15]. However, in practice, any type of lignocellulosic material, such as recycled fibers, side streams from agricultural practices, or even industrial byproducts, can be added to plastics as reinforcement [16]. In this context, the current investigation aimed to incorporate dyed cotton flocks, an industrial textile byproduct, into polypropylene, with the purpose of valorizing the residue, contributing to a circular economy, reducing the pressure on natural resources, and developing competitive composite materials that can replace the existing ones.

The case of cotton flocks is considered particularly interesting given the huge availability of the residue and its favorable chemical composition. Cotton is a cellulose-rich material with high availability of hydroxyls groups at the fibers' surface [17]. The abundance of hydroxyl groups can aid the development of bonds between the polymeric and lignocellulosic phases under favorable conditions. For instance, in polypropylene (PP)-based composites, with PP probably being the most representative polyolefin within the composite sector, the use of maleic anhydride grafted polypropylene (MAPP) as a coupling agent has effectively proved to enhance the interfacial adhesion by connecting the hydroxyl groups in the fiber surface and maleic acid chains. The action of MAPP is based on two mechanisms: first, the maleic groups form covalent bonds through esterification with the hydroxyl groups in the surface of the fiber; second, MAPP's PP chains diffuse through entanglement (physical interactions) between the unmodified PP chains [18–20]. Hence, an elevated presence of hydroxyls groups combined with the action of an adequate coupling agent can develop an optimal scenario to enhance the fiber–plastic compatibility. Otherwise, poor compatibilities may lead to fiber agglomeration, uneven dispersion within the matrix, and low stress-transfer capacity, ultimately hindering the composite's properties. Strengthening the interfacial adhesion with coupling agents may also contribute to the water barrier properties of the composite material by reducing the gaps between the fiber and the matrix [21]. In previous work from the research team dealing with the tensile and

flexural strength of cotton fiber-reinforced PP composites, a 6 wt.% of MAPP concerning the fiber content was established as an optimal percentage of coupling agent to effectively address the issue of the interfacial adhesion. At this MAPP content, the higher tensile and flexural strength increments were obtained concerning the uncoupled composite. For this reason, in this work, composite materials were prepared both without and with a 6 wt.% of MAPP. It must be stated that other grades of natural fiber-reinforced PP composites may require lower MAPP contents. This may be explained by the greater contribution of hydroxyl groups in the case of cotton fibers in comparison with other fiber sources (i.e., wood) [18,22].

As mentioned, cotton flocks may contain dyes resulting from the manufacture of denim products. The presence of dyes in cotton flocks has been reported to increase the hydrophobicity of the fibers, and thus, better dispersion of the phases is expected [9,23]. It is even possible to find some studies where the use of coupling agents was deemed unnecessary due to the presence of dyes acting as a hydrophobic agent of the fiber surface. Indeed, such dyes could also be interfering with the action of the coupling agents by reducing the accessibility to the hydroxyls groups [24]. However, disposing of coupling agents may lead to insufficient strength increments and limit the potential of the composite material. Overall, there seems to be widespread rather ambiguous results on the influence of dyes and coupling agents in cotton flocks-reinforced plastic composites.

The development of novel materials might fill demands that cannot be satisfied with the existing materials. In this sense, it is important to evaluate the potential of such materials in their specific application sectors, which are principally the automotive and building/construction sectors for the case of natural fiber composites. In such sectors, the composites are transformed, mainly by injection molding or extrusion processes, to obtain products such as door panels, roofing sheets, seat backboards, windows, and floor tiles, amongst others. These components principally develop structural or semi-structural functions and hence are typically subjected to bending forces, whereas tensile forces are scarce in comparison. This makes the flexural behavior of composite materials particularly relevant for gauging the potential of these products. Engineers and architects have a particular interest in previewing the materials' behavior under use conditions. When it comes to mechanical properties, Neagu et al. [25] explained that the most important characteristics of composite materials aiming at structural functions are dimensional stability and stiffness, whereas strength has a less important role. Overall, there seems to be an interest in the flexural behavior and stiffness of composite material, altogether making necessary the study of the flexural modulus as a key parameter for determining the technical viability of any product. Further, modeling the flexural modulus of composite materials via micromechanics analysis can be useful in understanding the fiber reinforcing mechanism, in determining the intrinsic flexural modulus of the fibers, and in evaluating the contribution of the fibers to the flexural modulus of the composite. Further, micromechanics analysis allows relevant characteristics of the fibers to be obtained, making it possible to predict their performance in similar systems. Some well-known micromechanical models include the Hirsch and Tsai-Pagano models, which can be used for the prediction of the intrinsic flexural modulus, the Cox-Krenchel model, the Fukuda model, and the Kawata model, amongst others—all of them contributing to a better understanding of the role of natural fibers in polymer composites. These micromechanics models have offered an effective prediction of the intrinsic properties and behavior of natural fiber composites, as reflected in numerous studies [26–28].

The present work examines the flexural moduli of PP-based composites processed using injection molding and charged up with 10–50 wt.% of cotton flocks, with the main purpose of valorizing this residue and reducing the pressure on other types of reinforcements, either synthetic or extracted from natural resources. Further, the influence of the coupling agent, MAPP, and dyes on the composites is evaluated. The competitiveness of the developed composites is assessed from macro- and micromechanics analyses of the flexural moduli, hereby considered a relevant mechanical prop-

decalin (decahydronaphthalene) as solvent. The whole extraction process lasted about 24 h, and then the fibers were rinsed with acetone and distilled water to remove the remaining solvent. The morphology of the fibers was evaluated using a MorFi Compact from Techpap SAS (Gières, France). The equipment measures about 30,000 fibers per test and, amongst other parameters, returns the average fiber lengths and diameters of the fibers.

Scanning electron microscopy (SEM) was performed on the cross-sectional area of the fractured specimens using a Zeiss DMS 960 SEM microscope by Zeiss (Jena, Germany).

2.2.4. Density Measurement and Void Volume Percentage

The density of the composite (ρ^c) and matrix (ρ^m) was determined using a pycnometer and distilled water as reference liquid. Then, the density of the fibers (ρ^F) was obtained from Equation (1), whereas the fiber volume fraction (V^F) was calculated following Equation (2):

$$\rho^C = \frac{w^C}{w^m/\rho^m + w^F/\rho^F} \quad (1)$$

$$V^F = \frac{w^F/\rho^F}{w^F/\rho^F + w^m/\rho^m} \quad (2)$$

where w^C, w^m, and w^F represent the composite, matrix, and fiber weight fractions, respectively. Void volume percentage (V_{void}) was estimated using the expression in Equation (3) [31]:

$$V_{void} = \left(\frac{{\rho^C}_{th} - {\rho^C}_{ex}}{{\rho^C}_{th}}\right) \cdot 100 \quad (3)$$

where ${\rho^C}_{th}$ and ${\rho^C}_{ex}$ are the theoretical and experimental density of the composites. The theoretical density of the composites is calculated assuming a fiber density of 1.54 g/cm^3, which agrees with accepted values in the literature.

2.2.5. Modeling the Flexural Modulus

Modeling the behavior of natural fiber composites is often required to gain a deeper understanding of the reinforcing mechanisms and to take advantage of the potential of the composites. Additionally, natural fiber-reinforced composites exhibit complex behavior under load due to their anisotropy, which further supports the use of such micromechanics models. One of the simplest ways to compute the contribution of the fibers and matrix to the flexural modulus of the composite is through a modified Rule of Mixtures (mRoM). The rule was initially developed to model Young's modulus [30], although it was rapidly adapted to the flexural modulus [32]. The mRoM for the flexural modulus is presented in Equation (4):

$$E_f^C = \eta_e \cdot E_f^F \cdot V^F + E_f^M \cdot \left(1 - V^F\right) \quad (4)$$

where E_f^C, E_f^F, and E_f^M are the flexural modulus of the composite, fiber, and matrix, respectively. The fiber volume fraction is represented by V^F, whereas the contribution of the fibers to the flexural modulus of the composite is corrected by incorporating a modulus efficiency factor (η_e). The fiber volume fraction may be simply calculated from the density of the composite (ρ^C) and the polymer (ρ^M), both measured using a pycnometer, and from the fiber (w^F) and matrix (w^M) weight fractions [33].

The contribution of the fibers to the overall flexural modulus of the composite can be determined from a Fiber Flexural Modulus Factor (FFMF) by rearranging the mRoM. The contribution of the fibers to the flexural modulus of the composite, expressed by $E_f^C - E_f^M \cdot (1 - V^F)$, is graphically represented as a function of the fiber volume fraction (V^F) at each fiber content (Equation (5)). The FFMF is obtained from the slope of the regression line that joins the contributions at different reinforcement volume fractions. The

parameter has been typically used in the literature for comparison purposes with other types of reinforcement within the same matrix.

$$\text{FFMF} = \eta_e \cdot E_f^F = \frac{E_f^C - E_f^M \cdot (1 - V^F)}{V^F} \tag{5}$$

The mRoM, in its current shape, contains two unknowns, which are the intrinsic flexural modulus of the fibers (E_f^F) and modulus efficiency factor (η_e). Following previously published methodologies, the intrinsic flexural modulus can be effectively determined using either (i) the Hirsch model [34] or (ii) the Tsai–Pagano model employing Halpin–Tsai equations, hereby abbreviated as TP&HT [35–37].

The Hirsch model is a combination of Reuss and Voigt models. The Reuss model defines a system where the load is applied parallel to the fiber axis, whereas in the Voigt model, the stress happens perpendicular to the fiber axis. From the combination of both models and, by the inclusion of a stress-transfer coefficient (β), the Hirsch model is obtained. Generally, in those short fiber polymer composites processed using injection molding, a value of β close to 0.4 has shown good agreement between theoretical and experimental values [38]. The Hirsch model is reported in Equation (6):

$$E_f^c = \beta \cdot \left(E_f^F \cdot V^F - E_f^M \left(1 - V^F \right) \right) + \left(1 - V^F \right) \cdot \frac{E_f^F \cdot E_f^M}{E_f^M \cdot V^F + E_f^F \cdot (1 - V^F)} \tag{6}$$

Unlike the Hirsch model, where only experimental data from the flexural test are used, the TP and HT model also considers morphological features of the fibers, such as mean fiber length (l^F) and diameter (d^F). Tsai–Pagano model is described in Equation (7), whereas the longitudinal modulus (E^{11}) and transverse modulus (E^{22}) may be determined following Halpin–Tsai equations according to Equations (8) and (9):

$$E_f^C = \frac{3}{8} \cdot E^{11} + \frac{5}{8} \cdot E^{22} \tag{7}$$

$$E^{11} = \frac{1 + 2 \cdot (l^F / d^F) \cdot \eta_l \cdot V^F}{1 - \eta_l \cdot V^F} \cdot E_f^m \; ; \; \eta_l = \frac{\left(E_f^F / E_f^M \right) - 1}{\left(E_f^F / E_f^M \right) + 2 \cdot (l^F / d^F)} \tag{8}$$

$$E^{22} = \frac{1 + 2 \cdot \eta_t \cdot V^F}{1 - \eta_t \cdot V^F} \cdot E_f^m \; ; \; \eta_t = \frac{\left(E_f^F / E_f^M \right) - 1}{\left(E_f^F / E_f^M \right) + 2} \tag{9}$$

Once the intrinsic flexural modulus is computed, either by Hirsch or TP&HT models, the modulus efficiency factor may be obtained from the mRoM in Equation (4). Such modulus efficiency factor is mainly influenced by the orientation and length of the fibers inside the composite, which makes it possible to decompose the factor in a modulus orientation factor (η_l) and modulus length factor (η_o) according to Equation (10):

$$\eta_e = \eta_l \cdot \eta_o \tag{10}$$

Both η_l and η_o can be obtained by initially calculating the η_l through the Cox and Krenchel model (Equation (11)) [39,40] and then isolating the η_o from Equation (10). It should be noted that the factor ξ in Equation (11) refers to the stress concentration rate at the ends of the fibers, whereas ν is the Poisson's ratio of the matrix—in this case, 0.36 for PP.

$$\eta_l = 1 - \frac{\tan h \left(\xi \cdot l^F / 2 \right)}{\xi \cdot l^F / 2} \; ; \; \xi = \frac{1}{(d^F / 2)} \cdot \sqrt{\frac{E_f^M}{E_f^F \cdot (1 - \nu) \cdot \sqrt{\ln(\pi / 4 V^F)}}} \tag{11}$$

Once the orientation factor is obtained from Equation (10), it is possible to relate such factor to a limiting angle of the fibers (α_o) following the Fukuda and Kawata model (Equation (12)) [41]. Then, Sanomura and Kawamura [42] proposed an orientation parameter (f_p) from which a theoretical average orientation of the fibers (α) can be obtained ((Equation (13)):

$$\eta_o = \frac{\sin(\alpha_o)}{\alpha_o} \cdot \left(\frac{3-\nu}{4} \cdot \frac{\sin(\alpha_o)}{\alpha_o} + \frac{1-\nu}{4} \cdot \frac{\sin(3\alpha_o)}{3\alpha_o} \right) \tag{12}$$

$$f_p = \frac{\sin(2\alpha_o)}{2\alpha_o} = 2 \cdot \cos^2(\alpha) - 1 \tag{13}$$

The workflow of the current investigation, from experimental to micromechanics modeling, is presented in Figure 1.

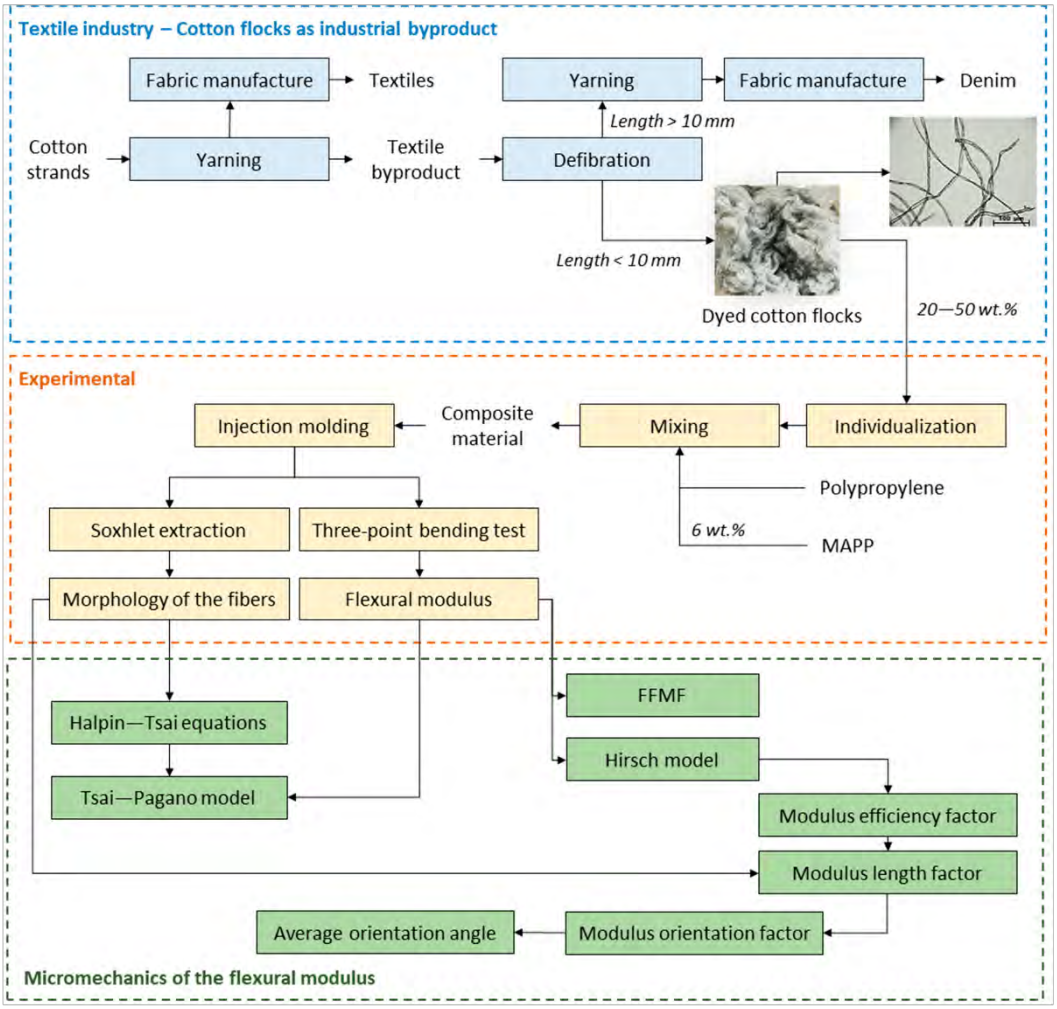

Figure 1. Workflow of the present investigation.

3. Results

3.1. Density and Void Volume Percentage of the Composites

The effect of fiber loading on the density and void volume percentage of the composites was evaluated and the results are collected in Table 1.

Table 1. Fiber content, matrix density (ρ^m), experimental composite density ($\rho^C{}_{ex}$), fiber density (ρ^F), fiber volume fraction (V^F), theoretical composite density ($\rho^C{}_{th}$), and void volume percentage (V_{void}).

Fiber Content (wt. %)	ρ^m (g/cm^3)	$\rho^C{}_{ex}$ (g/cm^3)	ρ^F (g/cm^3)	V^F	$\rho^C{}_{th}$ (g/cm^3)	V_{void} (%)
20	0.905	0.983	1.500	0.131	0.986	0.339
30		1.028	1.505	0.205	1.033	0.460
40		1.076	1.502	0.287	1.084	0.715
50		1.129	1.504	0.376	1.140	0.881

The density of the composites is observed to increase with the fiber content due to the notably higher density of cotton fibers in comparison with the neat matrix. In this sense, the density of cotton fibers was calculated to be 1.50 g/cm^3, assuming fully dense composite materials. However, the reported density in the literature for cotton fibers has been set at 1.54 g/cm^3, from which the theoretical density of the composite can be back calculated with the purpose of obtaining the void volume percentage of the composites (Equation (3)). Accordingly, the manufactured composites yielded void volume percentages of 0.339, 0.460, 0.715, and 0.881% concerning the 20, 30, 40, and 50 wt.% fiber content.

Porosity or void content in natural fiber composites is usually due to the intra fiber voids, such as natural fiber lumen, or due to the formation of voids between fibers. The first phenomenon affects composites with low fiber content, and the second increases with the percentage of fibers, uneven dispersion, or low individualization. Indeed, it is observed that void content increased with the fiber volume fraction. In this work, the relatively low void volume percentages are principally attributed to the compression forces that the materials undergo due to the mold injection process. Fibers' morphology changes noticeably during this phase. The lumen disappears as the fibers are compressed. On the other hand, the authors individualized the fibers prior to their processing to minimize the apparition of fiber bundles and to ensure a proper and regular dispersion of the reinforcements in the composite. This fact decreases the formation of voids between fibers.

Voids may affect the mechanical performance of composite materials. Madsen et al. [43] stated that for natural fiber-reinforced thermoplastic composites, the effect of porosity on the stiffness could be approximated by a factor of $(1 - V_{void})^2$. This roughly means that the void content in the composites reduced the stiffening potential by 0.68, 0.92, 1.42, and 1.75% concerning the composites containing a 20, 30, 40, and 50 wt.% of cotton fibers. These are considered almost negligible effects. Indeed, it has been considered that void content up to 4% has minimal effect on natural fiber composites [44]. Neglecting the possible effects of porosity on the materials' stiffness, the flexural modulus of the manufactured composites was evaluated.

3.2. Analysis of the Flexural Modulus

Table 2 presents the flexural modulus (E_f^C) and flexural strain (ε_f^C) of the coupled (6 wt.% MAPP) and uncoupled (0 wt.% MAPP) polypropylene (PP) composites containing 20–50 wt.% of cotton fibers (CF). In addition, the evolution of such parameters with the fiber volume fraction is graphically represented in Figure 2.

Table 2. Flexural modulus (E_f^C) and flexural deformation (ε_f^C) of the uncoupled and coupled composites reinforced with cotton fibers.

Fiber Content (wt. %)	V^f	0 wt.% MAPP		6 wt.% MAPP	
		E_f^c (GPa)	ε_f^c (%)	E_f^c (GPa)	ε_f^c (%)
0	0	1.1 ± 0.1	9.6 ± 0.2	1.1 ± 0.1	9.6 ± 0.2
20	0.131	2.4 ± 0.2	5.8 ± 0.2	2.4 ± 0.1	6.7 ± 0.0
30	0.205	2.9 ± 0.1	4.7 ± 0.3	2.7 ± 0.2	5.5 ± 0.1
40	0.287	3.5 ± 0.2	4.0 ± 0.1	3.2 ± 0.2	4.9 ± 0.2
50	0.376	4.1 ± 0.2	3.8 ± 0.1	3.9 ± 0.1	4.1 ± 0.1

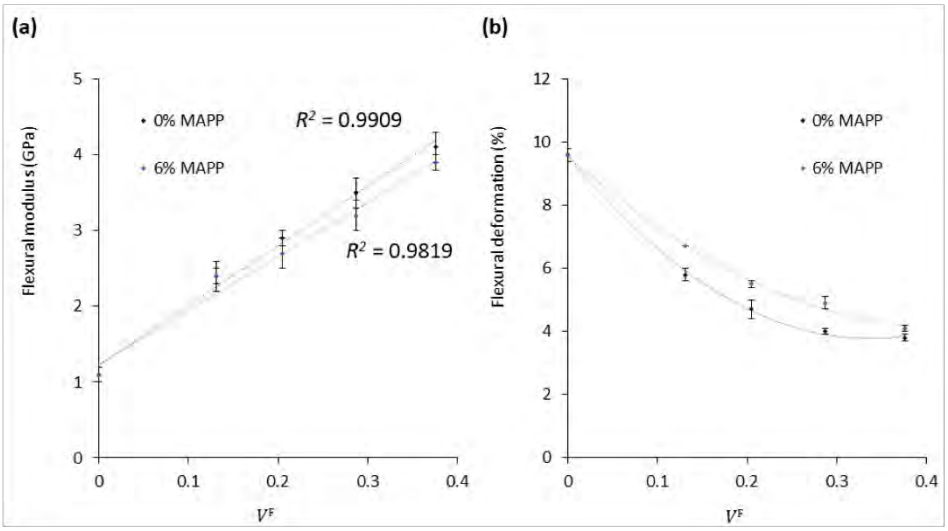

Figure 2. Evolution of the (**a**) flexural modulus and (**b**) flexural deformation with the fiber volume fraction of the composites against reinforcement volume fraction.

It is observed in Table 2 that the flexural modulus of the composites increased noticeably with the fiber content from 1.1 GPa, corresponding to neat PP, to 4.1 and 3.9 GPa (uncoupled and coupled materials, respectively) at 50 wt.% of CF. The increments in the flexural moduli were linearly correlated with the fiber contents as reflected in the high, close to 1, linear correlation coefficients (R^2) in Figure 2a. Such linear increase between both variables has been reported to be an indicator of good dispersion of the fibers within the polymeric phase [33]. This behavior contrasts with other studies reporting that lignocellulosic fibers, especially those with high cellulose contents, tend to aggregate when combined with hydrophobic polymers such as PP or PE, ultimately reducing or hindering the increment of the flexural modulus [45]. The literature suggests that optimum fiber content is found between 15 and 25 wt.% for polyolefin or polyester-based composites [46–48]. Hence, keeping a good dispersion of the phases at elevated fiber contents is considered relevant to effectively replace part of the plastic material with natural fibers, contributing to cost reductions and environmental impact reductions.

Since cotton is a high cellulose content material, precisely 93.8 wt.% of cellulose and 0.5 wt.% of lignin [23], its good dispersion inside the composite material can be presumably attributed to the presence of dyes. Such dyes, which are also a residue in the industrial production of denim products, can act as hydrophobic agents of the fiber surface and thus improve the fiber-matrix compatibility. As it was reported in a previous study, the cationic demand (CD) of the dyed cotton flocks was 16.39 μeq·g/g, whereas the virgin

cotton fibers containing no dyes exhibited a CD of about 58.7 μeq·g/g [23,49]. This means that the presence of dyes reduces the anionic nature of the fiber surface and thus makes the reinforcement more affine to the plastic material. For this reason, the presence of dyes in cotton flocks should not be viewed as inconvenient if the purpose is to valorize the residue in the composite sector.

The differences in flexural moduli of both coupled and uncoupled composites were not statistically significant as determined by ANOVA analysis at 95% confidence. Indeed, the presence of coupling agents that enhance the fiber-matrix interfacial adhesion has been reported to have almost no influence on the stiffness of composite materials [48], which is mainly governed by other factors, such as fiber and matrix properties, fiber content, grade of dispersion, and distribution of the phases [26,50,51]. Hence, coupling agents such as MAPP may not be required for purely stiffening purposes. However, composites containing MAPP were able to withstand higher flexural deformations and in addition, a recent study indicated that the flexural strength of coupled composites was higher than uncoupled [52]. Contrary to the flexural modulus, the analysis of variance (ANOVA) for the flexural deformation revealed significant differences between coupled and uncoupled composites. Such effects on deformation and strength properties are explained by the presence of MAPP favoring the bond formation between PP and cotton fibers, which consequently improves the stress transfer at the interfacial boundary when the material is subjected to load. Additionally, MAPP may also contribute to the water barrier properties of the composite material by reducing the availability of hydroxyl groups [53]. It is concluded that MAPP may not be necessary to increase the flexural modulus of the composite, though, its addition may add a competitive advantage over uncoupled composites in terms of strength, deformation capacity, and water barrier properties. Scanning electron microscopy (SEM) images were taken at the cross-sectional area of the specimens to assess how the presence of MAPP affected the dispersion and adhesion of the phases (Figure 3).

In Figure 3a, several holes in the material can be observed, presumably due to fiber slippage because of poor fiber-matrix adhesion in those uncoupled composites. A rather smother surface is observed in Figure 3b for the coupled composite, and the fibers seem to be more attached to the matrix. Such effects are more pronounced at higher magnifications. Composites without MAPP (Figure 3c,d) showed weaker interfacial adhesion than those containing MAPP (Figure 3e,f), as denotes the poor fiber-matrix anchoring and fiber pull-out tendency. Moreover, coupled composites showed improved wetting of the polymer on the fiber mainly due to the improved interactions between both phases. These effects on the material can explain the lower deformation capacities of uncoupled composites over coupled ones.

3.3. Contribution of Cotton Fibers to the Flexural Modulus of the Composites

The Fiber Flexural Modulus Factor (FFMF) is used to compute the contribution of the fibers to the flexural modulus of the composite. The parameter is considered an adequate indicator of the stiffening potential of natural fibers and thus can be used for comparison purposes with other fibers. In this work, the FFMF of cotton fibers was compared with other PP-based composites reinforced with wood fibers [54] and glass fibers [55] and reported in the literature. In Figure 4, the net contribution of cotton fibers, wood fibers, and glass fibers to the flexural modulus of PP composites is represented against the fiber volume fraction to obtain the FFMF. For comparison purposes, the fiber weight percentage is also presented in Figure 4.

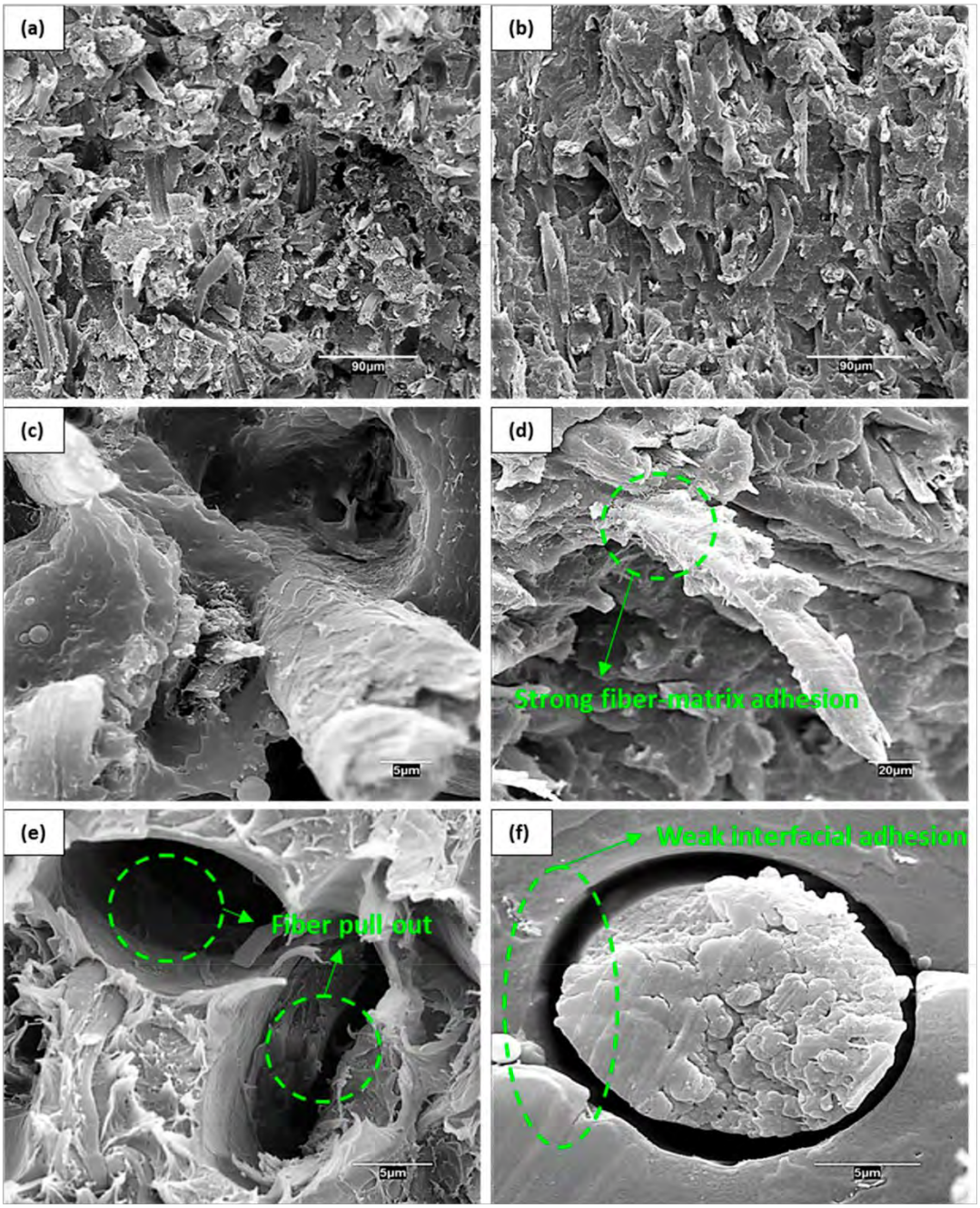

Figure 3. SEM micrographs at the cross-sectional area of the flexural specimens in composites containing 40 wt.% of cotton fibers. Observation of the composites with (**a**) and without (**b**) MAPP at low magnifications. Observation at higher magnification of composites with MAPP (**c**,**d**) and without MAPP (**e**,**f**).

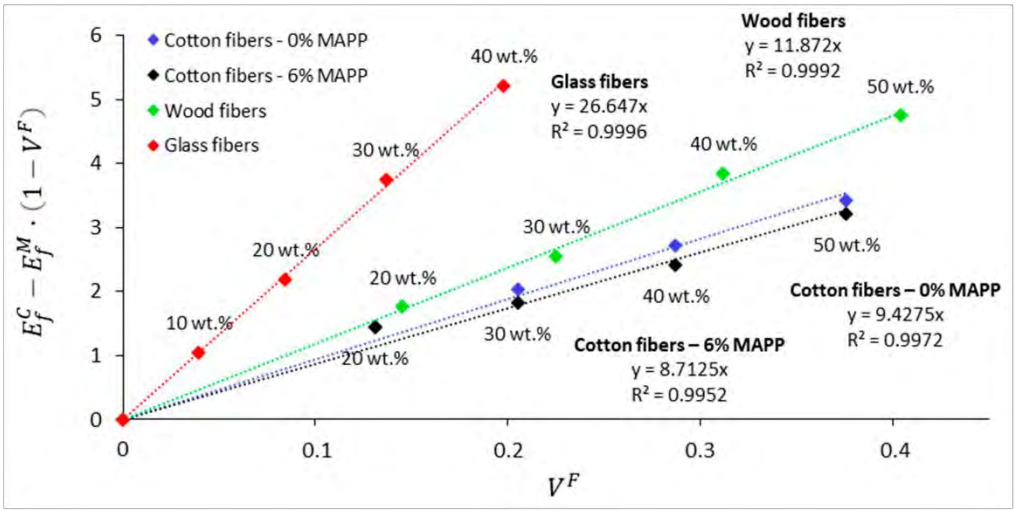

Figure 4. Representation of the Fiber Flexural Modulus Factor (FFMF) of cotton fibers, wood fibers, and glass fibers as PP reinforcement.

The FFMFs of cotton fiber uncoupled and coupled composites were 9.43 and 8.71, respectively. The FFMFs of wood fibers and glass fibers reinforced PP were 11.87 and 26.65, respectively. This roughly means that with equal increases in the fiber volume fraction, wood fibers and glass fibers are expected to have a stiffening effect of about 1.3 and 2.9 times higher than cotton fibers. From Figure 4 it is further possible to estimate that, for instance, 40 wt.% of cotton fibers, 30 wt.% of wood fibers, and 20 wt.% of glass fibers showed similar stiffening potential. It is also worth noting that at the mentioned weight percentages, cotton fiber composites show rather higher flexural deformation than wood composites (4.7%), which can be principally attributed to a better grade of dispersion within the matrix. Other types of lignocellulosic residues resulting from the textile industrial activity have shown slightly lower FFMFs. This is the case of hemp core fibers, which are an industrial residue from the production of hemp strands, which when combined with PP exhibited an FFMF around 8 [56].

Following the same methodology as for the calculus of the FFMF, a Fiber Tensile Modulus Factor (FTMF) can be calculated from the measurement of Young's modulus. The ratio between the FFMF and FTMF has been proposed in recent works as a simple modus for predicting the intrinsic flexural modulus of natural fibers [19]. Such a hypothesis is built on the fact that the modulus efficiency factor (η_e) does not depend upon the type of test, either tensile or flexural. η_e is mainly influenced by fibers' morphology, dispersion, and average orientation within the composite material, and such characteristics should not vary with the type of test. Assuming this hypothesis is correct, the following expression is obtained (Equation (14)):

$$\frac{\text{FFMF}}{\text{FTMF}} = \frac{\eta_e \cdot E_f^F}{\eta_e \cdot E_t^F} = \frac{E_f^F}{E_t^F} \quad \text{then,} \quad E_f^F = \frac{\text{FFMF}}{\text{FTMF}} \cdot E_t^F \tag{14}$$

The FTMF and intrinsic tensile modulus of cotton fibers (E_t^F) were studied in previous work [9]. The FTMF was set at 12.603, whereas the E_t^F was 31.5, 28.1, 26.5, and 25.5 GPa with respect to the composites containing 20, 30, 40, and 50 wt.% of cotton fibers, respectively. From these values, the intrinsic flexural strength of cotton fibers may be obtained following Equation (14). It is noted that the resulting values should be further contrasted with more established models such as Hirsch or Tsai–Pagano ones. However, finding models that

connect, in a rather effective way, tensile and flexural properties of composite materials is interesting from a research perspective, as reflected in several works, especially in the study of fibers' intrinsic properties owing to the difficulty of direct measuring their properties [57,58]. For instance, Hashemi [59] proposed a linear relationship combining macro- and micromechanical parameters by using the ratio between the tensile and flexural modulus of the composite, resulting in the following expression: $E_f^F = \left(E_f^c / E_t^c\right) \cdot E_t^F$. The main difference between this expression and the one in Equation (14) is that the latter one accounts only for the fiber contribution, whereas the expression of Hashemi considers both the matrix and fiber contribution to the flexural modulus of the composite.

3.4. Determination of the Intrinsic Flexural Modulus

The difficulty in measuring the flexural modulus of natural fibers by direct testing glimpses the opportunity of applying micromechanics models. In this context, the intrinsic flexural modulus of cotton fibers was calculated using (i) the Hirsch model and (ii) the Tsai–Pagano model using Halpin–Tsai equations, abbreviated as TP&HT. Since Halpin–Tsai equations require the mean fiber length (l^F) and diameter (d^F) of the fibers, the composite materials were subjected to Soxhlet extraction using decalin as a solvent to dissolve polypropylene and recover the fibers, which were then submitted to morphological analysis. The results from the morphological test are reported in Table 3. Further, SEM images of the cotton fibers before processing are provided in Figure 5 to further evaluate the morphology of the fibers.

Table 3. Evolution of morphological parameters, mean fiber length (l^F), mean fiber diameter (d^F), and aspect ratio (l^F/d^F) with the fiber content.

Fiber Content (wt. %)	0 wt.% MAPP			6 wt.% MAPP		
	l^F (μm)	d^F (μm)	l^F/d^F	l^F (μm)	d^F (μm)	l^F/d^F
20	512 ± 9	16.5	31.0	509 ± 9	16.5	30.8
30	459 ± 5		27.8	406 ± 5		24.6
40	396 ± 13		24.0	339 ± 7		20.5
50	351 ± 15		21.3	299 ± 11		18.1

A clear overall tendency of the mean fiber length to decrease as the fiber content increases was observed. This is explained by an increment of the composite viscosity concerning the matrix when natural fibers are incorporated into the material, which by consequence increases the shear forces created during the internal mixing process leading to fiber attrition and fiber length shortening. Additionally, the diameter was less affected by the compounding process and thus remained very stable at 16.5 μm. Such diameter agrees with the images in Figure 5, where the fibers present approximate diameters in the range of 16 and 17 μm. In addition, from SEM images in Figure 5, one can see that cotton fibers present a smooth surface, probably due to low lignin content and to the presence of dyes covering the surface. The attrition phenomena of the fibers were more pronounced in coupled composites, as reflected in a more sudden decrease of the average fiber length. This is explained by the stronger fiber-matrix adhesion in coupled composites that promotes the more efficient transmission of the shear forces from the matrix to the fibers [60]. The lower length of natural fibers in coupled composites, combined with very stable diameters, also led to smaller aspect ratios. Such differences observed in the aspect ratio of the fibers depending on the presence of MAPP can justify the slight discrepancies in the flexural moduli between uncoupled and coupled composites. The relationship between fiber aspect ratio and the stiffness of composite materials has been previously studied by Shibata et al. (2005) [61] and Hsueh (2000) [62]. According to their results, the stiffness of composites increases with the average fiber length up to approximately 2.8 mm length. Hence, the uncoupled composites are expected to show slightly higher flexural modulus owing to

the superior aspect ratios of the fibers. This also justifies the somewhat higher FFMF of uncoupled composites.

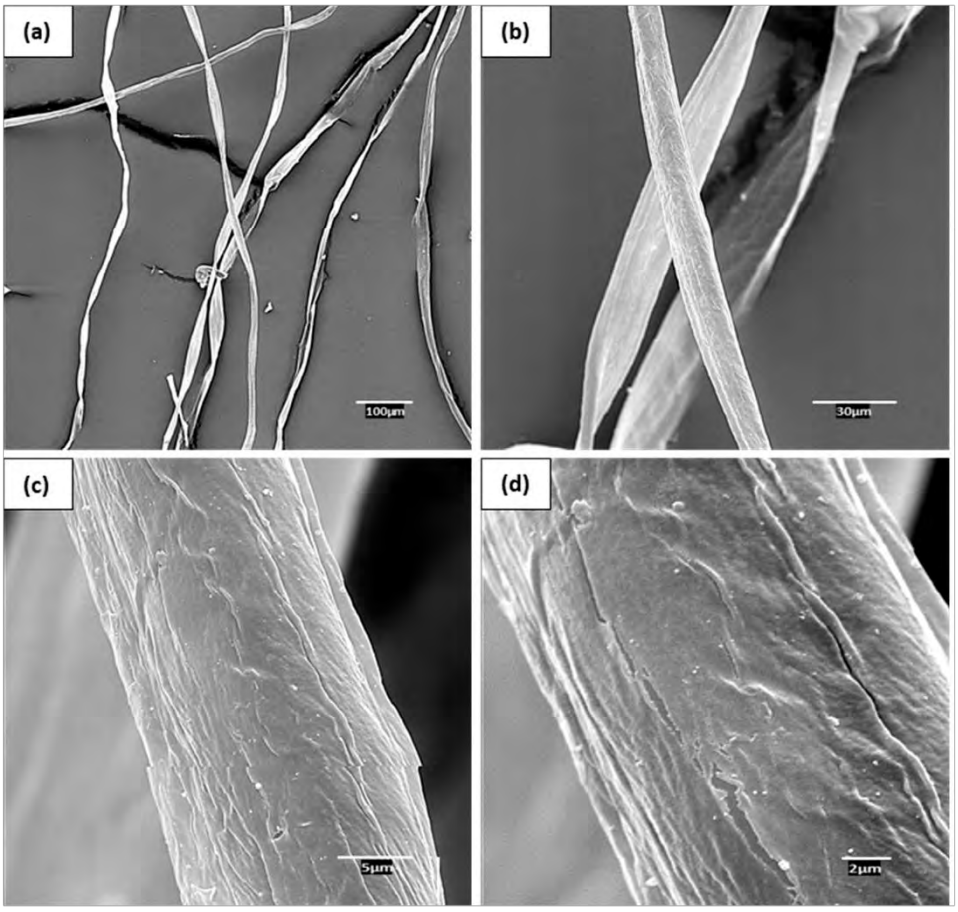

Figure 5. SEM images of cotton fibers before processing at different magnifications: (**a**) Cotton fibers at 100 µm of magnification; (**b**) Cotton fibers at 30 µm of magnification; (**c**) Cotton fiber at 5 µm of magnification; (**d**) Cotton fiber at 2 µm of magnification.

Both average fiber length and diameter were incorporated into Halpin–Tsai equation. The intrinsic flexural modulus of cotton fibers was determined following three different routes being (i) the Hirsch model, (ii) the TP&HT model, and (iii) the one proposed in this work using the FFMF/FTMF ratio. The results are presented in Table 4.

The different models applied for the calculus of the intrinsic flexural modulus showed good agreement, especially above the 20 wt.% fiber content. The similarities between methodologies support the utility of the Hirsch model, as well as the approach proposed in this work by using the FFMF/FTMF ratio, in front of Tsai–Pagano model, because these models do not require morphological data. It is further observed that the intrinsic flexural moduli of the fibers tended to decrease as the fiber content was increased. This could be due to fiber attrition phenomena suffered during compounding, which is intensified at higher fiber contents. Assuming the values obtained from the Hirsch model as being accurate, the intrinsic flexural modulus of cotton fibers was compared with other fiber-reinforced PP

composites, as shown in Figure 6. The specific intrinsic flexural modulus (E_f^F/ρ^F) of the fibers are also included in Figure 6 to attain the different densities of the fibers.

Table 4. Intrinsic flexural modulus of cotton fibers obtained using (i) Hirsch model, (ii) Tsai–Pagano model using Halpin–Tsai equation (TP&HT) (iii), and the ratio between the FFMF and FTMF.

Fiber Content (wt. %)	Intrinsic Flexural Modulus (E_f^F) (Gpa)					
	0 wt.% MAPP			6 wt.% MAPP		
	Hirsch	TP&HT	$\frac{\text{FFMF}}{\text{FTMF}}$	Hirsch	TP&HT	$\frac{\text{FFMF}}{\text{FTMF}}$
20	24.1	29.4	21.8	24.1	29.4	23.3
30	21.1	23.7	19.4	18.7	20.4	20.8
40	19.9	21.4	18.3	17.3	18.1	19.6
50	18.6	18.9	17.6	17.3	17.6	17.6
Average	20.9	23.4	20.7	19.4	21.4	19.3

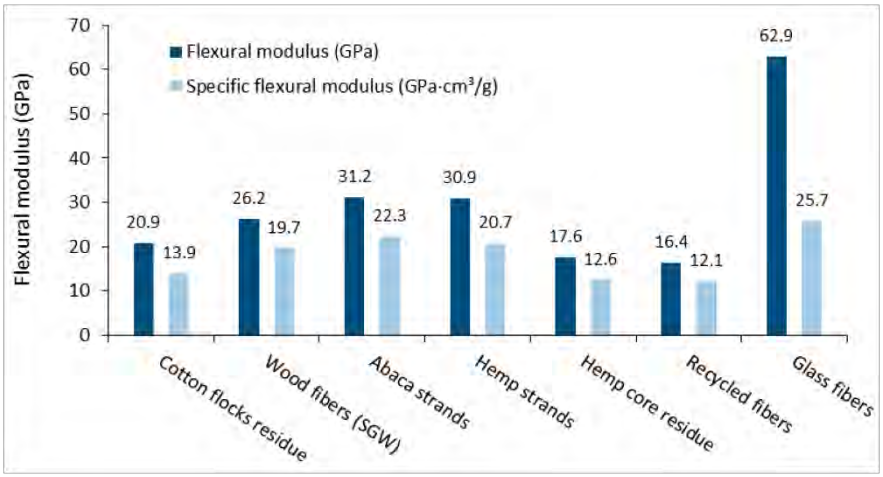

Figure 6. Flexural modulus and specific flexural modulus of different fiber-reinforced PP composites (wood fibers [52], abaca strands [53], hemp strands [61], hemp core residues [54], recycled fibers [32], and glass fibers [53]).

The intrinsic flexural modulus of cotton fibers was higher than other lignocellulosic residues, such as hemp core and recycled fibers, though still slightly below those of wood fibers and strands from annual plants such as abaca or hemp. The intrinsic flexural modulus of glass fibers was notably higher than those of natural fibers, though its high density (2.45 g/cm^3) makes the specific property comparable with the others.

3.5. Modulus Efficiency, Length, and Orientation Factors

The modulus efficiency factor was computed considering the intrinsic flexural strength of cotton fibers and the modified Rule of Mixtures (mRoM). The implication of fiber morphology and orientation on the flexural modulus of the composite was evaluated using the modulus length and orientation factors. Further, from the orientation factor, the limiting and average orientation angles were determined. The results are given in Table 5.

Table 5. Micromechanics of the flexural modulus. Intrinsic flexural strength (E_f^F), modulus efficiency factor (η_e), length factor (η_l), orientation factor (η_o), limit angle (α_o), mean orientation angle (α).

Coupling Agent Content	Factor	Fiber Content (wt. %)				Average
		20	30	40	50	
0 wt.% MAPP	E_f^F (Hirsch)	24.1	21.1	19.9	18.6	20.9
	η_e	0.46	0.47	0.48	0.49	0.47
	η_l	0.89	0.90	0.90	0.91	0.90
	η_o	0.52	0.52	0.53	0.54	0.53
	α_o	66.0°	65.2°	64.3°	63.1°	64.7°
	α	30.6°	30.6°	30.6°	30.6°	30.6°
6 wt.% MAPP	E_f^F (Hirsch)	24.1	18.7	17.3	17.3	19.4
	η_e	0.46	0.48	0.49	0.49	0.48
	η_l	0.89	0.89	0.89	0.89	0.89
	η_o	0.52	0.54	0.55	0.55	0.54
	α_o	65.8°	63.5°	61.9°	61.2°	63.1°
	α	30.6°	30.6°	30.6°	30.6°	30.6°

First, the slight differences between the micromechanics of coupled and uncoupled composites are not considered significant, as the variations are almost negligible. The modulus efficiency factor is in line with those reported in the literature for natural fibers, around 0.5, supporting the relevance of the results and indicating that the composite material took full advantage of the stiffening potential of the fiber. Noteworthily, the efficiency factor is in the same order as the one obtained from the micromechanics of Young's modulus in a recent work, with an average value of 0.47. The similarities between the efficiency factors obtained from Young's and flexural moduli analyses support the theoretical hypothesis regarding the calculus of the intrinsic flexural modulus from the FFMF/FTMF ratio.

The modulus orientation factor typically ranges between 0.4 and 0.6 in composites processed using injection molding and is mainly influenced by the compounding conditions and mold geometry [46]. In this work, the values for the modulus orientation factor were around 0.53–0.54. Such factor equals 1 when the fibers are completely aligned, whereas for planar random configuration the factor tends to be 3/8 and for completely random systems the factor may decrease to 1/5 [63,64]. Hence, for the present case a certain alignment of the fibers inside the composite is noticed, which as mentioned, can be principally attributed to the injection process. The modulus length factor was close to 1, which indicates that fibers' morphology, particularly their aspect ratio, plays a key role in stiffening the composite material by providing an adequate load transfer.

By using the modulus orientation factor and estimating a square packing distribution of the fibers inside the composite, a limiting angle around 63–64° was obtained. The limiting angle refers to the angle of orientation for which the axial stress of the fiber tends to 0. From such value, the mean orientation of the fibers inside the composite may be set at 30.6°, both for uncoupled and coupled composites, considering that a fully aligned fiber/matrix system would reach 0°. Comparatively, the micromechanics of Young's modulus for the same composites returned a limiting angle of 53.3° and mean orientation about 36.1°. It is observed that, again, the micromechanics of the Young's modulus and flexural modulus deliver similar results. Similarities are also found in the micromechanics analysis of the tensile strength, which was the subject of study in previous work [24]. In such work, the strength orientation factor (x_1) was set at 0.3, from which a limiting angle of 61° could be calculated in agreement with the expression $x_1 = \cos^4(\alpha_0)$ developed by Mittal et al. [65], finally obtaining a mean orientation of the fibers of 35.4°. It is observed that from tensile strength, Young's modulus, and flexural modulus analysis of the materials' similar orientation angles are attained, which supports the relevance of the micromechanics models and the results obtained.

In general, the developed cotton-reinforced PP composites are presented as an attractive opportunity to replace virgin lignocellulosic feedstocks with industrial residues, attaining economically and technically competitive materials. The composites could exhibit potential for semi-structural/construction given their relatively high stiffness/weight ratio, making their use particularly adequate for lightweight applications, such as panels, ceilings, and partition boards. Other fields where the composites could be directly implemented concern the automotive sector. Indeed, the global production of natural fiber composites in the automotive sector has grown considerably in recent years from 90,000 tons in the year 2010 to 350,000 tons by 2020 [66]. Additionally, the similar appearance of the composites to solely wood materials also makes the composites suitable for furniture and indoor applications.

4. Conclusions

The textile industry generates huge amounts of cotton byproducts yearly, from which only a minor part is recycled, and the rest is either landfilled or incinerated, resulting in serious environmental issues. To enhance the sustainability of the textile sector, the potential of these cotton byproducts in the composite sector was evaluated. The cotton flocks were mechanically defibrated and incorporated into a polypropylene matrix up to 50 wt.%. The flexural modulus of the composites was studied to assess their potential and competitiveness. The results indicate that the flexural modulus increased steadily up to 50 wt.% of fiber contents, increasing the flexural modulus of the matrix by 272%. The good dispersion of the phases in comparison with other fiber typologies was attributed to the presence of dyes, whereas the good interfacial adhesion was attributed to the presence of maleic anhydride polypropylene (MAPP), which was used as a coupling agent. From the micromechanics analysis of the flexural modulus, the following remarks are pointed out: (i) An alternative methodology, which connected Young's and flexural moduli, was used for the calculus of the intrinsic flexural modulus of cotton fibers, which agreed with more established models such as Hirsch or Tsai–Pagano; (ii) The intrinsic flexural modulus (around 20 GPa) was found in line with other natural fibers, though still far from glass fibers; (iii) It was shown that the composite took advantage of the stiffening potential of cotton fibers; (iv) The fibers showed a certain degree of alignment, whereas the aspect ratio was found to play a key role on stiffening the material. Overall, the developed composites showed similar stiffening potential as other natural fibers, with the environmental and economic advantage of valorizing a low value-added residue.

Author Contributions: Investigation, A.S.; Data curation and writing—original draft preparation, F.S.-P.; Conceptualization and methodology, F.V.; Supervision, M.D.-A.; Visualization and writing—review and editing, F.X.E.; Project administration and validation, Q.T. All authors have read and agreed to the published version of the manuscript.

Funding: This research received no external funding.

Institutional Review Board Statement: Not applicable.

Informed Consent Statement: Not applicable.

Acknowledgments: The authors wish to acknowledge the University of Girona for providing the basic resources to develop this research. Marc Delgado-Aguilar is a Serra Húnter Fellow.

Conflicts of Interest: The authors declare no conflict of interest.

References

1. Liakos, N.; Kumar, V.; Pongsakornrungsilp, S.; Garza-Reyes, J.A.; Gupta, B.; Pongsakornrungsilp, P. Understanding circular economy awareness and practices in manufacturing firms. *J. Enterp. Inf. Manag.* **2019**, *32*, 563–584. [CrossRef]
2. Stahel, W.R. The circular economy. *Nature* **2016**, *531*, 435–438. [CrossRef]
3. Malinauskaite, J.; Jouhara, H.; Czajczyńska, D.; Stanchev, P.; Katsou, E.; Rostkowski, P.; Thorne, R.J.; Colón, J.; Ponsá, S.; Al-Mansour, F.; et al. Municipal solid waste management and waste-to-energy in the context of a circular economy and energy recycling in Europe. *Energy* **2017**, *141*, 2013–2044. [CrossRef]

4. Chemiefaser, I. *Worldwide Production Volume of Chemical and Textile Fibers from 1975 to 2018*; Statista Inc.: Hamburg, Germany, 2018.
5. Patti, A.; Cicala, G.; Acierno, D. Eco-Sustainability of the Textile Production: Waste Recovery and Current Recycling in the Composites World. *Polymers* **2021**, *13*, 134. [CrossRef] [PubMed]
6. De Silva, R.; Wang, X.; Byrne, N. Recycling textiles: The use of ionic liquids in the separation of cotton polyester blends. *RSC Adv.* **2014**, *4*, 29094–29098. [CrossRef]
7. Shen, F.; Xiao, W.; Lin, L.; Yang, G.; Zhang, Y.; Deng, S. Enzymatic saccharification coupling with polyester recovery from cotton-based waste textiles by phosphoric acid pretreatment. *Bioresour. Technol.* **2013**, *130*, 248–255. [CrossRef]
8. Jeihanipour, A.; Karimi, K.; Niklasson, C.; Taherzadeh, M.J. A novel process for ethanol or biogas production from cellulose in blended-fibers waste textiles. *Waste Manag.* **2010**, *30*, 2504–2509. [CrossRef] [PubMed]
9. Serra, A.; Tarrés, Q.; Chamorro, M.-À.; Soler, J.; Mutjé, P.; Espinach, F.X.; Vilaseca, F. Modeling the Stiffness of Coupled and Uncoupled Recycled Cotton Fibers Reinforced Polypropylene Composites. *Polymers* **2019**, *11*, 1725. [CrossRef]
10. Mohanty, A.K.; Misra, M.; Drzal, L.T. *Natural Fibers, Biopolymers, and Biocomposites*; Lawrence, T., Ed.; Taylor & Francis: Boca Raton, FL, USA, 2005; ISBN 9780203508206.
11. Bledzki, A.K.; Gassan, J.; Theis, S. Wood-filled thermoplastic composites. *Mech. Compos. Mater.* **1998**, *34*, 563–568. [CrossRef]
12. Holbery, J.; Houston, D. Natural-fiber-reinforced polymer composites in automotive applications. *JOM* **2006**, *58*, 80–86. [CrossRef]
13. Serrano, A.; Espinach, F.X.; Tresserras, J.; Pellicer, N.; Alcala, M.; Mutje, P. Study on the technical feasibility of replacing glass fibers by old newspaper recycled fibers as polypropylene reinforcement. *J. Clean. Prod.* **2014**, *65*, 489–496. [CrossRef]
14. Puglia, D.; Biagiotti, J.; Kenny, J.M. A review on natural fibre-based composites—Part II: Application of natural reinforcements in composite materials for automotive industry. *J. Nat. Fibers* **2004**, *1*, 23–65. [CrossRef]
15. Serra-Parareda, F.; Tarrés, Q.; Delgado-Aguilar, M.; Espinach, F.X.; Mutjé, P.; Vilaseca, F. Biobased Composites from Biobased-Polyethylene and Barley Thermomechanical Fibers: Micromechanics of Composites. *Materials* **2019**, *12*, 4182. [CrossRef]
16. Väisänen, T.; Haapala, A.; Lappalainen, R.; Tomppo, L. Utilization of agricultural and forest industry waste and residues in natural fiber-polymer composites: A review. *Waste Manag.* **2016**, *54*, 62–73. [CrossRef] [PubMed]
17. Chokshi, S.; Parmar, V.; Gohil, P.; Chaudhary, V. Chemical Composition and Mechanical Properties of Natural Fibers. *J. Nat. Fibers* **2020**, *18*, 1–12. [CrossRef]
18. Zabihzadeh, S.M.; Ebrahimi, G.; Enayati, A.A. Effect of Compatibilizer on Mechanical, Morphological, and Thermal Properties of Chemimechanical Pulp-reinforced PP Composites. *J. Thermoplast. Compos. Mater.* **2011**, *24*, 221–231. [CrossRef]
19. Belgacem, C.; Serra-Parareda, F.; Tarrés, Q.; Mutjé, P.; Delgado-Aguilar, M.; Boufi, S. Valorization of Date Palm Waste for Plastic Reinforcement: Macro and Micromechanics of Flexural Strength. *Polymers* **2021**, *13*, 1751. [CrossRef] [PubMed]
20. Ndiaye, D.; Gueye, M.; Malang Badji, A.; Thiandoume, C.; Dasylva, A.; Tidjani, A. Effects of Reinforcing Fillers and Coupling Agents on Performances of Wood–Polymer Composites. In *Bio-Based Composites for High-Performance Materials: From Strategy to Industrial Application*; CRC Press: Boca Raton, FL, USA, 2014; pp. 113–132.
21. Sanjay, M.R.; Madhu, P.; Jawaid, M.; Senthamaraikannan, P.; Senthil, S.; Pradeep, S. Characterization and properties of natural fiber polymer composites: A comprehensive review. *J. Clean. Prod.* **2018**, *172*, 566–581. [CrossRef]
22. Mohanty, S.; Nayak, S.K.; Verma, S.K.; Tripathy, S.S. Effect of MAPP as a Coupling Agent on the Performance of Jute-PP Composites. *J. Reinf. Plast. Compos.* **2004**, *23*, 625–637. [CrossRef]
23. Serra, A.; Tarrés, Q.; Claramunt, J.; Mutjé, P.; Ardanuy, M.; Espinach, F.X. Behavior of the interphase of dyed cotton residue flocks reinforced polypropylene composites. *Compos. Part B Eng.* **2017**, *128*, 200–207. [CrossRef]
24. Serra, A.; Tarrés, Q.; Llop, M.; Reixach, R.; Mutjé, P.; Espinach, F.X. Recycling dyed cotton textile byproduct fibers as polypropylene reinforcement. *Text. Res. J.* **2019**, *89*, 2113–2125. [CrossRef]
25. Neagu, R.C.; Gamstedt, E.K.; Berthold, F. Stiffness Contribution of Various Wood Fibers to Composite Materials. *J. Compos. Mater.* **2006**, *40*, 663–699. [CrossRef]
26. Espinach, F.X.; Julián, F.; Alcalà, M.; Tresserras, J.; Mutjé, P. High Stiffness Performance Alpha-Grass Pulp Fiber Reinforced Thermoplastic Starch-Based Fully Biodegradable Composites. *BioResources* **2013**, *9*, 738–755. [CrossRef]
27. Wang, F.; Chen, Z.Q.; Wei, Y.Q.; Zeng, X.G. Numerical Modeling of Tensile Behavior of Fiber-reinforced Polymer Composites. *J. Compos. Mater.* **2010**, *44*, 2325–2340. [CrossRef]
28. Delgado-Aguilar, M.; Oliver-Ortega, H.; Alberto Méndez, J.; Camps, J.; Espinach, F.X.; Mutjé, P. The role of lignin on the mechanical performance of polylactic acid and jute composites. *Int. J. Biol. Macromol.* **2018**, *116*, 299–304. [CrossRef] [PubMed]
29. ASTM. *ASTM D618—13: Standard Practice for Conditioning Plastics for Testing*; ASTM: West Conshohocken, PA, USA, 2013.
30. ASTM. *ASTM D790—17 Standard Test Methods for Flexural Properties of Unreinforced and Reinforced Plastics and Electrical Insulating Materials*; ASTM: West Conshohocken, PA, USA, 2017.
31. Rao, P.D.; Kiran, C.U.; Prasad, K.E. Effect of fiber loading and void content on tensile properties of keratin based randomly oriented human hair fiber composites. *Int. J. Compos. Mater.* **2017**, *7*, 136–143.
32. Tarrés; Soler; Rojas-Sola; Oliver-Ortega; Julián; Espinach; Mutjé; Delgado-Aguilar Flexural Properties and Mean Intrinsic Flexural Strength of Old Newspaper Reinforced Polypropylene Composites. *Polymers* **2019**, *11*, 1244. [CrossRef] [PubMed]
33. Vilaseca, F.; Serra-Parareda, F.; Espinosa, E.; Rodríguez, A.; Mutjé, P.; Delgado-Aguilar, M. Valorization of Hemp Core Residues: Impact of NaOH Treatment on the Flexural Strength of PP Composites and Intrinsic Flexural Strength of Hemp Core Fibers. *Biomolecules* **2020**, *10*, 823. [CrossRef]

34. Hirsch, T.J. Modulus of elasticity of concrete affected by elastic moduli of cement paste matrix and aggregate. *J. Am. Concr. Inst.* **1962**, *59*, 427–452.
35. Halpin, J.C.; Pagano, N.J. The Laminate Approximation for Randomly Oriented Fibrous Composites. *J. Compos. Mater.* **1969**, *3*, 720–724. [CrossRef]
36. Halpin, J.C. *Effects of Environmental Factors on Composite Materials*; Air Force Materials Lab Wright-Patterson AFB: Dayton, OH, USA, 1969.
37. Affdl, J.H.; Kardos, J.L. The Halpin-Tsai equations: A review. *Polym. Eng. Sci.* **1976**, *16*, 344–352. [CrossRef]
38. Reixach, R.; Espinach, F.X.; Franco-Marquès, E.; Ramirez de Cartagena, F.; Pellicer, N.; Tresserras, J.; Mutjé, P. Modeling of the tensile moduli of mechanical, thermomechanical, and chemi-thermomechanical pulps from orange tree pruning. *Polym. Compos.* **2013**, *34*, 1840–1846. [CrossRef]
39. Cox, H.L. The elasticity and strength of paper and other fibrous materials. *Br. J. Appl. Phys.* **1952**, *3*, 72. [CrossRef]
40. Krenchel, H. *Fibre Reinforcement, Theoretical and Practical Investigations of the Elasticity and Strength of Fibre-Reinforced Materials*; Akademisk Forlag: Copenhagen, Denmark, 1964.
41. Fukuda, H.; Kawata, K. On Young's modulus of short fibre composites. *Fibre Sci. Technol.* **1974**, *7*, 207–222. [CrossRef]
42. Sanomura, Y.; Kawamura, M. Fiber orientation control of short-fiber reinforced thermoplastics by ram extrusion. *Polym. Compos.* **2003**, *24*, 587–596. [CrossRef]
43. Madsen, B.; Thygesen, A.; Lilholt, H. Plant fibre composites–porosity and stiffness. *Compos. Sci. Technol.* **2009**, *69*, 1057–1069. [CrossRef]
44. Shah, D.U.; Schubel, P.J.; Licence, P.; Clifford, M.J. Determining the minimum, critical and maximum fibre content for twisted yarn reinforced plant fibre composites. *Compos. Sci. Technol.* **2012**, *72*, 1909–1917. [CrossRef]
45. Saheb, D.N.; Jog, J.P. Natural fiber polymer composites: A review. *Adv. Polym. Technol.* **1999**, *18*, 351–363. [CrossRef]
46. Brahmakumar, M.; Pavithran, C.; Pillai, R.M. Coconut fibre reinforced polyethylene composites: Effect of natural waxy surface layer of the fibre on fibre/matrix interfacial bonding and strength of composites. *Compos. Sci. Technol.* **2005**, *65*, 563–569. [CrossRef]
47. Prasad, S.V.; Pavithran, C.; Rohatgi, P.K. Alkali treatment of coir fibres for coir-polyester composites. *J. Mater. Sci.* **1983**, *18*, 1443–1454. [CrossRef]
48. Arrakhiz, F.Z.; El Achaby, M.; Malha, M.; Bensalah, M.O.; Fassi-Fehri, O.; Bouhfid, R.; Benmoussa, K.; Qaiss, A. Mechanical and thermal properties of natural fibers reinforced polymer composites: Doum/low density polyethylene. *Mater. Des.* **2013**, *43*, 200–205. [CrossRef]
49. Carrasco, F.; Mutjé, P.; Pelach, M.A. Control of retention in paper-making by colloid titration and zeta potential techniques. *Wood Sci. Technol.* **1998**, *32*, 145–155. [CrossRef]
50. Karmaker, A.C.; Youngquist, J.A. Injection molding of polypropylene reinforced with short jute fibers. *J. Appl. Polym. Sci.* **1996**, *62*, 1147–1151. [CrossRef]
51. Koronis, G.; Silva, A.; Fontul, M. Green composites: A review of adequate materials for automotive applications. *Compos. Part B Eng.* **2013**, *44*, 120–127. [CrossRef]
52. Serra-Parareda, F.; Julián, F.; Espinosa, E.; Rodríguez, A.; Espinach, F.X.; Vilaseca, F. Feasibility of Barley Straw Fibers as Reinforcement in Fully Biobased Polyethylene Composites: Macro and Micro Mechanics of the Flexural Strength. *Molecules* **2020**, *25*, 2242. [CrossRef]
53. Li, X.; Xiao, R.; Morrell, J.J.; Zhou, X.; Du, G. Improving the performance of hemp hurd/polypropylene composites using pectinase pre-treatments. *Ind. Crops Prod.* **2017**, *97*, 465–468. [CrossRef]
54. López, J.P.; Gironès, J.; Mendez, J.A.; Pèlach, M.A.; Vilaseca, F.; Mutjé, P. Impact and flexural properties of stone-ground wood pulp-reinforced polypropylene composites. *Polym. Compos.* **2013**, *34*, 842–848. [CrossRef]
55. Gironès, J.; Lopez, J.P.; Vilaseca, F.; Bayer, R.; Herrera-Franco, P.J.; Mutjé, P. Biocomposites from Musa textilis and polypropylene: Evaluation of flexural properties and impact strength. *Compos. Sci. Technol.* **2011**, *71*, 122–128. [CrossRef]
56. Serra-Parareda, F.; Espinach, F.X.; Pelach, M.À.; Méndez, J.A.; Vilaseca, F.; Tarrés, Q. Effect of NaOH Treatment on the Flexural Modulus of Hemp Core Reinforced Composites and on the Intrinsic Flexural Moduli of the Fibers. *Polymers* **2020**, *12*, 1428. [CrossRef] [PubMed]
57. Wisnom, M.R. The relationship between tensile and flexural strength of unidirectional composites. *J. Compos. Mater.* **1992**, *26*, 1173–1180. [CrossRef]
58. Mujika, F.; Carbajal, N.; Arrese, A.; Mondragon, I. Determination of tensile and compressive moduli by flexural tests. *Polym. Test.* **2006**, *25*, 766–771. [CrossRef]
59. Hashemi, S. Hybridisation effect on flexural properties of single- and double-gated injection moulded acrylonitrile butadiene styrene (ABS) filled with short glass fibres and glass beads particles. *J. Mater. Sci.* **2008**, *43*, 4811–4819. [CrossRef]
60. Arbelaiz, A.; Fernandez, B.; Ramos, J.A.; Retegi, A.; Llano-Ponte, R.; Mondragon, I. Mechanical properties of short flax fibre bundle/polypropylene composites: Influence of matrix/fibre modification, fibre content, water uptake and recycling. *Compos. Sci. Technol.* **2005**, *65*, 1582–1592. [CrossRef]
61. Shibata, S.; Cao, Y.; Fukumoto, I. Press forming of short natural fiber-reinforced biodegradable resin: Effects of fiber volume and length on flexural properties. *Polym. Test.* **2005**, *24*, 1005–1011. [CrossRef]

62. Hsueh, C.H. Young's modulus of unidirectional discontinuous-fibre composites. *Compos. Sci. Technol.* **2000**, *60*, 2671–2680. [CrossRef]
63. Espinach, F.X.; Julian, F.; Verdaguer, N.; Torres, L.; Pelach, M.A.; Vilaseca, F.; Mutje, P. Analysis of tensile and flexural modulus in hemp strands/polypropylene composites. *Compos. Part B Eng.* **2013**, *47*, 339–343. [CrossRef]
64. Sanadi, A.R.; Young, R.A.; Clemons, C.; Rowell, R.M. Recycled Newspaper Fibers as Reinforcing Fillers in Thermoplastics: Part I-Analysis of Tensile and Impact Properties in Polypropylene. *J. Reinf. Plast. Compos.* **1994**, *13*, 54–67. [CrossRef]
65. Mittal, R.K.; Gupta, V.B.; Sharma, P. The effect of fibre orientation on the interfacial shear stress in short fibre-reinforced polypropylene. *J. Mater. Sci.* **1987**, *22*, 1949–1955. [CrossRef]
66. Peças, P.; Carvalho, H.; Salman, H.; Leite, M. Natural Fibre Composites and Their Applications: A Review. *J. Compos. Sci.* **2018**, *2*, 66. [CrossRef]

Discusión general de resultados

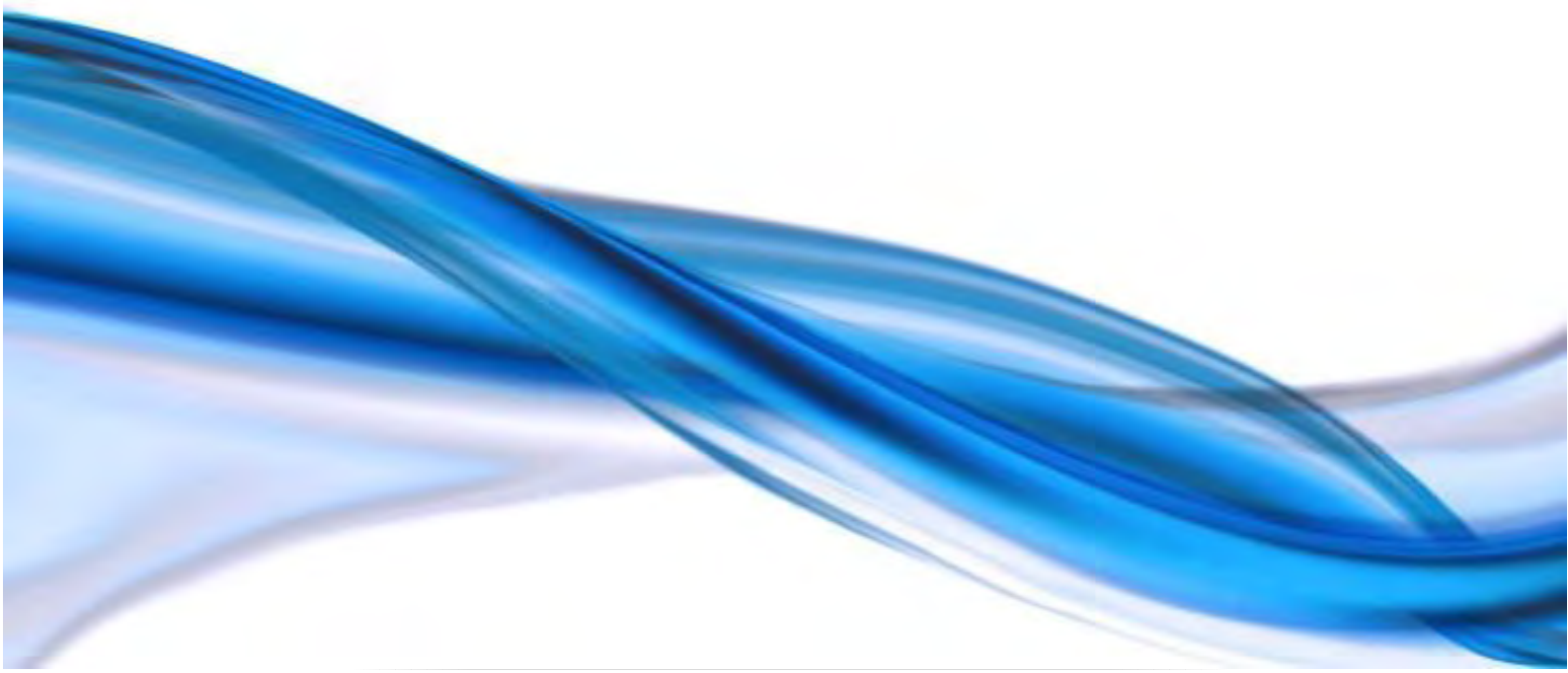

5. Discusión general de resultados

5.1. Optimización del contenido de agente de acoplamiento.

La utilización de fibras naturales hidrófilas para el refuerzo de una matriz hidrófoba, como el PP, así como el uso de agentes de acoplamiento como el MAPP es una práctica común para obtener una buena resistencia a tracción y flexión [106,131,132]. Así para la utilización de un residuo celulósico de la industria textil como refuerzo de una matriz de PP se considera necesario el estudio del efecto del contenido de MAPP.

En la Figura 15 se reflejan los resultados obtenidos al aplicar porcentajes progresivos de MAPP en materiales compuestos de PP reforzados con fibras de algodón (CF) en un 30 y 40% (w/w).

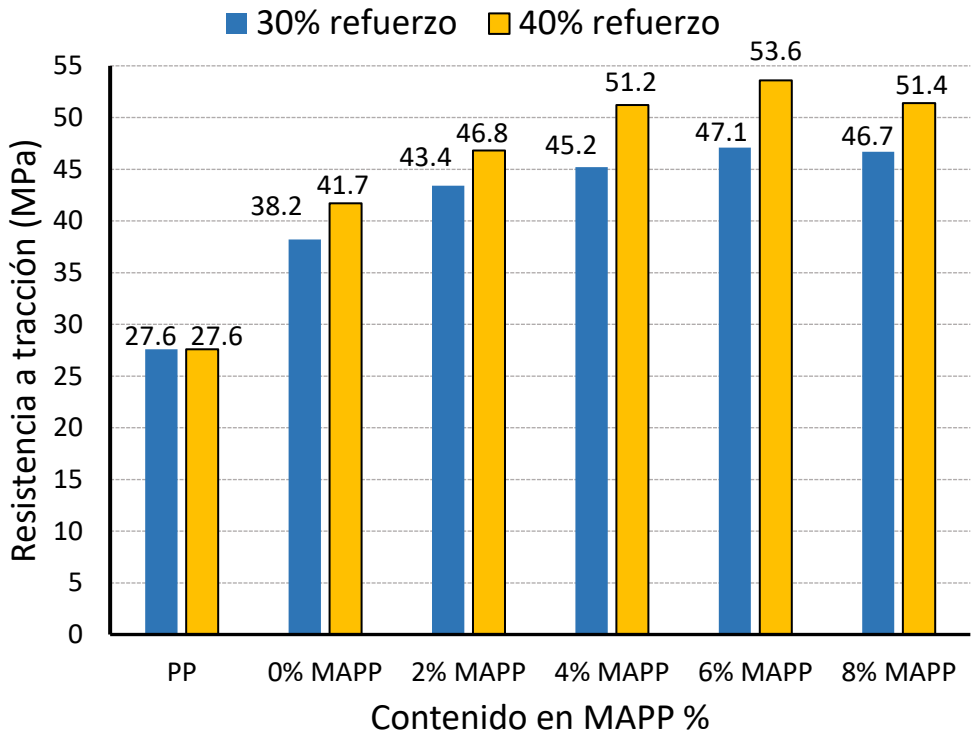

***Figura 15**. Resistencia a tracción de los compuestos en función del % de MAPP*

Se puede constatar como la presencia de distintos porcentajes de agente de acoplamiento (MAPP) conduce a incrementos progresivos de la resistencia a tracción para ambos contenidos de refuerzo. Los materiales reforzados en un 30 % con una adición del 2, 4 y 6 % de MAPP en peso sobre el contenido de refuerzo, muestran incrementos de la resistencia a tracción (σ^c_t) del 57,2, 63,7, y 70,6% respecto a la resistencia a tracción de la matriz (σ^m_t). Una adicción superior de agente de acoplamiento, presenta una disminución de la σ^c_t respecto del compuesto formulado con un 6% de MAPP. Este hecho es causado por el mismo agente de acoplamiento, porqué muestra una cadena significativamente más corta que la del polipropileno utilizado como matriz [90]. Un comportamiento similar se observa cuando el contenido de refuerzo es del 40% (w/w). Así para porcentajes del 30 y 40% de refuerzo se observa que la cantidad optima de MAPP es del 6% dando lugar a incrementos de resistencia del 70,6 y 94,2% sobre la matriz de PP. Sin embargo, si se compara con materiales compuestos reforzados al 30 y 40% (w/w), sin

adición de MAPP, el incremento de la resistencia es solo del 23,3 y del 28,5% respectivamente. Se observa que en el caso de los materiales compuestos reforzados con CF en un 30% y 40% (w/w) sin adición de MAPP, presentan incrementos de resistencia respecto a la matriz del 38,4 y 51,1%, respectivamente. Todo lo contrario de lo que describe en varias publicaciones donde se obtienen materiales compuestos de PP reforzados con fibras celulósicas [91,106,126]. Esto permite deducir que la presencia de tintes parece favorecer la interfase entre las fibras de algodón y la matriz de PP.

5.2. Resistencia a tracción de los compuestos.

Como se ha observado anteriormente, las fibras de algodón teñidas son capaces de reforzar la matriz de PP sin un agente de acoplamiento. Sin embargo, los compuestos con una adición de un 6% (w/w) de MAPP presentan mayores σ^{c}_{t}. Por lo tanto, se decidió estudiar la evolución de la resistencia en función del contenido de refuerzo de los materiales formulados con un 0 y 6% (w/w) de MAPP. La Tabla 3 muestra los resultados obtenidos de los ensayos a tracción de los materiales compuestos formulados con distintos porcentajes de refuerzo y de MAPP.

Compuesto	V^{F}(%)	σ^{C}_{t} (MPa)	ε^{C}_{t} (%)	σ^{m*}_{t} (MPa)
PP	-	27,6 ± 0,51	9,3 ± 0,23	---
20CF80PP0MAPP	0,127	35,0 ± 0,45	3,8 ± 0,12	20,86
30CF70PP0MAPP	0,200	38,2 ± 0,78	3,5 ± 0,09	20,01
40CF60PP0MAPP	0,280	41,7 ± 0,84	3,3 ± 0,14	19,38
50CF50PP0MAPP	0,368	45,4 ± 1,14	3,1 ± 0,16	18,70
20CF80PP6MAPP	0,127	41,7 ± 0,66	4,3 ± 0,18	22,08
30CF70PP6MAPP	0,200	47,1 ± 0,74	3,9 ± 0,15	21,13
40CF60PP6MAPP	0,280	53,6 ± 0,97	3,7 ± 0,13	20,59
50CF50PP6MAPP	0,368	58,3 ± 1,23	3,2 ± 0,08	19,05

Tabla 3. *Datos experimentales de los ensayos a tracción de los distintos compuestos.*

Los compuestos formulados con un 0 y 6% en peso de MAPP muestran un incremento notable de la resistencia a tracción de la matriz. Todos ellos también muestran un incremento lineal de sus resistencias a tracción cuando el porcentaje de refuerzo es incrementado. En particular, los compuestos con un 0% (w/w) de MAPP incrementaron la resistencia a tracción de la matriz en un 27, 38, 51 y 64% cuando el contenido en refuerzo fue incrementado des de 20% hasta 50% respectivamente.

La razón del incremento de la resistencia a tracción de los compuestos sin MAPP, se debe a los tintes que provocan una mejora de la interfase entre la matriz y las fibras. La polaridad superficial de las fibras de algodón es modificada debido al bloqueo parcial de los grupos hidroxilos por parte del tinte. Dicha modificación en la polaridad de las fibras puede asimilarse a la obtenida mediante el tratamiento alcalino [133] o el tratamiento superficial con AKD de las mismas [134,135]. Mediante el análisis de la demanda catiónica de las CF, 16,39 µeq/g, y de las

fibras de algodón virgen, 58,7 µeq/g, se constató la hidrofobización parcial de las fibras como consecuencia de la presencia de tinte. La menor polaridad de las fibras de algodón teñido permite una mayor afinidad con el PP, el cual tiene naturaleza hidrofóbica.

Por otro lado, los compuestos con un 6% (w/w) de MAPP aumentaron la resistencia a la tracción de la matriz en un 51, 70, 94 y 111% cuando el contenido de refuerzo se incrementó del 20 al 50% respectivamente. En este sentido, los resultados obtenidos mostraron como la adición de un agente de acoplamiento en la formulación de los compuestos mejora la resistencia a la tracción de éstos.

El material compuesto comercial comúnmente utilizado es el formado por una matriz de PP reforzada con fibras de vidrio (GF), las cuales proporcionan grandes incrementos de la resistencia a tracción de la matriz. En la industria actual, estos compuestos se consideran productos básicos y se utilizan ampliamente en la industria automotriz, en el diseño de productos y como materiales de construcción [82,136,137]. Sin embargo, debido a la baja sostenibilidad de estos compuestos, los investigadores han realizado un intenso esfuerzo para substituir la fibra de vidrio con refuerzos más sostenibles, como las fibras de Stone Ground Wood (SGW), obteniendo resultados notables [52,138]. En la Figura 16 muestra la evolución de las resistencias a tracción de los compuestos mencionados anteriormente frente a sus fracciones en volumen de refuerzo. También muestra la resistencia a la tracción de los compuestos de PP reforzados con fibra de vidrio [52].

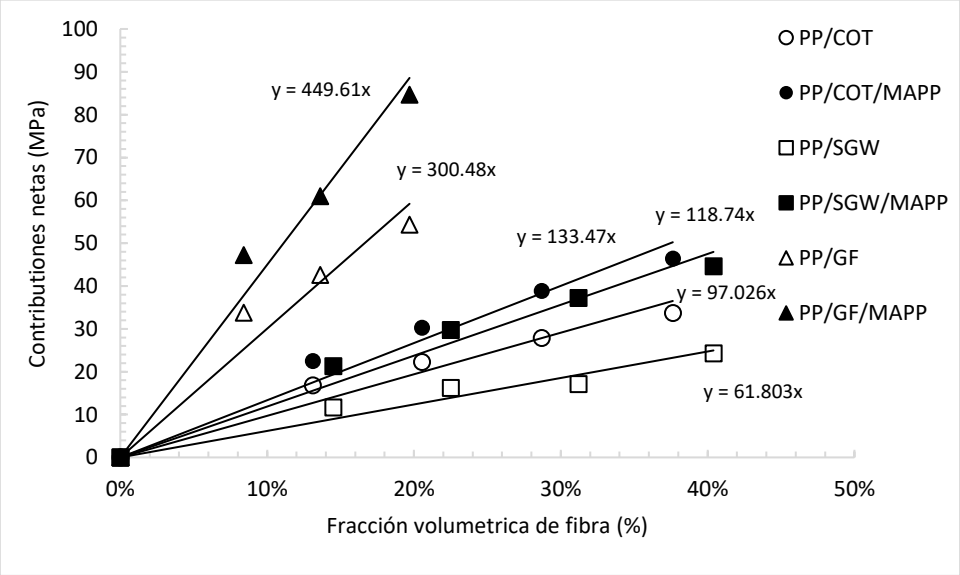

Figura 16. *Resistencia a tracción de los refuerzos de PP en función de los contenidos de refuerzo.*

Las resistencias a la tracción de los compuestos de PP reforzados con fibras naturales, son inferiores a las resistencias de los compuestos de fibra de vidrio, si se comparan con el mismo porcentaje de refuerzo. No obstante, hay compuestos que presentan σ^c_t similares que contienen distintos porcentajes de refuerzo. En el caso de los compuestos de CF sin MAPP, es necesario

reforzar la matiz de PP con un 50% (w/w) de fibra para obtener una σ^c_t equivalente a la de un compuesto de fibra de vidrio al 5% (w/w).

Por otro lado, los compuestos de CF formulados con MAPP presentan resistencias a tracción similares a los compuestos sin MAPP y reforzados con un contenido de fibra de vidrio del 10 y 20% (w/w). Estos porcentajes de refuerzo disminuyen para los compuestos de fibra de vidrio formulados con un agente de acoplamiento. Un compuesto de algodón con un contenido del 50% presenta una resistencia a tracción similar a la de un compuesto formulado con MAPP y un 10% de fibra de vidrio. Por lo tanto, es necesario el diseño de una ingeniería inteligente para que los compuestos de CF puedan substituir una parte de los compuestos de fibra de vidrio.

Si se comparan los compuestos de CF y de SGW, ambos formulados sin la adición de MAPP, éstos exhiben un comportamiento claramente diferente. Mientras los compuestos de SGW muestran un nulo incremento de la resistencia a tracción de la matriz, los compuestos de CF presentan un incremento lineal de la σ^M_t cuando aumenta el porcentaje de refuerzo. Este comportamiento es similar al de los compuestos de PP reforzado con fibra de periódico (ONPF) y sin la adición de MAPP [139,140].

Todos los materiales compuestos con un 6% (w/w) de MAPP ofrecen mayores resistencias a la tracción que sus respectivos materiales compuestos sin MAPP y con el mismo contenido de refuerzo. Sin embargo, los compuestos de SGW con un 6% (w/w) de MAPP muestran un mayor incremento respecto a sus respectivos compuestos sin MAPP que los compuestos de CF. Aun así, los compuestos reforzados con CF presentan mayores resistencias que los reforzados con SGW y con el mismo contenido en fibra. La razón principal puede deberse a la mayor resistencia intrínseca de las CF que las de SGW. Según datos bibliográficos, la resistencia intrínseca de las fibras de SGW y de CF a tracción son de 612 y 950 MPa, respectivamente [52,116].

Con el fin de establecer el impacto de los tintes en la resistencia a tracción de los compuestos, se calcularon los factores de resistencia a tracción de la fibra (FTSF) para evaluar la contribución neta de las fibras a la resistencia a tracción de los materiales compuestos. Mediante los FTSF se puede intuir la fortaleza de la interfase porque si una interfase es débil, la transferencia de carga por cargas cortantes en la interfase será limitada, y en consecuencia el valor de FTSF será bajo.

	FTSF (Mpa)	
Fibra de refuerzo	**Materiales sin MAPP**	**Materiales con MAPP**
Fibra de vidrio	300,48	449,61
SGW	61,80	118,74
Fibra de algodón	97,03	133,47

***Tabla 4**. FTSF de los materiales de PP, formulados con o sin MAPP,y reforzados con CF, SGW y fibra de vidrio.*

En la Tabla 4 se observa como la contribución de las fibras de algodón aumentó con la adicción de MAPP en un 37,5%, con un incremento de 36,4 MPa respecto de los materiales sin agente de acoplamiento. Este incremento es menor que el obtenido para las fibras SGW, donde la adicción de MAPP supuso un aumento del 92%, unos 56,9 MPa de aumento. Por lo tanto,

presumiblemente, la fortaleza de la interfase de los compuestos basados en SGW tuvo un incremento mayor que la de los compuestos basados en algodón. Los compuestos a base de fibra de vidrio aumentaron su FTSF en un 46,6%, pero el aumento neto fue de 149,1 MPa. En comparación con los compuestos de algodón, el resto de los materiales mostraron aumentos notables en las contribuciones netas de las fibras y presumiblemente mayores aumentos de la fortaleza de sus interfases. Así, se propuso el modelado micromecánico con el fin de evaluar la fortaleza de la interfase de los compuestos reforzados con fibras de algodón.

Para evaluar la interfase de los materiales reforzados con CF, se calculó mediante modelos micromecánicos la resistencia interfacial al cizallamiento. Esta resistencia explica la capacidad de la interfase para transmitir cargas desde la matriz a la fibra [140]. En el caso de los compuestos semi-alineados de fibra corta, se puede usar el criterio de von Mises ($\sigma^m_t.3^{-1/2}$) para predecir la τ de un material compuesto con una muy buena interfase.

$$\tau = \frac{\sigma_t^m}{\sqrt{3}} \tag{40}$$

Donde τ es la resistencia interfacial al cizallamiento y σ^m_t es la resistencia a tracción de la matriz. La matriz utilizada para la confección de los materiales de CF ha sido el PP Isplen PP090 62M que presenta una resistencia de 27,6 MPa. Por lo tanto, según el criterio de von Mises, se tendría que obtener un valor de τ igual a 15,9 Mpa para considerar que los compuestos de CF presentan una buena interfase [141]. A partir de la ecuación modificada de Kelly y Tyson y la solución proporcionada por Bowyer y Bader, se calculó la resistencia interfacial al cizallamiento de la interfase y la resistencia intrínseca a tracción de los refuerzos de CF. La Tabla 5 muestra los valores obtenidos.

Compuesto	X_1	τ (MPa)	L_c (µm)	σ_t^F (MPa)
20CF80PP0MAPP	0,312	9,14	878	973
30CF70PP0MAPP	0,307	8,70	861	908
40CF60PP0MAPP	0,293	9,31	833	940
50CF50PP0MAPP	0,301	9,17	746	829
20CF80PP6MAPP	0,297	14,41	710	1240
30CF70PP6MAPP	0,316	13,96	686	1162
40CF60PP6MAPP	0,310	14,55	776	1368
50CF50PP6MAPP	0,310	14,53	735	1295

Tabla 5. *Propiedades micromecánicas de la interfase y de las fibras después de resolver la ecuación de Kelly y Tyson.*

La τ varía notablemente con la adicción de MAPP. Los compuestos formulados sin MAPP presentan una τ media de 9,1±0,26 MPa, mientras que los formulados con un 6% (w/w) MAPP presentan una resistencia media interfacial de 14,36±0,27 MPa. Las resistencias interfaciales al cizallamiento de los compuestos sin agente de acoplamiento son un 74% más bajas que las de von Mises. No obstante, los valores de τ son superiores a los compuestos de SGW formulados sin MAPP, con valores por debajo de 4 MPa [52]. Aunque los compuestos formulados sin la

adición de MAPP muestran una interfase débil, su resistencia interfacial es superior a la que presentan diferentes compuestos de PP reforzados con fibras naturales y formulados sin un agente de acoplamiento [139,142,143].

Por otro lado, los compuestos de CF formulados con MAPP dan τ más altas, sólo un 11% más bajas que los criterios de von Mises. A pesar de obtener unas interfases cercanas al criterio de von Mises, los compuestos de SGW con un 6% (w/w) MAPP muestran mayores resistencias al cizallamiento interfacial, con valores cercanos a 16 MPa [52]. Además, los compuestos basados en fibras de periódicos también muestran τ similares a 16 MPa [140]. Por lo tanto, los tintes superficiales de las fibras de algodón tienen un comportamiento opuesto para los compuestos formulados con y sin MAPP. Para los compuestos formulados sin MAPP, los tintes han reducido la hidrofilidad de las fibras, y en consecuencia han aumentado la compatibilidad entre el refuerzo y la matriz. En cambio, para los compuestos formulados con MAPP, los tintes probablemente obstaculizaron la reacción entre el ácido maleico y los grupos OH superficiales de las fibras, impidiendo mejores interfaces.

En la Tabla 5 se pueden observar que las resistencias intrínsecas a la tracción de las fibras de los compuestos sin MAPP, muestran valores cercanos a 950 MPa. Estos valores son muy similares a la resistencia intrínseca a tracción de las fibras de algodón obtenida mediante ensayos de tracción de una sola fibra [116]. Sin embargo, las fibras de algodón dentro de los compuestos formulados con MAPP presentan una resistencia a la tracción intrínseca media de 1266 ± 87 MPa, un 33% más alta que las fibras de algodón de los compuestos formulados sin MAPP. Esto concuerda con investigaciones anteriores, las cuales señalaron que las propiedades de un refuerzo medido experimentalmente pueden variar de las que se calculan de forma retrospectiva [144]. Seguramente, al medir la resistencia de los textiles mediante el ensayo a tracción de una sola fibra, se subestimaron las capacidades de resistencia de las fibras [145].

Según Kelly y Tyson, la resistencia a tracción de un material compuesto se debe a las contribuciones de las fibras subcríticas, las fibras supercríticas y de la matriz. En la Figura 17 se muestran las tres contribuciones para los compuestos de CF.

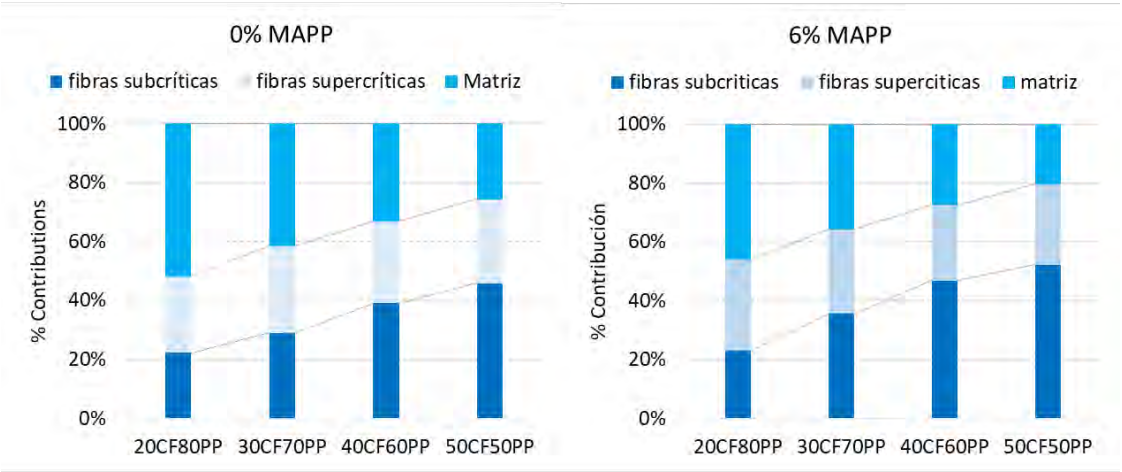

Figura 17. *Contribución de la matriz y de las fibras subcríticas y supercríticas a la resistencia a tracción de los compuestos de CF.*

En los gráficos anteriores se puede observar que los compuestos con MAPP presentan mayores contribuciones de las fibras a la resistencia a tracción que los compuestos sin MAPP. Esto es debido a una interfase más débil en los compuestos sin MAPP y, por ende, una menor capacidad de refuerzo por parte de las fibras. La aportación de las fibras se incrementó con el porcentaje de refuerzo debido a la disminución de la aportación de la matriz, y por el aumento de la aportación de las fibras subcríticas. La contribución de las fibras subcríticas fue notablemente mayor que la observada para otros compuestos a base de fibras naturales: alrededor del 10% [146]. Este hecho era esperado, debido al aumento de fibras supercríticas y a la disminución de la longitud crítica [147].

Por otro lado, la contribución de las fibras supercríticas se mantiene prácticamente constante en torno al 30%, a pesar de la presencia de agentes de acoplamiento o la cantidad de refuerzo. La resistencia interfacial obtenida dificulta la explotación completa de las capacidades de fortalecimiento de las fibras supercríticas, pero permite una explotación completa de las fibras subcríticas.

5.3. Módulo a tracción.

La *Tabla 6* presenta los valores de los Módulos de Young obtenidos en los compuestos con y sin agente de acoplamiento (E_t^C).

	CF con 0% MAPP	***CF con 6% MAPP***
W^f	**E_t^C(GPa)**	**E_t^C(GPa)**
0	1,5 ± 0,1	1,5 ± 0,1
20	3,2 ± 0,1	3,3 ± 0,1
30	3,9 ± 0,2	3,9 ± 0,1
40	4,7 ± 0,2	4,8 ± 0,2
50	5,6 ± 0,2	5,4 ± 0,2

Tabla 6. *Módulos de Young de los compuestos de PP formulados con distintos porcentajes de CF y de MAPP.*

Los compuestos con y sin MAPP muestran incrementos de la rigidez de la matriz al incrementar el porcentaje de refuerzo. Por otro lado, la adicción de MAPP presenta un efecto casi nulo sobre el E_t^C y se realizó un estudio ANOVA con un intervalo de confianza del 95%, para un análisis más exhaustivo. Este estudio determinó que los valores del Módulo de Young obtenidos para una misma cantidad de refuerzo no presentan diferencias significativas. No obstante, la adición de MAPP si tuvo un efecto notable sobre la resistencia a tracción de los compuestos, el cual se puede observar en la Tabla 3. Este comportamiento es similar al que presentan otros compuestos de PP reforzados con fibras naturales [148,149]. Según datos bibliográficos, la fuerza de la interfase entre la matriz y los refuerzos tiene un impacto limitado sobre la rigidez de los compuestos [150,151].

Para determinar su competitividad, los valores del Módulo de Young de los compuestos obtenidos fueron comparados con los de los compuestos de PP reforzados con otras fibras (Tabla 7).

% refuerzo (w/w) / fibra	SGW	HS	ONPF	GF
0	1,5 ± 0,1	1,5 ± 0,1	1,5 ± 0,1	1,5 ± 0,1
20	2,7 ± 0,1	2,8 ± 0,1	2,8 ± 0,1	4,1 ± 0,1
30	3,5 ± 0,1	3,8 ± 0,1	3,8 ± 0,1	5,7 ± 0,1
40	4,3 ± 0,1	5,2 ± 0,2	4,2 ± 0,1	7,7 ± 0,1
50	5,2 ± 0,1	6,3 ± 0,2	5,3 ± 0,1	----

Tabla 7. *Módulos de Young de los compuestos acoplados de PP reforzados con SGW, HS, ONPF y GF.*

Los compuestos reforzados con CF muestran Módulos de Young superiores a los compuestos reforzados con SGW y ONPF, y son similares a los compuestos reforzados con filamentos de cáñamo (HS) u otras hebras [127,151,152]. Sin embargo, los materiales reforzados con GF presentan Módulos de Young mayores que los compuestos a base de fibras naturales [52]. Con el mismo contenido en refuerzo, el Módulo de Young de los compuestos reforzados con CF es menor que el E^T_C de los compuestos reforzados con GF. No obstante, ciertos compuestos de CF presentan módulos similares a compuestos de GF que contienen un 20% (w/w) menos de refuerzo.

El factor de módulo a tracción de las fibras (FTMF) se puede utilizar como medida de la capacidad de refuerzo de una fibra [148]. La Figura 18 muestra los FTMF para diferentes fibras como refuerzo de PP.

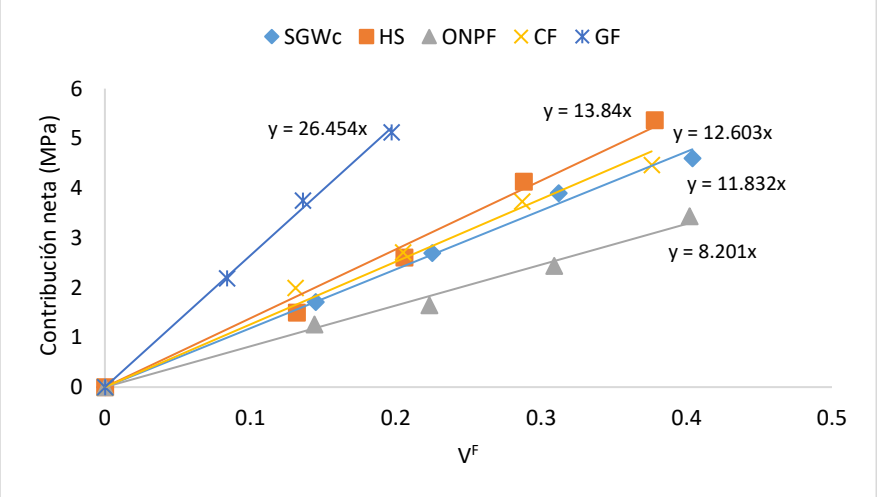

Figura 18. *Módulos a tracción de la fibra de SGW, HS, CF y GF.*

Los FTMF de los refuerzos basados en fibras naturales muestran un comportamiento similar al de los Módulos de Young de sus respectivos compuestos. En particular, el FTMF de los compuestos de CF están entre el de HS y el de SGW. Con este el valor de FTMF, es posible la aplicación de los compuestos de CF en propósitos de construcción o diseño de productos [153,154]. Otra posible aplicación es la sustitución de algunos compuestos de GF por compuestos de CF. Vallejos y colaboradores utilizaron un compuesto de OPNF que presenta un FTMF ligeramente inferior al de los compuestos de CF para sustituir uno basado en GF [139]. Por otro lado, las fibras artificiales de GF mostraron una mayor capacidad de refuerzo que el resto

de las fibras naturales debido a las propiedades intrínsecas más estables y a una morfología más regular.

Por lo tanto, las diferencias entre dichos módulos parecen centrarse en el módulo intrínseco de Young del refuerzo y en el factor de eficiencia del módulo. Para analizar tales diferencias, se realizó un estudio micromecánico empleando el modelo de Hirsch.

A través de Hirsch, se obtuvo un Módulo de Young intrínseco medio de 27,87 GPa para los compuestos de CF (Tabla 8). Este valor es ligeramente superior al de HS, con un E_t^F de 26,8 GPa [151]. Sin embargo, este E_t^F obtenido para las fibras de CF contrasta con los valores inferiores que se encuentran en la literatura. Algunas publicaciones sitúan este Módulo de Young intrínseco en el rango de 5 a 13 GPa [79,155,156]. Usando tales valores con la regla de las mezclas modificada no es posible alcanzar los valores experimentales obtenidos sin usar factores de eficiencia del módulo fuera del rango habitual.

(w/w) refuerzo (%)	E_t^F (GPa)	η_e	η_l	η_o
20	31,48	0,52	0,89	0,58
30	28,06	0,47	0.89	0,53
40	26,48	0,45	0,89	0,51
50	25,46	0,45	0,9	0,49
Media	27,87 ± 2,63	0,47 ± 0,03	0,89 ± 0,01	0,53 ± 0,04

Tabla 8. *Datos micromecánicos de los compuestos acoplados de PP reforzados con CF.*

Por otro lado, el valor de las CF es superior al valor obtenido para SGW y ONPF, 21,2 y 22,8 GPa respectivamente [127,140]. Esto también concuerda con las contribuciones netas de estas fibras. Sin embargo, las fibras de GF mostraron un Módulo de Young intrínseco de 76 GPa, el cual es superior a los Módulos de Young de los compuestos reforzados con fibras naturales.

Mediante los todos los valores experimentales (Tabla 6) y el Módulo de Young intrínseco medio de las CF (E_t^F) se calcularon los valores del factor de eficiencia (Tabla 8), obteniendo un valor medio de 0,47. El valor medio obtenido está a dentro del rango habitual de valores, entre 0,45 y 0,56 para dicho factor [127,141,143,151].

Aunque las fibras de CF presentan un E_F^t superior a los HS, los compuestos basados en CF muestran Módulos de Young menores que los compuestos reforzados con HS, con el mismo contenido de refuerzo para ambos compuestos. Este hecho es debido a los distintos factores de eficiencia del módulo, porque los compuestos reforzados con HS tienen un η_e superior al de los compuestos de CF [141].

Probablemente los compuestos reforzados con CF no han aprovechado las capacidades de refuerzo de las fibras de algodón en su totalidad. En la Tabla 8 se puede observar que los valores de η_e disminuyen cuando aumenta el contenido de fibra. El compuesto con un 20% en peso de CF presenta un factor de eficiencia del módulo más alto que los otros compuestos basados en CF, y también un Módulo de Young intrínseco más alto. Las razones deben encontrarse en la orientación media de las fibras, la morfología de los refuerzos o su dispersión.

Por un lado, el factor de eficiencia de longitud permaneció casi igual para todas las formulaciones compuestas, con un valor medio de 0,89. Por lo general, este factor disminuye cuando aumenta el porcentaje de refuerzo [149]. Sin embargo, el impacto de la morfología de las fibras de algodón parece tener poco impacto en el módulo de Young, aunque los refuerzos disminuyeron su longitud media de 293 a 185 µm [147].

Por otro lado, el factor de eficiencia de orientación cambió claramente con la cantidad de refuerzo (Tabla 3). Este factor disminuye a medida que se incrementa el contenido de refuerzo, debido a que las fibras estaban menos orientadas al incrementar su contenido. Normalmente el factor de eficiencia de orientación es más estable que el factor de eficiencia de longitud, porque la orientación media de las fibras se ve afectada por las condiciones de inyección y por geometría del molde de inyección [146,157].

5.4. Resistencia a flexión de los compuestos.

En el estudio de las propiedades a flexión se estudió el efecto del porcentaje de MAPP sobre los compuestos reforzados con un 30% de fibra. Los resultados muestran que, para la adición del 0, 2, 4 y 6% (w/w) de MAPP sobre el refuerzo implica incrementos de la resistencia a flexión (σ_t^F) de 59,7, 80,3, 94,8 y 99,5% sobre la resistencia a flexión de la matriz (σ^m_f). Sin embargo, la adición de un 8 y 10% implica una disminución de la σ_f^c del 3,5 y 8,8% respecto al compuesto formulado con un 6% de MAPP, respectivamente. Por lo tanto, la adición del 6% (w/w) de MAPP da la mayor resistencia a flexión para los compuestos reforzados con un mismo contenido de fibra. También se concluye que por la adición de MAPP, las propiedades de flexión de los compuestos se vieron afectadas de una forma similar a las propiedades de tracción (Figura 15).

Una vez determinado el % MAPP optimo, se analizó el efecto del contenido de fibra en las propiedades a flexión de los compuestos con un 0 y 6% (w/w) de MAPP. Los compuestos de CF sin la adición de MAPP (Tabla 9), aparte de incrementar la resistencia a tracción de la matriz (Tabla 3), también aumentaron la resistencia a flexión. Estos compuestos presentan aumentos de la resistencia a la flexión de la matriz en un 41, 59,7, 76,4 y 96,3%, cuando el porcentaje de CF es incrementado de 20 a 50% (w/w). La razón de los incrementos de la σ^c_f es debido a los tintes superficiales de las fibras de algodón que aumentan la compatibilidad de éstas con el PP.

Generalmente, los compuestos reforzados con fibras naturales y sin un agente de acoplamiento muestran un comportamiento distinto. Según datos bibliográficos, estos compuestos presentan ligeros incrementos en la resistencia a flexión de la matriz, y en algunos casos, presentan una disminución de σ^m_f para elevados contenidos en fibra [53,158,159]. Este hecho se debe a la interfase débil o nula entre las fibras naturales y el PP debido a su distinta polaridad, y por ende la contribución de las fibras está bastante comprometida.

Compuesto	σ^C_f (MPa)	ε^C_f (%)
PP	40,2 ± 0,84	9,6 ± 0,32
20CF80PP0MAPP	56,7 ± 0,95	5,8 ± 0,21
30CF70PP0MAPP	64,2 ± 1,05	4,7 ± 0,14
40CF60PP0MAPP	70,9 ± 1,16	4,0 ± 0,16
50CF50PP0MAPP	78,9 ± 1,24	3,8 ± 0,22
20CF80PP6MAPP	70,1 ± 0,84	6,7 ± 0,19
30CF70PP6MAPP	80,2 ± 1,19	5,5 ± 0,23
40CF60PP6MAPP	88,3 ± 2,07	4,9 ± 0,22
50CF50PP6MAPP	96,2 ± 2,15	4,1 ± 0,16

Tabla 9. *Evolución de la resistencia a flexión de los compuestos en función del contenido de CF y de MAPP.*

En el caso de los compuestos formulados con MAPP, los incrementos fueron del 74,4, 99,5, 119,7 y 139,3% para los mismos porcentajes de contenido de refuerzo. Esos compuestos presentan un comportamiento similar a compuestos de PP reforzados con diferentes fibras naturales [53,159].

En la Figura 19, se grafican los valores experimentales y teóricos de la resistencia a la flexión frente a las fracciones de volumen de fibra.

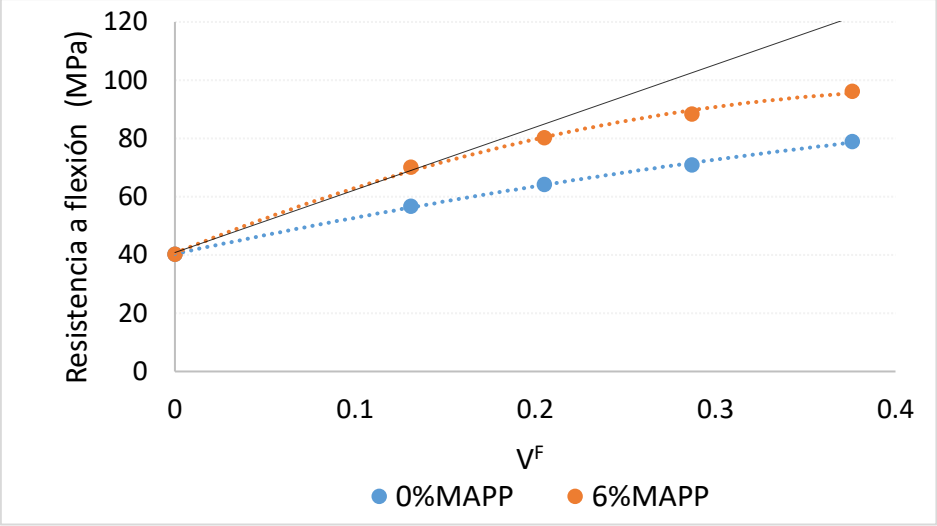

Figura 19*. Evolución de la resistencia a flexión de los compuestos respecto de su contenido en fibra. El gráfico también exhibe una regresión lineal que muestra la teórica evolución lineal de los compuestos.*

Se puede observar que los compuestos formulados con y sin MAPP muestran una evolución no lineal de la resistencia a flexión respecto del contenido de refuerzo. También presentan una desviación respecto al valor teórico, la cual se incrementa cuanto mayor es el contenido de refuerzo. Por lo tanto, el gráfico parece mostrar un deterioro de la contribución de las fibras a la resistencia a flexión del compuesto.

Aunque los compuestos de CF no permitan el desarrollo de toda la resistencia intrínseca a flexión de las fibras, estos compuestos pueden ser competitivos frente a los compuestos de PP reforzados con GF bajo algunas consideraciones. Los compuestos de CF (Tabla 9) pueden reemplazar a los compuestos formulados sin MAPP y reforzados con un 20 y 30% (w/w) de GF, los cuales presentan resistencias a la flexión de 78,0 y 88,1 MPa [53]. Sin embargo, los compuestos de CF no pueden reemplazar a todos los compuestos de PP reforzados con GF. Este es el caso para un compuesto reforzado al 30% (w/w) de GF y con MAPP, porqué presenta una σ^C_f de 125,1 MPa [53] .

Para analizar con más detalle el efecto de la presencia de tintes en las propiedades mecánicas de los compuestos de CF, es necesario un análisis micromecánico. En este caso, se calculó la contribución neta de las fibras (FFSF), evaluando la resistencia de la interfase y la resistencia intrínseca a flexión de las fibras mediante el método descrito en estas investigaciones [105,160]. La tabla 9 muestra los valores para la resistencia intrínseca a flexión de las fibras obtenidos.

Compuesto	σ_f^{M*} (MPa)	σ^F_t (MPa)	σ_f^F (MPa)	FTSF	FFSF	Fc*
20CF80PP0MAPP	36,4	973	1713	97,02	170,88	0,083
30CF70PP0MAPP	37,2	908	1599	97,02	170,88	0,082
40CF60PP0MAPP	29,6	940	1655	97.02	170,88	0,076
50CF50PP0MAPP	28,6	829	1460	97,02	170,88	0,071
20CF80PP6MAPP	38,5	1240	2069	133,47	222,73	0,122
30CF70PP6MAPP	35,5	1162	1939	133,47	222,73	0,111
40CF60PP6MAPP	33,5	1368	2282	133,47	222,73	0,098
50CF50PP6MAPP	30,1	1295	2161	133,47	222,73	0,090

Tabla 10. *Evaluación de las resistencias intrínsecas a flexión de las fibras y del factor de acoplamiento de los compuestos, asumiendo que σ_f^F es igual a 2282 MPa.*

Los compuestos con un 0 y 6% (w/w) MAPP presentan un FFSF de 170,9 y 222,7 respectivamente. Los compuestos de PP reforzados con fibras alfa, las cuales son muy similares a las de algodón, presentan valores de 173 MPa para los compuestos sin MAPP y 335 MPa para los compuestos con MAPP [161]. Si bien los valores de los compuestos sin MAPP son similares, las capacidades de refuerzo de las fibras alfa parecen ser superiores a las del algodón. Por otro lado, comparando los compuestos formulados con MAPP, los reforzados con fibras alfa presentan un FFSF superior y una evolución lineal σ_f^F en función del contenido de fibra. Estas diferencias son debidas a los tintes superficiales de las fibras, los cuales impiden mejores interfaces y provocan una menor contribución de las CF.

Las resistencias intrínsecas teóricas a flexión (σ_f^F) de los materiales compuestos oscilaron entre 1460 MPa y 2282 MPa para los materiales reforzados con CF. Esta oscilación en la σ_f^F no tendría que producirse porque se utilizaron las mimas fibras para todos los compuestos. Muy probablemente, las diferencias entre los valores obtenidos se deben a los cambios en la fuerza de la interfase. Por lo tanto, la propiedad intrínseca del refuerzo es igual o superior a los valores calculados más altos. Por tanto, la resistencia a la flexión intrínseca de las fibras teñidas de algodón como polipropileno es igual o superior a 2282 MPa.

Para calcular los factores de acoplamiento que se presentan en la Tabla 10, se estableció en 2282 MPa el valor de la resistencia a la tracción intrínseca. Los factores de acoplamiento obtenidos para los materiales con MAPP están muy lejos de los valores esperados para dichos compuestos, los cuales suelen estar en el rango de 0,18 a 0,20 [105,150]. Sin embargo, los valores obtenidos para los compuestos sin MAPP son superiores a los esperados [158].

Como se ha mencionado anteriormente, los tintes presentan dos efectos opuestos sobre la interfase. Por un lado, reducen la hidrofilidad de las fibras y permiten crear una interfase débil entre las fibras y la matriz, pero suficiente para permitir la transferencia de carga. Por otro lado, los tintes inhiben la creación de una interfase completamente fuerte. Este efecto aumenta con la cantidad de refuerzo y no permite una evolución lineal de la resistencia a flexión de los compuestos.

5.5. Módulo a flexión.

Los módulos a flexión obtenidos de los compuestos de CF se muestran en la Figura 20.

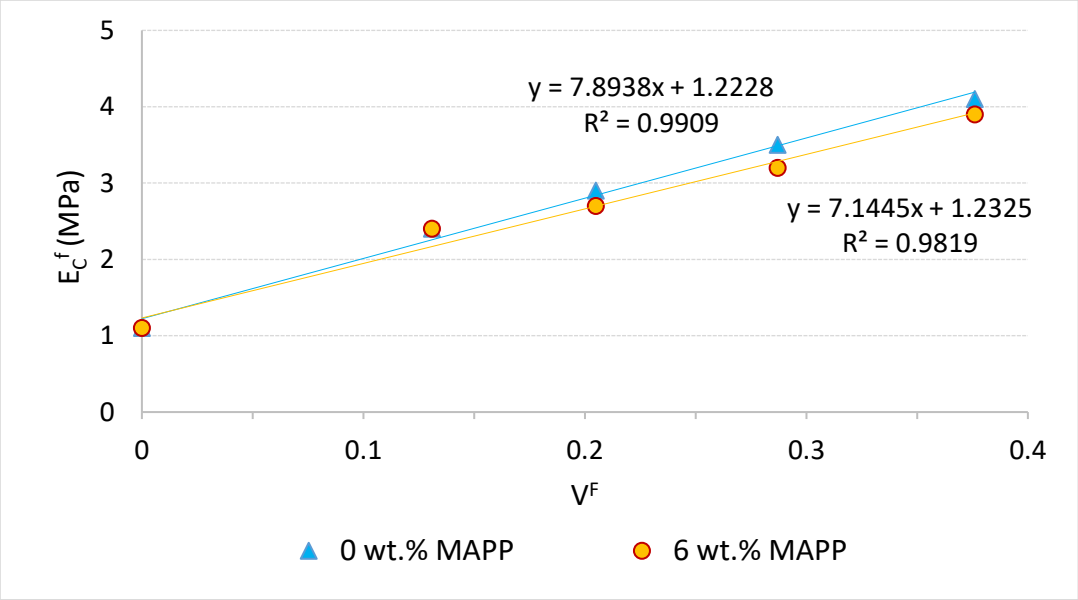

Figura 20. *Evolución de los módulos a flexión de los compuestos de CF.*

En la Figura 20 se observa que los módulos de flexión de los compuestos de CF aumentan linealmente con el contenido de fibra. Esta correlación lineal entre las dos variables, cuyos coeficientes de correlación lineal presentan valores cercanos a 1, es un buen indicador de una buena dispersión de las fibras dentro de la fase polimérica [162]. Este comportamiento no es propio de las fibras con un alto contenido en celulosa, porqué dichas fibras tienden a agregarse cuando se combinan con polímeros hidrófobos como el PP, reduciendo el incremento del módulo de flexión [163]. Dado que el algodón es un material con un alto contenido de celulosa [147], su buena dispersión dentro del material compuesto puede atribuirse presumiblemente a la presencia de tintes.

Por otro lado, la adicción de MAPP presenta un efecto casi nulo sobre los módulos de flexión de los materiales compuestos de CF. Según datos bibliográficos, la adición de agentes de

acoplamiento influye levemente en la rigidez de los materiales compuestos [99], que se rige principalmente por otros factores como las propiedades de la fibra y la matriz, el contenido de fibra, grado de dispersión y distribución de las fases [103,164]. Por lo tanto, es posible que no se requieran agentes de acoplamiento como MAPP con fines puramente de refuerzo. Sin embargo, los compuestos que contienen MAPP pueden soportar mayores deformaciones por flexión y muestran mayores resistencias que los compuestos sin MAPP (Tabla 9).

La contribución de las fibras al módulo a flexión del material compuesto se puede calcular a través del factor de módulo a flexión de la fibra (FFMF). Este factor se considera un indicador del potencial de endurecimiento de las fibras, y se puede usar para la comparación con otras fibras. En la Tabla 11 se muestra el FFMF de los compuestos reforzados con CF, fibras de madera [165] y fibras de vidrio [166].

Tipo de refuerzo	FFMF
CF 0% MAPP	9,43
CF 6% MAPP	8,71
SGW	11,87
GF	26,65

Tabla 11. *Factores de modulo a flexión de la fibra (FFMF) de los compuestos de CF, SGW y GF.*

Los compuestos 0 y 6% (w/w) MAPP de fibra presentan FFMF de 9,43 y 8,71, respectivamente. Estos FFMF son superiores a los que muestran otros compuestos reforzados con residuos lignocelulósicos resultantes de la actividad industrial textil. Este es el caso para el residuo de fibras de cáñamo, que cuando se utiliza como refuerzo del PP, presenta un FFMF de 7,9 [167]. No obstante, los compuestos de PP reforzados con SGW y GF muestran FFMF superiores a los de CF. Esto implica que, para compuestos de PP reforzados con el mismo contenido en fibra, las SGW y las GF tengan un efecto de endurecimiento 1,3 y 2,9 veces mayor a las CF.

La medición del módulo de flexión de las fibras (E^F_f) mediante pruebas directas es muy compleja y, por ende, se procedió a la obtención de su valor mediante modelos micromecánicos. Por lo tanto, el módulo de flexión intrínseco de las fibras de algodón se calculó usando el modelo de Hirsch, el modelo de Tsai-Pagano y un modelo que utiliza como base la relación FFMF / FTMF. Este último se ha propuesto en estudios recientes como un método simple para calcular el módulo de flexión intrínseco de las fibras naturales [168].

Los diferentes modelos mostraron valores similares entre ellos (Tabla 12), especialmente por los compuestos reforzados con un contenido de fibra superior al 20% en peso. Las similitudes entre los tres métodos apoyan la utilidad del modelo propuesto en este trabajo y del modelo de Hirsch frente al modelo Tsai-Pagano, debido a que estos dos no requieren datos morfológicos. También se observa que E^F_f tiende a disminuir a medida que aumenta el contenido de fibra. Esto podría deberse a los fenómenos de desgaste de las fibras sufridos durante su composición, los cuales se intensifican con contenidos de fibra elevados.

Contenido de fibra (w %)	Módulo de flexión de las fibras (E^F_f) (GPa)					
	0 % (w/w) MAPP			6 % (w/w) MAPP		
	Hirsch	Tsai-Pagano	FFMF/FTMF	Hirsch	Tsai-Pagano	FFMF/FTMF
20	24,1	29,4	21,8	24,1	29,4	23,3
30	21,1	23,7	19,4	18,7	20,4	20,8
40	19,9	21,4	18,3	17,3	18,1	19,6
50	18,6	18,9	17,6	17,3	17,6	17,6
Media	**20,9**	**23,4**	**20,7**	**19,4**	**21,4**	**19,3**

Tabla 12. *Módulos de flexión de las fibras de los compuestos de CF calculados mediante Hirsch, Tsai-Pagano y la relación FFMF/FTMF.*

Los factores de eficiencia se calcularon mediante el E^F_f obtenido por Hirsch y la Regla de mezclas modificada. Por lo tanto, los compuestos de CF con un 0 y 6% (w/w) MAPP muestran coeficientes de eficiencia (η_e) de 0,47 y 0,48 respectivamente. Estos factores obtenidos están en línea con los reportados en la literatura para fibras naturales que presentan valores entre 0,45 y 0,56 [150,161,165]. Cabe destacar que el factor de eficiencia es prácticamente idéntico al obtenido a partir de la micromecánica del Módulo de Young, con un valor medio de 0,47 (Tabla 8). Las similitudes entre los factores de eficiencia obtenidos a partir del módulo de flexión y del Módulo de Young, confirman que se puede calcular el módulo de flexión intrínseco mediante la relación FFMF / FTMF.

Los valores para el factor de orientación del módulo estuvieron entre 0,53 y 0,5. Este factor suele oscilar entre 0,4 y 0,6 en materiales compuestos procesados mediante moldeo por inyección y está influenciado principalmente por las condiciones de composición y geometría del molde [169]. Dicho factor es igual a 1 cuando las fibras están completamente alineadas, mientras que para la configuración aleatoria plana el factor tiende a ser 3/8 y para sistemas completamente aleatorios el factor puede disminuir a 1/5 [57]. Por tanto, para el presente caso se advierte una cierta alineación de las fibras en el interior del material compuesto, que como se ha mencionado, se puede atribuir principalmente al proceso de inyección.

Utilizando el factor de orientación del módulo y, estimando una distribución de empaquetamiento cuadrado de las fibras dentro del compuesto, la orientación media de las fibras dentro del compuesto se fijó en 30,6°. Comparativamente, la micromecánica del módulo de Young para los mismos compuestos arrojó un ángulo límite de 53,3° y una orientación media de aproximadamente 36,1°. Se observa que, nuevamente, la micromecánica del módulo de Young y el módulo de flexión arrojan resultados similares.

5.6. Impacto

En la producción de materiales plásticos debe considerarse la resistencia al impacto como una propiedad relevante en muchas aplicaciones. Para evaluar el uso de los materiales plásticos en condiciones reales no es suficiente la evaluación de las propiedades de flexión y tracción. Estas propiedades evalúan el efecto de una fuerza constante que se incrementa ligeramente y representan sólo una parte de la información necesaria en el diseño o desarrollo de productos [170]. En la producción de materiales compuestos debe considerarse que la resiliencia al impacto depende en gran medida de las fases y sus interacciones. Una débil interfase entre las fibras y la matriz repercute significativamente en las propiedades de impacto. La mayor rigidez del material debido a la incorporación de fibras suele reducir la resistencia al impacto de los materiales compuestos.

Se evaluó la resistencia al impacto de los materiales compuestos obtenidos con y sin agente de acoplamiento. La Tabla 13 muestra los resultados del ensayo Charpy obtenidos sin entallar (I_U^C) y con entalla (I_N^C).

Contenido de fibra (w %)	Resistencia al Impacto					
	0 % (w/w) MAPP			6 % (w/w) MAPP		
	I_U^C (KJ/m²)	I_N^C (KJ/m²)	$I_U^C - I_N^C$ (KJ/m²)	I_U^C (KJ/m²)	I_N^C (KJ/m²)	$I_U^C - I_N^C$ (KJ/m²)
0	No rompe					
20	27,2 ± 0,8	4,5 ± 0,2	22,7	34,8 ± 1,2	4,9 ± 0,3	29,9
30	12,1 ± 0,5	4,2 ± 0,1	7,9	22,1 ± 1,4	4,6 ± 0,2	17,5
40	11,4 ± 1,0	4,0 ± 0,1	7,4	19,5 ± 1,5	4,4 ± 0,2	15,1
50	10,6 ± 0,8	3,9 ± 0,2	6,7	18,6 ± 0,9	4,2 ± 0,1	14,4

***Tabla 13**. Evolución de la resistencia al impacto Charpy con y sin entalla en función del contenido de fibra para los compuestos con y sin agente de acoplamiento.*

El equipo de ensayo no pudo romper la muestra de PP, lo que demuestra su alta tenacidad. En la literatura la resistencia al impacto de un PP se encuentra en torno a 85 kJ/m^2 [171]. Por otra parte, tal y como se esperaba, la adición de un porcentaje de refuerzo al material compuesto provoco una disminución considerable de la resistencia al impacto. Sin embargo, la disminución en la resistencia al impacto de los materiales con un 6% de agente de acoplamiento es significativamente inferior a la de los materiales sin este agente. Las diferencias entre las resistencias al impacto de los materiales compuestos con agente de acoplamiento y sin agente de acoplamiento pueden relacionarse con un cambio en el mecanismo de creación y propagación de la fractura. Las fracturas iniciales se desarrollarán en la fase más débil, que luego se propagarán de acuerdo con los mecanismos descritos en la literatura [172]. Esta disminución en la resistencia al impacto puede ser atribuida a diversos factores entre los que se encuentran una posible disminución de la resistencia de la interfaz, las aglomeraciones de fibras que dan lugar a concentraciones de tensiones, y a una reducción de la absorción de energía debido al contacto entre fibras [173].

Por otro lado, los resultados del ensayo Charpy con entalla no muestran diferencias significativas en función del porcentaje de refuerzo. Este resultado indica una escasa contribución de los refuerzos a la resistencia al impacto de los materiales compuestos. Un aumento de la resistencia al impacto en el ensayo Charpy con entalla indicaría una interfase débil. Este hecho se debe a que la fractura ya se ha producido y la energía absorbida es utilizada en la extracción de las fibras [174]. La disminución de la resistencia al impacto de los materiales compuestos no entallados puede estar relacionada con el aumento ya observado de la fragilidad de los materiales compuestos cuando se someten a los ensayos de tracción y flexión, y un cambio de fractura dúctil a frágil [175].

La creciente fragilidad al incrementar el porcentaje de fibras puede explicarse por la disminución de los porcentajes de la matriz de PP, la fase continua, y el aumento de los porcentajes de refuerzos más fuertes pero más frágiles. Así mismo también se puede atribuir al aumento de las concentraciones de tensión en las proximidades de la fibra [176] o la presencia de demasiados extremos de fibra dentro del material compuesto [166].

Uno de los principales materiales utilizados en la industria son los compuestos de polipropileno (PP) reforzado con fibra de vidrio (GF). La producción de este material de refuerzo mineral consume grandes cantidades de energía y conlleva riesgos para la salud humana [139]. Es por ello por lo que las propiedades de los materiales compuestos a partir de fibras de algodón deben compararse con materiales compuestos comerciales para evaluar su competitividad en aplicaciones similares. La resistencia al impacto de los materiales compuestos de PP/CF sin entallar son inferiores a los de PP/GF, donde un material con un 30 % en peso de fibra de vidrio alcanza 39,4 kJ/m^2 [166].

En cualquier caso, la literatura sitúa en 30 kJ/m^2 la resistencia al impacto de los materiales utilizados en la industria del automóvil [170]. Así pues, es posible preparar materiales compuestos que añadan un 20% de CF, fibras más baratas y sostenibles que las fibras de vidrio, y competir con los materiales comerciales de PP/GF.

5.7. Absorción de agua

El carácter hidrofílico de las fibras de celulosa puede tener un gran efecto en las propiedades mecánicas de los materiales compuestos. Ello podría reducir significativamente la vida útil de los materiales compuestos en sus aplicaciones, principalmente en exteriores [174,177,178]. Es por ello por lo que el estudio de la absorción de agua y su cinética es relevante para el uso de estos materiales compuestos y sus posibles aplicaciones. Además, el efecto de la interfaz en la absorción de agua es fundamental, ya que podría afectar a la cinética y a la permeabilidad del agua en el material compuesto [99]. La absorción de agua de los polímeros y materiales compuestos tiene un efecto significativo en su rendimiento mecánico. El agua es una molécula pequeña que puede fundirse fácilmente en los materiales sólidos. Sin embargo, en el caso de los materiales poliméricos, la penetración del agua en el interior de la fase polimérica produce una alteración en la disposición espacial de las cadenas, inhibiendo la interacción entre ellas, y desplazando las cadenas [179]. Esto provoca un hinchamiento del material y una pérdida de rendimiento mecánico. El hinchamiento de las fibras también puede producir el agrietamiento

del material [178]. No obstante, existen ejemplos de utilización de poliolefinas reforzadas con fibras naturales en el diseño de productos y de automóviles [180].

La Figura 21 muestra el comportamiento obtenido para el PP puro y sus compuestos de CF.

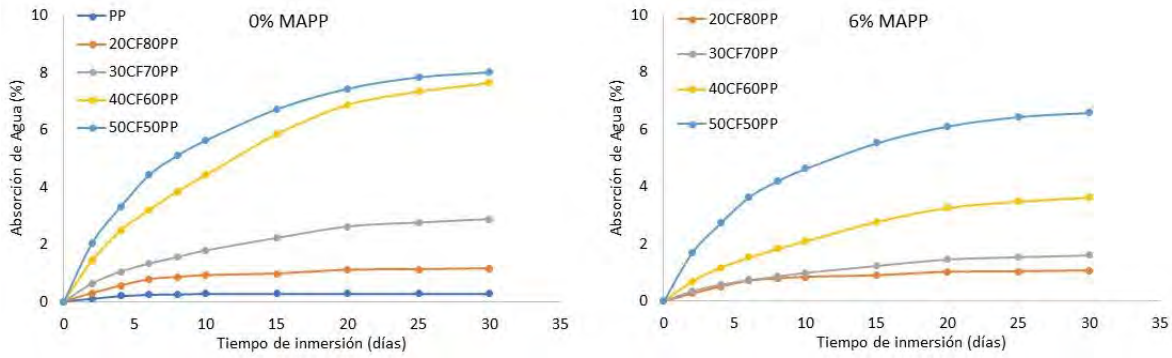

Figura 21. *Evolución de la absorción de agua de los compuestos de PP-CF: a) Sin agente de acoplamiento; b) con un 6% de agente de acoplamiento.*

Los materiales sin agente de acoplamiento presentaron un significativo aumento de la absorción de agua cuando el porcentaje de CF se incrementó. Tras 30 días de exposición, los materiales reforzados con 20, 30, 40 y 50 % en peso de CF mostraron porcentajes de absorción de agua del 1,16%, 2,89%, 7,65% y 8,02%, respectivamente. Por otra parte, la Figura 21 muestra la insignificante absorción de agua de la matriz. Por lo tanto, se ha constatado como las fibras hidrofílicas son responsables de la absorción de agua de los materiales compuestos obtenidos.

La presencia de un agente de acoplamiento en la formulación de los composites afectó a los porcentajes de absorción de agua. Después de 30 días, los composites con agente de acoplamiento presentaron porcentajes de absorción de agua del 1,06%, 1,62%, 3,64% y 6,59%, respectivamente. Esto puede deberse a la mayor adhesión entre las fases y a la ausencia de huecos en la zona interfacial, dificultando la difusión y acumulación de agua. Por otro lado, la hidrofilia de las fibras se reduce debido a la presencia del MAPP, ya que algunos grupos hidroxilos de la superficie de las fibras crean enlaces éster con el agente de acoplamiento [181].

La cinética de la absorción de agua en los materiales plásticos puede modelarse mediante la ecuación linealizada de la ley de Fick:

$$\log\left(M_t/M_\infty\right) = n\log\left(t\right) + \log\ K \tag{41}$$

donde M_t es el valor de saturación en un tiempo (t). El parámetro n y K son las constantes de Fick obtenidas directamente y referidas al tipo de caso de difusión de agua descrito en el modelo Fickiano [182]. La movilidad de las moléculas de agua en relación con las cadenas poliméricas es descrita por el parámetro n. La constante K se encuentra relacionada con las condiciones ambientales.

Contenido de fibra (w/w) (%)	M_∞ (%)	n	K
0	0,28 ± 0,06	0,51 ± 0,02	0,30 ± 0,01
20	1,06 ± 0,09	0,46 ± 0,09	0,24 ± 0,01
30	1,62 ± 0,12	0,56 ± 0,05	0,16 ± 0,02
40	3,64 ± 0,11	0,62 ± 0,07	0,13 ± 0,01
50	6,59 ± 0,17	0,50 ± 0,02	0,21 ± 0,01

Tabla 14. *Constantes de Fick obtenidas a partir de la linealización de los resultados experimentales de los compuestos de PP y fibras de algodón con un 6% de agente de acoplamiento.*

El parámetro n obtenido a partir de la linealización de los resultados experimentales de los compuestos de PP con distintos porcentajes de fibra de algodón y un 6% de MAPP está cerca de 0,5, lo que indica un caso de difusión de Fick o también conocido como caso de difusión I. Este comportamiento se traduce en la consecución rápida y fácil del equilibrio en el interior del polímero. Un caso de Fick se obtiene normalmente en polímeros semicristalinos en los que no se observa una fuerte interacción entre el polímero y el agua. Los resultados obtenidos son similares a los presentados en la literatura por otros compuestos de polipropileno reforzado con fibras naturales [176,183]. Por otra parte, el valor K relacionado con el entorno de las muestras, es similar para todos los compuestos. Estos resultados eran de esperar, debido a que todas las muestras han sido sometidas a las mismas condiciones ambientales.

El coeficiente de difusión (D) indica la facilidad del agua para penetrar en el material. El coeficiente de difusión de los distintos materiales compuestos puede ser obtenido, para un caso de difusión de Fick, a partir de la siguiente ecuación.

$$\frac{M_t}{M_\infty} = \frac{4}{L} \cdot (D/\pi)^{1/2} \cdot t^{1/2} \qquad (42)$$

Esta ecuación puede aplicarse para relaciones de $\frac{M_t}{M_\infty}$ inferiores a 0,5 y considerando la anchura de la muestra (L).

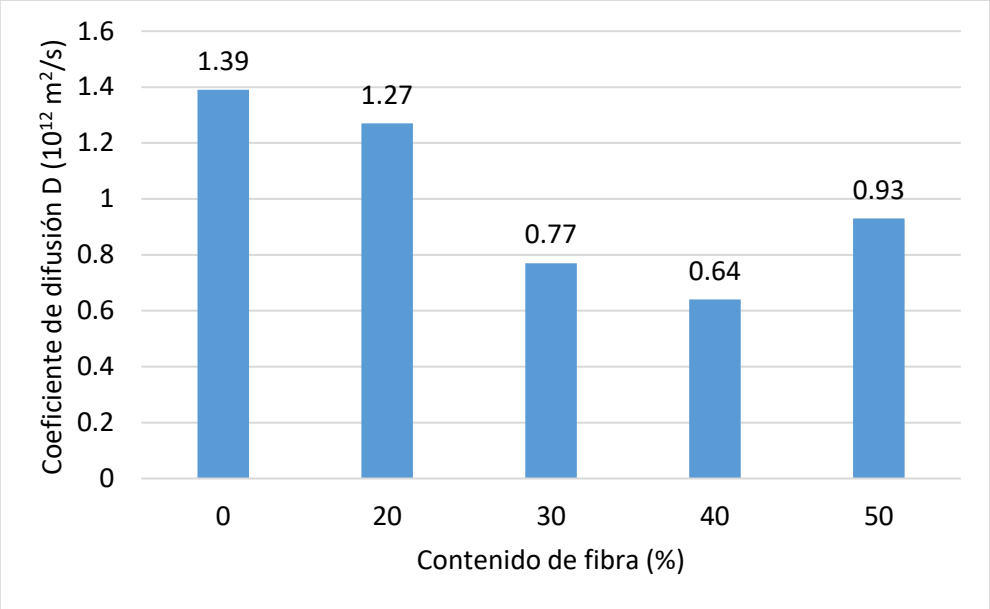

Figura 22. *Evolución del coeficiente de difusión en los materiales compuestos en función del contenido de fibra de algodón.*

En la Figura 22 se observa una mayor capacidad en el PP que en el caso de los materiales compuestos. La presencia de fibra redujo el coeficiente D para los materiales compuestos, lo que indica una mayor dificultad del agua para penetrar en estos materiales. Estos resultados pueden estar relacionados con la rigidez de las fibras que dificulta la movilidad de la cadena del polímero y aumenta el tiempo de saturación en muestras con una anchura similar. En este mismo sentido los resultados obtenidos son del mismo orden de los presentados en la literatura para compuestos de PP reforzados con fibras naturales [184].

Conclusiones generales

6. Conclusiones generales

La obtención exitosa de materiales compuestos a partir de polipropileno y borra de algodón teñida como refuerzo, ha permitido alcanzar el objetivo principal de esta tesis doctoral. Estos materiales compuestos de PP presentan propiedades relevantes y muestran que es posible recuperar subproductos textiles, los cuales pueden ser valiosos. El uso de tales fibras como refuerzo es una alternativa al difícil proceso de reciclado de textiles y una solución a su contaminación medioambiental causada por su vertido o incineración.

Se ha estudiado el efecto del agente de acoplamiento, mostrando un incremento las propiedades mecánicas de la matriz de polipropileno (PP), tanto si se usa un agente de acoplamiento como si no. Aunque todas las formulaciones incrementan las propiedades de la matriz, los materiales compuestos con un 6% (w/w) de MAPP son los que presentan mejores propiedades a tracción y a flexión. Sin embargo, los módulos de Young y los módulos de flexión de los compuestos se vieron poco afectados por la presencia de agentes de acoplamiento. Por lo tanto, para aplicaciones donde la rigidez es primordial, los compuestos sin un agente de acoplamiento se pueden utilizar con la misma respuesta que los compuestos con un 6% (w/w) de MAPP.

Se han determinado las propiedades mecánicas de los compuestos de CF. Estos materiales incrementan sus respectivos valores al incrementar la cantidad de refuerzo, tanto para los compuestos con y sin MAPP. Generalmente, la evolución de las propiedades mecánicas respecto del contenido de fibra fue lineal y siguieron la evolución descrita por la regla de las mezclas. Sin embargo, la evolución de la resistencia a la flexión de los compuestos con MAPP no fue lineal. Estos compuestos, sobre todo los reforzados con mayores porcentajes de algodón, muestran resistencias a la flexión más bajas que las esperadas por una evolución lineal. Esto se atribuyó a la presencia de interfases menos fuertes de lo esperado.

Se ha avaluado la calidad de la interfase mediante los análisis micromecánicos. Los compuestos sin MAPP muestran una τ mayor que otros compuestos de PP reforzados con fibras naturales y formulados sin un agente de acoplamiento. Este hecho se debe principalmente a los tintes superficiales de las fibras de algodón, los cuales reducen la hidrofilidad de las fibras, y en consecuencia aumentan la compatibilidad entre el refuerzo y la matriz. Por otro lado, los valores de τ obtenidos para los compuestos de CF con un 6% (w/w) de MAPP son un 11% más bajas que los criterios de von Mises. Aunque la adicción de MAPP aumentó la calidad de la interfase de los compuestos mostrando buenos valores, el aumento de τ es menor al que muestran varios compuestos de PP reforzados con fibras naturales o con fibra de vidrio. Esta causa se debe principalmente a los tintes que probablemente obstaculizan la reacción entre el ácido maleico y los grupos OH superficiales de las fibras, impidiendo mejores interfases.

Se ha estudiado el cambio morfológico de las fibras de algodón durante la fabricación de los materiales compuestos. La longitud media de las fibras dentro de los materiales compuestos disminuye al incrementar el contenido de refuerzo. Además, los compuestos con MAPP muestran longitudes medias más bajas que los que los compuestos sin MAPP. Aunque el tiempo de mezcla se redujo para los compuestos reforzados con un alto contenido en fibra, fue lo

suficientemente largo para que la interfase transfiriera mayores cargas de cizallamiento a las fibras y se redujeran sus longitudes. La forma de las distribuciones de longitud de las fibras también cambia con las cantidades de refuerzo. Los materiales compuestos con mayor cantidad de refuerzo muestran una mayor presencia de fibras cortas y una distribución gradual de las fibras largas presentes. No obstante, el diámetro medio de las fibras se mantuvo muy estable a 16,5 micrómetros.

Se han determinado las contribuciones de las fibras en las propiedades mecánicas:

- La resistencia intrínseca a tracción de las fibras de algodón calculada mediante modelos micromecánicos muestra un valor de 1266 MPa, mientras que la σ_t^F obtenida mediante ensayos de tracción de una sola fibra muestra un valor de 948 MPa. Este hecho se debió a la subestimación de las capacidades de resistencia de las fibras cuando se realizó el ensayo de tracción de una sola fibra. Cabe destacar que las dos σ_t^F presentan valores superiores a los encontrados en la bibliografía para las fibras de algodón.

- Aunque las resistencias intrínsecas a flexión oscilan entre 1460 MPa y 2282 MPa, se estable un valor de 2282 MPa para σ_f^F. Esta oscilación se atribuye a los cambios en la fuerza de la interfase y por ende, a un cambio del factor de acoplamiento. Dichos factores de acoplamiento presentan valores muy lejos de los esperados para los compuestos reforzados con fibras naturales y formulados con MAPP, los cuales suelen estar en el rango de 0,18 a 0,20. Sin embargo, los valores obtenidos para los compuestos sin MAPP son superiores a los esperados.

- Los compuestos de CF presentan un Módulo intrínseco de Young de 27,87 GPa, que se determinó mediante el modelo de Hirsch. Este valor es ligeramente superior al mostrado por las fibras naturales pero inferior a los 76 GPa que muestran los compuestos reforzados con fibra de vidrio. Por otro lado, se utilizó una metodología alternativa para el cálculo del módulo intrínseco de flexión, que conecta los Módulos de Young y los de Flexión, y que proporcionó un valor de 20 GPa para E^F_f. Este valor obtenido se comparó con los valores obtenidos mediante modelos más establecidos como Hirsch o Tsai-Pagano. Las tres metodologías usadas proporcionan un valor similiar de E^F_f. Aunque este valor está en línea con otras fibras naturales, las fibras de vidrio muestran un módulo intrínseco de flexión superior.

Se han calculado los coeficientes de eficiencia a partir de la micromecánica del Módulo de Young y del módulo de flexión, los cuales son muy similares. Los compuestos de CF muestran coeficientes de eficiencia (η_e) alrededor de 0,47, los cuales están en línea con los reportados en la literatura para fibras naturales. Las similitudes entre los factores de eficiencia obtenidos a partir del módulo de flexión y del Módulo de Young, confirman que se puede calcular el módulo de flexión intrínseco mediante la relación FFMF / FTMF.

Se ha realizado el análisis de la resistencia a impacto de los materiales de CF. La adición de un agente de acoplamiento muestra un aumento de la resistencia al impacto de los materiales respecto de los materiales sin MAPP. Por otro lado, el incremento del contenido de refuerzo

provoca una disminución significativa de la resistencia a impacto. Este aumento de la fragilidad puede explicarse por los el aumentos de los porcentajes de los refuerzos, los cuales son más frágiles.

Se ha determinado el comportamiento de los compuestos de CF en ambientes húmedos. La presencia de un agente de acoplamiento en la formulación de los composites de CF reduce la absorción de agua. Esto puede deberse a la mayor adhesión entre las fases y a la ausencia de huecos en la zona interfacial, dificultando la difusión y acumulación de agua. Por otro lado, los materiales con y sin agente de acoplamiento presentan un aumento de la absorción de agua cuando el porcentaje de CF se incrementa.

Se ha evaluado su posible aplicación teniendo en cuenta las propiedades mecánicas de los compuestos obtenidos. Este estudio muestra la oportunidad de recuperar fibras textiles de algodón, que son inútiles para la industria textil, para la obtención de materiales compuestos capaces de sustituir a los materiales reforzados con fibra de vidrio. Aunque los compuestos de PP reforzados con fibra de vidrio muestran propiedades mecánicas más altas, ciertos compuestos de CF presentan propiedades similares a compuestos de PP con bajo refuerzo de fibra de vidrio. Si bien ambas propiedades son diferentes, un diseño de ingeniería inteligente puede permitir la sustitución de compuestos de fibra de vidrio por compuestos reforzados con fibra de algodón. Esta sustitución podría conllevar a varios beneficios, por un lado, sería la no utilización de un material artificial, de compleja manipulación y muy costoso de producción. Otro beneficio seria la reducción de la cantidad de PP usada en la formación de los compuestos porqué es necesario un porcentaje mayor de CF para obtener propiedades similares. También se andaría valor a un residuo textil evitando su vertido e incineración de dichas fibras.

En cuanto a las perspectivas de futuro, se podían usar otros residuos celulósicos procedentes de la industria textil como refuerzo de PP. Por otro lado, las fibras teñidas de algodón podrían ser un buen refuerzo para otras matrices, especialmente para las matrices procedentes de fuentes renovables y sostenibles. Esto permitiría la obtención de materiales compuestos con un grado de sostenibilidad ambiental superior. En esta línea, son muchos los esfuerzos en investigación que deben producirse para encontrar una utilidad a los varios residuos celulósicos provenientes de la industria textil y que permitan alcanzar propiedades acordes a las solicitadas para la aplicación correspondiente.

Bibliografía general

7. Bibliografía general

[1] Kaza S, Yao L, Bhada-Tata P, Van Woerden F. What a Waste 2.0: A Global Snapshot of Solid Waste Management to 2050. 2018:231.

[2] European Union. The case for increasing recycling : Estimating the potential for recycling in Europe Key messages 2020:1–13.

[3] European Environmental Agency. Textiles in Europe's circular economy Key messages. 2020.

[4] Sánchez CM. La industria textil, la segunda más contaminante del planeta. XL Sem 2020.

[5] Drew D, Reichart E. These are the Economic, Social and Environmental Impacts of fashion 2019.

[6] Ryu C, Phan AN, Sharifi VN, Swithenbank J. Combustion of textile residues in a packed bed. Exp Therm Fluid Sci 2007;31:887–95. https://doi.org/10.1016/j.expthermflusci.2006.09.004.

[7] European Environmental Agency. Plastic in textiles : towards a circular economy for synthetic textiles in Europe Key messages 2021:1–12.

[8] Barbero-Barrera MDM, Pombo O, Navacerrada MDLÁ. Textile fibre waste bindered with natural hydraulic lime. Compos Part B Eng 2016;94:26–33. https://doi.org/10.1016/j.compositesb.2016.03.013.

[9] Illge L, Preuss L. Strategies for Sustainable Cotton: Comparing Niche with Mainstream Markets. Corp Soc Responsib Environ Manag 2012;19:102–13. https://doi.org/10.1002/csr.291.

[10] United States Enviromental protection Agency n.d.:www.epa.gov.

[11] Jha MK, Kumar V, Maharaj L, Singh RJ. Studies on Leaching and Recycling of Zinc from Rayon Waste Sludge. Ind Eng Chem Res 2004;43:1284–95. https://doi.org/10.1021/ie020949p.

[12] Liu W, Liu S, Liu T, Liu T, Zhang J, Liu H. Eco-friendly post-consumer cotton waste recycling for regenerated cellulose fibers. Carbohydr Polym 2019;206:141–8. https://doi.org/10.1016/j.carbpol.2018.10.046.

[13] European Union. Directive 2018/851 amending Directive 2008/98/EC on waste Framework. Off J Eur Union 2018:(L-150/109-140).

[14] Shirvanimoghaddam K, Motamed B, Ramakrishna S, Naebe M. Death by waste: Fashion and textile circular economy case. Sci Total Environ 2020;718:137317. https://doi.org/10.1016/j.scitotenv.2020.137317.

[15] Mulinari DR, Voorwald HJC, Cioffi MOH, Lima CAA, Baptista CAPR, Rocha GJM. Composite materials obtained from textile fiber residue. J Compos Mater 2011;45:543–7. https://doi.org/10.1177/0021998310376098.

[16] Kant Hvass K, Pedersen ERG. Toward circular economy of fashion: Experiences from a brand's product take-back initiative. J Fash Mark Manag 2019;23:345–65. https://doi.org/10.1108/JFMM-04-2018-0059.

[17] EURATEX. The textile and clothing industry in 2019. Euratex 2020:29.

[18] Commission E. Textiles and clothing industries 2016:https://ec.europa.eu/growth/sectors/fashion/texti.

[19] Fohlen C. La Revolución industrial. Barcelona: Vicens-Vives; 1978.

[20] Roig V, Jaime. Problemas actuales y futuros en el suministro de materias primas para la industria textil. 1979.

[21] Houck M. Identification of textile fibers 2009.

[22] García Reyes LE. La industria textil y su control de calidad. 2013.

[23] Marín FL-A. Determinación de la longitud en la fibra de lana. Boletín Intexter Del Inst Investig Text y Coop Ind 1974.

[24] Solutions TT. Textile Fibres. vol. I. 2019.

[25] Textile Exchanges. Preferred Fiber & Materials Market Report 2020 2020:103.

[26] Sánchez Maza MÁ. Iniciación en materiales, productos y procesos textiles. 2012.

[27] United Sattes Depertament of agriculture. Cotton Outlook 2021. 2021.

[28] Ansell MP, Mwaikambo LY. The structure of cotton and other plant fibres. vol. 2. Woodhead Publishing Limited; 2009. https://doi.org/10.1533/9781845697310.1.62.

[29] Abdouramane N, Cécile A, Dydimus Efeze N, Anicet Noah PM, Betene FE, Gomdjé Valery H, et al. Class of Mineral Textile Fibres Review. Int J Polym Text Eng 2021;8:6–8. https://doi.org/10.14445/23942592/ijpte-v8i2p102.

[30] Nayak L. The mineral fibre: Asbestos - Its manufacture, properties, toxic effects and substitutes. Nat Environ Pollut Technol 2016;15:477–82.

[31] Shaikh T, Chaudhari S, Varma A. Viscose Rayon: A Legendary Development in the Manmade Textile. Mrs Alpa Varma / Int J Eng Res Appl 2012;2:675–80.

[32] Tecnología de los plásticos n.d.:https://tecnologiadelosplasticos.blogspot.com/2012.

[33] More Reyes PM. El algodón pima peruano: cultivo y manejo agronomico. J Chem Inf Model 2019;53:1689–99.

[34] Neefus JD, Ivester AL. Industria De Productos Textiles. Encicl Salud Y Segur En El Trab 1991:36.

[35] Lord PR. Handbook of Yarn Production: Technology, Science and Economics. 2003.

[36] Halimi MT, Hassen M Ben, Sakli F. Cotton waste recycling: Quantitative and qualitative assessment. Resour Conserv Recycl 2008;52:785–91. https://doi.org/10.1016/j.resconrec.2007.11.009.

[37] Wanassi B, Azzouz B, Hassen M Ben. Value-added waste cotton yarn: Optimization of recycling process and spinning of reclaimed fibers. Ind Crops Prod 2016;87:27–32. https://doi.org/10.1016/j.indcrop.2016.04.020.

[38] El-Molla MM, Schneider R. Development of ecofriendly binders for pigment printing of all types of textile fabrics. Dye Pigment 2006;71:130–7. https://doi.org/10.1016/j.dyepig.2005.06.017.

[39] Shen F, Xiao W, Lin L, Yang G, Zhang Y, Deng S. Enzymatic saccharification coupling with

polyester recovery from cotton-based waste textiles by phosphoric acid pretreatment. Bioresour Technol 2013;130:248–55. https://doi.org/10.1016/j.biortech.2012.12.025.

[40] Jeihanipour A, Karimi K, Niklasson C, Taherzadeh MJ. A novel process for ethanol or biogas production from cellulose in blended-fibers waste textiles. Waste Manag 2010;30:2504–9. https://doi.org/10.1016/j.wasman.2010.06.026.

[41] Peña-Pichardo P, Martínez-Barrera G, Martínez-López M, Ureña-Núñez F, dos Reis JML. Recovery of cotton fibers from waste Blue-Jeans and its use in polyester concrete. Constr Build Mater 2018;177:409–16. https://doi.org/10.1016/j.conbuildmat.2018.05.137.

[42] Yousef S, Tatariants M, Tichonovas M, Kliucininkas L, Lukošiūtė SI, Yan L. Sustainable green technology for recovery of cotton fibers and polyester from textile waste. J Clean Prod 2020;254. https://doi.org/10.1016/j.jclepro.2020.120078.

[43] Hesser F. Environmental advantage by choice: Ex-ante LCA for a new Kraft pulp fibre reinforced polypropylene composite in comparison to reference materials. Compos Part B Eng 2015;79:197–203. https://doi.org/10.1016/j.compositesb.2015.04.038.

[44] Hull D. An introduction to composite materials. 2014. https://doi.org/10.1007/s13398-014-0173-7.2.

[45] Lubin G. Handbook of Composites. Boston, MA: Springer US; 1982.

[46] McMullen P. Fibre/resin composites for aircraft primary structures: a short history. Composites 1984;15:222–30.

[47] Suarez SA, Gibson RF, Sun CT, Chaturvedi SK. The influence of fiber length and fiber orientation on damping and stiffness of polymer composite materials. Exp Mech 1986;26:175–84. https://doi.org/10.1007/BF02320012.

[48] Drzal LT. The role of the fiber-matrix interphase on composite properties. Vacuum 1990;41:1615–8.

[49] Ribeiro MCS, Fiúza A, Ferreira A, Dinis M de L, Castro ACM, Meixedo JP, et al. Recycling approach towards sustainability advance of composite materials' industry. Recycling 2016;1:178–93. https://doi.org/10.3390/recycling1010178.

[50] Thomason J, Jenkins P, Yang L. Glass Fibre Strength—A Review with Relation to Composite Recycling. Fibers 2016;4:18. https://doi.org/10.3390/fib4020018.

[51] Amer AAR, Abdullah MMAB, Ming LY, Tahir MFM. Performance and properties of glass fiber and its utilization in concrete - A review. AIP Conf Proc 2018;2030. https://doi.org/10.1063/1.5066937.

[52] López JP, Méndez JA, Mansouri NE El, Mutjé P, Vilaseca F. Mean intrinsic tensile properties of stone groundwood fibers from softwood. BioResources 2011;6:5037–49. https://doi.org/10.15376/biores.6.4.5037-5049.

[53] Tarrés Q, Oliver-Ortega H, Espinach FX, Mutjé P, Delgado-Aguilar M, Méndez JA. Determination of mean intrinsic flexural strength and coupling factor of natural fiber reinforcement in polylactic acid biocomposites. Polymers (Basel) 2019;11. https://doi.org/10.3390/polym11111736.

[54] Dai Q, Kelly J, Sullivan J, Elgowainy A. Life-Cycle Analysis update of glass and glass fiber for the GREET model. Argonne Natl Lab 2015:25.

[55] Greenberg MI, Waksman J, Curtis J. Silicosis: A Review. Disease-a-Month 2007;53:394–416. https://doi.org/10.1016/j.disamonth.2007.09.020.

[56] Donaldson K, Tran CL. An introduction to the short-term toxicology of respirable industrial fibres. Mutat Res 2004;553:5–9. https://doi.org/10.1016/j.mrfmmm.2004.06.011.

[57] Joshi S V., Drzal LT, Mohanty AK, Arora S. Are natural fiber composites environmentally superior to glass fiber reinforced composites? Compos Part A Appl Sci Manuf 2004;35:371–6. https://doi.org/10.1016/j.compositesa.2003.09.016.

[58] Granda LA, Espinach FX, Tarrés Q, Méndez JA, Delgado-Aguilar M, Mutjé P. Towards a good interphase between bleached kraft softwood fibers and poly(lactic) acid. Compos Part B Eng 2016;99:514–20. https://doi.org/10.1016/j.compositesb.2016.05.008.

[59] Selke SE, Wichman I. Wood fiber/polyolefin composites. Compos Part A Appl Sci Manuf 2004;35:321–6. https://doi.org/10.1016/j.compositesa.2003.09.010.

[60] Woodhams RT, Thomas G, Rodgers DK. Wood fibers as reinforcing fillers for polyolefins. Polym Eng Sci 1984;24:1166–71. https://doi.org/10.1002/pen.760241504.

[61] Association of Plastics Manufacters in Europe & European Association of plastics. Plastics – the Facts 2020. PlasticEurope 2020:1–64.

[62] Konvar V. Smart Textiles for in situMonitoring of composites. Matthew Deans; 2018.

[63] Ku H, Wang H, Pattarachaiyakoop N, Trada M. A review on the tensile properties of natural fiber reinforced polymer composites. Compos Part B Eng 2011;42:856–73. https://doi.org/10.1016/j.compositesb.2011.01.010.

[64] Sauter DW, Taoufik M, Boisson C. Polyolefins, a success story. Polymers (Basel) 2017;9:1–13. https://doi.org/10.3390/polym9060185.

[65] Noureddine Abidi, Hequet E, Ethridge D. Thermogravimetric Analysis of Cotton Fibers: Relationships with Matury and Fineness. J Appl Polym Sci 2006;103:3476–82. https://doi.org/10.1002/app.24465.

[66] Cossee P. Ziegler-Natta catalysis I. Mechanism of polymerization of α-olefins with Ziegler-Natta catalysts. J Catal 1964;3:80–8.

[67] E.J Arlman PC. Ziegler-Natta catalysis III. Stereospeecific polymerization of propene with the catalyst system TiCl3 AlEt3. J Catal 1964;3:99–104.

[68] Wypych G. Handbook of polymers. first Edit. 2011.

[69] Thomason JL. The influence of fibre length and concentration on the properties of glass fibre reinforced polypropylene: 5. Injection moulded long and short fibre PP. Compos Part A Appl Sci Manuf 2002;33:1641–52. https://doi.org/10.1016/S1359-835X(02)00179-3.

[70] Bledzki AK, Gassan J, Theis S. Wood-filled thermoplastic composites. Mech Compos Mater 1998;34:563–8. https://doi.org/10.1007/BF02254666.

[71] Akil HM, Omar MF, Mazuki AAM, Safiee S, Ishak ZAM, Abu Bakar A. Kenaf fiber reinforced composites: A review. Mater Des 2011;32:4107–21. https://doi.org/10.1016/j.matdes.2011.04.008.

[72] Khalil AHPS, Bhat AH, Yursa IAF. Green composites from sustainable cellulose nanofibrils: A review. Carbohydr Polym 2012;87:963–79. https://doi.org/10.1016/j.carbpol.2011.08.078.

[73] Yang HS, Kim HJ, Park HJ, Lee BJ, Hwang TS. Water absorption behavior and mechanical properties of lignocellulosic filler-polyolefin bio-composites. Compos Struct 2006;72:429–37. https://doi.org/10.1016/j.compstruct.2005.01.013.

[74] Hu W, Ton-That M, Perrin-Sarazin F, Denault J. An Improved Method for Single Fiber Tensile Test of Natural Fibers. Polym Eng Sci 2010;50:819. https://doi.org/10.1002/pen.21593.

[75] Peltola H, Pääkkönen E, Jetsu P, Heinemann S. Wood based PLA and PP composites: Effect of fibre type and matrix polymer on fibre morphology, dispersion and composite properties. Compos Part A Appl Sci Manuf 2014;61:13–22. https://doi.org/10.1016/j.compositesa.2014.02.002.

[76] Zierdt P, Theumer T, Kulkarni G, Däumlich V, Klehm J, Hirsch U, et al. Sustainable wood-plastic composites from bio-based polyamide 11 and chemically modified beech fibers. Sustain Mater Technol 2015;6:6–14. https://doi.org/10.1016/j.susmat.2015.10.001.

[77] Balart JF, García-Sanoguera D, Balart R, Boronat T, Sánchez-Nacher L. Manufacturing and properties of biobased thermoplastic composites from poly(lactid acid) and hazelnut shell wastes. Polym Compos 2016. https://doi.org/10.1002/pc.24007.

[78] Hoang D, Pham T, Nguyen T, An H, Kim J. Organo-Phosphorus Flame Retardants for Poly(vinyl chloride)/Wood Flour Composite. Polym Compos 2018;39:961–70. https://doi.org/10.1002/pc.24026.

[79] Faruk O, Bledzki AK, Fink HP, Sain M. Progress report on natural fiber reinforced composites. Macromol Mater Eng 2014;299:9–26. https://doi.org/10.1002/name.201300008.

[80] Oliver-Ortega H, Julian F, Espinach FX, Tarrés Q, Ardanuy M, Mutjé P. Research on the use of lignocellulosic fibers reinforced bio-polyamide 11 with composites for automotive parts: Car door handle case study. J Clean Prod 2019;226:64–73. https://doi.org/10.1016/j.jclepro.2019.04.047.

[81] Holbery J, Houston D. Natural-fiber-reinforced polymer composites in automotive applications. JOM 2006;58:80–6.

[82] Siengchin S. Editorial corner – a personal view Potential use of 'green' composites in automotive applications. Express Polym Lett 2017;11:600. https://doi.org/10.3144/expresspolymlett.2017.57.

[83] Granda LA, Méndez JA, Espinach FX, Puig J, Delgado-Aguilar M, Mutjé P. Polypropylene reinforced with semi-chemical fibres of Leucaena collinsii: Thermal properties. Compos Part B Eng 2016;94:75–81. https://doi.org/10.1016/j.compositesb.2016.03.017.

[84] Lu JZ, Wu Q, McNabb HS. Chemical coupling in wood fiber and polymer composites: A review of coupling agents and treatments. Wood Fiber Sci 2000;32:88–104.

[85] Hill CAS, Khalil HPSA, Hale MD. A study of the potential of acetylation to improve the properties of plant fibres. Ind Crops Prod 1998;8:53–63. https://doi.org/10.1016/S0926-6690(97)10012-7.

[86] Bessadok A, Marais S, Gouanvé F, Colasse L, Zimmerlin I, Roudesli S, et al. Effect of chemical treatments of Alfa (Stipa tenacissima) fibres on water-sorption properties. Compos Sci Technol 2007;67:685–97. https://doi.org/10.1016/j.compscitech.2006.04.013.

[87] Vilaseca F, Corrales F, F.Llop M, Pelach MÀ, Mutjé P. Chemichal treatment for improving wettability of biofibers into thermoplastic matrices. Taylor Fr 2005;12:725–38. https://doi.org/10.1163/156855405774984075.

[88] Lee SY, Chun SJ, Doh GH, Kang IA, Lee S, Paik KH. Influence of Chemical Modification and Filler Loading on Fundamental Properties of Bamboo Fibers Reinforced Polypropylene Composites. J Compos Mater 2009;43:1639–57. https://doi.org/10.1177/0021998309339352.

[89] Naghmouchi I, Mutjé P, Boufi S. Olive stones flour as reinforcement in polypropylene composites: A step forward in the valorization of the solid waste from the olive oil industry. Ind Crops Prod 2014;72:183–91. https://doi.org/10.1016/j.indcrop.2014.11.051.

[90] Beckermann GW, Pickering KL. Engineering and evaluation of hemp fibre reinforced polypropylene composites: Micro-mechanics and strength prediction modelling. Compos Part A Appl Sci Manuf 2009;40:210–7. https://doi.org/10.1016/j.compositesa.2008.11.005.

[91] Naghmouchi I, Espinach FX, Mutjé P, Boufi S. Polypropylene composites based on lignocellulosic fillers: How the filler morphology affects the composite properties. Mater Des 2015;65:454–61. https://doi.org/10.1016/j.matdes.2014.09.047.

[92] Jordi Gironès, Méndez JA, Boufi S, Vilaseca F, Mutjé P. Effect of Silane Coupling Agents on the Properties of Pine Fibers/Polypropylene Composites. J Appl Polym Sci 2006;103:3706–17. https://doi.org/10.1002/app.

[93] Qiu W, Zhang F, Endo T, Hirotsu T. Effect of maleated polypropylene on the performance of polypropylene/ cellulose composite. Polym Compos 2005;26:448–53. https://doi.org/10.1002/pc.20119.

[94] Heinen W, Rosenmöller CH, Wenzel CB, De Groot HJM, Lugtenburg J, Van Duin M. 13C NMR study of the grafting of maleic anhydride onto polyethene, polypropene, and ethene-propene copolymers. Macromolecules 1996;29:1151–7. https://doi.org/10.1021/ma951015y.

[95] Mutjé P, Vallejos ME, Gironès J, Vilaseca F, López A, López JP, et al. Effect of maleated polypropylene as coupling agent for polypropylene composites reinforced with hemp strands. J Appl Polym Sci 2006;102:833–40. https://doi.org/10.1002/app.24315.

[96] Singh B, Gupta M, Verma A, Tyagi OS. FT-IR microscopic studies on coupling agents: Treated natural fibres. Polym Int 2000;49:1444–51.

[97] Kazayawoko M, Balatinecz JJ, Woodhams RT. Diffuse reflectance Fourier transform infrared spectra of wood fibers treated with maleated polypropylenes. J Appl Polym Sci 1997;66:1163–73.

[98] Etcheverry M, Barbosa SE. Glass fiber reinforced polypropylene mechanical properties enhancement by adhesion improvement. Materials (Basel) 2012;5:1084–113. https://doi.org/10.3390/ma5061084.

[99] Karmaker AC, Youngquist JA. Injection molding of polypropylene reinforced with short jute fibers. J Appl Polym Sci 1996;62:1147–51. https://doi.org/10.1002/(SICI)1097-4628(19961121)62:8<1147::AID-APP2>3.0.CO;2-I.

[100] Malkapuram R, Kumar V, Singh Negi Y. Recent development in natural fiber reinforced polypropylene composites. J Reinf Plast Compos 2009;28:1169–89. https://doi.org/10.1177/0731684407087759.

[101] Pauskstza D, ManKowski J, Kolodziej J, Szostak M. Polypropylene (PP) Composites Reinforced with Stinging Nettle (Utrica dioica L.) Fiber. J Nat Fibers 2013;10:147–58. https://doi.org/10.1080/15440478.2013.789287.

[102] Sullins T, Pillay S, Komus A, Ning H. Hemp fiber reinforced polypropylene composites: The effects of material treatments. Compos Part B Eng 2017;114:15–22. https://doi.org/10.1016/j.compositesb.2017.02.001.

[103] Koronis G, Silva A, Fontul M. Green composites: A review of adequate materials for automotive applications. Compos Part B Eng 2013;44:120–7. https://doi.org/10.1016/j.compositesb.2012.07.004.

[104] Delgado-Aguilar M, Vilaseca F, Tarrés Q, Julián F, Mutjé P, Espinach FX. Extending the value chain of corn agriculture by evaluating technical feasibility and the quality of the interphase of chemo-thermomechanical fiber from corn stover reinforced polypropylene biocomposites. Compos Part B Eng 2018;137:16–22. https://doi.org/10.1016/j.compositesb.2017.11.006.

[105] Serra-Parareda F, Tarrés Q, Delgado-Aguilar M, Espinach FX, Mutjé P, Vilaseca F. Biobased composites from biobased-polyethylene and barley thermomechanical fibers: Micromechanics of composites. Materials (Basel) 2019;12. https://doi.org/10.3390/ma1224182.

[106] Reixach R, Espinach FX, Arbat G, Julián F, Delgado-Aguilar M, Puig J, et al. Tensile properties of polypropylene composites reinforced with mechanical, thermomechanical, and chemi-thermomechanical pulps from orange pruning. BioResources 2015;10:4544–56. https://doi.org/10.15376/biores.10.3.4544-4556.

[107] Araújo RS, Rezende CC, Marques MFV, Ferreira LC, Russo P, Emanuela Errico M, et al. Polypropylene-based composites reinforced with textile wastes. J Appl Polym Sci 2017;134:1–10. https://doi.org/10.1002/app.45060.

[108] Haque MS. Processing and Characterization of waste demin fiber reinforced polymer composites. 2014.

[109] Petrucci R, Nisini E, Puglia D, Sarasini F, Rallini M, Santulli C, et al. Tensile and fatigue characterisation of textile cotton waste/polypropylene laminates. Compos Part B Eng 2015;81:84–90. https://doi.org/10.1016/j.compositesb.2015.07.005.

[110] Zhong T, Dhandapani R, Liang D, Wang J, Wolcott MP, Van Fossen D, et al. Nanocellulose from recycled indigo-dyed denim fabric and its application in composite films. Carbohydr Polym 2020;240:116283. https://doi.org/10.1016/j.carbpol.2020.116283.

[111] TAPPI. T204cm-07: Solvent extractives of wood and pulp. 2007.

[112] TAPPI. T211 om-12: Ash in wood, pulp, paper and paperboard: combustion at 525°C. 2012.

[113] TAPPI. T222 om-15: Acid-insoluble lignin in wood and pulp. 2015.

[114] TAPPI. Alpha-, beta- and gamma-cellulose in pulp, Test Method T 203 cm-09. 2009.

[115] ISO. ISO 5351:2010 Pulps-Determination of limiting viscosity number in cupri-ethylenediamine (CED) solution. 2010.

[116] Serra A, Tarrés Q, Claramunt J, Mutjé P, Ardanuy M, Espinach FX. Behavior of the interphase of dyed cotton residue flocks reinforced polypropylene composites. Compos Part B Eng 2017;128:200–7. https://doi.org/10.1016/j.compositesb.2017.07.015.

[117] ISO. ISO 16065:2014 Pulp-Determination of fibre length by automated optical analysis. 2014.

[118] ASTM. ASTM D618 - 13: Standard Practice for Conditioning Plastics for Testing. 2013.

[119] ASTM. ASTM D3039 / D3039M - 17 Standard Test Method for Tensile Properties of Polymer Matrix Composite Materials. 2017.

[120] ASTM. ASTM D790 - 17 Standard Test Methods for Flexural Properties of Unreinforced and Reinforced Plastics and Electrical Insulating Materials. 2017.

[121] ISO. ISO 179:2010: Plastics - Determination of Charpy Impact properties. 2010.

[122] ISO. ISO 180:2001: Determinación de la Resistencia al Impacto Izod. 2001.

[123] Tucker CL, Liang E. 1999 - Sti□ness predictions for unidirectional short-fiber composites.pdf. Compos Sci Technol 1999;59:655–71.

[124] Kelly A, Tyson W. Tensile porperties of fibre-reinforced metals-copper/tungsten and copper/molybdenum. J Mechanocs Phys Solids 1965;13:329–38.

[125] Bowyer WH, Bader HG. On the reinforcement of thermoplastics by imperfectly aligned discontinuous fibres. J Mater Sci 1972;7:1315–1312.

[126] Hirsch TJ. Modulus of Elasticity of Concrete Affected by Elastic Moduli of Cement Paste Matrix and Aggregate. J Proc 1962;59:427–52.

[127] López JP, Mutjé P, Angels Pèlach M, El Mansouri NE, Boufi S, Vilaseca F. Analysis of the tensile modulus of polypropylene composites reinforced with stone groundwood fibers. BioResources 2012;7:1310–23. https://doi.org/10.15376/biores.7.1.1310-1323.

[128] Cox HL. The elasticity and strength of paper and other fibrous materials. Br J Appl Phys 1952;3:72–9. https://doi.org/10.1088/0508-3443/3/3/302.

[129] Tarrés Q, Soler J, Rojas-Sola JI, Oliver-Ortega H, Julián F, Espinach FX, et al. Flexural properties and mean intrinsic flexural strength of old newspaper reinforced polypropylene composites. Polymers (Basel) 2019;11:1–13. https://doi.org/10.3390/polym11081244.

[130] Reixach R, Espinach FX, Franco-Marquès E, Cartagena FR de, Pellicer N, Tresserras J, et al. Modeling of the Tensile Moduli of Mechanical, Thermomechanical, and Chemi-Thermomechanical Pulps from Orange Tree Pruning Rafel. Polym Compos 2013;34:1840 1846. https://doi.org/10.1002/pc.

[131] Li Y, Pickering KL, Farrell RL. Determination of interfacial shear strength of white rot fungi treated hemp fibre reinforced polypropylene. Compos Sci Technol 2009;69:1165–71. https://doi.org/10.1016/j.compscitech.2009.02.018.

[132] Granda LA, Espinach FX, López F, García JC, Delgado-Aguilar M, Mutjé P. Semichemical fibres of Leucaena collinsii reinforced polypropylene: Macromechanical and micromechanical analysis. Compos Part B Eng 2016;91:384–91. https://doi.org/10.1016/j.compositesb.2016.01.035.

[133] Serra A, Tarrés Q, Chamorro M-À, Soler J, Mutjé P, Espinach FX, et al. Modeling the Stiffness of Coupled and Uncoupled Recycled Cotton Fibers Reinforced. Polymers (Basel) 2019;11:1725. https://doi.org/10.3390/polym11101725.

[134] Vilaseca F, López A, Llauró X, Pèlach MA, Mutjé P. Hemp strands as reinforcement of polystyrene composites. Chem Eng Res Des 2004;82:1425–31. https://doi.org/10.1205/cerd.82.11.1425.52038.

[135] Mutjé P, Gironès J, Lòpez A, Llop MF, Vilaseca F. Hemp strands: PP composites by injection molding: Effect of low cost physico-chemical treatments. J Reinf Plast Compos 2006;25:313–27. https://doi.org/10.1177/0731684406059784.

[136] Julián F, Espinach FX, Verdaguer N, Pèlach MA, Vilaseca F. Design and development of fully biodegradable products from starch biopolymer and corn stalk fibres. J Biobased Mater Bioenergy 2012;6:410–7. https://doi.org/10.1166/jbmb.2012.1228.

[137] Galan-Marin C, Rivera-Gomez C, Garcia-Martinez A. Use of natural-fiber bio-composites in construction versus traditional solutions: Operational and embodied energy assessment. Materials (Basel) 2016;9. https://doi.org/10.3390/ma9060465.

[138] López JP, Méndez JA, Espinach FX, Julián F, Mutjé P, Vilaseca F. Tensile strength characteristics of polypropylene composites reinforced with stone groundwood fibers from softwood. BioResources 2012;7:3188–200. https://doi.org/10.15376/biores.7.3.3188-3200.

[139] Serrano A, Espinach FX, Tresserras J, Pellicer N, Alcala M, Mutje P. Study on the technical feasibility of replacing glass fibers by old newspaper recycled fibers as polypropylene reinforcement. J Clean Prod 2014;65:489–96. https://doi.org/10.1016/j.jclepro.2013.10.003.

[140] Serrano A, Espinach FX, Julian F, Del Rey R, Mendez JA, Mutje P. Estimation of the interfacial shears strength, orientation factor and mean equivalent intrinsic tensile strength in old newspaper fiber/polypropylene composites. Compos Part B Eng 2013;50:232–8. https://doi.org/10.1016/j.compositesb.2013.02.018.

[141] Vallejos ME, Espinach FX, Julián F, Torres L, Vilaseca F, Mutjé P. Micromechanics of hemp strands in polypropylene composites. Compos Sci Technol 2012;72:1209–13. https://doi.org/10.1016/j.compscitech.2012.04.005.

[142] Franco-Marquès E, Méndez JA, Pèlach MA, Vilaseca F, Bayer J, Mutjé P. Influence of coupling agents in the preparation of polypropylene composites reinforced with recycled fibers. Chem Eng J 2011;166:1170–8. https://doi.org/10.1016/j.cej.2010.12.031.

[143] Vilaseca F, Valadez-Gonzalez A, Herrera-Franco PJ, Pèlach MÀ, López JP, Mutjé P. Biocomposites from abaca strands and polypropylene. Part I: Evaluation of the tensile properties. Bioresour Technol 2010;101:387–95. https://doi.org/10.1016/j.biortech.2009.07.066.

[144] Shah DU, Nag RK, Clifford MJ. Why do we observe significant differences between measured and 'back-calculated' properties of natural fibres? Cellulose 2016;23:1481–90.

https://doi.org/10.1007/s10570-016-0926-x.

[145] Üreyen ME, Kadoglu H. Regressional Estimation of Ring Cotton Yarn Properties from HVI Fiber Properties. Text Res J 2006;76:360–6. https://doi.org/10.1177/0040517506062262.

[146] Reixach R, Franco-Marquès E, El Mansouri NE, de Cartagena FR, Arbat G, Espinach FX, et al. Micromechanics of mechanical, thermomechanical, and chemi-thermomechanical pulp from orange tree pruning as polypropylene reinforcement: A comparative study. BioResources 2013;8:3231–46. https://doi.org/10.15376/biores.8.3.3231-3246.

[147] Serra A, Tarrés Q, Llop M, Reixach R, Mutjé P, Espinach FX. Recycling dyed cotton textile byproduct fibers as polypropylene reinforcement. Text Res J 2019;89:2113–25. https://doi.org/10.1177/0040517518786278.

[148] Granda LA, Espinach FX, Méndez JA, Tresserras J, Delgado-Aguilar M, Mutjé P. Semichemical fibres of Leucaena collinsii reinforced polypropylene composites: Young's modulus analysis and fibre diameter effect on the stiffness. Compos Part B Eng 2016;92:332–7. https://doi.org/10.1016/j.compositesb.2016.02.023.

[149] Serrano A, Espinach FX, Tresserras J, del Rey R, Pellicer N, Mutje P. Macro and micromechanics analysis of short fiber composites stiffness: The case of old newspaper fibers-polypropylene composites. Mater Des 2014;55:319–24. https://doi.org/10.1016/j.matdes.2013.10.011.

[150] Espinach FX, Chamorro-Trenado MA, Llorens J, Tresserras J, Pellicer N, Vilaseca F, et al. Study of the flexural modulus and the micromechanics of old newspaper reinforced polypropylene composites. BioResources 2019;14:3578–93. https://doi.org/10.15376/biores.14.2.3578-3593.

[151] Espinach FX, Julian F, Verdaguer N, Torres L, Pelach MA, Vilaseca F, et al. Analysis of tensile and flexural modulus in hemp strands/polypropylene composites. Compos Part B Eng 2013;47:339–43. https://doi.org/10.1016/j.compositesb.2012.11.021.

[152] Tarrés Q, Vilaseca F, Herrera-Franco PJ, Espinach FX, Delgado-Aguilar M, Mutjé P. Interface and micromechanical characterization of tensile strength of bio-based composites from polypropylene and henequen strands. Ind Crops Prod 2019;132:319–26. https://doi.org/10.1016/j.indcrop.2019.02.010.

[153] Julian F, Méndez JA, Espinach FX, Verdaguer N, Mutje P, Vilaseca F. Bio-based composites from stone groundwood applied to new product development. BioResources 2012;7:5829–42. https://doi.org/10.15376/biores.7.4.5829-5842.

[154] Oliver-Ortega H, Chamorro-Trenado MÀ, Soler J, Mutjé P, Vilaseca F, Espinach FX. Macro and micromechanical preliminary assessment of the tensile strength of particulate rapeseed sawdust reinforced polypropylene copolymer biocomposites for its use as building material. Constr Build Mater 2018;168:422–30. https://doi.org/10.1016/j.conbuildmat.2018.02.158.

[155] Bledzki AK, Gassan J. Composites reinforced with cellulose based fibres. Prog Polym Sci 1999;24:221–74.

[156] Rogovina SZ, Prut E V., Berlin AA. Composite Materials Based on Synthetic Polymers Reinforced with Natural Fibers. Polym Sci - Ser A 2019;61:417–38. https://doi.org/10.1134/S0965545X19040084.

[157] del Rey R, Serrat R, Alba J, Perez I, Mutje P, Espinach FX. Effect of sodium hydroxide treatments on the tensile strength and the interphase quality of hemp core fiber-reinforced polypropylene composites. Polymers (Basel) 2017;9:6–8. https://doi.org/10.3390/polym9080377.

[158] Granda LA, Espinach FX, Méndez JA, Vilaseca F, Delgado-Aguilar M, Mutjé P. Semichemical fibres of Leucaena collinsii reinforced polypropylene composites: Flexural characterisation, impact behaviour and water uptake properties. Compos Part B Eng 2016;97:176–82. https://doi.org/10.1016/j.compositesb.2016.04.063.

[159] Sood M, Dwivedi G. Effect of fiber treatment on flexural properties of natural fiber reinforced composites: A review. Egypt J Pet 2018;27:775–83. https://doi.org/10.1016/j.ejpe.2017.11.005.

[160] Espinach FX, Granda LA, Tarrés Q, Duran J, Fullana-i-Palmer P, Mutjé P. Mechanical and micromechanical tensile strength of eucalyptus bleached fibers reinforced polyoxymethylene composites. Compos Part B Eng 2017;116:333–9. https://doi.org/10.1016/j.compositesb.2016.10.073.

[161] Espinach FX, Delgado-Aguilar M, Puig J, Julian F, Boufi S, Mutjé P. Flexural properties of fully biodegradable alpha-grass fibers reinforced starch-based thermoplastics. Compos Part B Eng 2015;81:98–106. https://doi.org/10.1016/j.compositesb.2015.07.004.

[162] Vilaseca F, Serra-Parareda F, Espinosa E, Rodríguez A, Mutjé P, Delgado-Aguilar M. Valorization of hemp core residues: Impact of NaOH treatment on the flexural strength of PP composites and intrinsic flexural strength of hemp core fibers. Biomolecules 2020;10. https://doi.org/10.3390/biom10060823.

[163] Nabi Saheb D, Jog JP. Natural fiber polymer composites: A review. Adv Polym Technol 1999;18:351–63.

[164] Espinach FX, Julián F, Alcalá M, Tresserras J, Mutjé P. High stiffness performance alpha-grass pulp fiber reinforced thermoplastic starch-based fully biodegradable composites. BioResources 2014;9:738–55. https://doi.org/10.15376/biores.9.1.738-755.

[165] López J. P, Gironés J, Mendez JA, Pelach MA, Vilaseca F, Mutjé P. Impact and Flexural Properties of Stone-Ground Wood Pulp-Reinforced Polypropylene Composites. Polym Compos 2013;34:842–8. https://doi.org/10.1002/pc.

[166] Gironès J, Lopez JP, Vilaseca F, Bayer R, Herrera-Franco PJ, Mutjé P. Biocomposites from Musa textilis and polypropylene: Evaluation of flexural properties and impact strength. Compos Sci Technol 2011;71:122–8. https://doi.org/10.1016/j.compscitech.2010.10.012.

[167] Serra-Parareda F, Espinach FX, Pelach MÀ, Méndez JA, Vilaseca F, Tarrés Q. Effect of NaOH treatment on the flexural modulus of hemp core reinforced composites and on the intrinsic flexural moduli of the fibers. Polymers (Basel) 2020;12:1–21. https://doi.org/10.3390/polym12061428.

[168] Belgacem C, Serra-Parareda F, Tarrés Q, Mutjé P, Delgado-Aguilar M, Boufi S. Valorization of date palm waste for plastic reinforcement: Macro and micromechanics of flexural strength. Polymers (Basel) 2021;13. https://doi.org/10.3390/polym13111751.

[169] Serra-Parareda F, Julián F, Espinosa E, Rodríguez A, Espinach FX, Vilaseca F. Feasibility of barley straw fibers as reinforcement in fully biobased polyethylene composites: Macro

and micro mechanics of the flexural strength. Molecules 2020;25:1–16. https://doi.org/10.3390/molecules25092242.

[170] Bax B, Müssig J. Impact and tensile properties of PLA/Cordenka and PLA/flax composites. Compos Sci Technol 2008;68:1601–7. https://doi.org/10.1016/j.compscitech.2008.01.004.

[171] Khan MA, Ganster J, Fink HP. Hybrid composites of jute and man-made cellulose fibers with polypropylene by injection moulding. Compos Part A Appl Sci Manuf 2009;40:846–51. https://doi.org/10.1016/j.compositesa.2009.04.015.

[172] Guettler BE, Moresoli C, Simon LC. Mechanical properties and crack propagation of soy-polypropylene composites. J Appl Polym Sci 2013;130:175–85. https://doi.org/10.1002/app.39151.

[173] Thomason JL, Rudeiros-Fernández JL. A review of the impact performance of natural fiber thermoplastic composites. Front Mater 2018;5:1–18. https://doi.org/10.3389/fmats.2018.00060.

[174] Arbelaiz A, Fernández B, Cantero G, Llano-Ponte R, Valea A, Mondragon I. Mechanical properties of flax fibre/polypropylene composites. Influence of fibre/matrix modification and glass fibre hybridization. Compos Part A Appl Sci Manuf 2005;36:1637–44. https://doi.org/10.1016/j.compositesa.2005.03.021.

[175] Candido VS, Silva ACR da, Simonassi NT, Luz FS da, Monteiro SN. Toughness of polyester matrix composites reinforced with sugarcane bagasse fibers evaluated by Charpy impact tests. J Mater Res Technol 2017;6:334–8. https://doi.org/10.1016/j.jmrt.2017.06.001.

[176] Huda MS, Drzal LT, Mohanty AK, Misra M. Chopped glass and recycled newspaper as reinforcement fibers in injection molded poly(lactic acid) (PLA) composites: A comparative study. Compos Sci Technol 2006;66:1813–24. https://doi.org/10.1016/j.compscitech.2005.10.015.

[177] Arbelaiz A, Fernández B, Ramos JA, Retegi A, Llano-Ponte R, Mondragon I. Mechanical properties of short flax fibre bundle/polypropylene composites: Influence of matrix/fibre modification, fibre content, water uptake and recycling. Compos Sci Technol 2005;65:1582–92. https://doi.org/10.1016/j.compscitech.2005.01.008.

[178] Orue A, Eceiza A, Peña-Rodriguez C, Arbelaiz A. Water uptake behavior and young modulus prediction of composites based on treated sisal fibers and poly(lactic acid). Materials (Basel) 2016;9. https://doi.org/10.3390/ma9050400.

[179] Yew GH, Mohd Yusof AM, Mohd Ishak ZA, Ishiaku US. Water absorption and enzymatic degradation of poly(lactic acid)/rice starch composites. Polym Degrad Stab 2005;90:488–500. https://doi.org/10.1016/j.polymdegradstab.2005.04.006.

[180] Alonso-Montemayor FJ, Tarrés Q, Oliver-Ortega H, Espinach FX, Narro-Céspedes RI, Castañeda-Facio AO, et al. Enhancing the mechanical performance of bleached hemp fibers reinforced polyamide 6 composites: A competitive alternative to commodity composites. Polymers (Basel) 2020;12. https://doi.org/10.3390/POLYM12051041.

[181] Mohebby B, Fallah-Moghadam P, Ghotbifar AR, Kazemi-Najafi S. Influence of maleic-anhydride-polypropylene (MAPP) on wettability of polypropylene/wood flour/glass fiber hybrid composites. J Agric Sci Technol 2011;13:877–84.

[182] Ashori A. Wood-plastic composites as promising green-composites for automotive

industries! Bioresour Technol 2008;99:4661–7. https://doi.org/10.1016/j.biortech.2007.09.043.

[183] Rhim JW, Mohanty KA, Singh SP, Ng PKW. Preparation and properties of biodegradable multilayer films based on soy protein isolate and poly(lactide). Ind Eng Chem Res 2006;45:3059–66. https://doi.org/10.1021/ie051207+.

[184] Méndez JA, Vilaseca F, Pèlach MA, López JP, Barberà L, Turon X, et al. Evaluation of the reinforcing effect of ground wood pulp in the preparation of polypropylene-based composites coupled with maleic anhydride grafted polypropylene. J Appl Polym Sci 2007;105:3588–96. https://doi.org/10.1002/app.26426.